Numerical Simulation of Groundwater Flow and Solute Transport

Editor
L. ELANGO

Numerical Simulation of Groundwater Flow and Solute Transport

Editor
Prof. L. Elango
Department of Geology
Anna University, Chennai

Sponsored by
Department of Science and Technology
Ministry of Science and Technology
Government of India, New Delhi

Allied Publishers Pvt. Ltd.

New Delhi • Mumbai • Kolkata • Chennai • Nagpur
Ahmedabad • Bangalore • Hyderabad • Lucknow

ALLIED PUBLISHERS PVT. LTD.
Regd. Off.: 15, J.N. Heredia Marg, Ballard Estate, Mumbai – 400 001
Prarthna Flats (2nd Floor), Navrangpura, Ahmedabad – 380 009
3-5-844/6 & 7, Kachiguda Station Road, Hyderabad – 500 027
Patiala House, 16-A Ashok Marg, Lucknow – 226 001
5th Main Road, Gandhi Nagar, Bangalore – 560 009
17, Chittaranjan Avenue, Kolkata – 700 072
13/14, Asaf Ali Road, New Delhi – 110 002
81, Hill Road, Ramnagar, Nagpur – 440 010
751, Anna Salai, Chennai – 600 002

ISBN : 81 -

Published by
S.M. Sachdev
M/s. Allied Publishers Pvt. Ltd.
751, Anna Salai, Chennai – 600 002

Preface

Mathematical modelling is one of most important tools that is widely used around the world for answering many questions raised during the management of the groundwater resources. Models range from simple mathematical equations to complex computer generated models. Models are generally used to support remedial decisions where groundwater contamination exists above a prescribed action level. It is well known that modeling and simulation studies make a significant contribution to solving existing and emerging problems in science, engineering, economics, management, social and behavioral sciences. During the recent past, there have been widespread innovations in the application of these methodologies and tools in resolving many problems helping scientists, planners, administrators and decision makers. Realising the need for promoting the use of mathematical modelling in India, Department of Science and Technology, Government of India under the Earth System Science Division has initiated a programme to organize various types of inter-disciplinary and multi-institutional training activities in different parts of the country. One such training programme is organised by me at Anna University from 7-11-2005 to 30-11-2005. This book on Numerical Simulation of Groundwater Flow and Solute Transport is a result of this programme. It is expected that these thought provoking papers will lead to better understanding of techniques and application of groundwater modelling and enthuse many to work in this field of research.

All contributors are thanked for their willing co-operation and support in the publication of this book. Thanks are also due the reviewers who had given critical and constructive comments on the contents of this book.

I thank Dr. D.R. Ram, Director, Earth System Science Division, Department of Science and Technology, Ministry of Science and Technology for has constant support and his encouragement. I thank the Vice-Chancellor, Anna University who was a constant source of inspiration and guidance which enabled me to publish this book. I thank my teacher Prof. P. Ganesan, Department of Mathematics, Anna University for having introduced me to the field of Numerical Methods and for his guidance in the publication of this book. Thanks are also due to my colleagues Prof. S. Sanjeevi, Dr. R. Nagendra, Dr. Hema Achyuthan and Dr. S. Srinivasalu for their support.

I thank the Department of Science and Technology, Government of India for the funding to organise the training programme and for the publication of this book.

I also thank the Dept of Science and Technology, Govt of India, Council of Scientific and Industrial Research, All India Council for Technical Education and University Grants Commission for sponsoring research projects, which have gone a long way in enhancing my knowledge in this area of research. Thanks are also due to the Project Fellows Mr C. Sivakumar, Mr. D. Sreenivas and Mr. K.K. Ilayaraja for their untiring support during the preparation of this book.

October 2005 **L. Elango**

List of Contributors

Ballukraya, P. N.
Professor
Department of Applied Geology
University of Madras
Chennai.

Chaudhuri, A.
Department of Civil Engineering
Indian Institute of Science
Bangalore

Descloitres, M.
IFCWS
Indian Institute of Science
Bangalore

Elango, L.
Professor and Head
Department of Geology
Anna University
Chennai.

Ganesan, P.
Professor and Head
Department of Mathematics
Anna University
Chennai.

Gurunadha Rao, V.V.S.
Deputy Director
Environmental Hydrology Group
National Geophysical Research Institute
Hyderabad.

Kannan, R.
Project Fellow
Department of Geology
Anna University
Chennai.

Legchenko, A.
Laboratoire D'etude Des Transferts En
Hydrologie Et Environement
38041 Grenoble
Cedex 9, France

Mahesh Kumar, K.
Environmental Hydrology Group
National Geophysical Research Institute
Hyderabad.

Mohan, S.
Professor and Head
Department of Civil Engineering
Indian Institute of Technology, Madras
Chennai.

Pramada, S.K.
Department of Civil Engineering
Indian Institute of Technology, Madras
Chennai.

Rajmohan, N.
Post Doctoral Fellow
Water Research Center
Post Graduate Studies and Research
Sultan Qaboos University
Alkhouth 123, Oman

Sanjeevi, S.
Professor
Department of Geology
Anna University
Chennai

Sankaran, S.
Environmental Hydrology Group
National Geophysical Research Institute
Hyderabad.

Sekhar, M.
Assistant Professor
Department of Civil Engineering
Indian Institute of Science
Bangalore.

Senthil Kumar, M.
Scientist
Central Groundwater Board
Ahmedabad.

Sinha, A.K.
Professor and Head
Department of Geology
University of Rajasthan
Jaipur.

Sivakumar, C.
Project Fellow
Department of Geology
Anna University
Chennai.

Suresh, S.
Scientist
Central Groundwater Board
South Eastern Coastal Region
Chennai.

Thangarajan, M.
Retired Scientist and Head
Groundwater Modelling Group
National Geophysical Research Institute
Hyderabad.

Contents

Numerical Simulation of Groundwater Flow and Solute Transport, L. Elango (ed). pp.1-14

Basics of Groundwater Flow

L. Elango and **C. Sivakumar**

INTRODUCTION

Groundwater is the used for water that occurs beneath the ground surface. Groundwater forms a part of the hydrologic cycle. Water first passes through the zone of aeration or unsaturated zone. In this zone, a mixture of air and water fills the spaces between the rock and soil particles. From here, water is taken up by plant roots, discharged into a body of water, or flows down to the next zone, which is the zone of saturation or saturated zone. Here all the spaces between particles are completely filled with water. The top of this zone is called the water table. Geological formations are classified as aquifer or aquitard or aquiclude based on their capacity to transmit or store groundwater as follows.

Aquifer - a saturated permeable geologic unit that can transmit significant quantities of water under ordinary potential gradients. i.e. normally constitutes medium to coarse sands and gravels.

Aquitard - a saturated geologic unit that is capable of transmitting water under ordinary potential gradients but not it sufficient quantities to allow completion of production wells within them. i.e. normally constitutes clays and silts.

Aquiclude - a saturated geologic unit that is incapable of transmitting significant quantities of water under ordinary potential gradients. i.e. normally constitutes consolidated clays of very low permeability.

Aquifer Parameters

Porosity is the ratio of the volume of void spaces in a rock or sediment to the total volume of the rock or sediment. Primary porosity represents the original pore openings formed when a rock or sediment formed; whilst secondary porosity is that caused by fractures or weathering in a rock or sediment after it has been formed. Up to approximately **70**% of a rock or soil's volume (e.g. clays) may contain groundwater.

Specific Yield: It is the ratio of the volume of water that drains from a saturated rock owing to the attraction of gravity to the total volume of the rock.

$$n = \frac{V_v}{V_T} \quad \text{fraction}$$

$$n = 100\frac{V_v}{V_T} \quad \text{percentage}$$

Storage coefficient **or** ***storativity*** is the volume of water that a permeable unit will absorb or expel from storage per unit surface area per unit change in head.

Thus $S = bS_s$

Transmissivity This is a measure of the amount of water that can be transmitted horizontally by the full-saturated thickness of the aquifer under a hydraulic gradient of 1.

HOMOGENEITY AND HETEROGENEITY

Homogenous formations are those in which hydraulic conductivity K is independent of position. If the hydraulic conductivity K is dependent on the position within a geologic formation, the formation is heterogeneous.

There are probably as many types of heterogeneous configurations as there are geological environments; but is may be instructive to draw attention to three broad classes. Fig. 1(a). is vertical cross section that shows an example of layered heterogeneity, common in sedimentary reocks and unconsolidated lacustrine and marine deposits. Here, the individual beds making up the formation each have a homogenous conductivity value K1, K2…, but the entire system can be thought of as heterogeneous. Perhaps the most ubiquitous discontinuous feature is the overburden-bedrock contact. Fig. 1(b) is a map that shows a case of trending heterogeneity. Trends are possible in the any type of geological formation, but they are particularly common in response if the sedimentation processes that create deltas, alluvial fans, and glacial out wash plains. The A, B and C soil horizons often show vertical trends in hydraulic conductivity, as do rock types whose conductivity is primarily dependent on joint and fracture concentration, Trending heterogeneity in large consolidated or unconsolidated sedimentary formations can attain gradients of 2-3 order of magnitude in a few kilometers.

Fig. 1: Layered heterogeneity and trending heterogeneity

ISOTROPY AND ANISOTROPY

A formation is called as isotropic if the hydraulic conductivity k is independent of the direction of measurement. If the hydraulic conductivity k varies with the direction of measurement at a point in a geologic formation, the formation is anisotropic at that point. The primary cause of anisotropy on a small scale is the orientation of clay minerals in sedimentary rocks and unconsolidated sediments.

If an xyz coordinate system is set up in such a way that the coordinate direction coincide with the principal directions of anisotropy, the hydraulic conductivity values in the principal directions can be specified as K_x, K_y, and K_z. At any point (x, y, z), an isotropic formation will have $K_x=K_y=K_z$ whereas an anisotropic formation will have $K_x\neq K_y\neq K_z$. If $K_x,=K_y\neq K_z$, as is common in horizontally bedded sedimentary deposits, the formation is said to be transversely isotropic.

To fully describe the nature of the hydraulic conductivity in a geologic formation, it is necessary to use two adjectives, one dealing with heterogeneity and one with anisotropy. For example, for a homogenous, isotropic system in two dimensions: K_x (x,z)=K_z(X,Z)=C for all (x,z), where C is a constant. For a homogeneous, anisotropic system, K_x(X,Z)=C_1 for all(X,Z) and K_z (X, Z)=C_2 for all (X,Z) but C_1=C_2. Fig. 2 attempts to further clarify the four possible combinations. The length of the arrow vectors is proportional to the K_x and K_z values at the two points (X_1, Z_1) and (X_1, Z_2). In layerd formation as shown in Fig. 3 each layer is homogeneous and isotropic with hydraulic conductivity values K_1, K2, …..,K_n. But this system as a whole acts likes a single homogeneous, anistropic layer.

Homogeneous, Isotropic Homogeneous, Anisotropic

Heterogeneous, Isotropic Heterogeneous, Anisotropic

Fig. 2: Four possible combinations of heterogeneity and anisotropy

Fig. 3: Relation between layered heterogeneity and anisotrophy

Darcy's Law

Darcy's law states that the rate of water flow through a bed of a porous medium is proportional to the difference in the height of the water between two ends of the filter beds and inversely proportional to the length of the flow path. The quantity of flow is proportional to a coefficient, K, which is dependent upon the nature of the porous medium. Experimental verification of Darcy's law can be carried out by the movement of water through a porous media. Fig. illustrates a horizontal pipe filled with sand. Water is applied under pressure through one end. The pressure can be measured and observed by means of a thin vertical pipe open in the sand at point. The water flows through the pipe and discharge at another end. Darcy found that the discharge, Q, is proportional to the difference in the height of the water, h (hydraulic head), between the ends and inversely proportional to the flow length L.

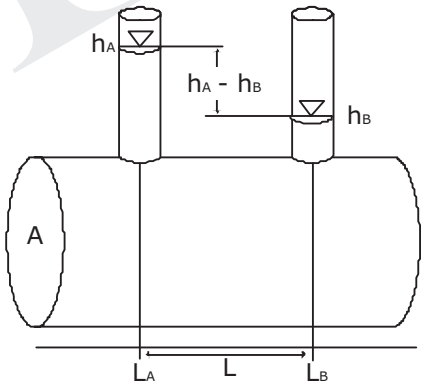

Fig. 4: Darcy's Law

The flow is also obviously proportional to the cross sectional area of the pipe. When combined with the proportionality constant, K, the result is expression known as Darcy's law.

$$Q = -AK\frac{dh}{dl}$$

where,Q = volumetric flow rate (m^3/s), A = flow area perpendicular to L (m^2), K = hydraulic conductivity (m/s), l = flow path length (m), h = hydraulic head (m), and Δ = denotes the change in h over the path L. the negative sign indicates that flow is in the direction of decreasing hydraulic head.

EQUATIONS OF GROUNDWATER FLOW

Groundwater moves from areas of higher elevation or higher pressure/hydraulic head (recharge areas) to areas of lower elevation or pressure/hydraulic head. Permeable material contains interconnected cracks or spaces that are both numerous enough and large enough to allow water to move freely. In some permeable materials groundwater may move several metres in a day; in other places, it moves only a few centimetres in a century. Groundwater moves very slowly through relatively impermeable materials such as clay and shale. The direction of groundwater flow normally follows the general topography of the land surface. Groundwater movement is governed by established hydraulic principles. The flow through aquifers, most of which are natural porous media. possesses energy in mechanical, thermal, and chemical forms. Because the amounts of energy vary spatially, groundwater is forced to move from one region to another in nature‘s attempt to eliminate these energy differentials. The flow of groundwater is thus controlled by the laws of physics and thermodynamics.

STEADY UNIDIRECTIONAL FLOW

Confined Aquifer

If there is the steady movement of groundwater in a confined aquifer, there will be a gradient or slope to the potentiometric surface of the aquifer. Likewise, we know that the water will be moving in the opposite direction of grad h. for flow of this type; Darcy's law may be used directly. A portion of a confined aquifer of uniform thickness is shown. The potentiometric surface has a linear gradient; i.e., it's two dimensional projection is a straight line. There are two observation wells where the hydraulic head can be measured.

The quantity of flow per unit width, q', may be determined from Darcy's law:

$$Q' = Kb\, dh/dl \qquad (1)$$

Where K is the hydraulic conductivity, B is the aquifer thickness, Dh/dl is the slope of potentiometric surface, Q' is the flow per unit width

One may wish to know the head, h, at some intermediate distance, a, between h_1 and h_2. This may be found from the equation.

$$H= h_1 – q'/Kb\ a \quad (2)$$

Unconfined Aquifer

In an unconfined aquifer, the fact that the water table is also the upper boundary of the region of flow complicates flow determinations. On the left side of the saturated flow region is h_1 feet thick. On the right side, it is h_2 feet thick, which is h_1-h_2 feet thinner than the left side. If there is no recharge or evaporation as the flow traverses the region, the quantity of water flowing through the left side is equal to that flowing through the right side. From Darcy's law, it is obvious that since the cross-sectional area is smaller on the right side, the hydraulic gradient must be greater. Thus, the gradient of the water table in unconfined flow is not constant; it increases in the direction of flow.

This problem was solved by Dupit and his assumptions are known as dupit flow. The assumptions are that (a) the hydraulic gradient is equal to the slope of the water table and (b) for small water-table gradients, the stream-lines are horizontal and the equipotential lines are vertical. Solutions based on these assumptions have proved to be very useful in many practical problems. However, the Dupit assumptions do not allow for a seepage face above the outflow side.

STEADY RADIAL FLOW

Flow toward a well has been termed radial flow. It moves as if along the spokes of a wagon wheel toward the hub. We can deal with radial flow by use of a coordinates system called polar coordinates. The position of a point in a plane is specified according to its distance and direction from a fixed point or pole. The distance is measured directly from the pole to the point in the plane. The direction is determined by the angle between the line from the pole to the point and a fixed reference line- the polar axis. However in the following discussions the radial flow is assumed to be axi-symmetric, which means head is independent of angle.

Confined Aquifer

To derive the radial flow equation for a well completely penetrating a confined aquifer the flow is assumed two-dimensional to a well centered on a circular island and penetrating a homogenous and isotropic aquifer. It is shown in Fig. 5.

Because the flow is everywhere horizontal, the Dupit assumptions apply without error. Using plane polar coordinates with the well as the origin, the well discharge Q at any distance r equals

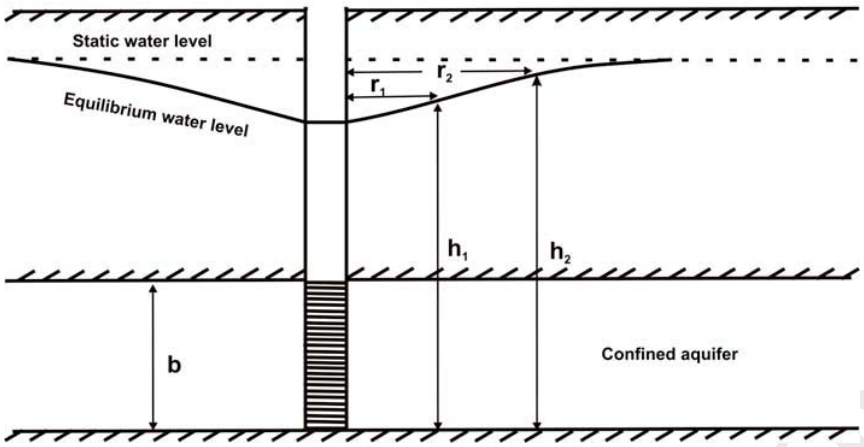

Fig. 5: Steady Radial flow in confined aquifer

$$Q = (2\pi r b) K (\frac{dh}{dr})$$

For steady radial flow to the well. Rearranging and integrating for the boundary conditions at the well at the edge of the island, h_2 and r_2 yields

$$h_2 - h_1 = \frac{Q}{2\pi T} \ln(\frac{r_2}{r_1})$$

Thus, from a theoretical aspect, steady radial flow in an extensive aquifer does not exist because the cone of dipression must expand identifiably with time. However, from a practical standpoint, h_1 approaches h_2 with distance from the well, and the drawdown varies with the logarithm of the distance from the well.

The above equation is known as the equilibrium or Thiem equation, enables the hydraulic conductivity or the Transmissivity of a confined aquifer to be determined from the pumped well. The Transmissivity is given by

$$T = \frac{Q}{2\pi (h_2 - h_1)} \ln(\frac{r_2}{r_1})$$

Unconfined Aquifer

An equation for steady radial flow to a well in an unconfined aquifer also can be derived with the help of the Dupit assumptions as shown in Fig. 6, the well completely penetrates the aquifer to the horizontal base and a concentric boundary of constant head surrounds the well. The well discharge is

$$Q = (2\pi rh)K(\frac{dh}{dr})$$

Which , when integrates between the limits h_1 and h_2 at r_1 and r_2, yields

$$h_2^2 - h_1^2 = \frac{Q}{\pi K}\ln(\frac{r_2}{r_1})$$

And rearranging to solve for the hydraulic conductivity

$$K = \frac{Q}{\pi(h_2^2 - h_1^2)}\ln(\frac{r_2}{r_1})$$

This equation fails to describe accurately the drawdown curve near the well because the large vertical flow components contradict the Dupit assumptions, however, estimates of K for given heads are good. In practice, drawdown should be small in relation to the saturated thickness of the unconfined aquifer.

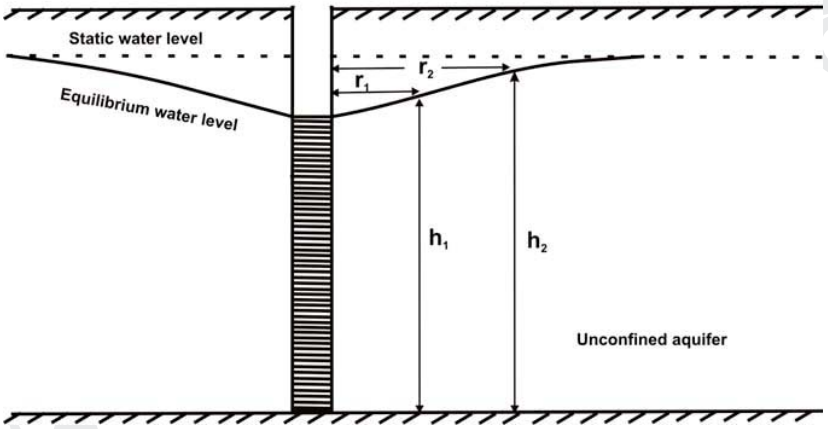

Fig. 6: Steady Radial flow in unconfined aquifer

UNSTEADY RADIAL FLOW

For purpose of analysis, the aquifers that we will consider will be assumed to be isotropic and homogeneous. It will be shown that solutions can be found for cases in which the value of the horizontal conductivity does not depend on the direction of flow in the aquifer.

Confined Aquifer

When well is pumped in a completely confined aquifer, the water is obtained from the

elastic or specific storage of the aquifer. You will recall that the elastic storage is water that is released from storage by the expansion of the water as pressure in the aquifer is reduced and as the pore space is reduced as the aquifer compacts. The product of the specific storage, Ss, and the aquifer thickness is an aquifer parameter called storativity. For a confined aquifer, it is generally small (0.005 or less), and pumpage affects a relatively large area of the aquifer. Further if there is no recharge, the area of drawdown of the potentiometric surface will expand indefinitely as the pumping continues.

We will assume the following conditions in applying the solution: flow is in the range of Darcy's law; water is discharged instantaneously from storage; and the aquifer is homogeneous and isotropic, has a constant thickness and a negligible slope, and is of infinite extent. We will also assume that the pumping well and any observation wells fully penetrate the aquifer (i.e., water can enter at any level from the top to the bottom) and that well diameter is infinitesimal.

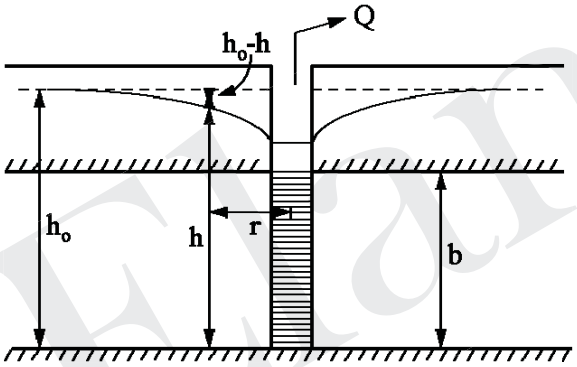

Fig. 7: Fully penetrating well pumping from a confined aquifer

Theis Method

The following equation for confined aquifers was first solved by C.V. Theis on the basis of the analogy between flow of water in an aquifer and flow of heat in a thermal conductor (2). The original level of the potentiometric surface is ho. The solution that Theis developed is

$$h_o - h = \frac{Q}{4\pi T}\int_u^\infty \frac{e^{-u}}{u}du$$

$$h_o - h = \frac{Q}{4\pi T}\left[-0.5772 - \ln u + u - \frac{u^2}{2\cdot 2!} + \frac{u^3}{3\cdot 3!} - \frac{u^4}{4\cdot 4!} + \cdots\right]$$

$$h_o - h = \frac{Q}{4\pi T}W(u) \qquad u = \frac{r^2 S}{4Tt}$$

Q is the constant pumping rate (L_3/T;ft^3/day or m^3/day) h is hydraulic head (L;ft or m) ho is hydraulic head before pumping started (L;ft or m) ho-h is the drawdown (L;ft or m) T is aquifer transmissivity (L_2/T; ft^2/day or m^2/day) t is time since pumping began (T;days) r is radial distance from the pumping well (L; ft or m) s is aquifer storativity (dimensionless) b is aquifer thickness (L; ft or m).

Jacob Straight Line Method

C.E. Jacob observed that after the pumping well had been running for some time, higher values of the infinite series became very small, and the nonequilibrium formula could be closely approximated by

$$h_0 - h = \frac{2.3Q}{4\pi T}\log\left(\frac{2.25Tt}{r^2 S}\right)$$

With consistent units. Equation (1) is valid for very small values of u. if (r^2S)/(4Tt) is less than 0.05,then all values for Equation beyond the first two terms of the infinite series are infinitesimal . Truncating eqn after the second term of the infinite series yield eqn (1) the logarithmic eqn (1) will plot as a straight line on semi logarithmic paper if the limiting condition is met. This may be true for large values of t or small values of r. thus, straight line plots of drawdown versus time can occur after sufficient time has elapsed. In pumping tests with multiple observation wells, the closer wells will meet the conditions before the more distant ones.

In the Jacob straight-line method, a straight line is drawn through the field-data points and extended backward to the zero drawdown axes. It should intercept this axis at some positive value of time (or t/r^2 if there are multiple observation wells). This value is designated t_0 [or (t/r^2)0]. The value of the drawdown per log cycle Δ (ho-h) is obtained from the slope of the graph. With consistent units for the parameters, the values of transmissivity and storativity may be found from the equations

$$T = \frac{2.3Q_w}{4\pi\Delta(H-h)}$$

and $$S = \frac{2.25Tt_0}{r^2}$$

where

Q is the constant rate of pumpage (gallons per minute)

Δ (h_0-h) is the drawdown per log cycle of time (feet)

t is the time since pumping began (minutes)

T is the transmissivity (square feet per day)

r is the distance to the pumped well (feet)

in comparing the Jacob solution with the Theis solution in the preceding problems, we see that the resulting answers are almost the same. As these are graphical methods of solution, there will often be a slight variation in the answers, depending upon the accuracy of the graph construction and subjective judgments in matching field data to type curves.

An aquifer test may be made even if there are no observation wells. In this case, drawdown must be measured in the pumping well. There are energy losses as the water rushes into the well, so that the head in the aquifer is higher than the water level in the pumping well. For this reason, aquifer storativity cannot be determined. However, a plot of drawdown versus time for the pumping well can be used to determine aquifer transmissivity. Either the theis or Jacob method can be used. It is important that the well be pumped at a constant rate, as any slight fluctuations will immediately affect the water level in the well. Likewise, drawdown data for the start of pumping are affected by the volume of water stored in the well casing. At the start of pumping, the water comes from the well casing rather than from the aquifer, especially when the well diameter is large and/or the pumping rate is small. The measured drawdown data should be adjusted to compensate for this factor.

Chow Method

Chow developed a method of solution with the advantages of avoiding curve fitting and being unrestricted in its application. Again, measurements of drawdown in an observation well near a pumped well are made. The observational data are plotted on semilograthmic paper in the same manner as for the cooper-Jacob method. On the plotted curve, choose an arbitrary point and note the coordinates, t and s. next, draw a tangent to the curve at the chosen point and determine the drawdown difference Δs, in feet, per log cycle of time. Compute F (u) from

$$F(u) = s/\Delta s$$

And find the corresponding values of W (u) and u from the curve.

Unconfined Aquifer

Water is derived from storage in water-table aquifer by vertical drainage of water in the pores. This drainage results in a decline in the position of the water table near a pumping well as time progresses. In the case of a confined aquifer, although the potentiometric surface declined, the saturated thickness of the aquifer remained constant. In the case of an unconfined aquifer, the saturated thickness can change with time. Under such conditions, the ability of the aquifer to transmit water- the transmissivity – changes, as it is the product of the conductivity K and the saturated thickness h (assuming that h is measured from the horizontal base of the aquifer).

DERIVATION FOR OF GENERAL GROUNDWATER FLOW EQUATION

Derivation Based on the Principles of Thermodynamics and Darcy's law, the main equations of ground-water flow can be derived.

Consider a small volume of the aquifer, called a Control volume. The three sides are of length dx,dy and *dz* respectively. Area of the faces normal to the x-axis is dydz; Area of the faces normal to the z-axis is dxdy. Assume that the aquifer is homogeneous and isotropic. The actual fluid motion can be subdivided on the basis of the components of flow parallel to the three principle axes.

Fig. 8: Control volume for flow through a confined aquifer

The inflow and outflow components in the X direction can be stated as

$$q_{x,i} = -T_z W\left(\frac{\partial h}{\partial x}\right)_i \text{ and } q_{z,o} = -T_z W\left(\frac{\partial h}{\partial x}\right)_o$$

Where Tx is the Transmissivity in the x direction, W is the length of a side of the square, (δh/δx)I and (δh/δx)o define the hydraulic gradient at the entry and exit faces of the element, respectively. The flow rate or released in the element as a result of these flows, by continuity, equals

$$\left(q_{x,i} - q_{x,o}\right) + \left(q_{y,i} - q_{y,o}\right) = -SW^2 \frac{\partial h}{\partial t}$$

Where S is storage coefficient. It follows that

$$-T_x \frac{\left(\frac{\partial h}{\partial x}\right)_i - \left(\frac{\partial h}{\partial x}\right)_o}{W} - T_y \frac{\left(\frac{\partial h}{\partial y}\right)_i - \left(\frac{\partial h}{\partial y}\right)_o}{W} = -S\frac{\partial h}{\partial t}$$

If the value of W becomes infinitesimally small, the derivatives on the left hand side become the second derivatives of h, so

$$T_x \frac{\partial^2 h}{\partial x^2} + T_y \frac{\partial^2 h}{\partial y^2} = S\frac{\partial h}{\partial t}$$

This is the general partial differential equation for unsteady flow of groundwater in the horizontal direction.

For these dimensions, employing an elemental cube rather than a square, it can be shown that

$$K_x \frac{\partial^2 h}{\partial x^2} + K_y \frac{\partial^2 h}{\partial y^2} + K_z \frac{\partial^2 h}{\partial z^2} = S_s \frac{\partial h}{\partial t}$$

Where Ss is the specific storage, defined as the volume of water a unit volume of saturatd aquifer releases from storage for a unit decline in hydraulic head

If the flow is steady, $\delta h/\delta t = 0$; therefore,

$$K_{xx} \frac{\partial^2 h}{\partial x^2} + K_{yy} \frac{\partial^2 h}{\partial y^2} + K_{zz} \frac{\partial^2 h}{\partial z^2} = 0$$

And for homogenous and isotropic aquifers, the above equation reduces to

$$\frac{\partial^2 h}{\partial x^2} + \frac{\partial^2 h}{\partial y^2} + \frac{\partial^2 h}{\partial z^2} = \frac{0}{K}$$

Which is the Laplace equation for potential flow.

Radial coordinates. For axisymmetric groundwater flow to wells, radial coordinates are preferable. In a homogenous and isotropic aquifer, it can be shown

$$h \frac{\partial^2 h}{\partial r^2} + \frac{h}{r} \frac{\partial h}{\partial r} = \frac{S}{K} \frac{\partial h}{\partial t}$$

Where r is the radial co ordinate from the well. And for steady flow this reduces to

$$\frac{\partial^2 h}{\partial r^2} + \frac{1}{r} \frac{\partial h}{\partial r} = 0$$

REFERENCES

[1] Anderson, M.P. and Woessner, W.W., (1992), "Applied groundwater modelling", Academic press, Newyork.

[2] Fetter, C.W., (1992), "Applied hydrogeology", Prentice hall

[3] Rushton, K.R. and Redshaw, (1979), "seepage and groundwater flow", Mc Graw Hill publishing Company, London.

[4] Todd, D.K., 1980. Groundwater hydrology, second edition John Wiley and Sons, New York. 535 p.

[5] Wang, H.F. and Anderson, M.P., (1982), "Introduction to Groundwater Modelling", Academic press, Newyork.

Numerical Simulation of Groundwater Flow and Solute Transport, L. Elango (ed). pp.15-28

Groundwater Modelling - An Emerging Tool for Groundwater Resource Management

A.K. Sinha

INTRODUCTION

Models are tools used in science to approximate natural phenomena. These models are applied to a variety of environmental issues and are particularly useful for interpreting and understanding the environmental issues having complex interaction of many variables in the system.

The use of aquifers is increasing both as a source of water supply and a medium for storing various hazardous wastes. Today a global withdrawal of 600-700 km^3/a (cubic kilometers per year) makes groundwater the world's most extracted raw material (IAH 2003). The increasing dependence on and dwindling groundwater resources has led to search for an appropriate scientific management skill. Groundwater modelling has emerged as an acceptable tool to support decision making process in groundwater management towards sustainability of Groundwater resources.

WHY DO WE NEED MODELLING STUDIES

It is not possible to see into the sub-surface, and observe the geological structure and the groundwater flow processes. The best we can do is to construct bores, use them for pumping and monitoring, and measure the effects on water levels and other physical aspects of the system. It is for this reason that groundwater flow models have been, and will continue to be, used to investigate the important features of groundwater systems, and to predict their behavior under varied conditions. Models also form an integral part of decision support systems in the process of managing water resources, salinity, drainage, and contaminant transport and should not be regarded as just an end point in themselves. The development and evaluation of resource management strategies for sustainable water allocation, and for control of land and water resource degradation, are heavily dependent on groundwater model interpretation and predictions. Regional scale groundwater flow modelling studies are commonly used for water resource evaluation and to help quantify sustainable yields and allocations to end-users.

GROUNDWATER MODELLING

Groundwater modelling involves simulation of aquifer and its response to various input /output systems. Groundwater Models have been applied to investigate a wide variety of hydrogeologic conditions**.** More recently, groundwater models are being applied to predict

the fate and transport of contaminants for risk evaluation. The use of groundwater models to simulate groundwater flow and contaminant transport has greatly increased over the past decade. Groundwater models represent or approximate a real system and are tools that help in the organization and understanding of hydrogeologic data or the prediction of future hydrogeologic events. Models are not a substitute for field investigations, but should be used as supplementary tools. Results are dependent on the quality and quantity of the field data available to define input parameters and boundary conditions (Wang and Anderson, 1982).

Model Classification

Groundwater modelling helps in analysis of many groundwater problems. In general, models are classified as **Predictive, Interpretive and Generic types**. Predictive model is used to understand the future availability of resources as well as aquifer responses under varied scenario and stress situation. Interpretive models are used to understand a system under different existing domain element such as how a system respond to different fracture densities or aperture widths and How a system would responds recharge from a flood event ? Generic type model helps in hypothesizing the situation. No calibration is required in case of such models.

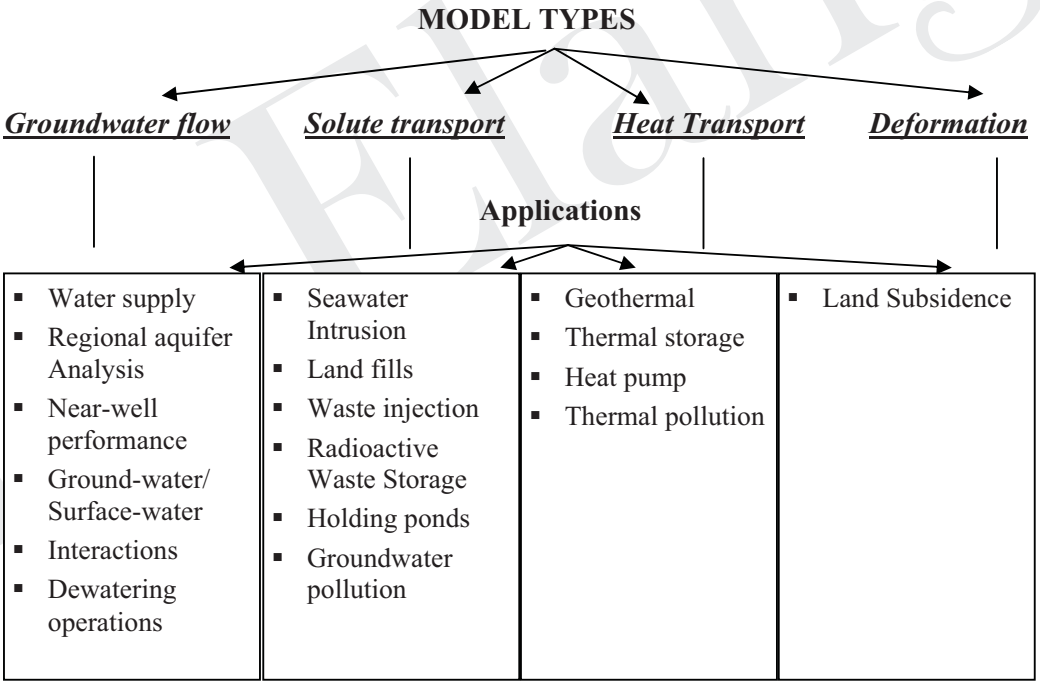

Fig. 1: Types of ground-water models and typical applications

Further, on the basis of applications **four general types of groundwater models** are identified (Fig. 1). The problem of water supply is normally described by one equation, usually in terms of hydraulic head. The resulting model providing a solution for this equation is referred to as a ***groundwater flow model***. If the problem involves water quality, then an additional equation(s) to the groundwater flow equation must be solved for concentration(s) of the chemical species(s). Such a model is referred to as a ***solute transport model***. Problems involving heat also require an equation, similar to the solute transport equation, but now in terms of temperature. This model is referred to as a ***heat transport model***. Finally, a ***deformation model*** combines a groundwater flow model with a set of equations that describe aquifer deformation. All of the models start with the basic equations of groundwater flow **(**Fetter, 1994).An example of groundwater flow equation to describe flow in a an unconfined aquifer is given by

$$\frac{\delta^2 h}{\delta x^2} + \frac{\delta^2 h}{\delta y^2} = \frac{S}{T}\frac{\delta h}{\delta t}$$

Groundwater flow models have been most extensively used for such problem as regional aquifer studies, groundwater basin analysis and near well performance. More recently, solute transport models have been used to aid in understanding and predicting the efforts of problems involving hazardous wastes. Some of the applications include sea-water intrusion, underground storage of radioactive wastes, movements of leachate from sanitary landfills, groundwater contamination from holding ponds, and waste injection through deep wells. Heat transport models have been applied to problems concerning geothermal energy, heat storage in aquifers, and thermal problems associated with high-level radioactive waste storage. Deformation models have been used to examine field problems where fluid withdrawal has decreased pressures and caused consolidation. This compaction of sediments results in subsidence at the land surface.

The classification of groundwater models is by no means complete. Models may be further subdivided into those describing porous media and those describing fractured media. Large numbers of models have come up to resolve diverse type of hydrogeological problems. One of the recent works (Thangarajan 2004) used Technique, Aquifer type and the dimension of the problem as basis for the classification of the model (Table 1).

However the survey of the literature reveals that it is techniques which has been used most and suitably modified to an applicable in diverse type of hydrological and hydrogeological situations. Therefore it would be pertinent to discuss briefly here only those models which are technique based.

Physical Scale Model is made from the same material as those of the natural system . Sand Models have been used for different type of hydrogeological studies such as dispersion,

artificial recharge and seawater intrusion etc (Kimbler 1970; Peter Y 1970; James and Rubin 1972)

Table 1: Classification of Models (Thangarajan 2004)

1. Model- Aquifer Type	2. Model - Dimensional Type	3. Model- Techniques Type	4. Model-Problem (Flow-Conditions) Type
▪ *Unconfined Aquifer Model* ▪ *Semiconfined Aquifer(Leaky) Model* ▪ *Confined Aquifer*	▪ *1-D (one-dimensional model)* ▪ *2-D(two dimensional model)* ▪ *3-D (three dimensional model)* ▪ *Multi layer (Leaky)model*	▪ *Physical Model* ▪ *Analog Model* ▪ *Mathematical Model*	▪ *Saturated GW Flow Model* ▪ *Unsaturated GW Flow Models* ▪ *Solute Transport Models*

Analog Model may be developed using electrical circuits or viscous fluid flow as the governing equations of groundwater flow through porous media is similar to the flow of electricity through conductor .Two –dimensional groundwater flow can be analogous to the flow of a viscous fluid between two very closely spaced parallel plates. The model is known as Hele-Shaw model.

However all analog model and Scale model have definite disadvantages with regard to their flexibility, scale, Storage and economy.

Mathematical Models

The translation of the physics is done into mathematical terms that are to make appropriate simplifying assumptions and develop the governing equation. This constitutes the mathematical model. Mathematical models are used to simulate the components of the conceptual model and include a single equation or set of governing equations that represent the process (es) occurring (e.g., groundwater flow, solute transport, etc.). The mathematical models rely upon the solution of the basic equations of groundwater flow, heat flow and mass transport. The most simple mathematical model of groundwater flow is Darcy's law. Darcy's law is an example of an Analytical **Model.**

The mathematical model for groundwater flow consists of a partial differential equation together with appropriate boundary and initial conditions that express conservation of mass and that describe continuous variables (for example, hydraulic head) over the region of interest. In additions, it entails various phenomenological "laws" describing the rate processes active in the aquifer. An example is Darcy's law for fluid flow through porous media; this is generally used to express conservation of momentum. Finally, various assumptions may b invoked such as those of one or two-dimensional flow and artesian or water table conditions.

Once the mathematical model is formulated, the next step is to obtain a solution using one of two general approaches. The groundwater flow equation can be simplified further for example, assuming radial flow and infinite aquifer extent, to form a subset of the general equation that is amenable to analytical solution. The equations and solutions of this subset are referred to as analytical models. The familiar theis type curve represents the solution of one such analytical model.

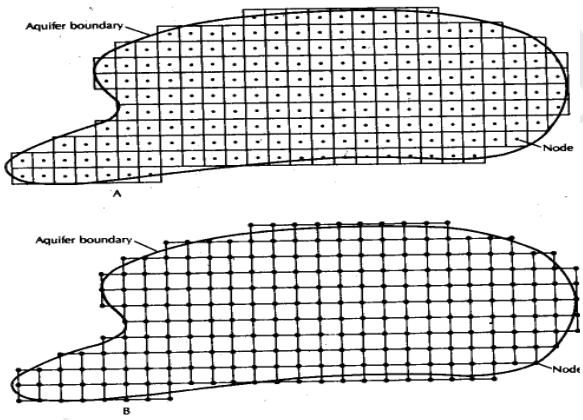

Fig. 2A and Fig. 2B: Block- Centered Finite difference grid and Mesh centered Finite difference grid

Alternatively, for problems where the simplified analytical models no longer describe the physics of the situation **Numerical Modelling** is used to approximate the partial differential equations, for example, with **Finite-difference techniques** or with the **Finite-element method** (Anderson and Woessner, 1992). In so doing, one replaces continuous variable with discrete variables that are defined at grid blocks (or nodes). Figures (Fig. 2) show Two variations of Finite –Difference grid(Fig. 2A & 2B) are Block-Centered Finite difference grid (Fig. 2A) and Mesh Centered Finite difference grid (Fig. 2B) .Associated with the grid are node points where the equations are solved to obtain unknown values . Transmissivity and storativity values associated with at each nodes are known. A block – Centered grid is one where the node points fall in the center of the grid, a mesh Centered has

the node points at the intersection of grid lines. The choice of whether to use a block – centered or a mesh –centered grid depends upon the boundary conditions. A block centered grid is most useful when a flux is specified across a boundary, and a mesh-centered grid is most convenient for situations where the head is specified at the boundary.

The basic grid is regular with rows and column at right angle to each other and the distance in x direction Δx being equal to Δy in y direction. Special notations are used to describe the positions of the nodes in the finite-difference grids. Fig. 3 shows a finite – difference grid centered on (xy). Adjacent points on the grid are located at a distance Δx away to the right or left and Δy away up nor down; x is positive to the right and y is positive downward.

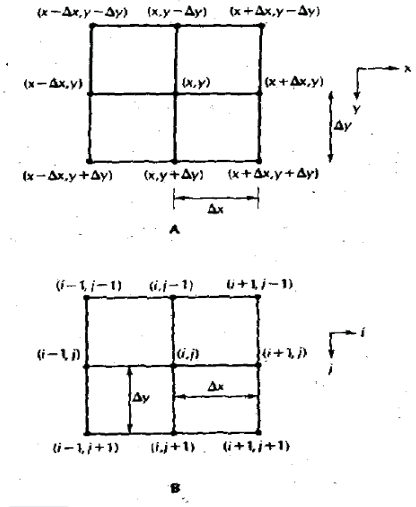

Fig. 3: Finite- Difference grid centered on (xy)

In the computer codes the locations of the nodes are designated with reference to node ij where i represent the column and j represents the row. The notation for i is positive to the right and for j it is positive downward .Thus the row above the j row is row j-i and the row below the j row is j+1. The column to the left of column i is column i-1 and the column to the right of column i is i+1.

Finite –element models offer an alternative approach to the numerical modelling of groundwater flow. In this model the aquifer is divided into polygonal cells typically triangular (Fig. 4) rather than rectangular as in Finite-difference model. The triangles intersect at the nodes that represent the points at which the unknown values such as heads will be computed .The value of the head in the interior of each cell is determined by interpolation between the nodal points.

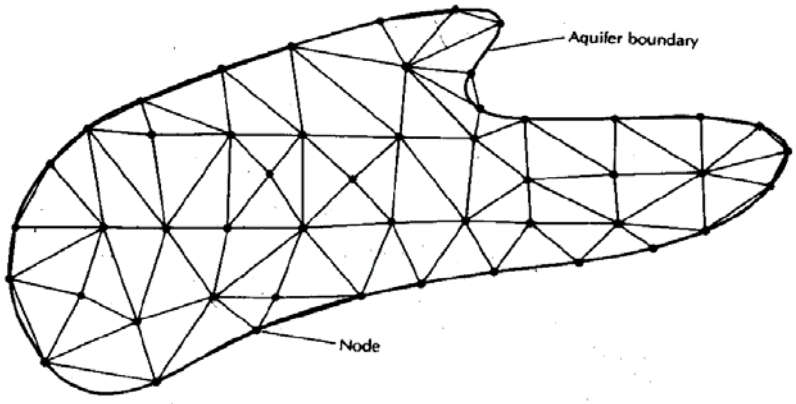

Fig. 4: Mesh with Triangular elements

Depending upon the Numerical technique(s) employed in solving in the mathematical model , there exist several types of numerical models such as Finite –difference Models, Finite Element Models, Boundary –element models, Particle tracking models, Method of characteristic models, random walk models and Integrated Finite –difference Models

The main features of the various numerical models are:

- The solution is sought for the numerical values of state variables only at specified points in the space and time domains defined for the problem (rather than their continuous variations in these domains)
- The partial differential equations that represent balances of the considered extensive quantities are replaced by a set of algebraic equations (written in terms of sought, discrete values of the state variables at the discrete points in space and time)
- The Solution is obtained for a specified set of numerical values of the various model coefficients (rather than as general relationship in terms of these coefficients)
- Because of the large number of equations that must be solved simultaneously, a computer program is prepared.

Although a number of numerical techniques exist, only finite-difference and finite-element techniques have been widely used (Anderson and Woessner, 1992).

Recently, a number of groundwater flow models have come into popular uses that are based on the Analytic element technique (Strack, 1989). This technique applies specific analytical solutions to various "elements" in an aquifer, such as streams, lakes, wells, and areas of recharge. The individual solutions then are superposed to obtain a solution (of hydraulic head) for any location. One attractive feature of this technique is its lack of a fixed grid, which allows the user to extend the model any distance to incorporate regional features

without sacrificing accuracy in the area of interest. However, the method's applicability currently is limited to steady-state, two-dimensional groundwater flow regimes.

Stochastic model: This approach utilizes hydraulic parameters having a probability distribution that results in all output having the same probability distribution. This method characterizes parameter uncertainty by incorporating uncertainty into the parameters and database utilized in the simulations.

BASIC INFORMATION

Groundwater modelling requires the following basic information:

- physical units
- model domain
- aquifer parameters
- time varying inputs
- boundary conditions

Physical Units

The physical units used to define aquifer parameters must be consistent within the model. For example, the following lists of units are consistent:

length	=	metres (m)
time	=	days (d)
flow rate	=	metres^3/day (m^3/d)
transmissivity	=	metres^2/day (m^2/d)

All input forms specify generic units for the input parameter in the terms of:

- L - length
- t - time
- M - mass

These generic units will be having superscripts indicating the degree of each generic unit. For example, flow rate, $q= L^3/t$

Model Domain

The model domain is the area of interest that is to be modelled. *Model Domain is* defined using a variable or regular grid. The grid divides the model domain into rectangular blocks or elements. The modeler specifies the aquifer properties for each block or element in the grid.

Aquifer Parameters

Aquifer parameters quantitatively describe the physical characteristics of aquifers, aquitards and aquicludes. For groundwater and solute transport models the following parameters are specified:

Transmissivity (KD or T) – It is the product of the average hydraulic conductivity K and the thickness of the aquifer D. It is also known as the capability of an aquifer to transmit water; having units L^3 / Tx L = L^2/T. and is expressed in m2/d or m2 /s. This parameter can range from 0 to greater than 10 000 m^2/day.

Hydraulic conductivity (K) - is the ability of a porous medium to allow water to flow; L/T. The range is typically between 10^{-5} and 10^6 m/day.

Storativity (s) - is the volume of water released or stored in an aquifer, over a unit area, for a unit change in head. Storativity is dimensionless and only applies to confined aquifers. The range is typically between 10^{-6} and 10^{-3}. Storativity is also known as the storage coefficient. It is defined as

$S_s=\gamma_w(\alpha + n\beta)$

- ***Specific yield*** - the volume of water that will drain from a unit volume of unconfined aquifer. This parameter is dimensionless and has a range between 0 and 1. For most geological materials the parameter is less than 0.5.

  $Sy = (1/A)dV/dh$

- ***Aquifer thickness*** - the vertical extent of a geological formation which contains, and can transmit water having units L. For a confined aquifer it is equal to the formation thickness. For an unconfined aquifer is equal to the saturated thickness.
- ***Static water level*** - the water level measured in a well or piezometer when the aquifer is not under stress (i.e. pumping or flowing) having units L. You will most often use static water levels as initial conditions to start the model.

Time Varying Inputs

- ***Pumping wells*** - locations defined within the model domain and where water is injected or abstracted from an aquifer having units L3/t. The magnitude of abstraction or injection generally varies with time.
- ***Observation wells*** - locations defined within the model domain at which heads are recorded. Generally the heads correspond to piezometers or monitoring wells at which water level measurements have been recorded in the field. They can also be locations of interest to the modeller, such as a *property* boundary.

Boundary Conditions

Boundary conditions specify how an aquifer interacts with the environment outside the model domain. To ensure a unique solution to a problem specify at least one unique boundary condition is specified. There are four basic types of boundary conditions:

No Flow Boundaries

There is physical or hydrological barriers that prevent water from flowing into or out of the model domain. No flow boundaries are specified either when defining the boundary of the model grid or by setting grid blocks as inactive (i.e. hydraulic conductivity = 0). This is in fact a very special type of the prescribed flux boundary and is also referred to as No-flux, Zero –Flux, impermeable, reflective or barrier boundary. In the analysis of model results, no-flow boundaries are identical to streamlines. The natural groundwater divides or streamlines act as No –Flow boundaries.

Constant Head Boundary

A source of water that has an invariant water level at the model boundary. This condition is used to model an aquifer in good communication with a lake, large river or another external aquifer. This is also known as a first type boundary condition which is mathematically referred as **Dirichlet** boundary. The constant head boundary or prescribed head boundaries can occur when surface water bodies such as rivers, lakes, canals, seacoast, impondments and drains interact freely with the aquifer.

Mathematically, boundary condition are stated as

$h(x) = h_o(x), \quad x \in \delta\Omega_1$ **Dirichlet**

where h_o is the specified head along the boundary segment $\delta\Omega_1$ of the modelled domain Ω

Constant Flux Boundary

*E*ntering or leaving the aquifer is constant/prescribed flux. This boundary condition is used to simulate rainfall, or distributed discharge such as evaporation. It is also useful for specifying known recharge to the aquifer due to induced recharge or reticulation. This boundary condition is also referred to as second type boundaries, Neumann's condition or recharge boundaries.

$\delta h(x) / \delta n \quad === \quad \delta h(x)/ \delta n /_0 , \quad x \in \delta\Omega_2$ **Neumann**

where $\delta h(x)/ \delta n/o$ is the specified outward normal gradient to the boundary segment $\delta\Omega_2$

Stream or River Head Dependent Boundary

The rate of water flow into or out of the aquifer is a function of the aquifer head, elevation of stream bed, and the **leakage** between the aquifer and the stream or river. This condition is used to model streams or small rivers in poor connection with the aquifer, upward leakage in artesian aquifers, drains and overlying aquitards. This is also known as third type boundary condition, mixed or Induced Flux or mathematically Cauchi Condition/Robbins Conditions.

$\alpha h(x) + \beta \quad \delta h(x)/\delta n = C_{0,} \quad x \quad \in \delta \Omega_3$ **Cauchi/Robbins**

where $C_{0\ is}$ specified function value along the boundary segment $\delta\Omega$ and α and β are specified functions

GENERALIZED MODELLING APPROACH

Though details of modelling process is depicted here (Fig. 5) through flow chart (Fig. 6) Anderson, M.P. and Woessner, W.W. 1992 and Spitz & Moreno 1996), a brief generalised approach consists of

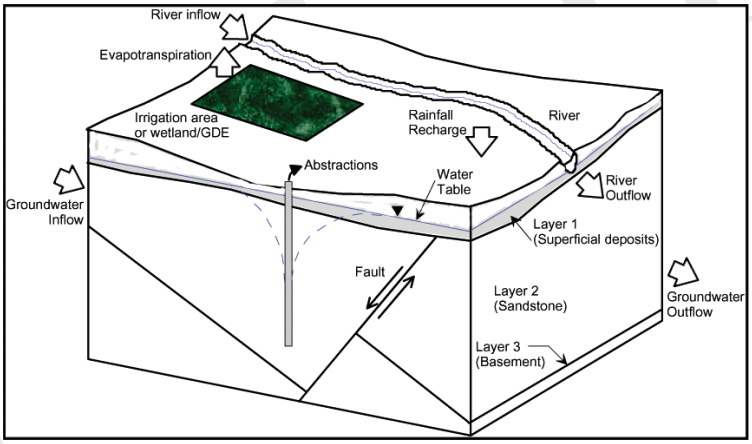

Fig. 5: Typical Block diagram type Conceptual Model

- The development of a conceptual model.
- Creation of the model and execution of various trials.
- Evaluation of the model results.
- The compilation of new data.
- Validation testing depending on the success of the calibration

However the development of conceptual framework is the most important step in the direction of modelling

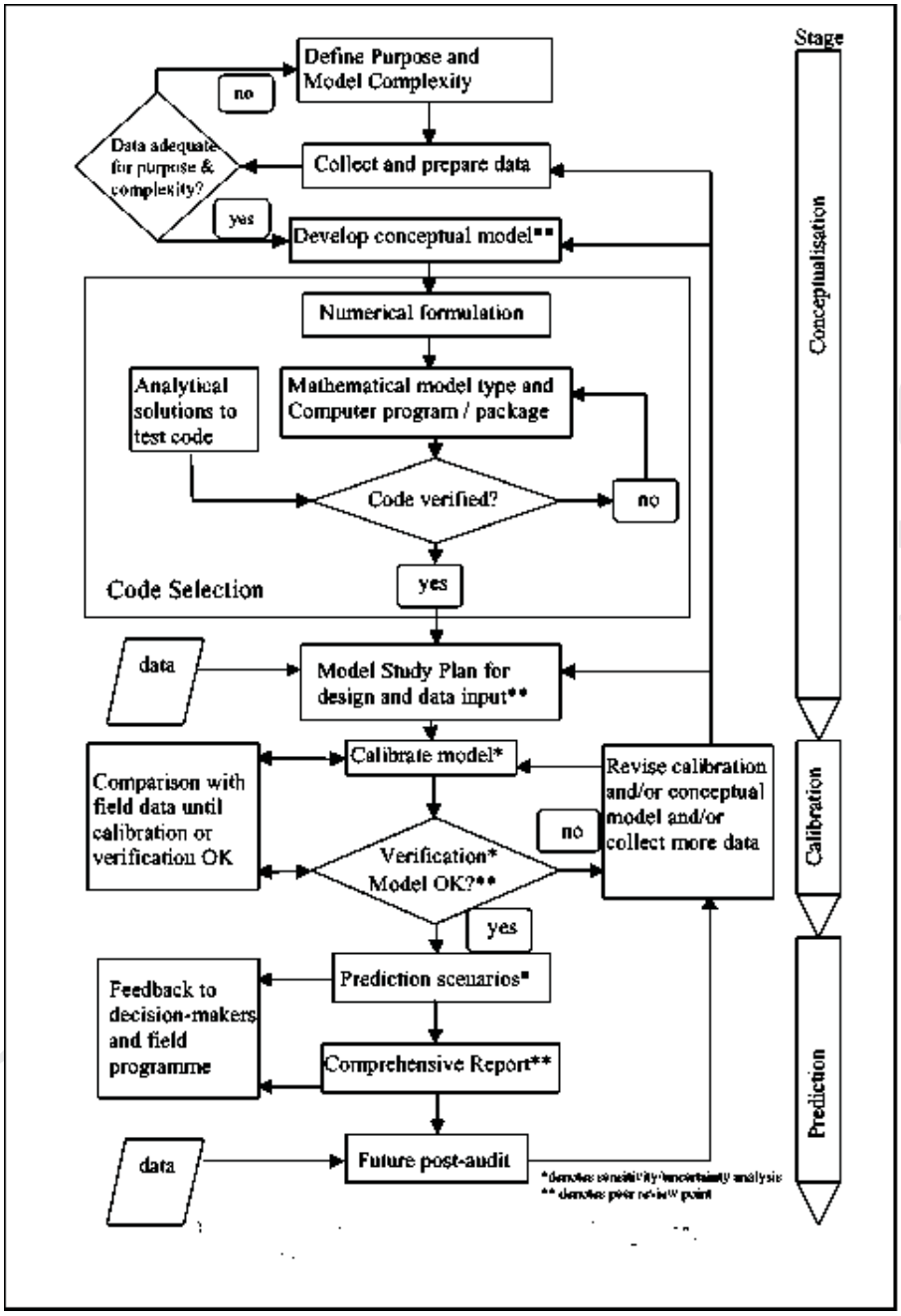

Fig. 6: The groundwater modelling Process

MODEL APPLICATION

Models are useful for reconnaissance studies preceding field investigations for interpretive studies following the field program, and for predictive studies in estimating future field behaviour. In addition to these applications, models are useful for studying various types of flow behaviour by examining hypothetical aquifer problems.

Few Important Areas of Application are

- Predict groundwater level changes for proposed developments and large-scale production wells
- Define wellhead protection areas for municipalities and water utilities
- Design effective storm water infiltration systems
- Show the effect from different types of land application systems
- Predict the effect on stream flow of land use changes
- Help to create better development design for groundwater protection
- Evaluation of regional groundwater resources.
- Tracking the migration of groundwater contamination.
- Evaluation of design of hydraulic containment and pump-and-treat systems
- Design of groundwater monitoring networks
- Prediction of the possible fate and migration of contaminants for risk evaluation

MODEL MISUSE AND MISTAKES

There are a variety of ways to misuse models (Prickett, 1975). The common and related ones are overkill, inappropriate prediction, and misinterpretation. The temptation to apply most sophisticated computational tool to a problem is difficult to resist. The following is a list of common misuses and mistakes related to groundwater flow modelling (Bear et al., 1992):

- **Improper conceptualization of the considered problem**
  - Wrong assumptions related to the significant processes, especially in cases of contaminant transport. These may include the type of sink/source phenomena, chemical and biological transformations, fluid-solid interactions, etc.
  - Selecting a model that involves coefficients that vary in space, but for which there are insufficient data for model calibration and parameter estimation.
  - Improper delineation of the model's domain.
  - Wrong selection of model geometry: a 2-D horizontal model, or a 3-D model.
  - Improper selection of boundary conditions.
  - Wrong assumptions related to homogeneity and isotropy of geologic material.

- **Selection of an inappropriate code for solving the model**
  - Code is more powerful/versatile than necessary.
  - Code is less powerful/versatile than necessary.
  - Code has not been verified and tested.

- **Improper model application**
  - Selection of improper values for model parameters and other input data.
  - Misrepresentation of aquitards in a multi-layer system.
  - Mistakes related to the selection of grid size and time steps.
  - Making predictions with a model that has been calibrated under different conditions.
  - Making mistakes in model calibration and other history matching.
  - Improper selection of computational parameters (closure criterion, etc.).

- **Misinterpretation of model results**
  - Mass balance is not achieved.
  - Applying the model beyond its true predictive capabilities.

REFERENCES

[1] Anderson, M.P. and Woessner, W.W., (1992). Applied Groundwater Modelling-Simulation of Flow and Advective Transport. Academic Press. San Diego, California.

[2] Bear J.,Beljin, M.S., and Ross, R.R., (1992). Fundamentals of Ground-Water Modelling. U.S. EPA.

[3] Fetter, C.W., (1994). Applied Hydrogeology, Third Edition. MacMillan College Publishing Company, New York.

[4] IAH, (2003). Groundwater-Development to Management presented at the 3rd World Water Forum, Japan

[5] James, R.V. and Rubin, J., (1972). Accounting for Apparatus –Induced Dispersion in Analysis of Miscible Displacement Experiments" Water Resource Research 8 717-21.

[6] Kimbler, O.K., (1970). "Fluid Model Studies of the Storage of Freshwater in Saline Aquifers" Water Resources Research 6, 1522-27.

[7] Peter, Y., (1970). "Model Tests for a horizontal Well "Groundwater 8 No. 5 30-34.

[8] Prickett, T.A., (1975). Modelling Techniques for Groundwater Evaluation. In: V.T. Chow (Editor) Advances in Hydroscience. Vol. 10. Academic Press New York.

[9] Thangarajan, M., (2004). Regional Groundwater Modelling, Capital Publishing Company pp. 20-21 New Delhi.

[10] Wang, H.F. and Anderson, M.P., (1982). Introduction to Groundwater Modelling-Finite Difference and Finite Element Methods. W.H. Freeman and Company. San Francisco, California.(Relocated to Salt Lake City, Utah.).

Numerical Simulation of Groundwater Flow and Solute Transport, L. Elango (ed). pp.29-40

Finite Difference Solution of Partial Differential Equations

P. Ganesan

INTRODUCTION

When using a finite-difference technique to solve a PDE (plus associated boundary and initial conditions), a network of *grid points* is first established throughout the region of interest occupied by the independent variables. Suppose, for example, we have two distance coordinates x and y, and time t as independent variables, and that the respective grid spacings are Δx, Δy, and Δt. Subscripts, i, j and n may then be used to denote that space point having coordinates $i\Delta x$, $j\Delta y$, $n\Delta t$, also called the grid-point (i, j, n). Let the exact solution to the PDE be $u = u(x,y,t)$, and let its approximation, to be determined at each grid point by the method of finite differences, be $v_{i,j,n.}$ We also use $u_{i,j,n}$ to denote the exact solution $u(i\Delta x, j\Delta y, n\Delta t)$ at a particular grid-point (i, j, n).

The partial derivatives of the original PDE are then approximated by suitable finite-difference expressions involving Δx, Δy, Δt, and the $v_{i,j,n.}$ whose values may then be determined. By making the grid spacings sufficiently small, it is hoped that $v_{i,j,n}$ will become a sufficiently close approximation to $u_{i,j,n}$ *at* any grid-point (i,j.n).

EXAMPLES OF PARTIAL DIFFERENTIAL EQUATION

The following PDEs, several of which bear obvious similarities are typical of those of practical importance to the engineer. The symbol ∇^2 denotes the Laplacian operator.

Unsteady Heat-conduction Equation

One-dimensional unsteady heat conduction in a rod is governed by

$$\frac{\partial}{\partial x}\left(k\frac{\partial T}{\partial x}\right) = \rho c_p \frac{\partial T}{\partial t},$$

where T denotes temperature, and k, ρ and c_p are the thermal conductivity, density, and specific heat of the rod. If k is constant, this equation may be rewritten as $\alpha\partial^2T/\partial x^2 = \partial T/\partial t$, in which $\alpha = k/\rho c_p$ is the thermal diffusivity. The introduction of new variables $X = x/L$ and $\tau = \alpha t/L^2$ where L is a characteristic dimension, leads to $\partial^2T/\partial X^2 = \partial T/\partial\tau$. A similar equation governs the interdiffusion of two substances.

Vorticity Transport Equation

The vorticity ζ of an incompressible fluid in two-dimensional motion varies according to

$$\frac{\partial \zeta}{\partial t} + u \frac{\partial \zeta}{\partial x} + v \frac{\partial \zeta}{\partial y} = \upsilon \nabla^2 \zeta$$

where u and v are the x and y velocity components, and v is the kinematic viscosity.

Poisson's Equation

Poisson's equation is $\nabla^2 \psi = -\sigma$. Three important applications occur: (a) in fluid dynamics, with ψ = stream function and σ = vorticity, (b) in electrostatics, with ψ = electric potential and σ = ratio of charge density to dielectric constant, and (c) in elasticity, with $\sigma = 2$, ψ is a function from which the angle of twist of a cylinder under torsion can be calculated.

Laminar Flow Heat – Exchanger Equation

The following equation governs variations of temperatures T with radial and axial distances r and z for steady, laminar flow in a cylindrical heat exchanger :

$$\frac{\partial^2 T}{\partial r^2} + \frac{1}{r}\frac{\partial T}{\partial r} + \frac{\partial^2 T}{\partial z^2} = \frac{\rho u c_P}{k} \frac{\partial T}{\partial z}$$

Here, ρ, c_P and k are the density, specific heat, and thermal conductivity of the fluid, and the axial velocity u is a known function of r. Note how the character of the equation changes if the term $\partial^2 T/\partial z^2$, corresponding to axial conduction, can be neglected.

Telephone Equation

The following equation can be used to predict variations of voltage V along a transmission cable.

$$\frac{\partial^2 V}{\partial x^2} = LC \frac{\partial^2 V}{\partial t^2} + (RC + GL) \frac{\partial V}{\partial t} + RGV .$$

Here, R and L denote the resistance and inductance per unit length of the cable, and C and G denote the capacitance and conductance to ground per unit length of the cable.

Wave Equation

The angle of twist ϕ at any section of a circular shaft undergoing torsional vibrations is governed by

$$\frac{\partial^2 \phi}{\partial t^2} = \frac{G}{\rho} \frac{\partial^2 \phi}{\partial x^2},$$

where G is the rigidity modulus of the shaft and ρ is its density.

Biharmonic Equation

The transverse deflection w of a thin plate of flexural rigidity D subject to a normal load q per unit area is governed by $\nabla^4 w = q/D$.

Vibrating Beam Equation

The transverse deflection y of a vibrating beam obeys

$$\frac{\partial^2 y}{\partial t^2} + \frac{EI\partial^4 y}{A\rho\partial x^4} = 0,$$

in which E = modulus of elasticity, I = cross-sectional moment of inertia, A = cross-sectional area, and ρ = density.

Ion-exchange Equation

For a flow of a solution through a packed column containing an ion-exchange resin,

$$\upsilon \frac{\partial c}{\partial x} + \varepsilon \frac{\partial c}{\partial t} + r = 0.$$

Here, c = concentration of a particular ion in solution, r = rate at which that ion is adsorbed per unit volume of column, ε = bed void fraction, and υ = superficial liquid velocity. A similar type of equation governs regenerative heat transfer.

THE APPROXIMATION OF DERIVATIVES BY FINITE DIFFERENCES

Here, suppose for simplicity that u = u(x,y). Assuming that u possesses a sufficient number of partial derivatives, the values of u at the two points (x,y) and (x + h, y + k) are related by the Taylor's expansion :

$$\begin{aligned} u(x + y,\ y+k) &= u(x, y) + \left(h \frac{\partial}{\partial x} + k \frac{\partial}{\partial y} \right) u(x, y) \\ &\quad + \frac{1}{2!} \left(h \frac{\partial}{\partial x} + k \frac{\partial}{\partial y} \right)^2 u(x, y) + ... \\ &\quad + \frac{1}{(n-1)!} \left(h \frac{\partial}{\partial x} + k \frac{\partial}{\partial y} \right)^{n-1} u(x, y) + R_n, \end{aligned} \tag{1}$$

where the remainder term is given by

$$R_n = \frac{1}{n!}\left(h\frac{\partial}{\partial x} + k\frac{\partial}{\partial y}\right)^n u(x+\xi h,\ y+\xi k), \quad 0 < \xi < 1 \tag{2}$$

That is,

$$R_n = O[(|h| + |k|)^n] \tag{3}$$

By (3), we mean there exists a positive constant M such that $|R_n| \leq M(|h| + |k|)^n$ as both h and k tend to zero.

The space point (i Δx, jΔy), also called the grid-point (i,j), is surrounded by the neighbouring grid points shown in Fig. 1. Expanding in Taylor's series of $u_{i-1,j}$ and $u_{i+1,j}$ about the central value $u_{i,j}$, we obtain

$$u_{i-1} = u_{i,j} - \Delta x u x + \frac{(\Delta x)^2}{2!} u_{x,x} - \frac{(\Delta x)^3}{3!} u_{xxx} + \frac{(\Delta x)^4}{4!} u_{xxxx}$$

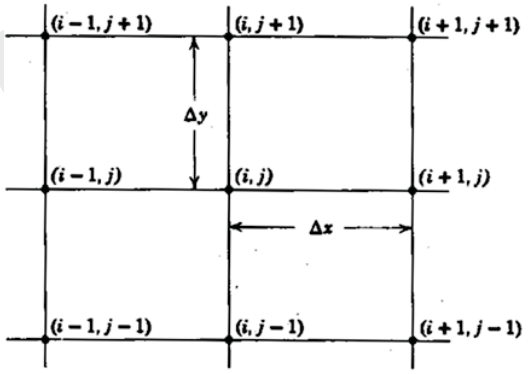

Fig. 1: Arrangement of grid points

$$u_{i+1,j} = u_{i,j} + \Delta x u_x + \frac{(\Delta x)^2}{2!} u_{x,x} + \frac{(\Delta x)^3}{3!} u_{xxx} + \frac{(\Delta x)^4}{4!} u_{xxxx}$$

Here, $u_x \equiv \partial u/\partial x, u_{xx} \equiv \partial^2 u/\partial x^2$, etc., and all derivatives are evaluated at the grid-point (i, j). By taking these equations singly, and by adding or subtracting one from the other, we

obtain the following finite-difference formulas for the first - and second - order derivatives at (i,j) :

$$\frac{\partial u}{\partial x} = \frac{u_{i+1,j} - u_{i,j}}{\Delta x} + O(\Delta x), \tag{4}$$

$$\frac{\partial u}{\partial x} = \frac{u_{ij} - u_{i-1,j}}{\Delta x} + O(\Delta x), \tag{5}$$

$$\frac{\partial u}{\partial x} = \frac{u_{i+1,j} - u_{i-1,j}}{2\Delta x} + O[(\Delta x)^2], \tag{6}$$

$$\frac{\partial^2 u}{\partial x^2} = \frac{u_{i-1,j} - 2u_{i,j} + u_{i+1,j}}{(\Delta x)^2} + O(\Delta x) \tag{7}$$

Formulas (4), (5) and (6) are known as the forward, backward, and central difference forms respectively. Similar forms exist for $\partial u/\partial y$ and $\partial^2 u/\partial y^2$. It may also be shown that

$$\frac{\partial^2 u}{\partial x\, \partial y} = \frac{u_{i+1,j+1} - u_{i-1,j+1} - u_{i-1,j-1}}{4\Delta x\ \Delta y} + O(\Delta x) \tag{8}$$

For a square grid ($\Delta x = \Delta y$), the following nine-point approximation is available for the Laplacian in two dimensions and will have the specified truncation error, provided that $u_{xx} + u_{rr} = 0$ is being solved :

$$\frac{\partial^2 u}{\partial x^2} + \frac{\partial^2 u}{\partial y^2} \frac{\begin{bmatrix} u_{i-1,j+1} + 4u_{i,j+1} + u_{i+1,j+1} \\ +4u_{i-1,j} - 20u_{i,j} + 4u_{i+1,j} \\ +u_{i-1,j-1} + 4u_{i,j-1} + u_{i+1,j-1} \end{bmatrix}}{6(\Delta x)^2} + O[(\Delta x)^4] \tag{9}$$

By taking more and more neighbouring points, an unlimited number of other approximations can be obtained, but the above forms are the most compact.

For convenience, the central – difference operator δ_x will be used occasionally. It is defined by

$$\delta_x u_{i,j} = \frac{u_{i+\frac{1}{2},j} - u_{i-\frac{1}{2},j}}{\Delta x} \tag{10}$$

$$\text{where } \delta_x^2 u_{i,j} = \frac{u_{i-1,j} - 2u_{i,j} + u_{i+1,j}}{(\Delta x)^2} \tag{11}$$

A SIMPLE PARABOLIC DIFFERENTIAL EQUATION

Consider an insulated bar with an initial temperature distribution at t = 0, having ends that are subsequently maintained at temperatures which may be functions of time. The temperature distribution u (x, t) in the bar at any t > 0 may be found by defining suitable dimensionless variables and by assuming that the physical properties for the bar are constant. The problem can be described by the following differential equation and initial and boundary conditions, also illustrated in Fig. 2.

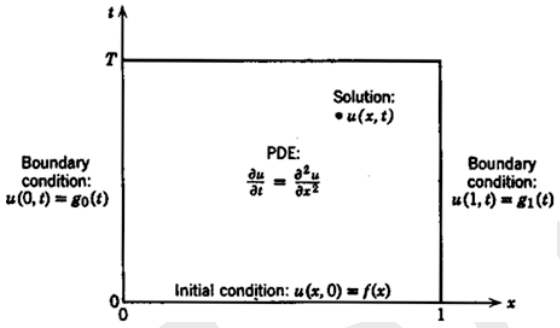

Fig. 2: The differential problem

$$\frac{\partial u}{\partial t} = \frac{\partial^2 u}{\partial x^2}, \quad \text{for } 0 < x < 1, \quad 0 < t < T, \tag{12}$$

$$\begin{aligned} u(x,0) &= f(x), \qquad 0 \le x \le 1, \\ u(0,t) &= g_0(t), \qquad 0 \le t \le T, \\ u(1,t) &= g_1(t), \qquad 0 \le t \le T. \end{aligned} \tag{13}$$

Here, f(x) is the initial condition, and $g_0(t)$ and $g_1(t)$ are the boundary conditions. The latter are of a particularly simple type, since they specify the temperature itself at the ends of the bar. We consider boundary conditions of a more general nature which involve also the derivatives of the dependent variable.

THE EXPLICIT FORM OF THE DIFFERENCE EQUATION

In order to approximate the solution of (12) and (13), a network of grid points is first established throughout the region $0 \le x \le t \le T$, as shown in Fig. 3, with grid spacings $\Delta x = 1/M$, $\Delta t = T/N$, where M and N are arbitrary integers. In this problem, it is easy to ensure that grid points lie on the boundaries of x and t, although, as well shall see later, this correspondence is seldom possible in two-dimensional problems when the boundaries are irregularly shaped. For any grid-point (i,n) that does not have i = 0, i = M, or n = 0, the derivatives of (12) are now replaced by the finite-difference forms suggested by (4) and (7):

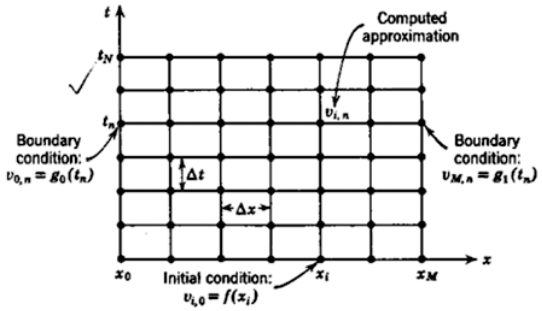

Fig. 3: The difference problem

$$\frac{\upsilon_{i,n+1} - \upsilon_{i,n}}{\Delta t} = \frac{\upsilon_{i-1,n} = 2\upsilon_{1,n} + \upsilon i + 1, n}{(\Delta x)^2} \tag{14}$$

or, defining

$$\lambda = \frac{\Delta t}{(\Delta x)^2} \tag{15}$$

then $\nu_{I,n+1} = \lambda\nu_{I-1,n} + (1 - 2\lambda)\nu_{1,n} + \lambda\nu_{I+1,n}$ (16)

In Fig. 4, the crosses and circles indicate those grid points involved in the time and space difference respectively.

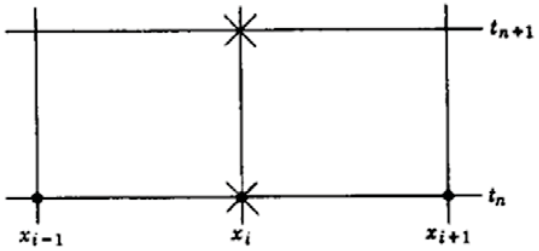

Fig. 4: The explicit form

If all the $\nu_{i,n}$ are known at any time level t_n, equation (15) enables $\nu_{i,n+1}$ to be calculated directly (that is, explicitly) at the time level t_{n+1} for $1 \leq I \leq M - 1$. For the boundary points i = 0, i = M, we also have

$$\nu_{o,n+1} = g_0 (t_{n+1}) \tag{17}$$

$$\nu_{M,n+1} = g_1(t_{n+1})$$

Since the initial values of ν are prescribed at t = 0 by

$$\nu_{i,0} = f(x_i) \tag{18}$$

the values of ν can evidently be obtained at all the grid points by repeated application of (15) and (16) ; we must calculate all values of ν at any one time level before advancing to the next time-step.

If the initial and boundary conditions do not match at (0,0) and (1,0), u(x,t) will be discontinuous at these corners, and the question arises as to what values should be assigned to, for example, $\nu_{0,0}$. It appears reasonable in such a case to use the arithmetic average of the values givens by f(x) ax x → 0 and $g_0(t)$ as t → 0; in programming, it is often simple to use either one value or the other and to recognize that a small error is thereby introduced.

Example **:** Consider the heat-conduction problem of (12) and (13), with the simple conditions f(x) = 0 and $g_0(t) = g_1(t) = 100$. Arbitrarily choose Δx = 0.2 and Δt = 0.017 corresponding to λ = 1/4, so that (15) becomes

$$\upsilon_{i,n+1} = \frac{\upsilon_{i-l,n} + 2\upsilon_{i,n} + \upsilon_{i+1.n}}{4}$$

we may then verify the tabulated values of $\nu_{I,n}$ in Table 1, computed to two decimal places.

Table 1: Illustration of the Explicit Method

Time subscription	Space Subscript, I					
	0	**1**	**2**	**3**	**4**	**5**
0	0	0	0	0	0	0
1	100	0	0	0	0	100
2	100	25	0	0	25	100
3	100	37.5	6.25	6.25	37.5	100
4	100	45.31	14.06	14.06	45.31	100
5	100	51.17	21.87	21.87	51.17	100
6	100	56.05	29.19	29.19	56.06	100
etc.						

A gradual diffusion of heat into the bar is evidenced by the general rise in temperature. Clearly, other values of Δx and Δt could be chosen (subject to a restriction mentioned below) each producing slightly different approximations to the true solution u(x,t).

THE IMPLICIT FORM OF THE DIFFERENCE EQUATION

In the explicit method previously described,$\nu_{i,n}$ depends only on $\nu_{i-1,\, n-1}$, $\nu_{i,n-1}$ and $\nu_{i+1,n-1}$. Referring to Fig. 5, only those values of ν within the pyramid-shaped area A can have any

influence on the value of $v_{i,n}$, whereas it is known that the solution u(x,y) of the PDE depends also on the values of u both in A and B for times earlier than t_n.

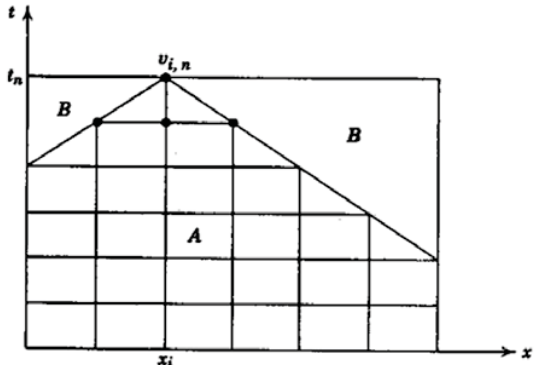

Fig. 5: Limitation of the explicit method

Furthermore, the requirement $0 < \Delta t / (\Delta x)^2 \leq ½$ places an undesirable restriction on the time increment which can be used. For problems extending over large values of time, this could result in excessive amounts of computation.

The implicit method, now to be described, overcomes both these difficulties at the expense of a somewhat more complicated calculational procedure. It consists of representing u_{xx} by a finite-difference form evaluated at the advanced point of time t_{n+1}, instead of at t_n as in the explicit method. Referring again to the problem of equations (12) and (13), the difference equation becomes

$$\frac{\upsilon_{i,n+1} - \upsilon_{i,n}}{\Delta t} = \frac{\upsilon_{i-1,n+1} - 2\upsilon_{i,n+1} + \upsilon_{i+1,n+1}}{(\Delta x)^2} \tag{19}$$

That is, the following relation exists between the values of v at the four points shown in the space-time grid of Fig.6.

$$-\lambda\upsilon_{i-1,n+1} + (1 \_ 2\lambda)\upsilon_{i,n+1} - \lambda\upsilon_{i+1,n+1} = \upsilon_{i,n} \tag{20}$$

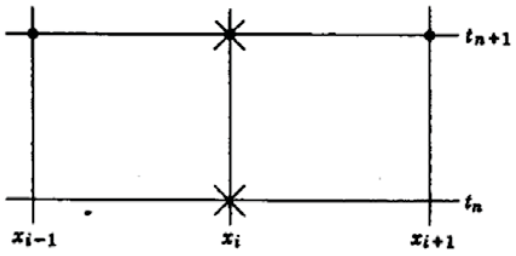

Fig. 6: The implicit form

The boundary and initial conditions of the explicit method still hold :

$$\begin{aligned} \nu_{0,n+1} &= g_0(t_{n+1}), \\ \nu_{M,n+1} &= g_1(t_{n+1}) \\ \nu_{i,0} &= f(x_i) \end{aligned} \tag{21}$$

At any one time level, equation (20) will be written once for each point $1 \leq i \leq M - 1$, resulting in a system of $M - 1$ simultaneous equations in the $M - 1$ unknowns $\nu_{i,n+1}$. The methods of solution for such a system will be discussed after we consider the convergence of the implicit method.

SOLUTION OF EQUATIONS RESULTING FROM THE IMPLICIT METHOD

Having established the convergence of the implicit scheme, we now return to study the solution of the $M - 1$ linear equations which result at each time step, namely,

$$\begin{aligned} &(1 + 2\lambda)\, \nu_{1,n+1} - \lambda\nu_{2,n+1} = \nu_{1,n}\, \lambda g_0(t_{n+1}), \\ &-\lambda\nu_{i-1,n+1} + (1 + 2\lambda)\nu_{i,n+1} - \lambda\nu_{i+1,\,n+1} = \nu_{i,n} \\ &\qquad\qquad\qquad\qquad \text{for } 2 \leq I \leq M - 2 \\ &-\lambda\nu_{M-2,n+1} + (1 + 2\lambda)\nu_{M-1,\,n+1} = \nu_{M-1,\,n} + \lambda g_1\,(t_{n+1}) \end{aligned} \tag{22}$$

Expressed more clearly equations (22) are a special form of system

$$\begin{aligned} &b_1\, \nu_1 + c_1\nu_2 = d_1 \\ &a_2\nu_1 + b_2\nu_2 + c_2\nu_3 = d_2 \\ &a_3\nu_2 + b_3\nu_3 + c_3\nu_4 = d_3 \\ &\ldots\ldots\ldots\ldots\ldots\ldots\ldots\ldots\ldots\ldots \\ &a_i\nu_{i-1} + b_i\nu_i + c_i\nu_{i+1} = d_i \\ &\ldots\ldots\ldots\ldots\ldots\ldots\ldots\ldots\ldots\ldots \\ &a_{N-1}\, \nu_{N-2} + b_{N-1}\nu_{N-1} + C_{N-1}\, \nu_N = d_{N-1} \\ &a_N\nu_{N-1} + b_N\nu_N \end{aligned} \tag{23}$$

In going from (22) and (23), the subscripts $(n + 1)$ on the ν's have been dropped, and the right-hand sides of (32), each of which is a known quantity, are called $d_1, d_2, \ldots. d_N$ for simplicity, with $N = M - 1$. The matrix of coefficients a, b, and c alone is called a tridiagonal matrix. The system (23) is readily solved by a Gaussian elimination method; with a maximum of three variables per equation, the solution can be expressed very concisely.

We first demonstrate the validity of a recursion solution of the form

$$\upsilon_i = \gamma_i - \frac{c_i}{\beta_i}\,\upsilon_{i+1},$$

in which the constants β_i and γ_i are to be determined. Substitution into the ith equation of (23) gives

$$a_i\left(\gamma_{i-1} - \frac{c_{i-1}}{\beta_{i-1}}\,\upsilon_i\right) + b_i\upsilon_i + c_i\upsilon_{i+1} = d_i$$

That is,

$$\upsilon_i = \frac{d_i - a_i\gamma_{i-1}}{b_i - \dfrac{a_i c_{i-1}}{\beta_{i-1}}} - \frac{c_i\upsilon_{i+1}}{b_i - \dfrac{a_i c_{i-1}}{\beta_{i-1}}}$$

which verifies the above form, subject to the following recursion relations :

$$\beta_i = b_i - \frac{a_i c_{i-1}}{\beta_{i-1}},\quad \gamma_i = \frac{d_i - a_i\gamma_{i-1}}{\beta_i}$$

Also, from the first equation of (23),

$$\upsilon_i = \frac{d_i}{b_i} - \frac{c_i}{b_i}\,\upsilon_2$$

whence $\beta_1 = b_1$ and $\gamma_1 = d_1/\beta_1$. Finally, substitution of the recursion solution into the last equation of (23) yields

$$\upsilon_N = \frac{d_N - a_N\upsilon_{N-1}}{b_N} = \frac{d_N - a_N\left(\gamma_{N-1} - \dfrac{c_{N-1}}{\beta_{N-1}}\,\upsilon_N\right)}{b_N}$$

whence

$$\upsilon_N = \frac{d_N - a_N\gamma_{N-1}}{b_N - \dfrac{a_N c_{N-1}}{\beta_{N-1}}} = \gamma_N$$

To summarize, the complete algorithm for the solution of the tridiagonal system is

$b_N = \gamma_N$,

$$\upsilon_i = \gamma_i - \frac{c_i\upsilon_{i+1}}{\beta_i},\quad i = N-1,\ N-2,\ \ldots,\ 1, \tag{24}$$

where the β's and γ's are determined from the recursion formulas

$$\beta_1 = b_1, \quad \gamma_1 = d_1 / \beta_1,$$

$$\beta_i = b_i - \frac{a_i c_{i-1}}{\beta_{i-1}}, \; i = 2,3,...N, \tag{25}$$

$$\gamma_i = \frac{d_i - a_i \gamma_{i-1}}{\beta_i}, \; i = 2,3,...N.$$

One of the disadvantages of a Gaussian elimination method is that round off error may accumulate seriously. However, Douglas [1] has conducted an analysis of the scheme of (24) and (25) and expects the round-off error to be small in comparison with the discretization error for usual choices of Δx and Δt.

We can now compare the amounts of computation required by the explicit and implicit methods. In making a rough estimate, we consider here only the number of multiplication and division steps. For M – 1 points at each time level, the explicit scheme of (15) requires 2M – 2 multiplication steps. Now if, as is the case with (22), the coefficients a, b and c of (23) remain constant, the β_I of (25) can be predetermined. In this case, the implicit scheme referred to requires some 3M – 3 steps. The absence of a restriction on the size of $\Delta t / (\Delta x)^2$ in the implicit method generally outweighs this moderate increase in computational effort.

Finally, note that (23) might also be solved by the Gauss-Seidel iteration scheme. However, each iteration consumes 2M – 2 steps, and since several iterations will generally be required for satisfactory convergence, such a procedure is not recommended.

Numerical Simulation of Groundwater Flow and Solute Transport, L. Elango (ed). pp.41-53

Understanding Water-bearing Properties of Rocks for Effective Conceptualization of Groundwater Flow Models

P.N. Ballukraya

INTRODUCTION

Groundwater is a naturally occurring substance, and is to be found filling the void spaces present in rock formations. Therefore the hydrogeological characteristics of an area is to a large extent dependant on the geological conditions prevailing there. Occurrence and movement of groundwater is thus controlled by the nature of rock types, their physical properties as well as the property of groundwater flowing through it. Such of these properties which control groundwater flow in rocks are therefore grouped under the name water-bearing properties of rock formations. A thorough knowledge of these properties is an essential necessity in understanding the science of groundwater and therefore a prerequisite while conceptualizing mathematical models of groundwater systems.

WATER-BEARING PROPERTIES OF ROCKS

From the point of view of hydrogeology, the following are the important water-bearing properties of rock formations:

1. Porosity
2. Permeability
3. Compressibility (of water and rock matrix)

These properties and related parameters largely define groundwater flow and all flow equations are based on these parameters.

Porosity

A rock matrix is generally made up of solid material (minerals) and void spaces in varying proportions. Obviously, the void spaces are important since it is in these open spaces that groundwater is stored and through which it moves with in the rock formation. Thus it is important to understand this basic water-bearing property in terms of its relative volume so that we can have an idea as to the possible volume of groundwater that can be stored in it.

Porosity, η can be defined as the volume of pore spaces present in unit volume of rock material ($\eta = V_v/V_t$, where V_v is the volume of void spaces and V_t is the total volume of the rock sample). Porosity of rock formations can vary from negligible to as high as 0.6. Two types of porosities can be recognized depending on the interconnectivity of the open spaces in a material. The volume of pores which are hydraulically interconnected with each other in

unit volume of aquifer constitutes the *effective porosity* as against the *total porosity* which is a measure of all the voids present in a sample irrespective of the degree of interconnection between them. In several rocks a substantial proportion of pores may be stand alone and not connected to one another. In groundwater science, it is the effective porosity which is of importance.

Porosity can be grouped in to several types based on different considerations.

Primary Porosity

Primary Porosity *i*s the porosity present in the rock when the rock was formed. The pores present in a sand sample or sandstone are examples.

Secondary Porosity

Secondary porosity on the other hand is the pore space developed in a rock due to geological processes affecting the rock after its formation. The joints and fractures in a granite rock or the cavities present in karstic limestones are examples of this type of porosity.

Intergranular Porosity

Intergranular porosity is the porosity due to the open spaces present around the mineral grains in a rock (such as in a sandstone or weathered regolith).

Fracture Porosity

Fracture porosity is developed when a rock undergoes breaking up along certain planes of weakness due to tectonic or other geological forces. The three sets of joints developed in granite is a good example.

Vesicular Porosity

Vesicular porosity is due to the presence of vesicles in the rock such as that present in vesicular basalt or in laterites.

The intergranular porosity is the most important from the point of view of groundwater availability. It also should be noted that most of the flow equations consider only this type of porosity, particularly where rock deformation is involved. This porosity of a granular medium is affected by several factors such as the shape, size and geometric arrangement of the grains present. For example, in a sandy formation, the larger pores formed by bigger grains may be filled by smaller grains, thus reducing its porosity. When stress is applied on such a medium, the grains may re-arrange themselves, leading to a change in the porosity. In fact, it is this ability to re-arrange, which leads to compression/expansion of the aquifer skeleton consequent to changed fluid pressure conditions in a granular medium.

Porosity of some common rocks			
Formation	porosity	Formation	porosity
Well sorted silt, sand, gravel	0.3 – 0.5	Limestone/dolomite	0 – 0.4
poorly sorted silt, sand gravel	0.2 – 0.35	Shale	0 – 0.1
Clay, clayey silt	0.35 – 0.6	Crystalline rocks	0 – 0.1
Sandstone	0.05 – 0.3		

Source: *Fitts*

Porosity is an index of the amount of water that can be stored in a rock formation, thus it is an important parameter in groundwater study. If a porous medium, saturated with water is allowed to drain, certain volume of water will be released from it due to gravity. The volume of groundwater that is drained by gravity from unit volume of aquifer material is called the *specific yield*, a parameter needed in mathematical modelling of unconfined aquifers.

***Problem*:** A 10m thick sandy unconfined aquifer extends over 10 km^2 area. If its specific yield is 0.1, what will be the volume of water obtained by completely draining the aquifer?

$V_w = V_a \times S_y$ and $dV_w = S_y A dh$

Volume of aquifer material = $\{(10m)\ (10 \times 10^6 m^2)\}$; the volume of water released is:

$V_w = (0.1) = 1 \times 10^6\ m^3$.

Permeability

Permeability is the ability of a rock formation to transmit a fluid through it. It quantifies the ease with which a fluid, say water can flow through a given material. Flow of groundwater through a rock formation is a mechanical process, involving conversion of mechanical energy to heat energy consequent to the resistance offered by the mineral grains to the flow of water. The mechanical energy in water having mass, m, pressure, P, volume V, velocity ν, and at elevation z is given by the Bernouli Equation (1738):

$$E = PV + mgz + \nu\ m^2/2$$

The first term on the right hand side being the elastic energy, the second is potential energy and the third is kinetic energy. This mechanical energy per unit mass of fluid at any point in the flow system can be defined as the work required to move that unit mass from a chosen standard state to a point in question. The energy per unit mass of fluid, called the *fluid potential*, θ is given by (Hubbert, 1940):

$$\theta = E/m = (P/\rho_w) + gz + (v^2/2)$$

for groundwater flow, a more convenient parameter is the energy per weight of water. By dividing the Bernouli equation by the weight of water, mg a new quantity, *hydraulic head* (h) is obtained:

$$h = E/mg = (P/\rho_w g) + z + (v^2/2g)$$

Since groundwater velocities are extremely low, the term can be ignored and thus we have,

$$h = (P/\rho_w g) + z$$

the value of g in the vicinity of ground surface is nearly constant and ρ_w can be taken as equal to 1, and therefore h can be equated to the sum of pressure head and elevation head.

In a non-pumping well, the pressure at the water surface is assumed to be zero. That is h = elevation of the water surface. As the depth increases, while h remains constant, $(P/\rho_w g)$ increases at the same rate z decreases. Therefore, the pressure anywhere in the water column is:

$P = (h-z)\ \rho_w g = (\text{depth})\ (\rho_w g)$

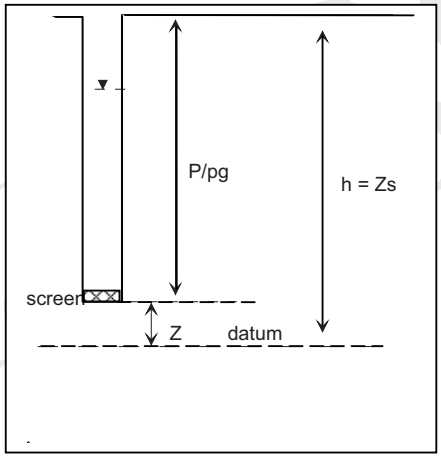

Henry Darcy studied the flow of water through porous medium and established certain relationships, which form the basis of modern hydrogeology. From his experiments, he concluded that when flow takes place through a porous material having a cross sectional area, A (L^2) over a flow length of L, for a given discharge of Q (L^3/T), the specific discharge, q = Q/A is proportional to the loss in hydraulic head Δh and inversely proportional to flow length L. Introducing a constant to describe the property of the rock formations, K this gives the relationship, Q = KiA, where $i = \Delta h/L$, is the hydraulic gradient. This is the basic Darcy's equation, which forms the basis of all groundwater flow equations. The property defined by K is the *hydraulic conductivity*, a basic water-bearing property of rock formations. It has the dimensions of velocity and thus has units of L/T. Since flow of a fluid through a medium is also dependant on the properties of fluid in addition to that of the granular material, the hydraulic conductivity is defined as the rate of flow through unit cross sectional area of a material under unit hydraulic gradient per unit of time under prevailing kinematic viscosity

of the fluid. Thus, we have K = k (ρg/ μ), where ρg is the specific weight of water and μ is the dynamic viscosity and k, the intrinsic permeability of the medium.

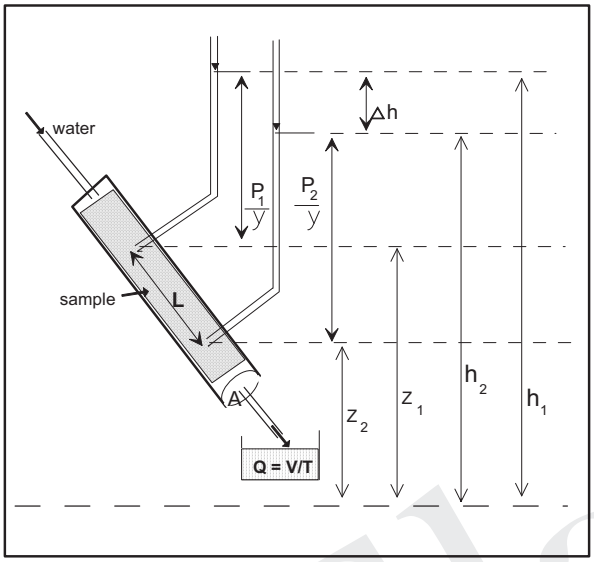

Darcy Experiment

Q = Discharge (Volume/Time)
H, pressure head

hydraulic head
L, length of flow
Z, elevation head
P/y,

Typical hydraulic conductivity (in m/sec) of some common rock formations	
Gravel: 10^{-1} to 10^{-2}	Clay: 10^{-10} to 10^{-6}
Sand 10^{-4} to 10^{0}	Sandstone: 10^{-8} to 10^{-3}
Siltty sand: 10^{-5} to 10^{-1}	Shale: 10^{-14} to 10^{-8}
Silt: 10^{-7} to 10^{-5}	Crystalline rocks: 10^{-11} to 10^{-2}

***Source**: Freeze and Cherry*

The intrinsic permeability, k of the rock formation is given by $k = cd^2$ (d, average pore diameter and c, a constant for shape, size and geometric arrangement of the grains).

Problem: A one km long trench was dug across a 3 m thick aquifer. Estimate the discharge in to this trench if the hydraulic conductivity of the aquifer is 0.8m per hour and the hydraulic gradient is 0.025.

Discharge, Q = KiA
= (0.8 m/hour) (10,000 m^2) (0.025) = 200 m^3.

A more commonly used parameter to define permeability in aquifers is the transmissivity, T. It is simply the rate of flow through the entire thickness of an aquifer

having unit cross sectional area under unit hydraulic gradient per unit of time and therefore, T = Kb, where b is the aquifer thickness.

The specific discharge, q is a macroscopic concept since the area A is made up of grains and open spaces. The average velocity at which water flows through the rock formation is given by the average linear velocity, ῡ is directly proportional to q and inversely proportional to η (effective porosity) and thus we have: ῡ = q/ η.

Sedimentary rocks form a majority of aquifers. These consist of a series of rock formations having varying hydraulic properties, that is, they are anisotropic and thus the flow through a cross section of such a sequence depends on the hydraulic conductivities of all the formations. The equivalent average hydraulic conductivity in such a multilayered sequence is given by:

$$K_{xe} = \Sigma Kxi\ d_i / \Sigma\ d_i$$

Where K_{xi} refers to the hydraulic conductivity of i^{th} layer in x direction and d_i is the thickness of i^{th} layer. The vertical hydraulic gradient will vary from one layer to another (but not the specific discharge, q_z). Since $q_z = -K_{zi}\ (\Delta_{hi}/d_i)$, the drop in hydraulic head across a given layer,i is

$$\Delta_{hi} = (q_z\ d_i)/\ (K_{zi})$$

The equivalent hydraulic conductivity in the vertical direction, K_{ze} must also have the same specific discharge, q_z over an equivalent single layer with the same total thickness and the loss in hydraulic head across is given by:

$$q_z = -\ K_{ze}\ \Sigma\Delta_{hi}/\ \Sigma\ d_i$$

Combining the above two equations for K_{xe} and q_z and solving for gives:

$$K_{ze} = \Sigma\ d_i/\ \Sigma\ (d_i/\ K_{zi}).$$

This relationship is a useful guide in evaluating source functions or leakage through overlying layers.

Deformation of Rocks

Most rock formations are elastic materials and therefore they expand/ compress in response to stress. Aquifers are generally at some depth below the ground surface, particularly the confined aquifers, and therefore they bear the weight of the overlying material plus that of the atmosphere. This load acting on the aquifers results in their volumetric deformation, the extent of which will depend up on their physical properties. Volumetric deformation leads to compression of the rock matrix, thus compressibility can be

defined as a material property describing the changes in volume or strain induced due to stress. Most porous materials are compressible and the volumetric deformations are brought about by 10 compression of intergranular pore water; 2) compression of the mineral grains and 3) compression of the rock matrix by way of rearrangement of the grains. Compressibility of grains is infinitely small and thus can be neglected.

Compressibility of Water

Water has a finite, low compressibility. Thus water at deeper zones are under stress and therefore undergo volumetric deformation leading to increased density and smaller volumes. As the pressure of water P increases by an amount dP at constant temperature, the density increases by $d\rho_w$ from its original density, ρ_w a given volume of water V_w will decrease in volume by dV_w according to:

$$\beta dP = \frac{d\rho_w}{\rho_w} = -\frac{dV_w}{V_w}$$

Where β is the compressibility of water and can be expressed in terms of either volumetric strain or density variation as

$$\beta = \frac{-dV_w / V_w}{dP}$$

This implies a linear elastic relationship between the volumetric strain and the stress induces in the fluid pressure. For a given mass of fluid, $\beta = \frac{d\rho_w / \rho_w}{dP}$.

The compressibility of water has a value of 4.5×10^{-10} m^2/N at 20°C (4.9×10^{-10} m^2/N at 0°C). Other important physical properties of waster are:

Mass density, $\rho_w = 1$ g/cc
Weight density, $\rho_w g = 9810$ N/m^3
Dynamic viscosity, $\mu = 1.4 \times 10^{-3}$ $N.sec/m^2$.

Assuming that the pressure of water at the surface (at water level in a well) is zero, its density at a depth of 100m will be:
$P_w = \rho_w gh = (1000 kg/m^3)\ (9.81 m/s^2)\ (100m) = 9.81 \times 10^5\ N/m^2$.
Since P at the top of the well is zero, dP = 9.81 x 105 N/m^2 and therefore, $d\rho_w$ is:
$\beta\ dP\rho_w = (4.5 \times 10^{-10}\ m^2/N)\ (9.81 \times 10^5\ N/m^2)\ (1000\ kg/m^3) = 4.415 \times 10^{-1} kg/m^3$.
Therefore the density of water at depth of 100m is: 1000 =0.4415 = 1000.4415 kg/m^3.

The weight of a vertical column of material acting on any horizontal plane is the total vertical stress, σ_{vt} (force per unit area, N/m^2) in a rock of density , the total weight, ω at depth b (from ground surface) is $\omega = \rho gbA$ (A being the cross sectional area of the vertical column). Thus, σ_{vt} at depth b is equal to ρgb. Under natural conditions, where the vertical lithological profile consists of several layers,

$$\sigma_{vt} = g \sum_{i=1}^{n} \rho_i b_i$$

Compressibility of the Aquifer Skeleton

The total stress, ω is thus borne by 1) force of pore water pressure and 2) force in the solid rock matrix. The force of pre water pressure is accounted for by its compressibility, and the second one is quantified by a property known as effective stress (Terzaghi, 1925), σ_{ve}, which is the matrix forces acting divided by the area.

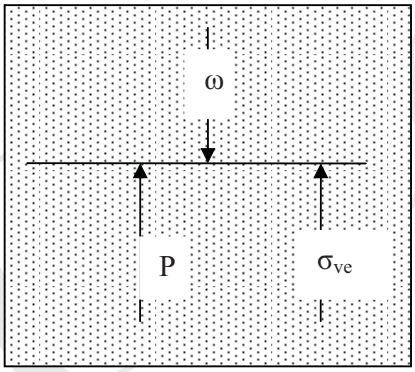

That part of the load which is not borne by the fluid pressure is the effective stress, σ_{ve}, which actually acts on the grains of the porous medium causing rearrangement of the grains leading to compression of the aquifer skeleton. The total stress, σ_{vt} is thus = σ_{ve} + P and $d\sigma_{vt} = dP + d\sigma_{ve}$. Since $d\sigma_{vt}$ is normally = 0,

$d\sigma_{ve} = -dP$.

As the pore pressure falls (consequent to a well pumping) effective stress increases.

Since hydraulic head, $h = (P/\rho_w g) + Z$, changes in h can be related to changes in P at a given location:

$dh = dP/ \rho_w g$ and assuming constant vertical stress,

$d\sigma_{ve} = - \rho_w g dh$.

The volumetric deformation in the aquifer skeleton is a measure of the compressibility of the rock matrix and is given by:

$$\alpha = \frac{dV_t / V_t}{d\sigma_{vt}}$$

Compressibility of rock formations lead to matrix compression to the extent permitted by its compressibility. Since volumentric deformation is essentially in the vertical direction, the thickness of the lithological unit decreases with increased effective stress in accordance with:

$\alpha = db / b_0 / d\sigma_{ve}$

Where db is the change in the thickness and b_0 is the original thickness of the formation.

compressibility (in m^2/N), of common lithological units

Soft clay: 3×10^{-7} to 2×10^{-6}	Stiff clay: 2×10^{-8} to 3×10^{-7}
Loose sand: 5×10^{-8} to 1×10^{-7}	Dense sand: 5×10^{-9} to 2×10^{-8}
Fractured rock: 3×10^{-10} to 7×10^{-9}	

***Source**: Fitts*

A common manifestation of material compaction is the instance of land subsidence, when groundwater is pumped on a large scale from a given aquifer. The extent of such subsidence can be estimated based on the above relationships. The change in the thickness of material due to changed effective stress is given by $db = -b_0 \alpha d\sigma_{ve}$.

When the aquifer is elastic and compressible and the load on the aquifer-aquiclude boundary remains constant, a reduction in fluid pressure due to pumping a well causes increase in effective stress leading to compaction of the aquifer skeleton and consequent reduction in porosity. Reduction in pressure leads to expansion of the pore water to the extent permitted by its elasticity. Both these actions lead to release of water from the aquifer. Cessation of pumping leads to gradual increase in pressure, compression of pore water, decreased effective stress, expansion of the aquifer skeleton, increase in porosity till the original state is reached. In a perfectly elastic aquifer, the initial piezometric surface will be restored.

Problem: A well tapping a 20 m thick confined aquifer is pumped over a long period during which the piezometric surface declined by 10 m. If the overlying material is 100m thick, has a density of 2500 kg/m^3, what would be the extent of reduction in the thickness of the aquifer if the initial water level was 10 m below ground level, assuming that the compressibility of the aquifer is 5×10^{-8} m^2/N?

Effective stress in the aquifer before pumping:

σ_{ve} = $\sigma_{vt} - P$
= {(height) (density of overburden) (g) } – (h-z) $\rho_w g$.
= [(100 m) (2500 kg/m^3) (9.81 m/s^2)] – [(90 m) (1000 kg/m^3) (9.81 m/s^2)]
= 1,569,600 N/m^2.

Effective stress when the water level declines by 10 m:
= [(100 m) (2500 kg/m^3) (9.81 m/s^2)] – [(80 m) (1000 kg/m^3) (9.81 m/s^2)]
= 1,667,700 N/m^2.

Thus, $d\sigma_{ve}$ is (1,667,700 N/m^2 - 1,569,600 N/m^2) = 98,100 N/m^2.
db = $-b_0 \alpha d\sigma_{ve}$. = (20 m) (5 x 10^{-8} m^2/N) (98,100 N/m^2)
= 9.81 x 10^{-2} m.

In an elemental volume ($\Delta V = \Delta A \Delta Z$) of compressible aquifer, with constant load and incompressible solid material and compression resulting in decrease in aquifer thickness,

$$\frac{d(\Delta V_s)}{\Delta A} = (1-\eta)d(\Delta z) - \Delta z d\eta = 0 \text{ and}$$

$$d\eta = \alpha(1-\eta)dP$$

If the mass of water in the elemental volume is $\Delta M = \rho\eta\Delta A\Delta Z$, with ΔA remaining constant, ΔM will vary with the density of water, the porosity and the vertical dimension of the elemental volume. The change in mass of water is given by:

$$\frac{d(\Delta M)}{\Delta V} = \eta dP + \rho d\eta + \frac{\rho\eta d(\Delta z)}{\Delta z}$$

Taking in to account the compressibility of the aquifer skeleton,

$$\frac{d(\Delta M)}{\Delta V} = (\eta\beta + \alpha)\, dP$$

The pressure p in an elemental volume, at a constant elevation within the aquifer directly changes with hydraulic head, h ($dP = \gamma dh$) and therefore,

$$\frac{d(\Delta M)}{\rho\Delta V} = \gamma\eta\beta\left(1 + \frac{\alpha}{\eta\beta}\right)dh = S_s dh$$

Where S_s is the specific storage (L^{-1}), defined as the volume of water which a unit volume of aquifer releases from storage (takes in to storage) because of expansion of pore water and compression of the porous medium (compression of the water and expansion of the porous medium per unit decline in head. i.e.,

$$S_s = \frac{dV_w}{V_t}\frac{1}{dh}$$

The storativity, S is the volume of water released from storage from a vertical column of aquifer having unit cross sectional area per unit decline in head (or vice versa) and is based on the equation:

$$S = \gamma\eta\beta b\ 1 + \frac{\alpha}{\eta\beta} = S_s b$$

For unit volume of material (V=1) and unit decline in head this simplifies to:

$S = \rho g\beta\ (\alpha + \eta\beta) = \gamma b\ (\alpha + \eta\beta)$ and

The change in the volume of water, dV_w due to change in elastic storage of an aquifer is given by:

$dV_w = -SAdh$

The normal range of storativity for common aquifers varies from 1×10^{-3} to 1×10^{-6}.

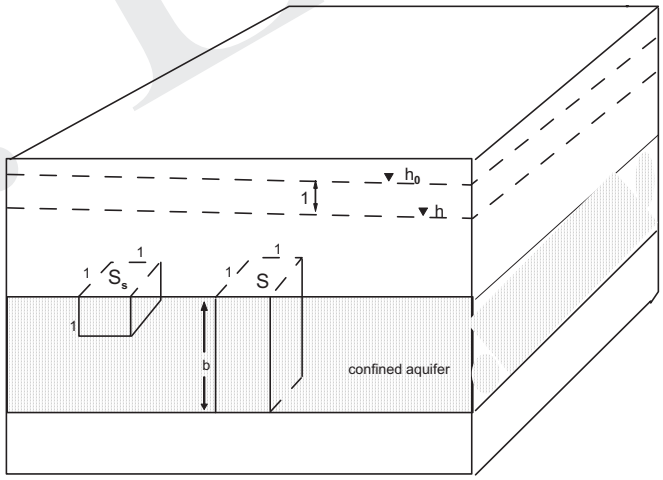

In the case of unconfined aquifer, the storativity is mainly the specific yield, Sy, since the elastic storage is negligible as compared to S_y. Therefore, for all practical purposes, S = S_y. Therefore, $dV_w = -S_yAdh$ for unconfined aquifers.

Barometric and Tidal Efficiency of Aquifers

The elevation of water surface in a well (h) is an important parameter in all groundwater studies. It forms the basis of calibration of mathematical models. Thus it is important that this data is accurately obtained from field measurements. Under normal circumstances, the water levels measured are true reflection of the pressure heads in the aquifer, without any extraneous influence. However, there are situations when external forces will lead to temporary changes in the elevation of water surface and two such instances are the transient changes in atmospheric pressure and the tidal stage in coastal aquifers.

Barometric Efficiency

When there is a change in the atmospheric pressure, the total load on the aquifer changes leading to changes in pore water pressure and effective stress. Also, in a well tapping the confines aquifer, the water surface in the well also is subjected to this changed pressure. The water surface is directly exposed to the atmosphere, and the entire pressure is transmitted to the water surface. Thus the pressure of water at the well increases by an amount equal to the extent by which the atmospheric pressure increases. For an increase of dP_a, in atmospheric pressure, the rise in water pressure at the water table in a well open to the atmosphere equals dP_{wt}.

$$dP_{water\ table} = dP_{well} = dP_a.$$

However, in the aquifer, the change in atmospheric pressure causes a corresponding change the total vertical stress, $d\sigma_{vt} = dP_a$.

A part of this increases stress is borne by the pore water and partly by the effective stress. The increase in pore water pressure in the aquifer is therefore less than the atmospheric pressure change and therefore, less than the pressure changed in the well, $dP_{well} > dP_{aquifer}$. This will result in a flow of water from the well in to the aquifer (through the screen) leading to decrease in water level elevation. A decrease in atmospheric pressure will result in the opposite reaction. The barometric efficiency, BE of an aquifer is the changes in water level in relation to changes in atmospheric pressures.

$$BE = \frac{\rho_w g dh}{dP_a}$$

Where dh is the change in head in the well during a change in atmospheric pressure (dP_a).

In fully confined aquifer, BE will be equal to 1, though normally it will be in the range of 0.9, since most confined aquifers leak to some extent. In an unconfined aquifer, BE will be nearly zero.

Tidal Efficiency

In a coastal confined aquifer extending under the sea floor, changes in sea level caused by tidal effects will induce changes in the piezometric level. An increase in sea level will lead to increased total vertical stress on the aquifer. This change in load will be borne partly by pore water pressure and partly by effective stress. Thus an increase in sea level of d_{sl} will lead to proportionate increase in effective stress as well as fluid pressure. Increase fluid pressure will lead to an equal increase in piezometric level. In a fully elastic confined aquifer, the change in water elevation will be directly proportional to changes in sea levels and this is defined as the tidal efficiency of the aquifer.

These two aspects have to be borne in mind while monitoring groundwater levels on a regular basis as otherwise the measurements are likely to be inaccurate.

CONCLUSIONS

A detailed account of the water-bearing properties of rock formations has been given in the above paragraphs. It can be seen from the theoretical treatment of the parameters that a thorough understanding of these is an essential prerequisite in conceptualizing groundwater regimes, and hence a necessary element in conceptualizing and modelling groundwater flow systems.

REFERENCES

[1] Fitts, C.R., 2002. Groundwater Science, Elsevier Science Ld., 450p.
[2] Freeze, R. A., and Cherry, J.A., 1979, Groundwater. Prentice HallInc. 603p.
[3] Todd, D.K., 1980, Groundwater hydrology, John Wiley and sons, 535p.

Numerical Simulation of Groundwater Flow and Solute Transport, L. Elango (ed). pp.55-60

Complexities in Hard Rock Hydrogeology

P.N. Ballukraya

INTRODUCTION

Groundwater is probably the most strategic natural resource of today. Groundwater is the only replenishible natural mineral resource available to man. Use of groundwater has been growing steadily over the years for domestic, agricultural and industrial purposes. In large parts of India, in the geographical areas away from surface water sources (rivers, lakes and man-made dams), it remains as the only source of water. In these areas, its exploitation has increased manifold in the last two to three decades. The report of the Groundwater Resources Estimation Committee (GWREC, 1997), has estimated that in India, during the period 1951-92, the number of dug wells increased from 3.86 million to 10.12 million, while the number of shallow tube wells increased from 3,000 to 5.38 million. World over, it has been estimated that the same amount of fresh water has to be shared by some 8 billion people in the year 2025 which was available for a mere 1.3 billion in the beginning of 20th century. As per the latest estimates by the Central Board of Groundwater, the total number of irrigation structures at present is 17.5 million which is in addition to about 3 million domestic/drinking water/industrial wells. Over 80% of rural and more than 50% of urban water requirements is currently met by groundwater. The total area irrigated by groundwater increased from 6.5Mha in 1951 to 35.38Mha in 1993. In the hard rock areas of India, where recharge is limited, such large scale abstraction has resulted in failure of shallow wells/ bore wells creating over-exploited zones. Of the 7163 blocks (mandals in A.P, taluks in Gujarat and water sheds in Maharashtra) in the country, 250 (3.5%) are over-exploited while 179 (2.5%) are dark areas (GWREC). The manifold increase in groundwater abstraction in the past two decades or so has meant that in many parts of the world, groundwater management and conservation are taking precedence over exploration and development. Over-exploitation has assumed alarming proportions with all its attendant undesirable consequences – socioeconomic as well as environmental.

Scientific development and management of groundwater is predicated on a proper understanding of local hydrogeology in terms of groundwater occurrence and movement. The mechanics of groundwater flow is well understood in case of granular aquifers and therefore they are readily amenable to mathematical modelling, which help predict aquifer responses under varying stress conditions. Therefore aquifer modelling is widely used as an effective tool in groundwater development and management programmes.

HARD ROCK HYDROGEOLOGY

However in the case of hard rocks, the picture is much more complex. From the

hydrogeological point of view the hard rocks are all those lithological units which basically lack primary porosity. All the igneous and metamorphic rocks can be grouped under this category. The water-bearing capacity of these rocks is based on their ability to develop secondary porosity which depends on the nature and extent of geological processes to which they have been subjected to. These processes generally show a very high degree of spatial variation even within a given lithological unit. This renders the hydraulic properties of hard rocks highly complex and often unpredictable.

Fracture Porosity

The development of secondary porosity in hard crystalline rock formations is essentially controlled by factors such as lithology, tectonics and climate. Development of joints and fractures are necessary components of this process of development of open spaces in an otherwise massive rock formation. Weathering is the next stage which enhances the porosity of the rock formation. When allowed to run their full course these two processes reduce the normally massive rock into a granular material.

The development of fractures and joints is controlled mostly by the lithology. Two types of fractures commonly develop, namely tension-release joints, which are basically due to unloading (removal of overlying material through erosion) and those due to compressional and tensional forces. Tension release joints are by and large nearly parallel to the existing ground surface and are closely spaced in the near surface zones. The second category of joints are mostly sub-vertical to vertical in disposition and the intensity of fracturing is generally related to the lithology. Rocks containing more felsic minerals develop more joints since they are relatively brittle in nature as compared to fewer joints in rocks having more mafic minerals. Thus granite will develop larger number of joints and fractures per unit volume of rock material as compared to say, charnockite under similar stress conditions. Even the process of weathering which attacks the rocks is lithology- controlled to a large extent. Granitic rocks generally produce more sandy products on weathering (physical weathering being predominant) while mafic rocks will normally give rise more clayey regoliths (chemical weathering predominant). Thus these two processes are the basic means by which a hard rock gets the ability to store and transmit groundwater. Therefore an understanding of these processes is important in hard rock hydrogeological studies.

Hard Rock Aquifers

Based on the physical condition of the rock formation which makes up the hard rock aquifer, two major divisions can be recognized which has a direct bearing on groundwater hydraulics. The first one is the weathered rock mantle occurring near the ground surface wherein the entire rock formation has been converted into more or less granular material. Here the porosity is essentially intergranular and thus this part of the hard rock aquifer behaves more or less like a granular aquifer medium. This is underlain by the bed rock where fracture porosity is the controlling factor. The rock matrix in this zone remains largely unaltered and devoid of water-bearing capacity. An intricate network of sub-horizontal to

horizontal and sub-vertical to vertical joints and fractures make up this aquifer system. The thickness of this zone varies spatially as does the number of joints per unit volume of rock. These fractures may or may not be interconnected with each other leading to a complex groundwater flow regime (Fig.1).

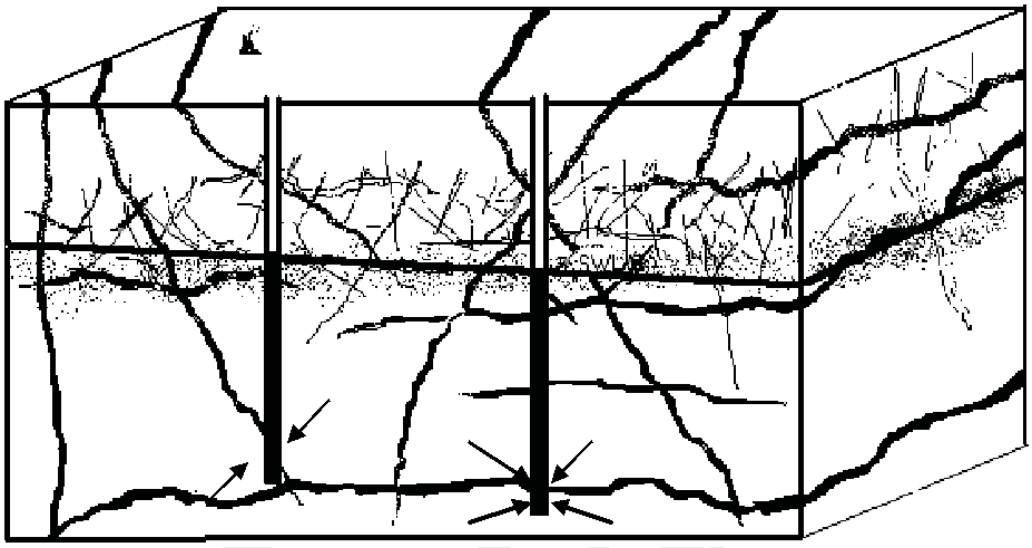

Fig. 1: Idealized schematic of hydrogeological conditions in a hard rock area

In the many parts of the hard rock areas of India it is these fractures which are the producing zones. The weathered and partly weathered zones may have long since become dry due to over abstraction and resulting decline in groundwater levels. Under normal circumstances the near-vertical joints act as conduits for the recharging/infiltrating water while the near-horizontal and sub-horizontal fractures act as the producing aquifers. The thickness of these water-bearing zones is seldom greater than a few tens of centimeters. The near-horizontal fractures being the main producing aquifers, a near-radial horizontal and radial flow into borewells occur, thus approximating one of the assumptions describing groundwater flow to a pumping well. However, there are some special conditions, which are encountered which need to be kept in mind. Some of these are discussed below.

1. In granular aquifers, the well discharge, Q is proportional to the drawdown, s. Thus, subject to well losses, by increasing the drawdown, the well discharge can be increased. However, in borewells tapping fractured aquifers, this is not generally true in that, the drawdowns sharply increase beyond a certain discharge, as seen from the following example

Borewell at SIPCOT, Hosur:

Borewell depth 51m; pump at 46m depth; SWL: 10.7m

Discharge in lpm	Drawdown in m	Duration of pumping, minutes
70	4.8	120
85	6.3	120
110	14.9	75
126	21.4	60
135	34.7	4; dry run.

At an increased discharge of 135 lpm, the drawdown sharply increases and the pumping water level reaches the depth at which the pump is located at which time the well runs dry for a few seconds after which the discharge is discontinuous in nature. This is one of the characteristic features of fracture aquifers.

2. In granular aquifers, Q is proportional to the hydraulic gradient (Q = KiA – Darcy's law). In hard rock areas, this may not be true in its general sense due to the highly heterogeneous nature of the fracture matrix. An example is given Fig.2. The example is from Tammapatti area (upper Sweta basin) in Tamil Nadu, It is seen that the yield of borewells, located close to each other is vastly different, even though their depths are essentially same. If it were a granular aquifer, the well yields would be essentially similar. This condition is the result of the non-uniformity of the fracture aquifers encountered by these borewells, and thus the yields do not correlate with the hydraulic gradient in the aquifer.

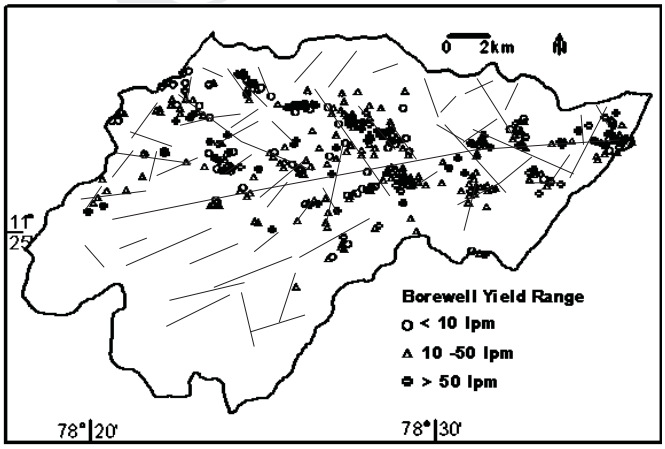

Fig. 2: Highly varying yields in small geographic area (upper Sweta Basin)

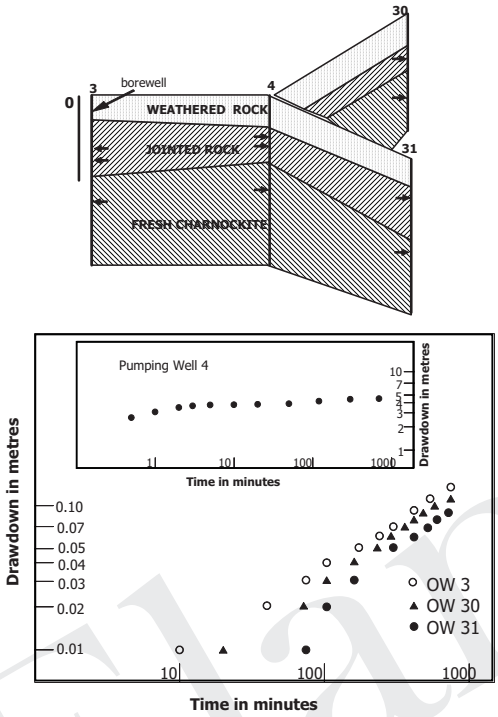

Fig. 3: Drawdown curves from Alathur area (top: location and litholog of borewells)

3. In a well field located in granular aquifers, the drawdowns in observation wells around a pumping well will be uniform for a given radial distance. It increases with increasing distance from the pumping well. However, in many instances in hard rock areas this may not be true. Observation wells located near the pumping well may register smaller drawdowns than those located far away. Also, the drawdowns tend to be direction dependant as seen in the example from Alathur, near Chennai (Fig 3). The aquifer parameters determined from such data will yield highly variable T and S in different directions, even with in short distances.

4. Presence of dykes or other hydrological boundaries are common in hard rock areas. At times these may not be seen near the ground surface and the pumping test data near such features will be affected by them without it being realized. For example, the drawdown curves in Alathur have been affected by the presence of a sub-surface barrier and this has been identified with the help of electrical resistivity surveys.

CONCLUSIONS

In the above paragraphs some of the more common features of hard rock hydrogeology are examined. The spatial complexities in aquifer behavior are a challenge that needs to be

addressed in conceptualizing groundwater flow in hard rock areas. In addition, several factors have to be considered and accounted for in understanding hard rock hydrogeology in order to model these aquifers for predictive purposes. Otherwise the predicted results will be wide off the reality and this has to be adequately addressed in any attempt at use mathematical modelling of a hard rock area. A solution to this would be in selecting very small areas like a micro watershed for modelling since most of the details could be then incorporated in to the model, thus ensuring a realistic outcome from the exercise of mathematical modelling.

REFERENCES

[1] Ballukraya, P.N., (2000). Over-exploitation and pollution of groundwater: a case study from Rasipuram area, Tamil Nadu. Jour. Geol. Soc., v.56, pp. 139-150.

[2] Ballukraya, P.N., (2004). Water balance studies in the overexploited Rasipuram area, Tamil Nadu. Jour. Geol. Society India, v.63, pp. 507-514.

[3] Center for Water Resources (CWR)., (2000). Baseline study of selected irrigation commands. Anna University, Chennai.

[4] CGWB., (1996). Groundwater resources of Tamil Nadu. Central Groundwater Board, SECR, Chennai. 95p.

[5] GWREC., (1997). Groundwater Resources Estimation Methodology 1997. Ministry of Water Resources, Govt. of India. 105p.

[6] Todd, D.K., (1980). Groundwater Hydrology. John Wiley and Sons. 535p.

Numerical Simulation of Groundwater Flow and Solute Transport, L. Elango (ed). pp.61-77

Remote Sensing – A Source of Thematic Input for Groundwater Studies

S. Sanjeevi

It is a known fact that groundwater is the most important natural resource requited for drinking, irrigation and for industrial use. The major problem with groundwater exploration is to identify the recharge and discharge areas in the ground. Also, a sound knowledge of the landforms present in the vicinity of the aquifer, that characterize the discharge or water availability, is a must to quantify the groundwater available in an aquifer. Groundwater potentiality of an area can be assessed through integration of the information on lithology, geomorphology, landuse/landcover, lineament and slope.

Remote sensing offers good guidelines for groundwater assessment by giving us information on the various recharge zones. Using remotely sensed images data, we can obtain information on geology, landuse/land-cover parameters, geomorphology, slope, time transgressive tectonics, fracture systems, water bearing fractures, water barren fractures and fractures of faster groundwater depletion, groundwater sinks and drains and spatial patterns of net recharge. We can also obtain preliminary information on possible sites for recharging the aquifer systems through natural recharge and artificial recharge mechanisms. Thus we can produce surface parameter maps for the regional and local aquifers and produce guidelines for further mapping and forward the same to governing local governing bodies/agencies. This article provides a synoptic view of the possible data/parameters that one can obtain using remote sensing.

Remote sensing data provide surface information, where as groundwater occurs at depth, may be a few meters or several tens of meters deep. The depth penetration of Electromagnetic radiation is only of the order of fractions of a millimeter in the visible region, to barely a few meters in the microwave region. Hence, in most cases, remotely sensed image data are unable to provide any direct information on groundwater. However, the surface regime (topograhical, hydrological, geological, landuse/landuse) which primarily governs the subsurface water conditions, can be studied and mapped using remotely sensed image data. Therefore, remote sensing acts as a very useful guide and an efficient tool for regional and local groundwater exploration. Gupta (2005) and Babar (2005) provide detailed information on the potential of remote sensing to derive certain groundwater parameters.

In the context of remote sensing for groundwater exploration, the various surface features or indicators can be grouped into two categories (1) first-order or direct indicators, and (2) Second-order or indirect indictors. The first-order indicators are directly related to the groundwater regime (Viz. recharge zones, soil moisture and vegetation). The second-order indicators are those hydrogeological parameters, which regionally indicate the

groundwater regime, e.g. rock/soil types, structures, including rock fractures, landforms, drainage characteristics etc (Gupta 2005).

The following table lists the components of the first and second order indicators.

Table 1: Components of the possible indicators of groundwater regime provided by remotely sensed images (Source: Gupta, 2005)

Indicators	Features
First-order or direct indicators	Features associated with recharge zones: rivers, channels, lakes, ponds etc
	Features associated with discharge zones: springs etc.
	Soil moisture
	Vegetation (anomalous)
Second-order or indirect indicators	Topographic features and general surface gradient.
	Landforms
	Depth of weathering and regolith
	Lithology: hard-rock and soft-rock area
	Geological structures
	Lineaments, joints and fractures
	Faults and shear zones
	Soil types
	Soil moisture
	Vegetation
	Drainage characteristics
	Special geological features, such as karst, alluvial fans, dykes and reefs, unconformities and buried channels which may have a bearing on groundwater occurrence and movement.

As far as the choice of wavelength for hydrogeological studies is concerned, it is understood that the NIR bands give much information about the recharge and discharge areas (Gupta 2005). The following figure illustrates this concept.

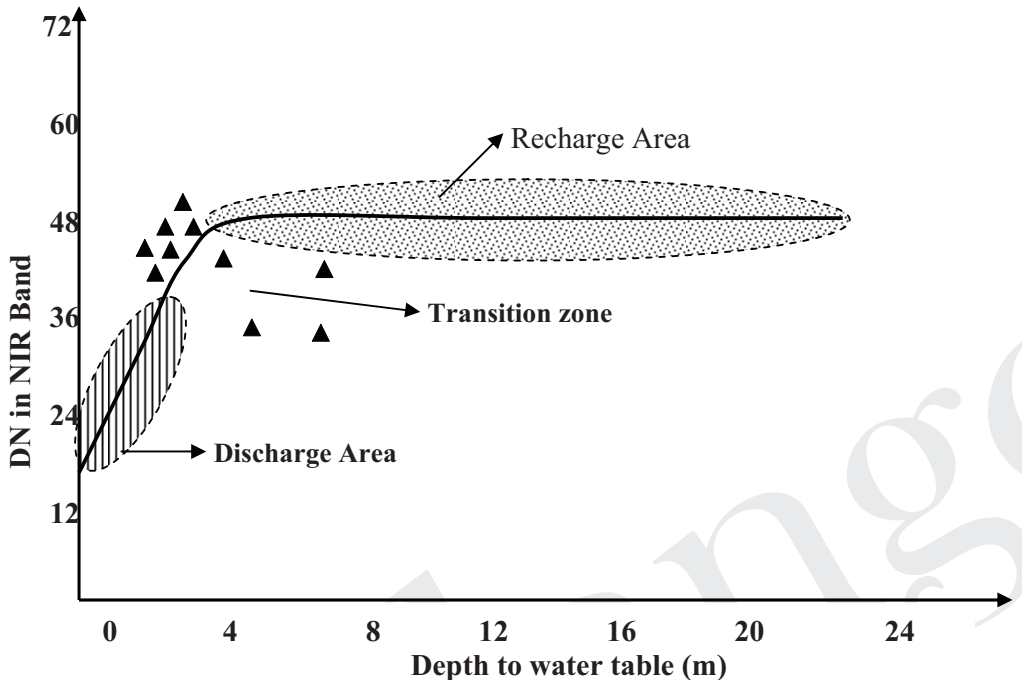

Hydrogeomorphic Information

Application of the principal of geomorphology provides information, which will be of value in predicting the geometry of the aquifers. On weathering and erosion, many geological formations develop landforms that are distinctive in respect of slope continuity of outcrops and symmetry of valley flanks. The surface topographic features of bedrocks can some times be extrapolated to reasonable depths to predict the thickness of alluvium or aeolian sands occurring as valley filled deposits, by treating slope profile as mathematical curves for which equations similar to regression equations can be found

It is well known that hydrologic processes are influenced by geomorphometric properties like local slope angle, convergences or drainage density. From the groundwater point of view integration of geological, structural and hydrogeological data with hydrogeomorphological data is very much useful in finding out the groundwater potential zones with fruitful results. Present day hydrogeomorphological research is the explanation of landscape and landforms: what they are, how they function and have developed with reference to the hydrological condition.

Landuse Information

Application of satellite remote sensing for land use surveys and mapping is gaining importance largely because of its ability to provide rapid and reliable data within a given

time of framework. Realising the relationship between landuse and hydrogeomorphology is important for planning and management activities. Accordingly, planning for agricultural landuse need detailed, timely, accurate and reliable data on the extent, location and quality of land and water resources and climate characteristics. The data on landuse potential and the conservation needs can help in planning for uses that will maintain the quality of land.

A Classification System for Use with Remote Sensing Techniques

There is no one ideal classification of land use and land cover, and it is unlikely that one could ever be developed. There are different perspectives in the classification process, and the process itself tends to be subjective, even when an objective numerical approach is used. There is, in fact, no logical reason to expect that one detailed inventory should be adequate for more than a short time, since land use and land cover patterns change in keeping with demands for natural resources. Each classification is made to suit the needs of the user, and few users will be satisfied with an inventory that does not meet most of their needs. In attempting to develop a classification system for use with remote sensing techniques that will provide a framework to satisfy the needs of the majority of users, certain guidelines of criteria for evaluation must first be established.

Classification Criteria

Anderson (1971) opines that A land use and land cover classification system which can effectively employ orbital and high-altitude remote sensor data should meet the following criteria:

1. The minimum level of interpretation accuracy in the identification of land use and land cover categories from remote sensor data should be at least 85 percent.
2. The accuracy of interpretation for the several categories should be about equal.
3. Repeatable or repetitive results should be obtainable from one interpreter to another and from one time of sensing to another.
4. The classification system should be applicable over extensive areas.
5. The categorization should permit vegetation and other types of land cover to be used as surrogates for activity.
6. The classification system should be suitable for use with remote sensor data obtained at different times of the year.
7. Effective use of subcategories that can be obtained from ground surveys or from the use of larger scale or enhanced remote sensor data should be possible.
8. Aggregation of categories must be possible.
9. Comparison with future land use data should be possible.
10. Multiple uses of land should be recognized when possible.

Table 2: Land use and land cover classification system for use with remote sensor data (Source: Anderson 1971 from Lillesand and Kiefer, 2000)

Level I	Level II
1 Urban or Built-up Land	11 Residential
	12 Commercial and Services
	13 Industrial
	14 Transportation, Communications, and Utilities
	15 Industrial and Commercial Complexes
	16 Mixed Urban or Built-up Land
	17 Other Urban or Built-up Land
2 Agricultural Land	21 Cropland and Pasture
	22 Orchards, Groves, Vineyards, Nurseries, and Ornamental Horticultural Areas
	23 Confined Feeding Operations
	24 Other Agricultural Land
3 Rangeland	31 Herbaceous Rangeland
	32 Shrub and Brush Rangeland
	33 Mixed Rangeland
4 Forest Land	41 Deciduous Forest Land
	42 Evergreen Forest Land
	43 Mixed Forest Land
5 Water	51 Streams and Canals
	52 Lakes
	53 Reservoirs
	54 Bays and Estuaries
6 Wetland	61 Forested Wetland
	62 Nonforested Wetland
7 Barren Land	71 Dry Salt Flats.
	72 Beaches
	73 Sandy Areas other than Beaches
	74 Bare Exposed Rock
	75 Strip Mines Quarries, and Gravel Pits
	76 Transitional Areas
	77 Mixed Barren Land
8 Tundra	81 Shrub and Brush Tundra
	82 Herbaceous Tundra
	83 Bare Ground Tundra
	84 Wet Tundra
	85 Mixed Tundra
9 Perennial Snow or Ice	91 Perennial Snowfields
	92 Glaciers

The type of remotely sensed image data to derive landuse details of different scales is as in Table 3.

Table 3: Image data types to be used to derive landuse information

Classification Level	Typical data characteristics
I	LANDSAT, IRS 1C, 1D LISS III type of data
II	High-altitude data at 40,000 ft (12,400 m) or above (less than l:8O,OOO scale)
III	Medium-altitude data taken between 10,000 and 40,000 ft (3,100 and 12,400 m) (1:20,000 to 1:80,000 scale)
IV	Low-altitude data taken below 10,000 ft (3,100 m) (more than 1:20,000 scale)

Joints, Faults and Lineaments

Joints of tectonic origin are most commonly subjected to mineralizations. The characters and extent of jointing depends also upon the composition and hardness of the rocks. Harder rocks are less rapidly disintegrated; hence joints penetrate them down to smaller depths. The process of weathering much more rapidly produces joints in comparatively softer rocks. Hard metamorphic rocks often exhibit an insignificant jointing and a very low water capacity. The hard rock formations are generally oriented and mutually intersecting joints, the groundwater flows along both the open joints are free from the products of mechanical weathering and the joints partly or completely filled with loose sandy clayey products of weathering.

From the hydrogeological points of view, the frequency and extent of joints and fractures in the rocks are the most significant parameters imparting permeability and porosity for forming suitable groundwater reservoirs in the basaltic terrain. The secondary porosity (joints and fractures) generally reduces with depth and hence the near surface (unconfined) aquifer system rarely, extends below 30 m depth. The distribution and migration of groundwater in jointed rocks are variable, being dependent on the character, origin, and size of cracks. Joints in hard rock contain both un-pressured and pressured waters. Groundwater head is commonly produced by the hydrostatic pressure in intersecting joints, some which occur in recharge area at higher altitudes, whereas the joints found at greater depths give rise to artesian springs.

It can be noticed that faults can affect groundwater in one of three general ways: (a) enhance flow rates, (b) inhibit flow, or (c) act in a neutral manner. Since this first part of a two-part paper is of a methodological nature, faults are considered to be neutral. The only effects of the relative positions of the layers of different, and perhaps sharply contrasted, hydrologic properties would affect the flow.

Table 4: Lists the image characters of certain landuse units in a typical hard rock terrain

Landuse category	Tone	Size	Shape	Texture	Pattern	Location	Association
Agriculture & Plantation	Dark red to red	Small to medium	Regular with sharp edges	Coarse to medium	Dispersed contiguous	Plains, foot hills and uplands	Dry lands or unirrigated lands, uplands occasionally cropland, proximity to rivers and on gentle slopes
Forest Plantation	Light red to red	Varying in size	Regular to irregular	Smooth to medium	Contiguous to non-contiguous	Uplands, foot slopes, coastal plains and within the notified area	Forest plantation of different types of sub-types, areas within thin soil cover and beach sands
River/ Streams	Light blue to dark blue	Long narrow to wide	Irregular, sinuous	Smooth to medium	Contiguous non linear to dendrite/sub dendrite etc	Natural rivers/streams, perennial and non-perennial.	Drainage pattern on hill slopes, flood plains, uplands etc. also with vegetation along the blanks and in river bed
Lake or Tank	Light blue to dark blue	Small/medium to large	Regular to irregular	Smooth to mottled subject to vegetation.	Non-contiguous dispersed, linear for canals	Tanks and lakes in lowlands/surrounded by hills and across river, canals in plains	Amidst cultivated lands, low lands, reservoirs with hilly terrain and rivers, canals with irrigated arable lands
Built-up land	Dark bluish green in the core and bluish on the periphery	Small to big	Irregular & discontinuous	Coarse & mottled	Clustered to scattered & non-contiguous	Plains, plateaus, on hill slopes, deserts, water front, road rail canal etc.	Surrounded by agricultural lands, forest cover, waste lands, network of river, road, rail etc
Fallow land	Yellow to greenish blue	Small to large	Regular to irregular	Medium to smooth	Contiguous to non-contiguous	Plains, valleys uplands etc	Amidst crop land as harvested agricultural fields etc
Degraded or scrub land	Light red to dark brown	Varying in size	Irregular, discontinuous	Coarse to mottled	Contiguous to non-contiguous	Mountain slopes, isolated hills and foot slopes and within notified forest areas	Hill slopes having skeletal soil, different forest types/sub-types and where a biotic interference
Barren rocky/stony waste	Greenish blue to yellow to brownish	Varying in shape	Irregular and discontinuous	Very coarse to coarse and medium	Linear to contiguous and dispersed	Steep isolated hillocks, hill slopes/crest, plateau and eroded plains.	Barren and exposed rock/stony wastes, laterites out-crops, mined areas and quarried sites, boulders

The study of the fault geomorphology involves 3 aspects of faulting *e.g.* (a) types of displacement of rock blocks and thus the resultant fault type; (b) tectonic expression of faulting and (c) geomorphic expression of faulting. The net thickness of fault gauge associated with the shear zone of the large fault depends upon the width of the zone and the characteristics of the small faults spacing ranging from 1 to 3 cm, with the individual faults having gouge zones from 0.1-1cm thick. The hydraulic conductance of a fault should reflect the net thickness and permeability of fault gouge associated with both the shear zones of the fault and the neighboring zones of associated small faults. Active faults act as paths of high permeability and concentrated groundwater flow and stable faults have little influence on flow paths due to secondary mineral deposits. These generalizations will aid in establishing relationship between springs and linear features. The fault itself may play a vital role in transporting or inhibiting water is where there is an overall tensional regional stress field that causes the fault to be much more likely to act as a conduit for flow.

Linear features on the surface on the earth have attracted the attention of geologists for over one hundred years. A lineament is defined as a large-scale linear feature, which expresses itself in terms of topography, which is in itself, an expression of the underlying structural features. This interest has grown most rapidly since the introduction of aerial photographs into geological studies. Geologists have recently proven that various structural features perceived in remotely sensed images are reliable indicators of geologic resources. These structures have been used in many applications: petroleum and mineral exploration, nuclear energy facility siting, geothermal assessments; and water resources investigations. Many scientists have established a relationship between the occurrence of groundwater and fracture traces, and in particular zone of localized weathering and increased permeability and porosity underlying these structures.

Lineaments are important in rocks where secondary permeability and porosity dominate and inter-granular characteristics combine in secondary openings influencing weathering, soil water and groundwater movements. They provide the pathways for groundwater movements and are hydrogeologically very important. Fracture zone forms an interlaced network of high transmissivity and serves as groundwater conduits in massive rocks in inter-fracture areas. Lineament intersection areas are considered as good groundwater potential zones. The combination of fractures and topographically low grounds can also serve as the best aquifers horizons. Geologists have recently proven that lineaments perceived in remotely sensed images are reliable indicators of geologic structures. From the groundwater point of view such features may include, valleys controlled by faulting and jointing, hill ranges and ridges, displacements and abrupt truncation of rocks, straight streams and right angles off setting of stream courses etc.

Folds

Fold geomorphology includes the development of drainage pattern and topographic features due to denudational processes on folded structures. One of the resultant features of

prolonged erosion of folded structure is the development of inversion of relief, i.e. inverted relief characterized by anticlinal valleys and synclinal ridges. Inversion of relief in folded structure is an important but unique phenomenon, which causes reverse sequence of topographic features. Structural influence on groundwater flow suggests that conduits tend to be oriented along structural strike in regions of strongly folded rocks. The nature and lateral and vertical extent of aquifers are controlled by the lithology, stratigraphy and structure of the rock formation. The structural features like fold are the manifestation of repetition and reversal of beds.

Landforms

In general the landforms can be classified as erosional, depositional, denudational and structural. Hydrological characteristics, composition of surface materials, soil conditions, drainage and vegetation pattern, depth of weathered materials which have specific recharging, storing and transmitting capacity are discussed. This would help in knowing the nature and water potentiality of different geomorphic units and landforms for identification of its groundwater prospects zone rating from excellent to poor. The groundwater prospects or various by hydrogeomorphic units and associated landforms can be identified.

The geomorphic surfaces are classified into different morpho-units (Landforms) on the basis of physiographic characteristics, morphological features, relief, slope, drainage density and lithology. These landforms are described below with reference to the groundwater studies point of view.

Erosional Landforms

River Valleys

The development of river valley starts from *splash erosion* by raindrops. It is a very effective method that causes soil erosion. During a torrential downpour, up to 100tons of soil per acre can be dislodged by splash erosion. *Sheet erosion* occurs when overland flow removes soil in uniform thin layers, often resulting in a denuded farm field. Sheet erosion may occur when rainwater completely fills all pore spaces in the soil (saturated conditions) causing enhanced runoff. In areas with a steep slope, runoff from torrential rains can cause *rill erosion.* Sometimes theses rills can develop into *gullies*, steep-walled trenches whose upper end grown progressively upslope. Gullies further develop into long V-shaped valleys.

River Terraces

These are bench like ledges or flat surfaces that occur on the sides of many stream valleys. The narrow flat surfaces on either sides of the valley floor are called river terraces. They represent the level of older floodplains. Sometimes several terraces on either side where the are arranged in step- like forms frequent the river valleys. River terraces are generally formed due to dissection of fluvial sediments of floodplains deposited along a valley floor. The rivers from extensive flood plains during the mature stage and attain their graded curves of profile of equilibrium. The flood plains consist of thick deposition of

alluvium and gravels. The rivers are rejuvenated due to sudden negative change in the sea level. Consequently, the erosive capacity of the rivers increases. Thus rejuvenated rivers deepen their valleys due to accelerated rate of vertical erosion. Now the rivers form their new narrow valley with in former valleys and thus terraces are formed on both the sides. Thus, the river terraces develop in succession over the earlier formed flat valleys.

Meanders

Meander channels forms where streams are flowing over a relatively flat landscape with a broad flood plane. Technically, s stream is said to be meandering when the ratio of actual channel length to the straight-line distance between two points on the stream channel is greater than 1.5. Channels in these streams are characteristically U shaped and actively migrate over the extensive flood plain

Dissected Plateau

An extensive flat top and steep slopes formed over horizondally-layered rocks criss-crossed by fractures/joints/lineaments etc. are called plateaus. Groundwater prospects are good moderate especially at lineament intersections. Deep valleys/gullies developed due to stream/river erosion on plateau and may be criss-crossed by lineaments.

Highly Dissected Plateau

The land of these units is severely dissected by the screams of giving size to a terrain consisting of flat toped ridges and steep scarps. These units can be expressed with reference to the evaluation range, total percentage of the area, morphologic attributes like slopes, runoff characteristics, drainage density, stream frequency and relative relief percentage. Groundwater potential in this unit is very poor. The runoff water can be arrested in the form of check dams and other suitable measures can be taken to boost the pasture, farm forestry and horticulture in these areas.

Moderately Dissected Plateau

These units can be expressed with reference to the evaluation range, total percentage of the area, morphometric attributes like slope, runoff characteristics, drainage density, stream frequently and relative relief percentage. The soils covering these plateau unit are moderately thick, dark brown to black in colour clayey, calcareous, moderate to well drained and high in moisture retentive capacity. Groundwater potential in this unit is moderate to high.

Undissected Plateau

The land of this unit is dissected by the streams of giving rise to undissected terrain consisting of flat-topped hills and steep scarps. These units can be expressed with reference to the elevation range, total percentage of the area, morphometric attributes like slope, runoff characteristics, drainage density, stream frequency and relative relief percentage. Groundwater potential in this unit is very poor. The runoff water can be arrested in the form

of check dam and other suitable measures can be taken to boost the pasture, hilltop forestry and horticulture in these areas.

Mesa and Buttes

These are the erosional features made up essentially of horizontally layered rocks, having a cap of hard and resistant tock that has escaped erosion. A mesa is generally produced in such horizontal layers of alternating characteristics that are exposed to river erosion. The small sized isolated patches of resistant horizontal layers covering the strata below are called buttes. These flat-topped isolated plateaus with steep sided slope at the top has poor groundwater prospect.

Peneplains

Peneplains represent low featureless plain having undulating surface and remnants of convexo-concave residual hills. These are, in fact, the end products of normal cycle of erosion. These are frequented with low residual hills known as monad-nocks, which are left out due to less erosion of relatively resistant rocks.

Pediment

The gently sloping smooth surface of erosional bedrock within veneer of detritus is called pediment. Pediments are noted as narrow scripts adjoining the highly dissected plateau and at foothill zones. Groundwater potential in pediments is poor except along fractures where limited quantity of groundwater can be obtained for domestic purpose.

Inselbergs

These are isolated residual hillocks being remnants of weathering and denudation. Inselbergs are mostly barren, rocky, usually smooth and rounded small hills. From groundwater point of these are all treated neither containing nor transmitting of water, i.e. aquifuge nature. Mostly acts as runoff zone.

Pediplain

This geomorphic unit is developed as a result of continuous processes of pedeplanation. The altitudinal variations is relatively high for rolling plain and this about 5-10 m. in this horizon there exists irregular dissected portions with a number of gully are present. The pediplain with sedimentary rock exposure are generally due to intensive weathering under semi arid climatic conditions representing final stage of the cyclic erosion. These are identified in the imageries with the grey tone on false color composite. Groundwater prospect in this unit is good due to the moderate thickness (15-20m) weathering materials. Pediplains are found to be good for groundwater potentiality. The weathered zone thickness range from 10- 15m. Irrigation in the zone can be done mainly through dug wells.

Shallow Weathered Buried Pediplain

A flat and smooth surface of buried pediplain with thickness of 0 to 5 m consisting of

shallow over burden of weathered derivative material. Groundwater prospects are moderate to poor but open wells yield good amount of potable water after monsoon.

Medium Weathered Buried Pediplain

A flat and smooth surface of buried pediplain with moderately thick 5 to 20 m overburden of weathered derivative material and has good potential for groundwater and less seasonal variations in water table is observed.

Deep Weathered Buried Pedeplain

A flat and smooth surface of buried pediplain with very thick i.e. more than 20m overburden of weathered derivative material and has good potential of groundwater and less seasonal variation in water table is observed. In this unit infiltration is moderately good. The thickness of the weathered zone varies from 10-20m and favours a good amount of water to circulate with in the zone before reaching the deeper fracture zone. Groundwater potential zone is very good and this unit is suitable for dug-well,dug-cum-bore wells and bore wells

Denudational Hills and Residual Hills

Denudational hills are marked by sharp to blunt crest lines with rugged tops indicating that the surface run off at the upper reaches of the hills has caused rill erosion. They can be interpreted from their massive size and glottal to elliptical shape. The rugged topography of this region is due to the erosion of the denudational hills to the plain region, leaving the rock exposed. Groundwater potential is moderate to poor.

Residual hills are the end products of the process of pediplanation, which reduces the original mountain masses in to a series of scattered knolls standing on the pediplain. The more resistant hills stand out prominently under the condition of differential erosion and weathering. The yield of groundwater in this area is very poor.

Structual Landforms

Escarpments

Escarpments are structurally controlled erosional features produced by streams in regions composed of alternating beds of hard and soft rocks. The stream easily erodes the soft layers of rocks were as the hard layers resist the erosion and stand projecting and ledges on the sides. A steep vertical cliff separates the alluvial and hard rock terrain has poor groundwater prospects.

Cuesta

Is the term given to a combined set of escarpments and dip slope occurring adjacently. obviously it results due to prolonged erosion of rocks forming the channel of the river and having an alternate hared and soft rock layers. This unit can be identified on satellite imagery by its darker tone, linear pattern isolated hillocks, parallel pattern o first order channels and

scanty or no vegetation. It exhibits asymmetrical and is controlled by gently dipping strata. In this unit groundwater prospect is poor.

Hogback

It is an erosional feature developed by river action. It is essentially an outcrop of hard resistant rock that is very steeply inclined. In satellite imagery it displays the tonal banding, linear zones, parallel drainage and symmetrical profile. It has erosional slopes on either side. It shows scanty vegetation cover and highly resistant to erosion. It has poor groundwater prospects.

Structural Hills

Structural hills are the linear or arcuate hills exhibiting definite trend lines. These hills are structurally controlled with complex folding, faulting, criss-crossed by numerous joints/fractures which facilitates some infiltration and mostly act as run off zones. The structural hills have poor to nil groundwater prospects because most of rainwater, which falls over them, goes down-slope as run-off.

Depositional Landforms

Soil particles that are removed by overland flow and deposited in the low-lying area forms colluvium. Soil particles that are picked up by streams, carried down streams and later deposited around the stream forms alluvium. Various landforms of depositional origin such as floodplain, alluvial plain, alluvial fan, river sand, ravines, meander scar, point bar deposits, delta etc.

Floodplain (FP)

The flat surface adjacent to stream/river composed of unconsolidated fluvial sediments subjected to periodic flooding in very good for groundwater development. Low lying areas are temporarily water logged during floods. This is the youngest geological unit and includes various landforms formed by fluvial action. This consists of sand, silt and clays and facilities channel bed infiltration. It is a highly permeable zone helping in partial bank recharge and sub surface flow groundwater occurs under semi-confined to perched water table conditions with shallow water levels. Groundwater prospects in floodplains are almost invariably found to be good (Sharma Jugran 1992). In this units are exists all along the Cauvery river course

Along side stream channels are relatively flat areas known as flood plain. Flood plain develops when streams over-top the levees spreading discharge and suspended sediments over the land surface during floods. Levees are ridges found along the sides of the stream channel composed of gravel or sand. Levees are approximately one half to four times the channel width in diameter. Upon retreat of floodwaters, stream velocity is reduced causing the deposition of the alluvium. Repeated flood cycles over time can result in the deposition of many successive layers of alluvial material. Flood plain deposits can raise the elevation of the stream bed. This process is called aggradation.

Flood plains can also contain sediments deposited from the lateral migration of the river channel. This process is common I both braided and meandering channels. Braided channels produce horizontal deposits of sands during times of reduced discharge. In meandering streams, channel migration leads to vertical deposition of point bar deposits. Both braided and meandering channel deposits are coarser than the materials laid down by flooding.

This unit forms the main source of groundwater in the region. Groundwater can be trapped through shallow and deep tube wells in alluvial plains and flood plains. The wells trapping the floodplains generally gives high yield with good quality of water.

Alluvial Plain (AP)

A flat to gently slopping surface formed by river consists of unconsolidated sediments. It has well to excellent prospect and promising zone or shallow unconfined aquifer.

Younger Alluvial Plains

These are primary sediments storage areas, especially on wide valley floors. This geomorphic unit occurs on either side of the major rivers and tributaries.

Older Alluvial Plains

This unit is seen as irregular patches with in the younger flood plains along the river channel. Features associated with this unit are point bar, severe gully erosion in the form of parallel gullies and meander scars. This morpho unit is located at the foot of the pediments.

Alluvial Fan

An alluvial fan is a large fan-shape deposits of sediment on which a braided stream flows over. Alluvial fans develop when streams carrying a heavy load reduce their velocity as they emerge from the mountainous terrain to a nearly horizontal plain. The fan is created as braided streams shift across the surface of this feature depositing sediments and adjusting their course.

Delta

Streams flowing into standing water normally create a delta. A delta is body of sediments that contains numerous horizontal and vertical layers. Deltas are created when the sediment load carried by the stream is deposited because of the sudden reduction of stream velocity. Small shifting channels that carry water and sediments away from the main river channel mark the surface of most deltas.

Deltaic plain is a major geomorphic unit in the areas of old stage of cycle of river erosion. It occupies areas comprising of finer loosely packed sediments. With in the deltaic plain some localized low lying areas, affected by water logging and soil salinity or alkalinity

can be found. The water logging and salinity problems may be due to the rising water level, low-lying topography and seepage from the cannels etc.

Valley Fills

Sediments deposited by stream/river/ narrow valley mostly fracture controlled. The materials in these surfaces consists mainly of weathered products of the surrounding basaltic rocks; mostly comprised moderately thick gravels, pebbles, sand and silt. The prospect varies depending on the thickness of the fills. Valley fill deposits are of good potentials for agriculture.

Valley fills act as good groundwater potential zones and water table is shallow. Valley fills has very good groundwater prospects as it is being recharged by surrounding hills as well as by the river water. Deep bore wells are preferable in these zones for intensive agriculture.

River Sand

Sandy material deposited along stream channel act as very good recharge zone for groundwater.

Ravines

Small narrow, depressions usually carved out by running water. they have poor groundwater yield.

Meander Scars

These are remnants of the highly sinuous paleo-drainage system, which where cut of from the main channel. They can be identified in the satellite imagery by arcuate shape, uniform tone, isolated occurrence, and depressed relief characterized by the loss of hydraulic continuity with parent channel. A crescent shaped scars of meandering stream still discernable on surface has excellent potential for groundwater.

Old Meander

Abandoned meandering loop of river/ streams has excellent potential for groundwater.

Paleo-channels

These are ancient drainage lines of streams or rivers through which it might have flown in past. Paleo channels can be recognized on the satellite imagery by their medium to dark tone. Curvelinear pattern, uniform texture and continuity of older stream. The remnant of the stream / river has buried or abandoned channels which are promising zones for shallow aquifer with excellent groundwater yield.

Coastal Landforms

The most important agents shaping the coastal landforms are waves, which are visible forms of energy produced by any of several processes, such as winds. Waves moves with little loss of energy until they reach shallow areas when the wave steepens and forms breakers. When these waves break against a weak or soft rock type, a marine scarp or marine cliff is produced.

Ria Coast

A ria coast is formed by the submergence of a continental land mass it may also be formed by a rise in sea level, inundating an area that has been dissected by streams. This situation creates many offshore islands that has previously been carved by steams.

Fiord Coast

A fiord coast is similar to the ria coast in that it has formed by the submergence of a land mass or rise in sea level. But valley glaciers had previously carved the area submerged. Hence the fiord coast has few beaches due to the depth of the fiord.

Bach Swamp

Low lying swamp / marshy area adjoining natural levees has good prospect.

Table 5: Relationship between the geomorphology and groundwater prospects in a hard-rock terrain

Land form	Description	Groundwater Prospects
Denudation Hill	Resistant hills resulting due to erosion	Mainly acts as runoff zone
Structural Hill	Linear to arcuate hills	Mainly acts as runoff zone
Pediment	Gently undulating plain, dotted with outcrops with or without veneer of soil	Runoff and recharge zone
Buried pediment-Deep	Pediment covered with thick alluvial material (>20m deep) or unconsolidated weathered rock	Good to moderate
Buried pediment - Moderate	Flat and smooth buried pediment with moderately thick (5-20m) over burden	Good to moderate
Buried pediment-Shallow	Flat and smooth surface of buried pediment with (0-5m) shallow over burden	Moderate to poor

Land form	Description	Groundwater Prospects
Pediment and inselberg complex	Pediment dotted with isolated hills	Acts as a runoff zone
Bajada	Alluvial deposit of varying grain size deposited along the foothill zone.	Forms highly productive shallow aquifers
Flood Plains	Landform adjacent to a river composed of unconsolidated fluvial sediments.	Excellent
Lineament	Fractures on the land surface or buried	Good

Digital Elevation Models as a Data Source

Digital Elevation Models (DEMs) are becoming an increasingly popular tool in many forms of environmental research including geomorphology, hydrology and environmental modelling. A DEM is an important component of hydrological models where it provides the topographic base information. A DEM can provide spatial information about several terrain features such as elevation, slope, aspect, drainage and other terrain attributes. Currently, digital elevation data are derived from one of the following alternative sources: ground surveys, photogrammetric data capture from aerial or satellite remote sensing images, digitized cartographic data, interferometric or stereo SAR or the direct measurement of elevation using LIDAR technology. Each of these sources has advantages and disadvantages in generating DEM. The geologic utility of DEM is best demonstrated when used to understand basin evolution in extensional and compressional tectonic basin regimes. The improved identification and interpretation of geomorphic features from DEMs, integrated with other geological and geophysical data into a geo-spatial database can now be used to test numerical models of mountain front catchment evolution. For hydrogeological studies, DEMs give information on slope, depression, phsiography etc.

CONCLUSION

This write-up has given a brief introduction to the type of surficial information that is required for groundwater studies and that can be derived from remotely sensed images. Such an information can act as a good source of input in a groundwater model or in a GIS model.

REFERENCES

[1] Gupta, R.P., (2005). Remote sensing Geology. Spenger Verlag. Second Edition. New Delhi.

[2] Babar. Md., (2005). Hydrogeomorphology. Fundamentals, applications and techniques. New India Publishing Agency, New Delhi.

[3] Lillesand and Kiefer, (2000). Remote Sensing and Image Interpretation, John Wiley & Sons, New York.

Numerical Simulation of Groundwater Flow and Solute Transport, L. Elango (ed). pp.79-86

Data Requirements for Groundwater Modelling

L. Elango

INTRODUCTION

A groundwater model provides a scientific means to draw together the available data into a numerical characterization of a groundwater system. The model represents the groundwater system to an adequate level of detail, and provides a predictive scientific tool to quantify the impacts on the system of specified hydrological, pumping or irrigation stresses. A groundwater model can be done for various purposes. It is not possible to see into the sub-surface, and observe the geological structure and the groundwater flow processes. The best we can do is to construct bore wells, use them for pumping and monitoring, and measure the effects on water levels and other physical aspects of the system. It is for this reason that groundwater flow models have been, and will continue to be, used to investigate the important features of groundwater systems, and to predict their behaviour under particular conditions. Models also form an integral part of decision support systems in the process of managing water resources, salinity and drainage, and should not be regarded as just an end point in themselves. Once the purpose has been established, the actual characteristics of the model are considered. The various characteristics to be considered developing a groundwater model include area to be modelled, wells to be included in the study aquifers and zones of interest, transport concerns (particle tracking and/or concentrations, transport times), steady-state or transient conditions, units and coordinate system to be used.

Data Collection

Before doing any field survey existing data should be assessed completely as a first step to any hydrogeologic site investigation for data collection. Much of the data necessary for developing a conceptual model may already have been collected during previous investigations of the site. Geologic, hydrologic, geographic, and other data can be obtained from electronic databases and from reports by the government agencies, and state, local, and private organizations. The level of detail desired will also affect the data needs. All data should be critically reviewed to validate their accuracy and applicability to investigation purposes. Data that should be reviewed include the following:

a) Regional hydrogeologic reports.
b) Previous investigations of aquifer and/or surface waters.
c) Available information on groundwater use, including purpose, quantities, and future projections.
d) Boring log data.

e) Cone penetrometer log data.
f) Monitoring well data.
g) Production well data.
h) Well construction characteristics.
i) Geophysical data.
j) Geologic, hydrologic, and topographic maps and cross sections of study area.
k) Aerial photographs.
l) Land use maps.
m) Soil maps.
n) Long-term climatic data.

After through study of the existing data and reports a field reconnaissance survey has to be carried out which will provide a more complete understanding of site hydrogeology and it will provide information on the following.

a) General character of local geology.
b) Prominent topographic features.
c) Location and flow rates of wells and adequacy of local wellhead protection.
d) Nature, volume, flow, and location of surface waters.
e) Nature of any potential surface and sub-surface contamination.
f) Nature and location of any significant impermeable areas.
g) Nature and location of areas of significant vegetative ground cover.

Data Requirements

Modelling studies require a large amount of data. In any king of numerical modelling it is necessary to divide t he study area into a number of cells where in it is necessary to assign various hydrogeological data. Groundwater modelling requires the basic information pertaining to physical framework of model area or domain, aquifer parameters, initial condition, time varying inputs and boundary conditions. However the type of data required might vary slightly according to the purpose for which a model is to be developed. Some of the common purposes fro which groundwater models are developed are give in Table.1.

Table 1: Purposes of groundwater model

Model	Purposes
Improving hydrogeological understanding	Synthesis of data
Aquifer simulation	Evaluation of aquifer behaviour
Designing practical solutions to meet specified goals	Engineering design

Model	Purposes
Optimising designs for economic efficiency and account for environmental effects	Optimisation
Evaluating recharge, discharge and aquifer storage processes	Water resources assessment
Predicting impacts of alternative hydrological or development scenarios	To assist decision-making
Quantifying the sustainable yield	Economically and environmentally sound allocation policies
Resource management	Assessment of alternative policies
Sensitivity and uncertainty analysis	To guide data collection and risk-based decision-making
Visualization	To communicate aquifer behaviour

Physical Frame Work of Model Domain

It is necessary to geomorphological features or land forms of the region and to evaluate the manner and degree in which they contribute to the basin's hydrology. Of, special importance are the areas open to deep percolation, the subsurface areas where inflow or outflow to or from the aquifer occurs, the type of material forming the aquifer system, including its permeable and less permeable confining formations, the location and nature of the aquifer's impermeable base, the hydraulic characteristics of the aquifer, and the location of any structures affecting groundwater movement. Important features like the Topography, basin boundary drainage, river course, canals, channel morphology surface water bodies, reservoirs like tanks, lakes and ponds should be demarcated. This is very important as the model domain or the area to be considered for modelling is based on this study. As model domain requires well defined hydrological boundaries the study has to be carried out with utmost care.

Aquifer Geometry

After identifying the area to be considered for modelling the aquifer type**,** thickness, lateral extent and lithological variation within aquifer have to be assessed. Geological information demarcated from the borehole litholog, depth to water table maps, cross-sections etc must be translated by the geologist to informations pertaining to the water bearing formation (aquifers) and non-water bearing formation (Impermeable or confining layers). The lateral variations, thickness and depth of aquifer may vary from place to place. The lateral extent of the aquifer, as found from well and bore logs, and geophysical data should be indicated on a map. From the same data sources, an isopach (thickness) map of the aquifer can be made. An isopach map requires two horizons, one at the top of the aquifer and one at the bottom. If the aquifer is unconfined, the two horizons are the impermeable base and the land surface. The net thickness of the aquifer can be calculated from the elevations of the

two horizons; local clay lenses within the aquifer, if any, are subtracted from the total thickness.

Aquifer Parameters

The next step is to assemble and evaluate the existing aquifer parameter data for modelling. These data include hydraulic parameters derived from aquifer pumping tests and slug test data, water level measurements (head), chemical concentrations, etc. which need to be collected or generated by field tests. Aquifer parameters such as hydraulic conductivity, transmissivity and storage coefficient are impartment data required for modelling groundwater flow and contaminant transport. In the case of solute transport modelling diffusion and dispersion coefficient of the formation is also need to be determined.

Initial Condition

Solution to a numerical model is possible if we know the initial groundwater head over the entire model domain. Hence, it is necessary that groundwater levels in all the well present in the area have to be measured and given as initial condition Similarly the initial concentration of solutes in the groundwater at all the cells is also necessary.

Time Varying Inputs

Groundwater model requires data related to aquifer recharge and abstraction at every time step in order to simulate the groundwater head over the model domain. Hence to calculate the groundwater recharge hydrometeorological data such as long term rainfall pattern, point of its measurements, evapotranspiration, areal distribution, surface runoff, soil thickness and infiltration rate of soils. Quantum of recharge from rainfall and other surface water bodies has to be given as model input for all the model cells and all time steps to be considered. If solute transport modelling need to be carried out the concentration of recharging water and different times is also required.

Similarly the other difficult task will be to estimate the groundwater abstraction with in the model domain from all the model cells. This can be assessed by the number of wells located in each model cells and determining the approximate of pumping from these wells.

Boundaries and Boundary Conditions

Boundary conditions are mathematical statements specifying the dependent variable (head or the derivative of the dependent variable (flux) at the boundaries of the problem domain. Boundary conditions are necessary to define how the site specific model interacts with entire flow system. It occurs at the edges of the active model area and it will make a piece of computer code a site specific model. Boundaries are largely responsible for how flow occurs in the system. The most likely source of error in the groundwater modelling process occurs while defining false boundary conditions. Physical boundaries of groundwater flow systems are formed by the physical presence of an impermeable body of

rock or a large body of surface water. Other boundaries form as a result of hydrologic conditions. These invisible boundaries are hydraulic boundaries that include groundwater divides and streamlines.

Selecting boundary conditions are a critical step in model design. In steady state simulations, the boundaries largely determine the flow pattern. Boundary conditions influence transient solutions when the effects of the transient stress reach the boundary. In this case, the boundaries must be selected so that the simulated effect is realistic.

Hydrogeologic boundaries are represented by the following three types of mathematical conditions:

Type 1 : Specified head boundaries (Dirichlet conditions) for which head are given.

Type 2 : Specified flow boundaries (Neumann conditions) for which the derivative of head (flux) across the boundary is given. A no-flow boundary condition is set by specifying flux to be zero.

Type 3 : Head dependent flow boundaries (Cauchy or mixed boundary conditions) for which flux across the boundary is calculated given a boundary head value. This type of boundary condition is sometimes called a mixed boundary condition because it relates boundary heads to boundary flows. There are several types of head-dependent flow boundaries.

The location of a boundary condition within the grid is dependent on whether a block-centered finite difference, mesh-centered finite difference, or finite element grid is used. In general it is advisable to use physical boundaries whenever possible. For example a lower impermeable hydrostratigraphic unit can be defined as the lower boundary.

Setting Boundaries

When selecting boundaries the one should visualize the probable flow pattern that will be induced by the boundaries. It is advisable to select physical boundaries whenever possible because they usually are stable features of the flow system. Impermeable rock typically forms the lower boundary of a modelled system. A two order of magnitude contrast in hydraulic conductivity may be sufficient to justify placement of an impermeable boundary. This type of contrast in hydraulic conductivity causes refraction of flow lines such that flow in the higher conductivity layer is essentially horizontal and flow in the lower conductivity layer is essentially vertical. If hydraulic gradients across the boundary are also low, flow out of the higher conductivity layer will be negligible, and the boundary can be considered impermeable. If leakage across the boundary is significant, boundary fluxes or heads can be specified, if known. Otherwise, it will be necessary to simulate the lower conductivity unit and continue down in the sequence until an impermeable lower boundary is found. Surface water bodies that fully penetrate the aquifer form ideal specified head boundaries. Termination of an aquifer at an impermeable rock unit forms a convenient physical no-flow

boundary. Some fault zones and the salt water interface in some coastal aquifers also form ideal no-flow boundaries.

A flow system will usually have a mix of specified head and specified flow boundaries but occasionally the conceptual model of the problem may be formulated entirely with flux boundaries. Steady state problems require at least one boundary node with a specified head in order to give the model a reference elevation from which to calculate heads. In transient solutions, the initial conditions provide the reference elevation for the head solution so that the use of all flux boundaries may be justified for certain types of problems.

In selecting boundaries that do not coincide with regional boundaries, two options are possible:

Distant Boundaries

In a transient simulation, boundaries may be arbitrarily located far from the center of the grid as long as the stresses to the system will not reach the boundaries during the simulation. That is, the assumption is that heads and flows in the vicinity of the boundaries will not change during the simulation.

Hydraulic Boundaries

Hydraulic boundaries that do not coincide with regional boundaries may be defined to create a smaller problem domain. The hydraulic boundaries may be specified head, no-flow, or specified flow boundaries. They are introduced for convenience to mimic the type of flow desired in a portion of the larger problem domain. Boundaries defined in this way are sometimes called artificial boundaries.

Simulating Boundaries

In finite element grids and mesh-centerd finite difference grids, nodes always fall directly on the boundary. In block centered finite difference grids, specified head boundaries are located directly at the node but flux boundaries are located at the outside edge of the block. Values for heads and fluxes at boundaries must be determined from field data. It is usually easier to measure heads; direct measurement of fluxes is possible using seepage meters placed in rivers or lakes or by measurement of baseflow or springflow.

Specified Head

A specified head boundary is simulated by setting the head at the relevant boundary nodes equal to known head values. When the boundary is a river, the head along the boundary is described by constant head conditions. In two dimensional areal simulations, specified head boundary nodes represent fully penetrating surface water bodies or the vertically averaged head in the aquifer at hydraulic boundaries. In profile and full three dimensional models, specified head nodes may represent the water table or surface water bodies.

Specified Flow

Specified flow conditions are used to describe fluxes to surface water bodies, springflow, unsteadyflow, underflow and seepage to or from bedrock underlying the modelled system. Specified flow conditions can also be used to simulate hydraulic boundaries defined from information on the regional flow system. Whenever possible, specified head conditions are selected over specified flow, however, because it is easier to measure head than to measure flow. Specified head conditions are also helpful in achieving calibration. In some situations, however, it may be advisable to use specified flow conditions.

No- Flow Boundaries

No-flow boundaries occur when the flux across the boundary is zero. A no-flow boundary may represent impermeable bedrock, an impermeable fault zone, a groundwater divide, or a streamline. A no-flow boundary also can be used to approximate the freshwater/saltwater interface in coastal aquifers. Groundwater in coastal aquifers discharges to the ocean through a zone of dispersion that forms the saltwater interface.

In a block centered finite difference grid, no-flow boundaries are simulated by assigning zeros to the transmissivities (or hydraulic conductivities) in the inactive cells just outside the boundary. In this way the boundary is set at the edge of the first active block. At no-flow boundaries the flux is simply set equal to zero. Most finite difference and finite element models automatically assume no-flow boundaries around the edge of the model. The user must activate another type of boundary condition to cancel the no-flow boundaries.

CONSISTENT DATA UNITS

To be able to be used in a modelling study, all data must be specified in consistent space and time units (metres and days are accepted standard modelling practice), and to a consistent horizontal and vertical datum. In addition, it is necessary for aquifer head measurements to be reduced to a common datum density (eg. fresh water), and to a standard temperature of 25°C (if temperature differences are significant), so that resulting heads can be contoured meaningfully. The need for consistent units and datum usually means that surveying of bores and other features is required before data compilation can be completed. Consistent units may be given as per the following suggestions.

a) Spatial coordinate and elevation data must be specified to a consistent standard datum.
b) Head measurements should be reduced to a common density (freshwater is suggested) and common temperature (25°C is suggested) datum.
c) Data with a length component should be specified in units of metres.
d) Data with a volume component should be specified in units of cubic metres.
e) Data with a time component should be specified in units of days.
f) Database compilations must explicitly state the units of the data.

IDENTIFICATION OF DATA GAPS

The process of collating data into a form for input to a model usually identifies data gaps, which can be used to guide monitoring efforts, or to modify the modelling objectives to establish achievable outcomes for the available level of data and understanding. The associated data analysis often provides an improved understanding of the groundwater flow system, and is often overlooked and under-resourced in the rush to develop a model. Owing to the initial hydrogeological interpretation, a computer model may be developed by inputting the data to groundwater modelling software, which is essentially a complex, three-dimensional, interactive database, with time variability. Then it is essential to assess whether the available data sources are sufficient to achieve the desired study objective and/or model complexity. If the assessment conclusion is that there is insufficient data or understanding, then the choices are to:

Acquire additional data to support the study objective/complexity.

Reduce the model complexity or commit to staged model development from low complexity to the desired level.

Conclude that a modelling study is not warranted for the time being.

Thus the data required for modelling need to be collected from the existing literature and by hydrogeological field investigation.

Numerical Simulation of Groundwater Flow and Solute Transport, L. Elango (ed). pp.87-96

Numerical Modelling of Solute Transport in a Fracture-matrix System

M. Sekhar

INTRODUCTION

Studies of conservative tracer movement in porous formations exhibiting heterogeneity due to variation in hydraulic conductivity have been the subject of considerable research over the past several years. In these studies focus has been on understanding the effective properties of solute velocity and macrodispersion, since these properties have a major influence on pollutant migration in an aquifer with regard to both dilution of concentrations and first-arrival times of solute at a given location. Transport through fractured rocks deals with special kind of heterogeneity, where the permeability of fractures differs markedly from the rest of the rock matrix. The movement and mixing of solutes in fractured media is of particular interest in an environmental context because of the possibility of very rapid and extensive movement of contaminants through fractures, cracks, or fissures in otherwise low-permeability rock (Gelhar, 1993).

The dual-media approach for analyzing fracture-matrix system is similar to the single continuum framework using an equivalent porous medium in place of fractured system. However, this approach is based on two continuums one for the fracture and the other for the matrix with the fluid and mass transfers between fractures and matrix conceptualized as exchange fluxes between both continuous media. This concept was first developed by Barenblatt et al. (1960) to solve flow problems in fractured porous rocks and later used for transport models (Bibby 1981; Tang et al. 1981; Huyakorn et al. 1983; Bodin et al. 2003) with an assumption that fracture and matrix both possess porosity while flow takes place only in the fracture. Transport equations are written for each medium considering advection-dispersion in fractures and diffusion in the matrix. Both equations are coupled by a sink-source term to account for the exchanges between fractures and matrix (Huyakorn et al. 1983).

Model Simulations in a Dual Porosity Medium

Fig. 1 presents the schematic representation of dual-porosity system characterizing fractured rock formation and the role of solute transport studies in a single fracture-matrix system. Several theoretical and experimental investigations relating to the solute transport in a single fracture have been attempted with emphasis on the following themes: (i) conceptualizing the interacting processes between fracture and matrix, (ii) behavior of hydrodynamic dispersion at the fracture scale due to heterogeneity of flow-velocity field in the fracture for constant as well as varying fracture apertures, (iii) dispersion characterization

and non-Fickian dispersion behavior, (iv) effect of matrix diffusion and channeling, and (v) inclusion of sorption and decay reactions. Kessler and Hunt (1994) provide also analytical expressions for the asymptotic value of the Taylor-Aris dispersion coefficient in partially clogged fractures. The influence of roughness on dispersion has been studied from experimental models (Dronfield and Silliman 1993; Detwiler et al. 1999). The relationship between geometrical characteristics of fracture aperture and hydrodynamic dispersion have been addressed numerically by several authors (Moreno et al. 1988; Amadei and Illangasekare 1994). Gelhar (1993) gave asymptotic dispersion for the case of variable fracture aperture using stochastic-dispersion theory, which compared well with the experiments. Channeling or preferential flow paths were observed to have noticeable effects on dispersion with increased dispersion if the flow paths are almost independent with contrasting velocities (Neretneiks et al. 1982; Lapcevic et al. 1999). Studies were made to estimate dispersion based on the calculation of temporal moments of solute concentration (Rasmuson 1985; Harvey and Gorelick 1995; Rubin et al. 1997). It was observed that hydrodynamic dispersion was either varying with time or with travel distance (Neretneiks 1983; Suresh Kumar and Sekhar 2004). Theoretical and experimental investigations have shown the great influence of matrix diffusion on transport causing slowdown in the migration of the solute and a decrease in the concentration peaks (Maloszewski and Zuber 1993; Zuber and Motyka 1994). Sorption is probably the major factor controlling the movement of many hazardous substances through the vadose zone and in groundwater aquifers. Sorption reactions are found to play a part in the slowdown and retention of solutes in geological formations similar to matrix diffusion, and Bodin et al. (2003) observed that there is a need for distinguishing between sorption and matrix diffusion processes. Cvetkovic et al. (1999) noted that most radionuclides that could be stored in the repository sites are subject to sorption on crystalline rocks. The effect of solute loss to the matrix is found to be profound and it is so significant that the effects of fracture dispersivity variations on the hydrodynamic dispersion in the fracture are completely overwhelmed by the matrix interaction properties. The matrix diffusion concept of transport of fractured geologic media has been the basis of numerous mathematical models. The most widely used model involves

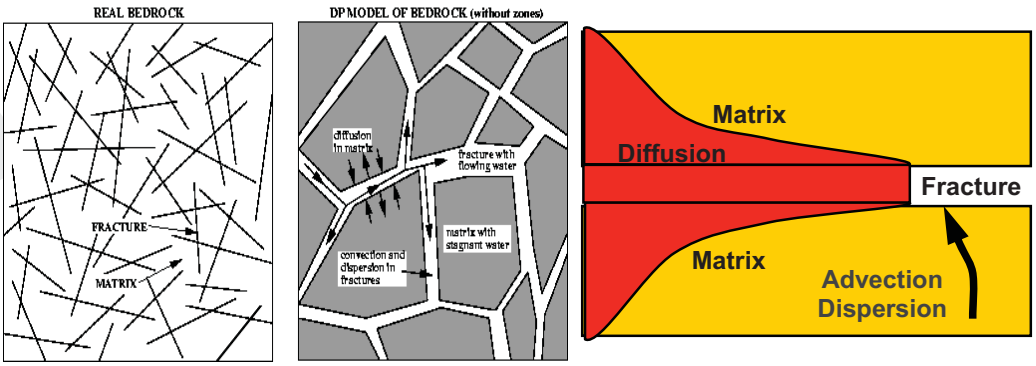

Fig. 1: Schematic representation of fracture-matrix system

advective and dispersive transport in the fracture coupled to diffusive transport into the porous matrix (Tang et al. 1981). This model and its successors have been used successfully to fit a number of field tracer tests in fractured rocks.

If the Fickian regime of dispersion is assumed in the fracture and if the transverse dispersion is neglected as compared to longitudinal dispersion, the volume concentration of solute in the fracture obeys the following 1-D transport equation:

$$R_f \frac{\partial c_f}{\partial t} = -V_o \frac{\partial c_f}{\partial x} + D_L \frac{\partial^2 c_f}{\partial x^2} - a_w \theta_m D_e' \frac{\partial c_m}{\partial y}\bigg|_{y=b} \tag{1}$$

where, $D_L = \alpha_0 V_o + D_m$; $D_e = \theta_m D_e' = F_f D_m$; $F_f = (\theta_m)^p$; and $a_w = \frac{1}{b}$

The equation for the impermeable matrix is given by

$$R_m \theta_m \frac{\partial c_m}{\partial t} = D_e \frac{\partial^2 c_m}{\partial y^2} \tag{2}$$

Here c_f and c_m are the volume concentrations of solute in fracture and matrix respectively (ML^{-3}), t is the time variable (T), x is the space coordinate along the flow direction in the fracture plane (L), y is the space coordinate perpendicular to the fracture plane (L), V_o is the mean groundwater velocity in the fracture (LT^{-1}), 2b is the constant fracture aperture (L), D_L is the hydrodynamic dispersion coefficient in the fracture (L^2T^{-1}) which is sum of molecular diffusion and microdispersion, and its expression is based on Tang et al. (1981), α_0 is the longitudinal dispersivity in the fracture (L), D_m is the molecular diffusion coefficient of the solute in free water (L^2T^{-1}), D_e is the effective diffusion coefficient at the scale of the rock matrix (L^2T^{-1}) which includes effects of porosity through a formation factor F_f (Neretnieks, 1993), θ_m is the matrix porosity, p is the exponent in the empirical relation between the formation factor and matrix porosity which is observed to be 1.57 for crystalline rocks (Sato, 1999) and 2.2 for sedimentary rocks (Boving and Gratwohl, 2001), and a_w is the flow wetted surface (Moreno and Nerernieks, 1993) or the specific surface area (Wels et al., 1996) which is the ratio between wall surface in contact with the solute and the volume of fluid in the fracture plane (L^{-1}). R_f and R_m are the retardation factors in fracture and matrix respectively and are expressed below:

$$R_f = 1 + \frac{K_f}{b} \tag{3}$$

$$R_m = 1 + \frac{\rho_m K_m}{\theta_m} \tag{4}$$

In Eqs. (3) and (4), K_f is the surface sorption coefficient of the fracture (L), ρ_m is the bulk density of the rock matrix (ML^{-3}) and K_m is the volume sorption coefficient of the rock matrix (L^3M^{-1}). Expressions (3) and (4) are valid for instantaneous linear equilibrium sorption.

It is assumed that there is no solute in the system at the start of the experiment and the upstream end in the fracture is subjected to a boundary condition of Dirichlet type with the reference concentration being the concentration in the incoming fluid. For field scale transport, it can sometimes be assumed that fracture extends to a large distance from the solute plume. For computational simplicity at the downstream boundary in the fracture a Neumann boundary condition with zero concentration gradient is assumed to exist all relevant times. This assumption required the location of the downstream boundary such that the concentration front does not reach this location during the simulation time for any of the cases. The initial and boundary conditions associated with equations (1) and (2) for the fracture and matrix respectively (Fig.1) are:

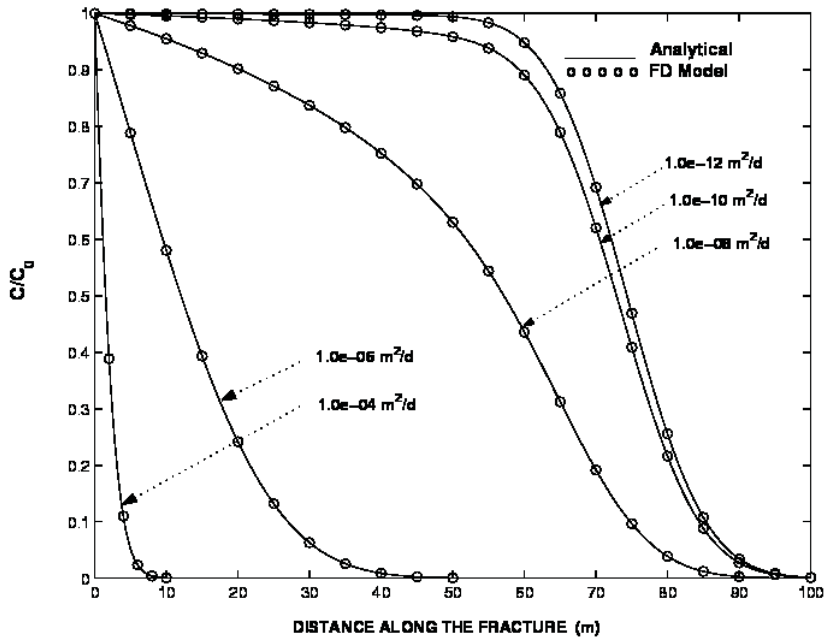

Fig. 2: Solute breakthrough in the fracture for various matrix diffusion coefficients

$$c_f(x,0) = 0\,; c_f(0,t) = c_0\,;\;\; c_f(l,t) = 0 \tag{5}$$

$$c_m(\mathrm{x,y,0}) = 0\,;\;\; c_m(\mathrm{x,b,t}) = c_f(\mathrm{x,t})\;;\;\; \left.\frac{\partial c_m}{\partial y}\right|_{(x,\,B,\,t)} = 0\;;$$

and for b≤ y ≤ B, $\left.\frac{\partial c_m}{\partial x}\right|_{(x=0,\ t)} = 0$, $\left.\frac{\partial c_m}{\partial x}\right|_{(x=l,\ t)} = 0$ (6)

where 2B is the fracture spacing (L), and l is the fracture length in the x space direction (L). Fig. 2 shows the numerically simulated spatial relative concentration profiles with various values of matrix diffusion coefficients in such a system. It is interesting to note that the effect of diffusion coefficient in the matrix plays a significant impact on the characteristics of the concentration profiles in the fracture. The simulated profiles are in good agreement with the analytical results of Sudicky and Frind (1982).

Spatial Moment Equations

Spatial moments describe the location and shape of the solute plume, i.e., the position of the centroid and the spreading around the centroid, and these moments are useful in describing the transport process. The advantage of plume spatial analysis is to permit characterization of the effective dispersion on the basis of the evolution of the concentration spatial moments over time (Bodin et al., 2003). The first spatial moment characterizing the displacement of the center of mass and the second spatial moment characterizing the spread around the center of mass of the solute based on the concentration distribution in the fracture are similar to the solute transport in one-dimensional porous media.

The following are the expressions for these moments using the fracture concentrations:

$$M_o = \int_0^{l'} c(x)dx\ ;\ M_1 = \int_0^{l'} xc(x,t)dx\ ;\ M_2 = \int_0^{l'} x^2 c(x,t)dx \tag{7}$$

and $X_1(t) = \frac{M_1}{M_0}$ and $X_{11}(t) = \frac{M_2}{M_o} - \left(\frac{M_1}{M_o}\right)^2$ (8)

Here M_o is the zeroth moment, X_1 is the first spatial moment, and X_{11} is the second spatial moment. From these moments, the effective properties of the solute velocity, the macrodispersion coefficient and the dispersivity can be obtained using the following expressions:

$$V(t) = \frac{d\{X_1(t)\}}{dt};\ D(t) = \frac{1}{2}\frac{d\{X_{11}(t)\}}{dt};\ \alpha(t) = \frac{1}{2}\frac{dX_{11}(t)}{dX_1(t)} \tag{9}$$

Since a constant continuous source boundary condition is used at the inlet of the fracture in the present study, the spatial moments are obtained using the same approach given by Suresh Kumar and Sekhar (2004).

In this section, the transient behavior of the first and second spatial moments are obtained from the numerical model described in the previous section. This review will discuss the behavior of solute front velocity and solute front dispersivity in the fracture for linearly sorbing solutes. It is observed that the effective solute velocity in the early time is a function of matrix diffusion coefficient, matrix porosity, fracture spacing, local fracture dispersivity and water velocity in the fracture. At larger solute residence time, equilibrium is established between the fracture and the matrix, and the solute velocity attains a steady state. At this asymptotic stage, the solute velocity (V∞) depends only on matrix porosity (θ), fracture porosity (b/L) and water velocity (Vo) and can be expressed as,

$$V_\infty = f\left(V_o, \frac{b}{L}, \theta, R_f, R_m\right) \tag{10}$$

Here b is the half fracture aperture, R_f and R_m are the retardation factors in the fracture and matrix respectively. The solute velocity in terms of the retardation factor can be expressed as,

$$V_\infty = \frac{V_o}{R_\infty} \tag{11}$$

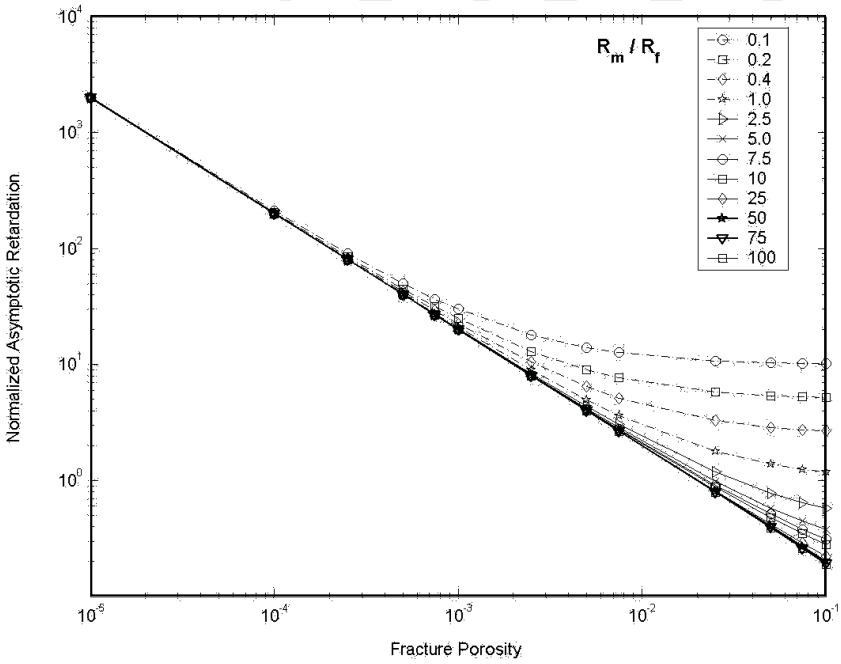

Fig. 3: Plot of normalized asymptotic retardation factor (R∞ /Rm) with respect to fracture porosity (b/L) for a low matrix porosity (θ) of 0.02 such as granitic rocks

Here R_∞ is the asymptotic retardation factor which is always greater than 1 for conservative solutes. It is observed that the following expression describes the behavior of retardation factor in the asymptotic stage.

$$R_\infty = R_f + R_m\,\theta\left(\frac{1}{b/L} - 1\right) \tag{12}$$

Fig. 3 presents a log-log plot of normalized asymptotic retardation (R_∞/R_m) with fracture porosity for the matrix porosity values of 0.02. This values of matrix porosity pertains to the approximate value observed for granite aquifers. In this plot a wide range of ratio of matrix to fracture retardation factors (R_m/R_f) are used to analyze the effect of sorption properties. It may be clearly noticed that two regimes of solute retardation exist based on effects of fracture porosity and ratio of matrix to fracture retardation factor. The effects of the matrix porosity and the matrix retardation factor dominate over fracture porosity and fracture retardation factor when fracture porosity is very small. As fracture porosity increases, matrix porosity and matrix retardation factor still continue to dominate when R_m/R_f is large. However as R_m/R_f becomes smaller and especially when it is less than 1 and as the fracture

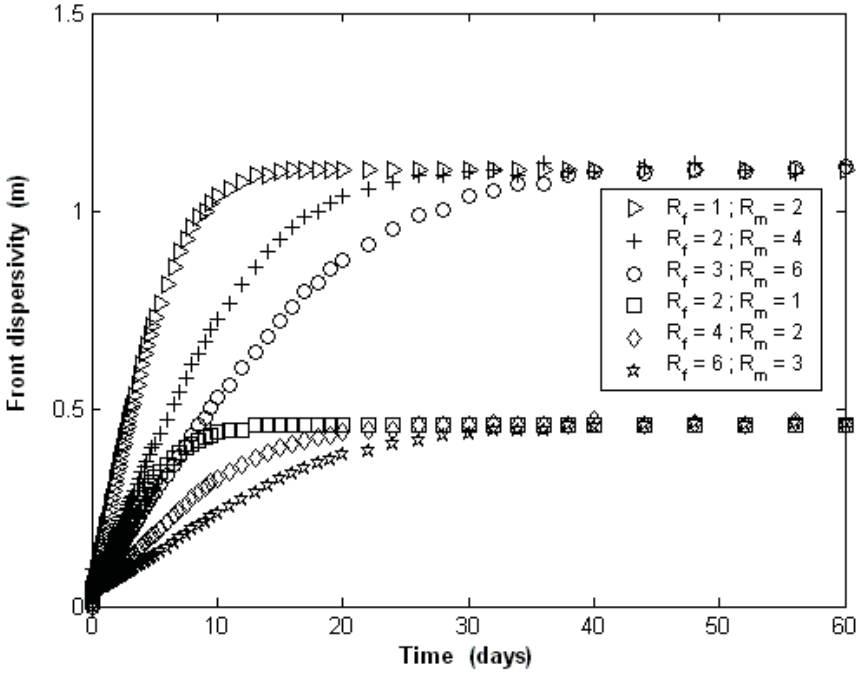

Fig. 4: Temporal variation of effective front dispersivity in the fracture, when surface sorption on the fracture wall and bulk sorption within the rock matrix are present

porosity increases (small fracture spacing), the effect of fracture porosity and fracture retardation factor on the solute velocity is clearly noticed. It is observed that the effect of fracture porosity on the solute velocity (V_∞) is clearly evident when the ratio of fracture porosity to matrix porosity is greater than $0.1R_m/R_f$. Alternatively, matrix porosity alone affects the solute velocity (V_∞) when the ratio of fracture porosity to matrix porosity is less than or equal to $0.1R_m/R_f$ in the case of linearly sorbing solutes.

By analyzing a large range of parameters affecting the fracture matrix system, it is observed that the effective longitudinal dispersivity of the plume in the fracture exhibits two regimes similar to the plume velocity in the fracture. The first regime is characterized as pre-asymtotic behavior wherein a temporal variation of longitudinal dispersivity is noticed while in the second regime, the longitudinal dispersivity has an asymptotic value. The temporal variation of longitudinal solute front dispersivity in the fracture reduces as surface sorption on the fracture walls increase in the absence of bulk sorption within the rock matrix, while the dispersivity increases with increase of bulk sorption in the absence of surface sorption. This shows the contrasting effects of surface and bulk sorption on solute front dispersivity in the fracture in the presence of matrix diffusion. Further it is observed that the asymptotic value of the front dispersivity is maintained a constant as the ratio between surface sorption on the fracture walls and bulk sorption within the rock matrix is a constant. Fig. 4 shows the comparison of asymptotic value of front dispersivity for two ratios of R_f/R_m. It is also observed that the front dispersivity is higher for a smaller value of ratio of surface sorption to bulk sorption. The longitudinal dispersivity is found to be a function of water velocity (V_o), local dispersivity in fracture (α_o), matrix porosity (θ_m), effective diffusion coefficient in the matrix (D_e), and half fracture spacing (B), in addition to the fracture and matrix retardation factors. The expression for the effective longitudinal dispersivity of the solute front in the fracture at asymptotic stage may be given as,

$$\alpha_\infty = \alpha_o + 0.3\, V_o \left(\frac{b}{B}\right)\left(B^2\right)\left(\frac{1}{\theta_m D_e^{'}}\right)\left(\frac{R_m}{R_f}\right) \tag{13}$$

The longitudinal macrodispersion coefficient in the fracture also follows a two regime behavior similar to plume velocity and longitudinal dispersivity in the fracture. The asymptotic longitudinal macrodispersion coefficient in the fracture is found to have the following expression,

$$D_\infty = \alpha_\infty V_\infty \tag{14}$$

By substituting Eqs.(2-4) in Eq.(5), the expression for longitudinal macrodispersion coefficient in the fracture at asymptotic stage for fracture-matrix system can be given as,

$$D_{\infty} = \frac{D_L}{R_{\infty}} + 0.3\, V_o^2 \left(\frac{1}{R_{\infty}}\right)\left(\frac{b}{B}\right)\left(B^2\right)\left(\frac{1}{\theta_m D_e^{'}}\right)\left(\frac{R_m}{R_f}\right) \tag{15}$$

where D_L (= $\alpha_o V_o$) is the longitudinal dispersion coefficient at local scale in the single fracture in the presence of no matrix coupling which is assumed constant. The macrodispersion coefficient in Eq.(6) indicates that it is affected by two terms. The first term pertains to the effective local dispersion coefficient in the fracture and the second term is the additional macrodispersion resulting in a smooth single fracture due to the presence of matrix diffusion.

SUMMARY

The solute transport behavior in fractured rock aquifers is assumed to be modelled by double-porosity model. Based on this concept, the asymptotic behavior of the solute front velocity and solute front dispersivity in the fracture is assessed while considering linearly sorbing solutes. Expressions are provided for solute front velocity, effective solute front dispersivity and macro-dispersion coefficient in such a system.

REFERENCES

[1] Amadei, B. and Illangasekare, T., (1994). A mathematical model for flow and solute transport in non-homogeneous rock fractures, Int. Journal of Rock Mechanics and Mineral Science Geomechanical Abstracts, 31: 719-731.

[2] Barenblatt, G.I., Zheltov, Iu.P. and Kochina, I.N., (1960). Basics concepts in the theory of seepage of homogeneous liquids in fissured rocks, J. Appl. Math. Mechanics. 24, 1286-1303.

[3] Bibby, R., (1981). Mass transport of solutes in dual-porosity media, Water Resources Research, 17(4): 1075-1081.

[4] Bodin, J., Delay, F. and de Marsily, G., (2003). Solute transport in a single fracture with negligible matrix permeability: 1. Fundamental mechanisms, Hydrogeology Journal, 11: 418-433.

[5] Cvetkovic, V., Selroos, J.O. and Cheng, H., (1999). Transport of reactive tracers n rock fractures, Journal of Fluid Mechanics, 378: 335-356.

[6] Detwiler, R.L., Pringle, S.E. and Glass, R.J., (1999). Measurement of fracture aperture fields using transmitted light: an evaluation of measurement errors and their influence on simulations of flow and transport through a single facture, Water Resources Research, 35(9): 2606-2617.

[7] Dronfield, D.G. and Silliman, S.E., (1993). Velocity dependence of dispersion for transport through a single fracture of variable roughness, Water Resources Research, 29(10): 3477-3483.

[8] Gelhar, L.W., (1993). Stochastic Subsurface Hydrology, Prentice-Hall, New Jersey.

[9] Harvey, C.F. and Gorelick, S.M., (1995). Temporal moment-generating equations: modelling transport and mass transfer in heterogenous aquifers, Water Resources Research, 31(8): 1895-1911.

[10] Huyakorn, P.S., Lester, B.H. and Mercer, J.W., (1983). An efficient finite element technique for modelling transport un fractured porous media. 1. Single species transport, Water Resources Research, 19(3): 841-854.

[11] Kessler, J.H. and Hunt, J.R., (1994). Dissolved and colloidal contaminant transport in a partially clogged fracture, Water Resources Research, 30(4): 1195-1206.

[12] Lapcevic, P.A., Novakowski, K.S. and Sudicky, E.A., (1999). The interpretation of a tracer experiment conducted in a single fracture under conditions of natural groundwater flow, Water Resources Research, 35(8): 2301-2312.

[13] Maloszewski, P. and Zuber, A., (1993). Tracer experiments in fissured rocks: matrix diffusion and the validity of models, Water Resources Research, 29(8): 2723-2735.

[14] Moench, A.F., (1984). Double porosity models for a fissured groundwater reservoir with fractured skin, Water Resources Research, Vol.20: 831-846.

[15] Moreno, L., Tsang, Y.W., Tsang, C.F., Hale, F.V. and Neretnieks, I., (1988). Flow and tracer transport in a single fracture: a stochastic model and its relation to some field observations, Water Resources Research, 24(12): 2033-2048.

[16] Neretnieks, I., Erksen, T. and Tahtinen, P., (1982). Tracer movement in a single fissure in granitic rock: some experimental results and their interpretation, Water Resources Research, 18(4): 849-858.

[17] Neretnieks, I., (1983). A note on fracture flow dispersion mechanisms in the ground, Water Resources Research, 19(2): 364-370.

[18] Rasmuson, A., (1985). Analysis of hydrodynamic dispersion in discrete fracture networks using the method of moments, Water Resources Research, 21(11): 1677-1683.

[19] Rubin, Y., Cushey, M.A. and Wilson, A., (1997). The moments of the breakthrough curves of instantaneously and kinetically sorbing solutes in heterogenous geologic media: prediction and parameter inference from field measurements, Water Resources Research, 33(11): 2465-2481.

[20] Sudicky, E.A. and Frind, E.O., (1982). Contaminant transport in fractured porous media: Analytical solutions for a system of parallel fractures, Water Resources Research, 18(6): 1634-1642.

[21] Suresh Kumar, G. and Sekhar M., (2004). Spatial moment analysis for transport of nonreactive solutes in a fracture matrix system, Jl. of Hydrologic Engineering, ASCE (Accepted).

[22] Tang, D.H., Frind, E.O. and Sudicky, E.A., (1981). Contaminant transport in fractured porous media: Analytical solution for a single fracture, Water Resources Research, 17(3): 467-480.

[23] Zuber, A. and Motyka, J., (1994). Matrix porosity as the important parameter of fissured rocks for solute transport at large scales, Journal of Hydrology, 158: 19-46.

Numerical Simulation of Groundwater Flow and Solute Transport, L. Elango (ed). pp.97-106

Guidelines, Documentation and Report Preparation for Groundwater Flow and Solute Transport Models

L. Elango and **M. Senthil Kumar**

INTRODUCTION

Groundwater models are prevalently used in the field of environmental hydrogeology. Groundwater-flow and transport models have been applied to investigate a wide variety of hydrogeologic conditions. Groundwater flow models are used to calculate the rate and direction of movement of groundwater through aquifers and confining units in the subsurface. Fate and transport models estimate the concentration of a chemical in groundwater beginning at its point of introduction to the environment to locations downgradient of the source. Fate and transport models require the development of a calibrated groundwater flow model or, at a minimum, an accurate determination of the velocity and direction of groundwater flow that has been based on field data. A groundwater model developed for a field or site, whether an analytical or numerical model, should be described in sufficient detail so that the model reviewer may determine the appropriateness of the model for the site or problem that is simulated. Submittal of a model documentation report and model datasets (in digital format) is required. The objective of this document is to summaries the steps and procedures that should be followed in the preparation of reports associated with ground investigations.

D.J. Palmer 2 wrote in 1957 on the framework and content of a report:

> *'The essentials to remember regarding content are that the report should be an account of the whole job from start to finish and should contain all the technical facts, good or bad, without reference to any personal administrative difficulties. The best approach is to make generalizations about the problem and then work to the particular, illustrating exceptions to the generalizations. Facts should be given first, theories afterwards. Drawings and sketches often help where words fail.'*

REPORT

Groundwater modelling documentation must detail the process by which the model was selected, developed, calibrated, verified and utilized. The model documentation report must include the following information:

Description of the Purpose and Scope of the Model Application

Groundwater models describe groundwater flow and fate and transport processes using mathematical equations that are based on certain simplifying assumptions. These

assumptions typically involve the direction of flow, geometry of the aquifer, the heterogeneity or anisotropy of sediments or bedrock within the aquifer, the contaminant transport mechanisms and chemical reactions. Because of the simplifying assumptions embedded in the mathematical equations and the many uncertainties in the values of data required by the model, a model must be viewed as an approximation and not an exact duplication of field conditions.

Groundwater models, however, even as approximations are a useful investigation tool that groundwater hydrologists may use for a number of applications. Among these are:

- Prediction of the possible fate and migration of contaminants for risk evaluation.
- Tracking the possible migration pathway of groundwater contamination.
- Evaluation of design of hydraulic containment and pump-and-treat systems.
- Design of groundwater monitoring networks.
- Wellhead protection area delineation.
- Evaluation of regional groundwater resources.
- Prediction of the effect of future groundwater withdrawals on groundwater levels.

Presentation of the Hydrogeologic Data used to Characterize the Site

The simulation of groundwater flow requires a thorough understanding of the hydrogeologic characteristics of the site. The hydrogeologic investigation should include a complete characterization of the following:

Subsurface extent and thickness of aquifers and confining units (hydrogeologic framework). Hydrologic boundaries (also referred to as boundary conditions), which control the rate and direction of movement of groundwater. Hydraulic properties of the aquifers and confining units. A description of the horizontal and vertical distribution of hydraulic head throughout the modelled area for beginning (initial conditions), equilibrium (steady-state conditions) and transitional conditions when hydraulic head may vary with time (transient conditions). Distribution and magnitude of groundwater recharge, pumping or injection of groundwater, leakage to or from surface-water bodies, etc. (sources or sinks, also referred to as stresses).These stresses may be constant (unvarying with time) or may change with time (transient).

Documentation of the Source of all Data Used in the Model, Whether Derived from Published Sources or Measured/calculated from Field / Laboratory Tests

Proper characterization of the hydrogeological conditions at a site is necessary in order to understand the importance of relevant flow or solute-transport processes. With the increase in the attempted application of natural attenuation as a remedial action, it is imperative that a thorough site characterization be completed. This level of characterization requires more site-specific fieldwork than just an initial assessment, including more

monitoring wells, groundwater samples, and an increase in the number of laboratory analytes and field parameters. Without proper site characterization, it is not possible to select an appropriate model or develop a reliably calibrated model. At a minimum, the following hydrogeological and geochemical information must be available for this characterization:

- Regional geologic data depicting subsurface geology.
- Topographic data (including surface-water elevations)
- Presence of surface-water bodies and measured stream-discharge (base flow) data
- Geologic cross sections drawn from soil borings and well logs.
- Well construction diagrams and soil boring logs.
- Measured hydraulic-head data.
- Estimates of hydraulic conductivity derived from aquifer by pumping test or slug test.
- Location and estimated flow rate of groundwater sources and sinks.
- Identification of chemicals of concern in contaminant plume.
- Vertical and horizontal extent of contaminant plume.
- Location, history, and mass loading or removal rate for contaminant sources or sinks.
- Direction and rate of contaminant migration.
- Identification of downgradient receptors.
- Organic carbon content of sediments.
- Appropriate geochemical field parameters (e.g. dissolved oxygen, Eh, pH)
- Appropriate geochemical indicator parameters (e.g. electron acceptors, and degradation by products)

Description of the Model Conceptualization

Model conceptualization is the process in which data describing field conditions are assembled in a systematic way to describe groundwater flow and contaminant transport processes at a site. The model conceptualization aids in determining the modelling approach and which model software to use. Questions to ask in developing a conceptual model include, but are not limited to:

- Are there adequate data to describe the hydrogeological conditions at the site
- In how many directions is groundwater moving
- Can the groundwater flow or contaminant transport be characterized as one-, two- or three-dimensional
- Is the aquifer system composed of more than one aquifer, and is vertical flow between aquifers important
- Is there recharge to the aquifer by precipitation or leakage from a river, drain, lake, or infiltration pond

- Is groundwater leaving the aquifer by seepage to a river or lake, flow to a drain, or extraction by a well
- Does it appear that the aquifer's hydrogeological characteristics remain relatively uniform, or do geologic data show considerable variation over the site
- Have the boundary conditions been defined around the perimeter of the model domain, and do they have a hydrogeological or geochemical basis
- Do groundwater-flow or contaminant source conditions remain constant, or do they change with time
- Are there receptors located downgradient of the contaminant plume
- Are geochemical reactions taking place in onsite groundwater, and are the processes understood

Other questions related to site-specific conditions may be asked. This conceptualization step must be completed and described in the model documentation report.

Identify the Model Selected to Perform the Task, Its Applicability and Limitations

After hydrogeological characterization of the site has been completed, and the conceptual model developed, computer model software is selected. The selected model should be capable of simulating conditions encountered at the site. The following general guidelines should be used in assessing the appropriateness of a model:

Analytical Models should be Used Where

- Field data show that groundwater flow or transport processes are relatively simple.
- An initial assessment of hydrogeological conditions or screening of remedial alternatives is needed.

Numerical Models should be Used Where

- Field data show that groundwater flow or transport processes are relatively complex.
- Groundwater flow directions, hydrogeological or geochemical conditions, and hydraulic or chemical sources and sinks vary with space and time.

One-dimensional Groundwater Flow or Transport Model should be Used Primarily for

- Initial assessments where the degree of aquifer heterogeneity or anisotropy is not known.
- Sites where a potential receptor is immediately downgradient of a contaminant source.

Two-dimensional Models should be Used for

- Problems which include one or more groundwater sources/sinks (e.g. pumping or injection wells, drains, rivers, etc.),

- Sites where the direction of groundwater flow is obviously in two dimensions (e.g. radial flow to a well, or single aquifer with relatively small vertical hydraulic head or contaminant concentration gradients),
- Sites at which the aquifer has distinct variations in hydraulic properties,
- Contaminant migration problems where the impacts of transverse dispersion are important and the lateral, or vertical, spread of the contaminant plume must be approximated.

Three-dimensional Flow and Transport Models should Generally be Used Where

- The hydrogeologic conditions are well known,
- Multiple aquifers are present,
- The vertical movement of groundwater or contaminants is important.

The rationale for selection of the appropriate model software should be discussed in the model documentation report. The choice of model software program for use at a site is the responsibility of the modeler. Any appropriate groundwater flow or fate and transport model software may be used provided that the model code has been tested, verified and documented. However, it is recommended that the model developer contact the Groundwater Modelling Program at the beginning of the investigation to discuss the selection of appropriate model software.

Summary of All Model Calibration, History Matching and Sensitivity Analysis Results

Model Calibration

Model calibration consists of changing values of model input parameters in an attempt to match field conditions within some acceptable criteria. This requires that field conditions at a site be properly characterized. Lack of proper site characterization may result in a model that is calibrated to a set of conditions which are not representative of actual field conditions. The calibration process typically involves calibrating to steady-state and transient conditions. With steady-state simulations, there are no observed changes in hydraulic head or contaminant concentration with time for the field conditions being modelled. Transient simulations involve the change in hydraulic head or contaminant concentration with time (e.g. aquifer test, an aquifer stressed by a well-field, or a migrating contaminant plume). These simulations are needed to narrow the range of variability in model input data since there are numerous choices of model input data values which may result in similar steady-state simulations. Models may be calibrated without simulating steady-state flow conditions, but not without some difficulty. At a minimum, model calibration should include comparisons between model-simulated conditions and field conditions for the following data:

- Hydraulic head data,
- Groundwater-flow direction,
- Hydraulic-head gradient,
- Water mass balance,
- Contaminant concentrations (if appropriate),
- Contaminant migration rates (if appropriate),
- Migration directions (if appropriate), and
- Degradation rates (if appropriate).

History Matching

A calibrated model uses selected values of hydrogeologic parameters, sources and sinks and boundary conditions to match field conditions for selected calibration time periods (either steady-state or transient). However, the choice of the parameter values and boundary conditions used in the calibrated model is not unique, and other combinations of parameter values and boundary conditions may give very similar model results. History matching uses the calibrated model to reproduce a set of historic field conditions. This process has been referred to by others as "model verification". The most common history matching scenario consists of reproducing an observed change in the hydraulic head or solute concentrations over a different time period, typically one that follows the calibration time period. The best scenarios for model verification are ones that use the calibrated model to simulate the aquifer under stressed conditions. The process of model verification may result in the need for further calibration refinement of the model. After the model has successfully reproduced measured changes in field conditions for both the calibration and history matching time periods, it is ready for predictive simulations.

Sensitivity Analysis

A sensitivity analysis is the process of varying model input parameters over a reasonable range (range of uncertainty in values of model parameters) and observing the relative change in model response. Typically, the observed changes in hydraulic head, flow rate or contaminant transport are noted. The purpose of the sensitivity analysis is to demonstrate the sensitivity of the model simulations to uncertainty in values of model input data. The sensitivity of one model parameter relative to other parameters is also demonstrated. Sensitivity analyses are also beneficial in determining the direction of future data collection activities. Data for which the model is relatively sensitive would require future characterization, as opposed to data for which the model is relatively insensitive. Model-insensitive data would not require further field characterization.

Present All Model Predictive Simulation Results as a Range of Probable Results Given the Range of Uncertainty in Values of Model Parameters

A model may be used to predict some future groundwater flow or contaminant transport

condition. The model may also be used to evaluate different remediation alternatives, such as hydraulic containment, pump-and-treat or natural attenuation, and to assist with risk evaluation. In order to perform these tasks, the model, whether it is a groundwater flow or solute transport model, must be reasonably accurate, as demonstrated during the model calibration process. However, because even a well-calibrated model is based on insufficient data or oversimplifications, there are errors and uncertainties in a groundwater-flow analysis or solute transport analysis that make any model prediction no better than an approximation. For this reason, all model predictions should be expressed as a range of possible outcomes which reflect the uncertainty in model parameter values. The range of uncertainty should be similar to that used for the sensitivity analysis.

The growth in errors resulting from projecting model simulation into the future need to be evaluated by monitoring field conditions over the time period of the predictive simulation or until appropriate cleanup criteria has been achieved. There is always some degree of uncertainty in predictive models. Predictive models should be conservative. That is, given the uncertainty in model input parameters and the corresponding uncertainty in predictive model simulations, model input values should be selected which result in a "worst-case" simulation. Site-specific data may be used to support a more reasonable worst-case scenario. Or stated another way, site-specific data should be collected to limit the range of uncertainty in predictive models.

MODELLING DOCUMENTATION MAY BE REPORTED

The organization of the report should include the following sections:

- Title Page
- Table of Contents
- List of Figures
- List of Tables
- Introduction
- Objectives
- Hydrogeologic Characterization
- Model Conceptualization
- Modelling Software Selection
- Model Calibration
- History matching
- Sensitivity Analysis
- Predictive Simulations or Use of Model for Evaluation of Remediation Alternatives
- Recommendations and Conclusions
- References

- Tables
- Figures
- Appendices

TABLES

The following is a list of tables that should appear within the body of the model documentation report or in attached appendices:

- Well and boring log data including:
- Name of all wells or borings,
- Top of casing elevation,
- Well coordinate data,
- Well screen interval,
- Hydraulic head data,
- Elevation of bottom of model,
- Hydraulic conductivity or Transmissivity, and
- Groundwater quality chemical analyses (if appropriate).
- Aquifer test or slug test data.
- Model calibration and verification result showing a comparison of measured and simulated calibration targets and residuals.
- Results of sensitivity analysis showing the range of adjustment of model parameters and resulting change in hydraulic heads or groundwater flow rates.

Other data, not listed above, may lend itself to presentation in tabular format. Where appropriate, the aquifer for which the data apply should be clearly identified in each table.

FIGURES

The following is a list of the types of figures (maps or cross sections) which should be included in the model documentation report:

- Regional location map with topography.
- Site map showing soil boring and well locations, and site topography.
- Geologic cross sections.
- Map showing the measured hydraulic-head distribution.
- Maps of top and/or bottom elevations of aquifers and confining units.
- Areal distribution of hydraulic conductivity/transmissivity.
- Map of areal recharge (if appropriate).

- Model grid with location of different boundary conditions used in the model.
- Simulated hydraulic-head maps.
- Contaminant distribution map(s) and/or cross sections showing vertical distribution of contaminants (if appropriate).
- Map showing simulated contaminant plume distribution (if appropriate).

Other types of information, not listed above, may be presented in graphic format. Figures that are used to illustrate derived or interpreted surfaces such as layer bottom elevations and hydraulic-head maps should have the data used for the interpolation also posted upon the figure. As an example, measured hydraulic-head maps should identify the observation points and the measured hydraulic-head elevation. Similarly, the simulated hydraulic-head maps should locate the calibration target points and the residual between the measured and modelled data.

All figures should provide the following information:

- North Arrow
- Date of figure preparation and data collection
- Title Bar
- Scale Bar
- Legend

All maps or cross sections should be drawn to scale with an accurate scale clearly displayed on each figure. When feasible, all figures should be the same scale. Figures that apply to specific aquifers should be clearly labeled.

ADDITIONAL DATA

Additional data may be required to be presented in the model documentation report. Examples of additional data are as follows:

- Additional studies work plans providing for the collection of additional data where model simulations show data deficiencies, and
- Groundwater monitoring plans/proposals/recommendations to collect data needed to verify model predictions.

Other data may be required, depending on the conditions at the site. These additional subjects should be addressed within the body of the report. This may include additional figures and tables, or report sections.

REFERENCES

[1] American Society for Testing and Materials (ASTM), Standard Guide for Defining Boundary Conditions in Ground-Water Flow Modelling. ASTM Standard D 5609-94, 4 p.

[2] ASTM, Standard Guide for Developing Conceptual Site Models for Contaminated Sites. ASTM Standard E 1689-95, 8 p.

[3] ASTM, Standard Guide for Application of a Ground-Water Flow Model to a Site-Specific Problem. ASTM Standard D 5447-93, 6 p.

[4] ASTM, Standard Guide for Subsurface Flow and Transport Modelling. ASTM Standard D 5880-95, 6 p.

[5] Anderson, M.P. and W.W. Woessner, (1992), Applied Groundwater Modelling. Academic Press, Inc., San Diego, CA., 381 p.

Numerical Simulation of Groundwater Flow and Solute Transport, L. Elango (ed). pp.107-129

Simulation Studies for Formulation of Groundwater Development Strategies in Waterlogged Areas of Hirakud Command Area, Orissa – A Case Study

S. Suresh

INTRODUCTION

The current irrigational practices in many parts of India are resulting in rise of water table and large areas are threatened by water logging and soil salinity. Water logging coupled with soil salinity contributes to progressive reduction in the agricultural production. In the canal command areas, there is usually an excess of water availability in head reaches and shortage in tail reaches, which also affect the agricultural production adversely. In order to sustain productivity and provide additional supply of water to the tail end areas, it becomes essential to develop both groundwater and surface water resources judiciously in conjunction.

In Hirakud Command Area, the canal irrigation system since 1960 has resulted in continuous rise of water table and large areas have become water logged. The water logging can be tackled by reducing surface water supply and utilization of groundwater in the area.

The coordinated and planned use of surface water and groundwater, whereby water is conserved is referred as Conjunctive Use (Todd, 1980). The conjunctive use plan takes into consideration the following.

A. Determination of
   i) Availability of surface water in space and time
   ii) Availability of groundwater in space and time
   iii) Demand for irrigation, domestic and industries.
B. Matching of Demand and Availability
C. Identification of critical water shortage/water surplus area
D. Development of mathematical model for simulation studies.
E. Groundwater Development Strategies in the light of simulation model
F. Economic Analysis of Conjunctive Use Plan
G. Operationalisation of Conjunctive use plan

In the present work, groundwater development has been suggested in the water logged area and the effect of groundwater development plan has been studied using aquifer response model.

REVIEW OF LITERATURE

The conjunctive use planning can be carried out using optimization approach or simulation approach or a combination of both. In the optimization approach, optimal solution is sought for a set of given constraints, where as in simulation approach, different strategies are tested by trail and error method and a best among the tested strategies are used. In the combined approach, both optimization and simulation are linked so that the laborious procedures of trial and error method are avoided. The review of work done is given separately for all the three approaches.

Optimization Approach

Coskunoglo and Shetty (1981) presented a mathematical programming model for conjunctive development of surface water and groundwater resources. The surface water has been used for power generation, irrigation and aquifer recharge purposes with the consideration of the downstream mandatory requirements. A confined aquifer has been developed for irrigation purpose only. The design and operation decisions have been considered simultaneously. Willis et al (1989) presented a conjunctive use of surface water and groundwater planning model for Yucheng country in China. The optimization model maximized the net revenues generated from existing cropping pattern over one year period. The groundwater response equations have been developed using finite element method and they have been used as constraints in the planning models. The results have been compared with that of the present allocation pattern. Onta et al (1991) suggested three steps modelling for conjunctive use of surface water and groundwater. As a first step long term operational policies are determined by stochastic dynamic programming model. In the second step, lumped simulation model is used to evaluate the alternatives. Finally, a multiple criteria decision making method is to be used to arrive at a satisfactory plan for deciding pumpage and water allocation policies.

Simulation Approach

Bredehoeft and Young (1970) suggested simulation approach for determining optimal temporal withdrawal policies for groundwater basins. They opined that the interdependency among the users could lead to inefficient allocation of groundwater resources over time in the absence of any regulation. Young and Bredehoeft (1972) formulated simulation models extending their work by including economic model, which represents the response of users to water supply and cost. However, the model does not provide optimal solution directly but can yield an objective function for each alternative. Singh et al (1984) used groundwater simulation model to predict dynamic behavior of water table in response to pumpage and net recharge in parts of Lower Ghagger basin in Haryana. In last two decades, the land use of

major portions of Ghagger river basin has been transformed from dry land farming to irrigated farming. The pumped water has been proposed to be used in conjunction with canal water for irrigation, considering the quality constraints. The study has been conducted to determine the management policies for controlling the rise of water table. Gupta et al (1985) have made a quantitative study of conjunctive use of surface water and groundwater to arrest water level decline in Dahi region using an interactive finite difference aquifer model. Illangasekhare and Morel-seytoux (1986) discussed about a stream-aquifer model to evaluate different conjunctive use strategies in the south latte river in Colorado using a discrete kernel approach. Kadi (1989) enumerated different techniques employed to simulate infiltration and subsurface flows for a number of available water shed models and conjunctive use models. Latifs and James (1991) presented conjunctive use model to arrest water logging and salinisation. The salt distribution in the root zone has been modelled and its effect on crop yield has been included in the model. Chawas-Morales et al (1992) used a simulation model for planning the conjunctive use of irrigation water from multipurpose reservoir and an aquifer for allocation of cropped area. Singh (1996) has carried out conjunctive use studies in Raipur-Luni command, in the Pali district of Rajasthan. He has suggested groundwater pumpage to alleviate water quality problem in the command area and at the same time use the withdrawn water to artificially recharge the aquifer outside the command area, showing depleting groundwater resources. The stresses created due to the groundwater pumpage within the command area have been studied using aquifer response model through IADIE scheme of solving the governing finite difference equations.

Approach Combining Optimization and Simulation

Prasad (1988) evolved an optimal operational strategy to augment the Firm Yield in the state of California. The author utilized a reservoir simulation model (Modified HEC3) in conjunction with an optimization model. Khare (1994) attempted distributed modelling for conjunctive use in a command area. He has combined Linear programming techniques with simulation model to arrive at the optimal policy. Ejas and Peralta (1995) have presented a simulation/optimization model to address the increasingly common conflicts between water quality and quantity objectives, maximizing steady conjunctive use of surface water and groundwater resources, maximizing waste loading from a sewage treatment plant to the stream without violating downstream quality. CGWB (1996) used the simulation model (MODFLOW, PM3) to evolve an optimal conjunctive use plan to increase the cropping intensity in the Hirakud command area. Linear programming technique has been used to increase the cropping intensity and the effect of groundwater development plan has also been studied in the simulation model.

BACKGROUND INFORMATION

The area of study comprised of a part of Hirakud Command of Orissa, situated within the North Latitudes 20°53';21°36' and East Longitudes 83°25';84°00' (Fig 1). The area is characterized by gently undulating topography dotted with low scattered residual hillocks

interspersed with low linear ridges. The elevation of land surface varies from 180 to 120 m above Mean Sea Level. The general slope is towards southeast.

The surface drainage of the command area is mainly controlled by Mahanadi River and its tributaries. The Mahanadi River has roughly southerly course while the tributaries have southeasterly flow direction. The Mahanadi River is perennial while the tributaries are ephemeral. The drainage is generally effluent in nature.

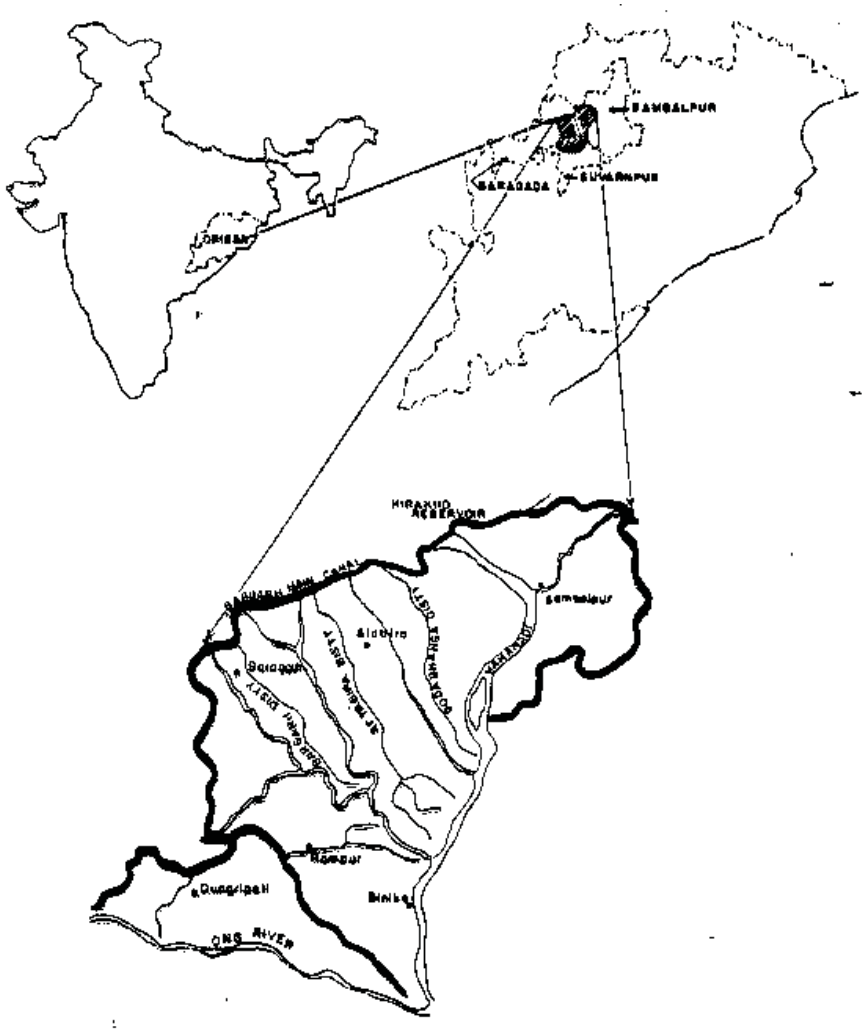

Fig. 1: Location Map of Hirakud Command Area

The rainfall in the area is mainly due to southwest monsoon. The average annual rainfall is in the order of 1500 mm, about 90% of which is received during Mid June to Mid October.

There are two principal crops grown in the area i.e., Kharif (June to October) and Rabi (Mid November to Mid April). The major kharif crops are paddy, sugarcane etc covering about 117917 Ha. The Rabi crops are paddy, oil seeds and pulses covering about 81882 hectares.

Irrigation is provided through a network of canals of Hirakud Canal system by gravitational flow. The distribution system comprises of two main canals, namely Bargarh on right bank and Sason on left bank, two branch canals, named as Attabira and Retamunda and a large number of distributaries, minors, sub-minors, water courses etc. the canals are mostly unlined and method of irrigation is by field to field flooding. The irrigation intensity varies from 162% to 175%.

Major parts of the study area are underlain by hard crystalline rocks of pre-Cambrian age. The most common rock types are granite, granite gneiss, charnockite, quartzite, quartz-mica schist etc. The country rocks are traversed by a number of dolerite dykes and veins of quartz and pegmatites. Recent alluvium occurs as thin discontinuous patches along river tributaries. Laterites occur as capping over the older rocks and occupy high land areas.

The weathered residuum and the fracture zones constitute main repository of groundwater. Ground water occurs under phreatic condition in the weathered residuum and under semi confined to unconfined conditions in the fracture zones.

Granite and granite gneisses generally occupy the undulating plains and are intensely weathered and highly jointed. The weathered residuum ranges in thickness from 10 to 30 m, average being 15 m and forms the phreatic aquifers suitable for development though open wells with the average yield being 5 lps.

Quartzites and Quartz Mica Schists form low hills & linear ridges and are very hard and resistant to weathering. There is paucity of well developed joint planes and thickness of weathered zone is also very less and is of the order of 5 to 8 m. Ground water development potential of these formations is poor. The yield of open wells located in these formations is less than 3 litres/second and yield of shallow bore wells down to 100 m depth is less than 5 litres/second.

Laterites and Alluvium locally form shallow aquifers suitable for exploitation by means of open wells.

The drilling data of the study area indicates that on an average 12 to 15 m of weathered zone occur in different boreholes underlain by fractured and massive rocks. Generally three to four water saturated fracture zones have been encountered within a depth of 100 m beyond

which the fractures are not very common. It is also observed that there is wide variation in occurrence and distribution of the fracture zones both laterally and vertically.

Depth to water level in the phreatic zone has been monitored on monthly basis through Key observation wells. The depth to water level varied from 0.80 to 9.70 m below land surface during pre monsoon period (June'93) and 0.3 to 4.03 m below land surface during post monsoon period (November'93). During the month of August'93 depth to water levels in most of the wells was recorded to be within 2 m below land surface.

Seasonal fluctuation of water level in the command area ranges from 0.02 m to 7.48 m, average being 2 m. In the high land wells seasonal fluctuation was recorded to be more than that of low land wells. Major part of the area had 2 to 4 m fluctuation (Sar et al., Op cit.)

OBJECTIVE OF THE STUDY

To identify the areas with development of groundwater mounds if any and thereby demarcate the areas where water logging conditions prevail or where the water table is showing a rising trend. Further, use modular three dimensional finite difference groundwater flow model developed by USGS (MODFLOW) for simulation of groundwater conditions in the area. Keeping in view the existing recharge conditions, different groundwater development strategies in the shallow water table areas are to be tested and the response of the aquifer to these different strategies to be studied.

METHODOLOGY

In any water management problem, the determination of water balance is a prerequisite. The study of water balance may involve use of surface water balance and groundwater balance equations. The latter is a specialized form of water balance equation that requires quantification of the terms of inflow and outflow from the groundwater regime as well as of changes in storage therein. As an initial exercise, water balance for the whole command area as a lumped model has been computed to ascertain the different recharging and discharging components. After the validation of lumped model, the distributed model has been considered to incorporate the variation in aquifer parameters, recharge and discharge components in the study area.

Groundwater Balance for Lumped Model

The equation for groundwater balance can be expressed as follows

$$R_r + R_c + R_i + R_d + S_i + I_g = E_l + T_p + S_e + O_g \pm \Delta S \quad (1)$$

Where,

R_r - Recharge from rainfall

R_c - Recharge from surface water bodies

R_i - Recharge from field irrigation
R_d - Recharge from depression storage
S_i - Influent seepage from rivers
I_g - Inflow from across the boundary
E_1 - Evapotranspiration
T_p - Draft from groundwater storage
S_e - Effluent seepage to the rivers
O_g - Outflow across the boundary
ΔS - Change in groundwater storage

In the present study, the groundwater balance has been carried out separately for Rabi and Kharif seasons for the year 1993-94. the area is bounded by ridge canals and rivers as boundary and hence it can be safely assumed that the inflow into the aquifer across the boundary is negligible.

Estimation of Different Components of Water Balance

The area is characterized by hard crystalline formations, comprising weathered residuum and fractured rock. It has been found in general, in the immediate vicinity of shallow fractures, a highly weathered zone due to the more circulation of water. Hence three layers have been considered for this area but modelling has been attempted only for the top layer due to the paucity of data for the other two layers.

I. Rabi Season

A. Discharge components

(i) Draft (T_p) : The unit draft of different groundwater structures has been taken as per the norms of Groundwater Estimation Committee (G.E.C, 1984) and the number of structures multiplied by the respective unit draft had yielded the total draft.

(ii) Evapotranspiration (E_1) : It is considered that the evapotranspiration is equal to the Potential Evapotranspiration (PET) in the area characterized by water table between 0-1 m bgl and evapotranspiration is equal to 50% of PET in the zone characterized by water table between 1-2 m bgl, while evapotranspiration is equal to 25% of PET in the zone characterized water table between by 2-3 m bgl. Accordingly, evapotranspiration in different months have been calculated by multiplying the areas of different water table zones with that of their corresponding P.E.T values and have been summed up to get the seasonal figure of evapotranspiration taking place in the area.

(iii) Outflow from the Aquifer (S_e) : The area is bounded by either canals or rivers. The Ong River in the south forms the southern boundary while the Mahanadi dividing the area into two parts forms a boundary for the parts of the area in the east. The watertable

contours in various months depicts the groundwater gradient towards the rivers. The quantum of baseflow has been computed using the Darcy's Law

$$Q = T * i * L * \text{No. of days} \quad (2)$$

Where,

Q = baseflow

T = transmissivity

L = length of the boundary across which flow takes place

i = hydraulic gradient

An average value of T and L along the length of the river has been considered and outflow has been determined for Rabi and Kharif seasons.

B. Change in storage (ΔS)

The watertable fluctuation map has been drawn (Nov 1993 - May 1994) and the change in storage has been calculated as follows:

$$\Delta S = W.T.F * A * S_y$$

where,

ΔS = change in storage

W.T.F = watertable fluctuation

A = area of each watertable zone

S_y = specific yield (An average of 2.5% has been taken for this purpose)

C. Recharge Components

(i) Canal seepage (R) : The length, wetted perimeter of each canal in the entire canal system, rate of flow and the period of flow are the data required for seepage calculation. Further the seepage is a function of the position of watertable in the vicinity of the canal. The change in the daily flow results in a change in the wetted perimeter. The length and bed width of the canal system are constant while the depth of the flow is a variable. The actual depth of flow is not available while the actual volume of the flow is available. Under these circumstances, the depth of flow is assumed to be in proportion to the actual discharge. The actual depth is obtained by multiplying the designed depth with the ratio of actual discharge and designed discharge. The actual wetted area is computed using the following expression:

$$A = L * (W + 2\,\text{sqrt}(1 + S^2)\, D * (Q_f/Q_d) \quad (3)$$

Where

A =Actual wetted area

L =Length of the canal

W =Bed width of the canal

S =Side Slope of the canal

D =Designed depth of flow

Q_f =Actual discharge in the canal

Q_d =Designed discharge of the canal

The seepage factor for different type of soil given in the report of G.E.C has been utilized for the computation seepage losses.(G.E.C., Op.cit.). the wetted area of the canal multiplied by the seepage factor gives the seepage losses from the canal system.

It is considered that the seepage in the area characterized by watertable between 0 – 1 m bgl would be negligible as the watertable is already high. Accordingly, figures of the seepage losses have been revised.

(ii) Rainfall recharge (Rr): The rainfall being negligible in the rabi season, it is supposed that the rainfall will go towards replenishing the soil moisture deficit and the recharge is taken as zero.

(iii) Return flow from Irrigation (R_i): The ministry of irrigation, Water Management Division, Govt. of India has prepared a manual giving guidelines to estimate Irrigation Water Requirements, (Saxena, 1984). The procedures/guidelines given in the manual have been used in the estimation of Irrigation Water Requirements. The irrigation is carried out predominantly by the canal in the command area but however the total Crop Water Requirements (CWR) for the existing cropping pattern was found to be more than the canal water supply made for the irrigation. The irrigation water applied at the Head reaches, flow down toward Tail reaches as lateral flow. This regeneration has resulted in more area being irrigated with the existing canal supply. Hence, the CWR has been proportionately reduced as per the canal water supply and return flow from irrigation has been calculated a follows:

$$\text{Total Outflow } (O_t) = S_e + E_t + T_p \quad (4)$$

$$\text{Total Recharge } (R_t) = O_t + S \quad (5)$$

$$R_i = R_t + R_c \quad (6)$$

$$\% \text{ of } R_i = [R_i/\text{CWR (corrected]} \quad (7)$$

II. Kharif Season

The discharge components have been computed in the similar way as that of Rabi season. The change in the storage has been calculated from the watertable fluctuation of June 1993-Nov.1993). The % of return flow from irrigation computed during rabi has been utilized to determine the Ri during Kharif season. Thus the total recharge has been computed using the equation no.4.6.

The rainfall recharge has been computed as follows

$$R_r = R_t - (R_c + R_i) \quad (8)$$

$$I.F = R_f/(A_g * \text{Monsoon rainfall}) \quad (9)$$

Where

I.F = infiltration factor

A_g = area suitable for groundwater recharge

If the infiltration factor so computed falls within the range reported in the literature, then the assumption made for various components in the computations may be justified.

Water Balance for Distributed Model

Conceptualization of Model

A model is a device that represents approximately the field conditions. A mathematical model simulates groundwater flow indirectly by means of governing equations thought to represent the physical process that occur in the system, together with equations that describe heads or flows along the boundary of the model (Anderson and Woessner, 1992). The mathematical model can be solved either analytically or numerically. A numerical model is useful in the case of non homogeneous terrain where the variation in the properties is to be included to approximate the field situations. The model allows more effective use of available data; more complexities can be accounted for; and the implications of the assumptions used in the analysis and the management decision can be evaluated (Mamilton, 1982). The Regional Aquifer System Analysis (RASA) program of USGS (Sun, 1986: Weeks and sun, 1987) has established the importance of modelling to improve the understanding of the regional flow system.

Once the need for numerical modelling is established, the task of model design and its applications begins. The steps involved in the model development (flow chart) are schematically presented in Fig 2.

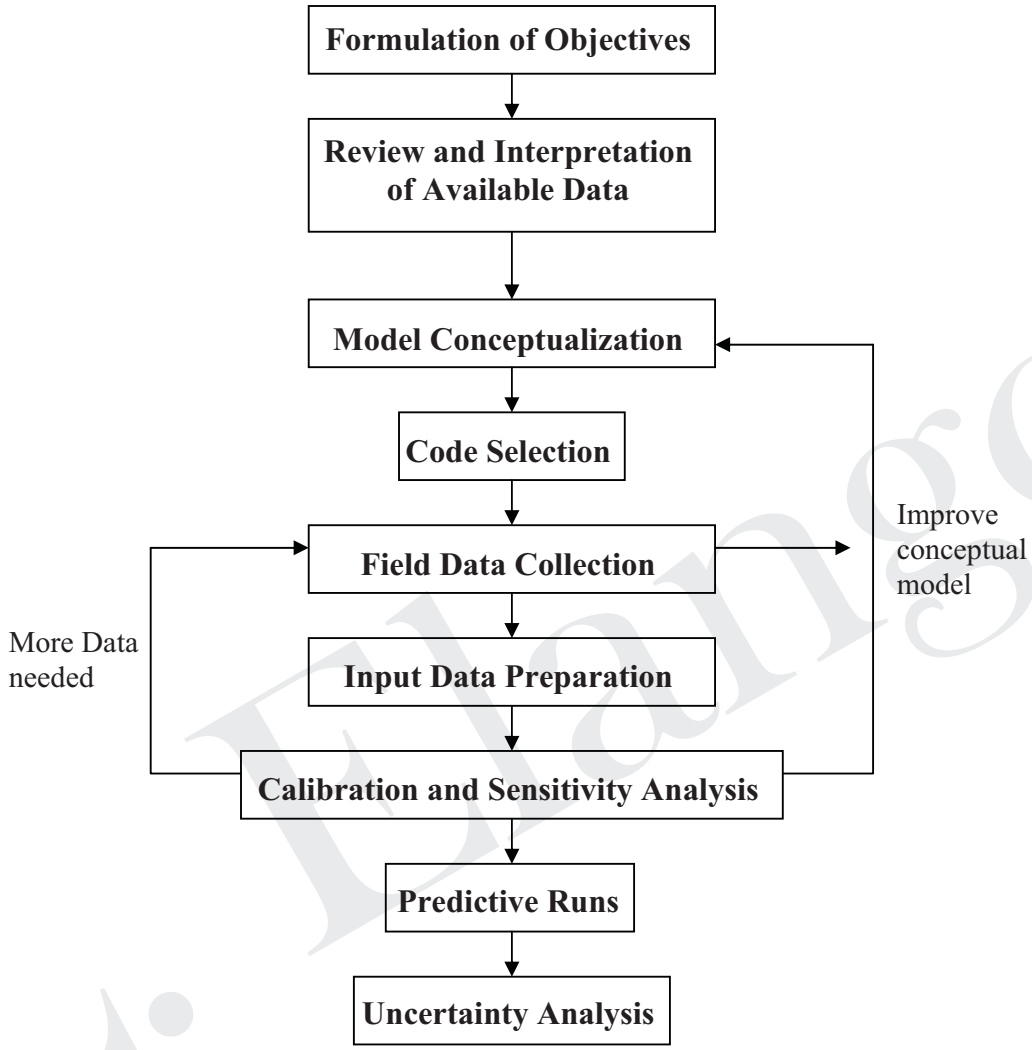

Fig. 2: Modelling Protocol

The hydrogeological investigations reveal that the study area is generally characterized by three zones, viz., weathered zone, followed by 1 m thick highly weathered permeable layer and a fractured zone. Thus a three layer model has been considered for the area, however, calibration and validation have been attempted for only top layer due to paucity of data for the other two layers. The layer characteristics have been summarized in Table 1.

Layer	Aquifer Material	Aquifer Type	Av.T	Av.S	Average thickness (m)
I	Weathered Zone	Unconfined	23	0.025	15
I	Highly wd. & Fr. zone	Unconfined/ Confined	50	0.050	1
III	Fractured zone	Confined/ Semi-confined	40	0.0005	54

A modular three dimensional finite difference groundwater flow model (MODFLOW) developed by USGS has been used for this study. Strongly Implicit Procedure (SIP) has been used for solving the system of equations.

Parameter Distribution

The geographical extent of the study area is 1758.7 sq.km. The area has been represented by a grid of 11 * 18 with a grid size of 4 sq.km. The study area is bounded by Ong river in the south, Mahanadi river in the east, Bargarh main canal in the west and a part of reservoir and Bargarh Main canal in the north.

The boundaries for the model consists of General head Boundary in the west and north except along the reservoir, were constant head boundary is considered. The boundaries formed by rivers, are considered as variable head boundary.

The modelling has been carried out on the monthly basis for the period June 1993-May 1994 with each month representing a stress period. A time step of 10 days has been taken for the modelling.

The aquifer parameters, elevation of top and bottom of the aquifers are available at some nodal points only. In the present study, the values of different parameters are either interpolated by contours or by demarcating the area of influence by theisson polygons.

CGWB has calculated draft for the whole command area. (Sar et al., 1994). In the computation, the Hirakud Command Area has been divided into 4 sectors and draft has been calculated for each sectors. The sector draft has been equally distributed to all cells falling in each sector.

In the present study, the recharge rate is used as an external input. The recharge term consists of components from rainfall, canal seepage and return flow from irrigation.

1) Rainfall recharge

The infiltration factor computed from Lumped model is utilized in the computations.

The recharge is computed for each cell using the expression;

$R_r = R.F * I.F$ (10)

R.F = rainfall (L)

I.F = infiltration factor in %

R_r = rainfall recharge (L)

2) Seepage from canal

The canal seepage has been estimated for each sector in Hirakud Command Area (Gupta and Suresh, 1994). The canal seepage has been equally distributed for each cell falling in the corresponding sectors. The cell wise seepage has been divided by cell area to get the canal seepage in terms of length per unit time.

3) Return flow from Irrigation

CGWB has compiled the crop coverage in each sector of Hirakud command Area. (Gupta and Sinha, 1994). The crop water requirement has been calculated for the study area and return flow from irrigation has been accordingly reduced as mentioned in the methodology of lumped model computations. The return flow from irrigation has been equally distributed for each cell falling in the respective sectors and has been divided by the cell area to get the return flow from irrigation in terms of length per unit time.

A sum of the recharge from the above mentioned sources have been considered as input of recharge rate for each cell.

The data of river stages in space and time and bottom of river bed are not available. The river bottom has been assumed to be 3.0 m below the elevation of adjacent cells and the river stage has been assumed to be proportionately reducing from the full flow of 3.0 m depth during July to October to zero flow in the month of Jun. The conductance has been calculated for each river nodes using the expression given in the manual of MODFLOW (McDonald and Harbough, 1984).

RESULTS AND DISCUSSIONS

Lumped Model

In the lumped model computations, the whole Hirakud command Area has been considered and hence the values of different components have been proportionately reworked as per the actual aerial extent of the study area, which is 79.71% of Hirakud Command Area (Table 2).

A perusal of the table2 shows that during Rabi season, there is a total outflow of 379.767 mcm and a recharge of 340.688 mcm with a change in storage of –39.079 mcm for Rabi season. This gave rise to the return flow from irrigation to be in the order or 17% and 12.7% of applied irrigation water for paddy and non paddy crops.

In Kharif season, there is a total outflow of 527.647 mcm and a recharge of 643.246 mcm with a change in storage of 115.599 mcm. The infiltration factor works out to be in the order of 13.95%, which is within the range of 10-15% for granitic terrain as per the G.E.C norms (G.E.C 1984).

Table 2: Lumped Model Results

		Rabi	Kharif	Annual
I	**Out flow (mcm)**			
	1 Evapotranspiration	364.872	517.795	882.667
	2 Draft	4.995	2.677	7.631
	3 Outflow from the aquifer	9.941	7.175	17.115
	Total	**379.767**	**527.647**	**907.414**
	Balance from watertable fluctuation	-39.079	115.599	76.520
	Total Recharge	340.688	643.246	983.934
II	**Inflow (mcm)**			
	1 Canal seepage	151.528	112.698	264.226
	2 Return flow from irrigation	189.160	177.868	367.028
	3 inflow to the aquifer	0.000	0.000	0.000
	4 Rainfall Recharge	0.000	352.680	352.680

In the lumped model, it is seen that the total outflow is in the order of 907.41 mcm, out of which 882.667 mcm is evapotranspiration 7.631 mcm is groundwater draft and 17.115 mcm is effluent seepage from the aquifer to the river, while the total recharge is in the order of 983.934 mcm with a change in storage of 76.520 mcm.

The recharge factor computed being within the permissible range, it appears to be justified that the values of parameters used in the lumped model can be utilized for the distributed model as an initial guess and may be modified at a later trial runs for calibrations.

Distributed Model

In the initial run, constant values of aquifer parameters and Constant Head boundary have been used for the river boundary. In the subsequent runs, the river package and spatial variation of in the aquifer parameters have been introduced.

Calibration and Validation

The analysis of the model results were carried out in three stages viz.,

1. Verification of water budget,
2. Comparison/validation of watertable elevation contours of simulated with that of observed at a given point.

3. Comparison and validation of hydrographs of simulated with that of observed at a given point of space over the model period.

Though the convergence has been obtained in the initial run but water budget for various components, (viz. recharge, draft, evapotranspiration were quite different and about two to three times the value obtained in the lumped model.

The introduction of river package and spatial variation in aquifer parameters in the model has brought about a sharp change in the water budget, hydrographs and watertable contours. The results, though not precise but are visibly closer to the lumped model results.

A perusal of the cumulative water budget of the study area shows that the % discrepancy varies from zero % (in most of the stress periods) to –0.02%, which is within the acceptable range of 1% as reported by Anderson and Woessner (1992). This strengthens the validity of the overall model.

It is also observed that the total inflow to the system varies from 460.24 mcm to 2142.7 mcm from the end of 1st to 12th stress period, out of which recharge contributes 349.57 mcm to 1447.9 mcm and river leakage from 33.84 mcm to 89.45 mcm respectively. Further, the total outflow from the system varies from 460.25 mcm to 2142.8 mcm at the end of 1st to 12th stress period, out of which well contributes .45 mcm to 7.21 mcm, evapotranspiration works out to be in the order of 46.18 mcm to 700.97 mcm and river leakage 180.8 mcm to 729.71 mcm respectively. The change in annual storage is in the order of 100 mcm.

The values of evapotranspiration and draft of lumped model computations corresponds well within that of distributed model while the effluent seepage to the river has been underestimated in the lumped model, probably due to the fact that the contribution to the tributaries has not been considered. However, the change in the storage values of lumped model amounting to 76.52 mcm is closer to the distributed model value of 100 mcm.

The watertable contours of both computed and observed for November 1993 have been given in Fig.3. A perusal of the figure shows that the contours are apparently close to each other in most of the areas, except at the nodes adjacent to either boundary or river nodes.

The hydrographs at some selected nodes have been given in the Fig.4. A glance of the figure shows that in general the trend of the observed and computed hydrographs are similar but the value of heads show a mismatch of about 0.5 to 1.0 m.

A sensitivity analysis of the aquifer parameters used in the model has also been carried out.

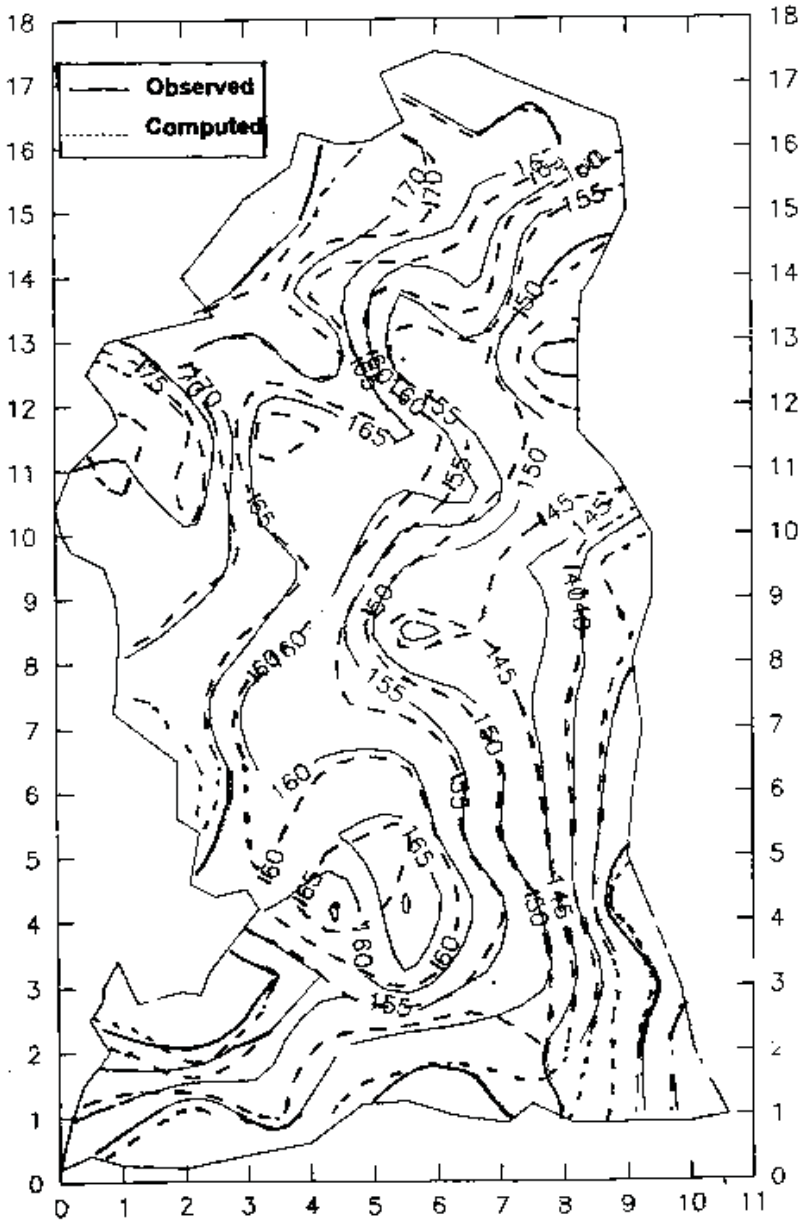

Fig. 3: Validated Waterable Elevation Contour Map Nov '93

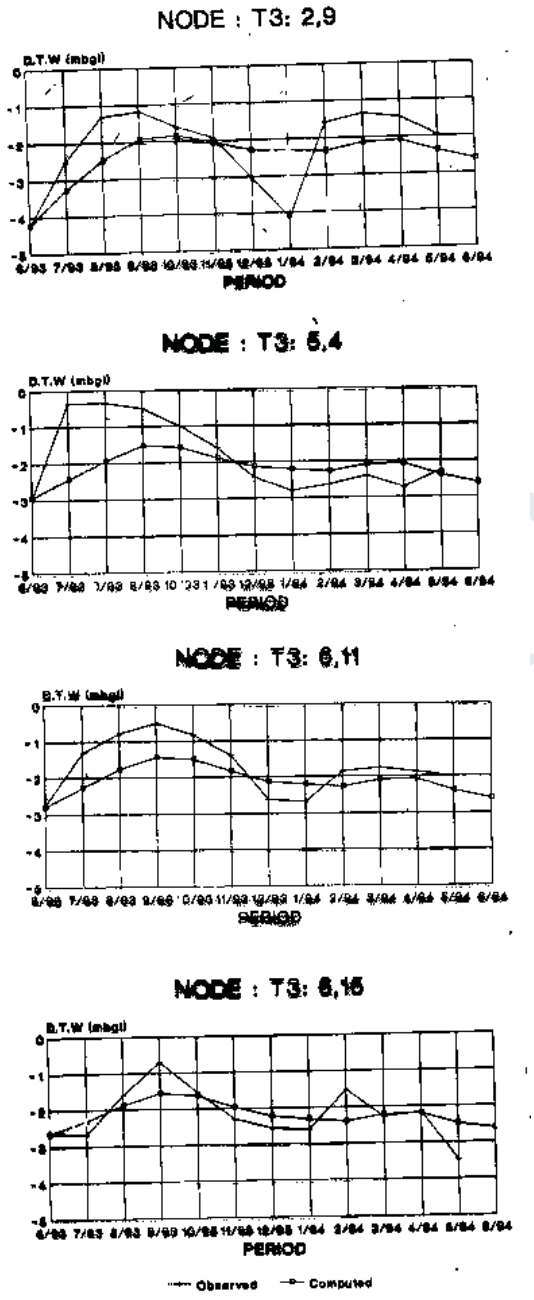

Fig. 4: Well Hydrographs (Observed and Computed) at selected nodes

The reasons for the mismatch between observed and simulated hydrographs can be attributed to the following factors.

1. Rainfall occurring on the last day of the month has also been considered as the recharge for the same month, ignoring the time lag in effecting the recharge.
2. Uniform distribution of recharge and discharge components over the area for want of discrete data at each nodes.
3. Assumptions relating to the stage/discharge data of river/tributaries.
4. The sparse data of aquifer parameters have been interpolated to get the value for each node.
5. Assumption for the seepage calculations can also introduce subjectivity in the results.

Various Scenarios for Conjunctive Use Plan

The simulation studies have shown that the major portion of the study area has been characterized by shallow watertable, even during the month of June. The conjunctive use planning using simulation techniques is a repetitive procedure wherein different scenarios are tested in the predictive simulation, to study the effect of extra stresses introduced in the system.

The influence of pumpage has been studied in the depth to water level maps prepared for the month of June. It has been noticed that the existing pumpage being very nominal (7.239 mcm while there is a recharge of 1447.9 mcm in the study area), there is a building up of dynamic storage of nearly 100 mcm in a year. This can be put to use effectively as well as reducing the depth to watertable in the shallow watertable zones, by increasing the pumping. Accordingly, the different scenarios of increased pumpage to 4 times (Scenario I), 25 times (Scenario II), 50 times (Scenario III) and 100 times (Scenario IV) of existing pumpage have been studied. Further, with 25 times of increased pumpage (Scenario V) and with a decrease of conductance of the river, which is tantamount to decreasing the recharge values indirectly vis-à-vis, increasing the canal seepage by the lining of canals have also been studied. Thus, five different scenarios have been generated for conjunctive use plan.

The area characterized by shallow water level (0 to 2 m bgl) during the month of Nov 93 has been earmarked for groundwater development. The area for groundwater development plan has been identified and it works out to be a total of 48 cells, covering a geographical extent of 768 sq.km. An additional draft has been introduced only in these cells to lower the shallow watertable. The change in the area characterized by shallow watertable at the end of predictive simulation period of three years, varies from 204.48 sq.km (Scenario I) to 185.6 sq.km (Scenario II) to 170.4 sq.km (Scenario III) to 62.88 sq.km (Scenario IV) to 209.792 sq.km (Scenario V). It is also noticed that in the second year of the predictive simulation, the shallow watertable area is found to increase while in the subsequent year, it is found to decrease. This may be attributed to the induced recharge in the

first year due to enhance withdrawal of groundwater, before the system stabilizes to the extra stresses.

In addition to the reduction of area characterized by shallow watertable zones, the other factors to be considered before finalizing the conjunctive use plan are as follows.

1. *The change in Storage* indicates the building up of storage in the system. The change in storage also denotes the availability of excess water for exploitation. The plan has to effectively reduce the change in storage without affecting the system as a whole.

2. *Net River Leakage* (Baseflow) depicts the quantum of water lost as out flow from the system, which can also be effectively exploited. Greater the exploitation, lesser would be the outflow and it indirectly affects the downstream users if they are more dependent on the flow in the river. Hence, the draft should be such that the system as a whole should not be obliterated.

3. *The Recharge* components indicate the ability of system to receive the induced recharge due to withdrawal of water from the aquifer.

Table 3: Comparison of different Scenarios for Groundwater Development Plan

Strategy No.	Increase of Draft	Period	Area of shallow W.T (Sq.km)	Recharge (mcm)	Draft (mcm)	Change in Storage (mcm)	Net river Leakage (mcm)
Existing	**Nil**	**June 94**	**200.96**	**1537.97**	**7.21**	**99.61**	**-640.26**
I	4 Times	June 94	216.64	1541.34	36.17	96.43	-629.21
		June 95	210.72	3224.61	72.34	129.90	-1068.39
		June 96	204.48	4907.81	108.51	138.30	-1508.16
II	25 Times	June 94	180.86	1559.04	188.19	76.20	-570.29
		June 95	180.16	3260.04	376.37	110.60	-950.41
		June 96	185.60	4960.97	564.56	120.50	-1331.08
III	50 Times	June 94	160.16	1598.76	369.16	33.87	-499.92
		June 95	170.88	3339.67	738.32	68.00	-809.43
		June 96	170.40	5080.54	1107.50	72.70	-1119.30
IV	100 Times	June 94	84.32	1704.46	731.11	-131.84	-356.39
		June 95	86.40	3552.38	1462.20	-199.90	-520.32
		June 96	62.88	5399.16	2181.70	-277.30	-683.50
V (Reduced River Conductance	25 Times	June 94	207.53	1556.44	188.19	76.25	-569.47
		June 95	212.38	3253.12	376.37	110.60	-949.03
		June 96	209.79	4949.75	564.56	120.60	-1329.00

Keeping in view the above, a summary of the predictive simulation of various Scenarios have been given in Table 3**.** A perusal of the table shows that in comparison to other scenarios, the Scenario III has shown more reduction in the area characterized by shallow watertable and considerable reduction in the building up of storage and at the same time the river leakage has also not been reduced appreciably.

Thus, the Scenario III has been inferred as most suitable for conjunctive use plan. However, there is still scope for finer tuning, for evolving an optimum conjunctive use plan to reduce the change in storage and area characterized by shallow watertable.

CONCLUSION

A predictive simulation period of three years has been considered and various scenarios of groundwater development plan, in the area characterized by shallow watertable (0-2 m bgl) have been carried out. The groundwater development plan of Scenario III has been chosen as the best amongst the generated scenarios. In this scenario, the annual groundwater draft of 369.16 mcm, has been recommended.

RECOMMENDATION

The analysis shows that the optimum groundwater development plan may fall somewhere in between 50 times to 100 times of excess pumpage to be added to the existing draft, with the present recharge conditions. A few more trial runs are needed to determine the optimum policy of groundwater development plan, with the existing recharge facilities.

Further, the local hydrogeological conditions have not been introduced while proposing the groundwater development plan. However, the occurrence of shallow watertable, though may be an indicator for the possible availability, the application of Geographical Information system (GIS), for verification of groundwater potential zones may authenticate the proposal on more sound footing.

Alternatively, canal lining may be suggested for reduction of canal seepage, which in turn would reduce the recharge and groundwater development plan combined with the canal lining may be studied on the aquifer response model to evolve an alternative scenario.

An economic analysis of different conjunctive use plans may bring out an optimum conjunctive use strategy for the study area.

REFERENCES

[1] Anderson, M.P. and Woessner, W.W., (1992). Applied groundwater modelling. Academic Press Inc., 381 p.

[2] Aron, G., (1969). Optimization of conjunctively managed surface and groundwater resources by dynamic programming. Water Resources Centre Contribution No. 129, University of California 158 p.

[3] Bredehoeft, J.D. and Young R.A., (1970). The temporal allocation of groundwater. Water Resources Res., vol 6 (1), pp 3-21.

[4] Buras.N., (1963). Conjunctive operation of Dams and Aquifers. J. of Hydr. Div. ASCE, Vol.89(6), pp 111-129.

[5] Burt, O.R., (1964). The economics of Conjunctive use of ground and surface water, Jhilgardia, Vol.36(2).

[6] C.G.W.B., (1996). Conjunctive use of surface water and groundwater in Hirakud Command Area, Orissa. A Technical Report of Central Groundwater Board, Ministry of Water Resources, Govt. of India (Unpublished).

[7] Chaudary, M.T., Labadie, J.W., Hall, W. and Abberston, M.L., (1974). Optimal conjunctive use model for Indus Basin. J. of Hydr. Div., ASCE, Vol.118(1), pp667-678.

[8] Chawas-Morales, J., Marino, M.A. and Holzapfel, A.H., (1992). Planning simulation model of irrigation district, J. of Irrig. And Drain, Engg., ASCE, Vol.118(1), pp 74-87.

[9] COE,J.J., (1990). Conjunctive used – Advantages, Constraints and Examples. J. of Irrig. And Drain. Engg., ASCE, Vol.116(3),pp 427-443.

[10] Coskunoglo, O. and Shetty, C.M., (1981). Optimal Stream-Aquifer Development, J. of Water Res. Planning & Management Div., ASCE, Vol. 107(2), pp 513-531.

[11] De Vries, J.J., (1990). Seasonal expansion and contraction of stream networks in shallow groundwater systems, J. of Hydrology, Vol. 170(1-4), pp 15-26.

[12] Ejas, M.S. and Peralta, R.C., (1995). Maximizing conjunctive use of surface groundwater under surface water quality constraints. Advances in Water Res., Vol. 18(2), pp 67-75.

[13] Groundwater Estimation committee, (1984). Groundwater Estimation Methodology. Central Groundwater Board, Ministry of Water Resources, Govt. of India.

[14] Gupta, J.P., (1995). Evaluation of the recharge techniques adopted for conjunctive use of surface and groundwater in the state of Haryana (India). Proc. Of the 2nd Intl. Symp. Of Artificial Recharge of Groundwater, ASCE., pp455-461.

[15] Gupta, C.P., Ahmed, S. and Gurunadharao, V.V.S., (1985). Conjunctive utilization of surface water and groundwater to arrest the water level decline in an alluvial aquifer, J. of Hydrology., Vol. 76(3-4), pp 351-362.

[16] Gupta, A.A. and Sinha, S.K., (1984). Crop water requirement in Hirakud Command Area. A Technical Report of Central Groundwater Board, Ministry of Water Resources., govt. of India (Unpublished).

[17] Gupta, A.A. and Suresh, S., (1994). Seepage losses from canal system to groundwater regime. A Technical Report of Central Groundwater Board, Ministry of Water Resources, Govt. of India (unpublished).

[18] Hamdan, A.S. and Ahmed Meredith, D.D., (1974). Model for conjunctive use water systems. J. of Hydraulics Div. ASCE, Vol. 101(10), pp 1343-1355.

[19] Illangasekhare, T.H. and Morel-Seytoux H.J., (1986). Algorithm for surface / groundwater allocation under appropriation doctrine. Groundwater, Vol. 24(2), pp 199-206.

[20] El-Kadi, A.I., (1989). Watershed models and their applicability to conjunctive use management. Water Res. Bul. Vol. 25(1), pp 125-137.

[21] Hamilton, D.A., (1982). Groundwater modelling: Selection, Testing and Use. Volume 1, Michigan Dept. of Water Resources, 199 p.

[22] Karanth, K.R., (1987). Groundwater Assessment Development and Management Tata McGraw Hill Pub., 720 p.

[23] Khare, D., (1994). Distributed Modelling of conjunctive use in a canal command. PH.D Thesis submitted in Dept. of Civil Engg., University of Roorkee, 243 p. (Unpublished).

[24] Latif, M. and James, L.D., (1991). conjunctive water use to control water logging and salinisation. J. of Water Res. Plan. And Manag., ASCE, Vol. 117(6), pp 611-628.

[25] Laxminarayana, V. and Rajagopalan, S.M., (1977). Optimum cropping pattern for basins in India J. of Irrig. And Drain. Engg. ASCE, Vol. 103(1), pp 53-70.

[26] Meddock, T. and Moody, D.W., (1974). Surface water and groundwater interaction phenomena in planning models. The use of computer techniques and automation for water resources systems. Washington, D.C., Vol. II pp 112-125.

[27] McDonald, M.G. and Harbough, A.W., (1984). A modular three dimensional finite difference groundwater flow model. A manual on MODFLOW. US Department of Interior, USGS, National Center, Reston, Virginia. 528 p.

[28] Mishra, G.C. and Singh, S.K., (1992). Groundwater and conjunctive use. Hydrological developments in India since independence. A contribution to Hydrological Sciences. National Institute of Hydrology, Roorkee. Pp 165-194.

[29] Onta, P.R., Das Gupta, A. and Harboe, R., (1991). Multistep planning model for conjunctive use of surface and groundwater resources. J. Water Res. Plan. and Manag., ASCE, vol. 117(6), pp 662-678.

[30] Prasad, M., (1988). Simulation –Optimization technique for firm yield in optimal conjunctive water resources management. J. Inst. Engrs. (India). Vol. 69(3), pp 178-185.

[31] RaoK.N. George, C.J. and Ramasatri, K.S., (1974). PET over India. IMD prepublished Scientific Report No. 136, 199 p.

[32] Sar, S.N., Roy, G.K. and Suresh, S., (1994). Hydrogeological studies for conjunctive use of surface water and groundwater in Hirakud command Area, Orissa. A Technical Report of Central Groundwater Board, Ministry of Water Resources, govt. of India (Unpublished).

[33] Singh, R., Sondhi, S.K. Singh, J. and Kumar, R., (1984). A groundwater model for stimulating the rise of water under irrigated conditions. J. of Hydrology., vol. 71(1-2), pp 165-179.

[34] Singh, R.P.,(1996). Hydrochemical and conjunctive use studies in surface and groundwaters in Raipur-Lunoi-command, district Pali, (Rajasthan). Pp 162. A dissertation submitted in Dept., of Hydrology, University of Roorkee (unpublished).

[35] Sun, R.J., (1986). Regional aquifer-system analysis program of the U.S. geological survey, summary of Projects, 1974-84, USGS, Circular 1002-264p.

[36] Todd, D.K., (1980). Groundwater Hydrology, John Willy and Sons Inc., New York, 535 p.

[37] Weeks, J.B. and Sun, R.J., (1987). Regional aquifer-system analysis program of the U.S Geological survey-Bibliography, 1978-1986, USGS Water Resources Investigations Report 87 –4138.

[38] Willis, R., Finney, B.A. and Zhang, D., (1989). Water resources management in North China Plain J. Water Res. Plan & Manag., ASCE.,Vol. 115(5),pp 598-615.

[39] Yan, J. and Smithy, K.R., (1994). simulation of integrated surface water and groundwater systems-Model formation. Water Res. Bul., Vol. 30(5), pp 879-890.

[40] Young, R.A. and Bredehoeft, J.D., (1972). Digital computer simulation for solving management problems of conjunctive groundwater system. Water Resour, Res., vol.8(3), pp 625-636.

Numerical Simulation of Groundwater Flow and Solute Transport, L. Elango (ed). pp.131-149

Modelling the Impact on the Groundwater Regime on Construction of Subsurface Barrierin Palar River, Southern India

M. Senthil Kumar and **L. Elango**

INTRODUCTION

Groundwater is a major renewable resource occurring below the earth's surface that supplies fresh water for living beings. Increasing demand for groundwater due to ever increasing population has initiated proper and effective management of available groundwater resources. Groundwater modelling is a powerful management tool which can serve multiple purposes such as providing a framework for organising hydrologic data, quantifying the properties and behaviour of the systems and allowing quantitative prediction of the responses of those systems to externally applied stresses. No other numerical groundwater management tool is as effective as a 3-dimensional groundwater model. A number of groundwater modelling studies have been carried out around the world for effective groundwater management (Corbet and Bethke, 1992; Storm and Mallory, 1995; Gnanasundar and Elango, 2000; SenthilKumar and Elango 2001 and SenthilKumar and Elango 2004). Such a study was attempted for the lower Palar River basin located in Southern India. As the Palar river flows only for a few days in a year, groundwater has been extensively used to meet the increasing demand for domestic, irrigational and industrial requirements. Industrial abstraction includes pumping for Madras Atomic Power Station (MAPS). Due to over dependence on groundwater for all these purposes, it is essential to develop a groundwater model in order to effectively manage this aquifer system. Hence, the present study was carried out with the objective of

- To asses accurately the quantum of groundwater potential available in the lower Palar Basin.
- To identify the most favourable areas of groundwater aquifer.
- To know the effect of pumping new wells on the existing wells.
- To predict the consequences/impact on the groundwater system both in the upstream and downstream side of the subsurface barrier due to the construction of subsurface barrier at Ayapakkam and also the effect, consequent on the construction of the barrier in the lower Palar Basin.
- To citing the new wells in the river bed and also in the adjacent flood plain area.
- To know the effects of increasing the abstraction rate of groundwater at anytime in future (during summer April-June and winter October – December separately) at the site of sub surface barrier.
- To know the rate of groundwater extraction to abate sea water intrusion.

- To know the movement of fresh water-salt water interface to be predicted depending upon the flow regime caused by changes in discharge / recharge as the aquifer is hydraulically connected with the sea (to avoid over standing of this coastal aquifer).
- To know the future pumping patterns and water balance at anytime, giving long predictions of draw down.

Constructing a numerical model and studying the effects of construction of subsurface barrier of the lower Palar River Basin, computer software Groundwater Modelling System (GMS) was used to simulate the groundwater flow for this study.

STUDY AREA

A part of the lower Palar River Basin, Tamil Nadu, India, considered for this study, is located 75 km south of Chennai (formerly Madras) and covers an area of 392 km^2 (Fig. 1). The eastern side of this area is bounded by the Bay of Bengal. This area enjoys sub-tropical monsoon climate with January and February as the dry periods, March to May as summer period, followed by the monsoon period. The maximum temperature in this area is about 42°C during the months of May and June. The minimum temperature is about 21°C recorded during the months of December and January. The southwest monsoon (June to September), the northeast monsoon (October to December) and the transition period contribute 40%, 51% and 9% respectively, of the total average annual rainfall (1167 mm/year) measured in the two rainfall stations. This area is bisected more or less into two halves by the Palar River. This is a seasonal river flowing during the months of November, December and January. Numerous tanks are present in the depressed parts of the undulating topography of the study area.

HYDROGEOLOGY

The study area exhibits varied physiographic features and the elevation ranges from 40 m in the west to sea level in the east. Geologically, the study area has two distinct formations: crystalline rocks of Archean age and recent alluvium (Fig. 2). These alluvial deposits occur along the present and paleo Palar River courses. Crystalline rocks comprising charnockites and gneiss form the basement and some exposures are found in the southern part of this area. Alluvium occurs as the upper layer and is characterised by sand, gravel and sandy clay. Its thickness ranges from 1 m at the northern and southern boundaries to 30 m along the river. The alluvium and weathered crystalline charnockites function as an aquifer system. Groundwater occurs in unconfined condition in both the alluvial and underlying weathered rocks. The groundwater table occurs at a depth of 2 to 5.5 m below ground level in the monitoring wells. The hydraulic conductivity of this alluvium ranges from 20 – 69 m/day. The specific yield value ranges from 0.037 to 0.32 (PWD, 2000). The lower layer is characterised by weathered crystalline rocks with there thickness varying from 0 to 7 m. The hydraulic conductivity of this layer ranges from 0.5 to 12 m/day, and specific yield value ranges from 0.002 to 0.01(PWD, 2000).

GROUNDWATER MATHEMATICAL MODELLING

Anisotrophic and heterogeneous three-dimensional flow of groundwater, assumed to have constant density, may be described by the partial-differential equation (Rushton. and Redshaw 1979).

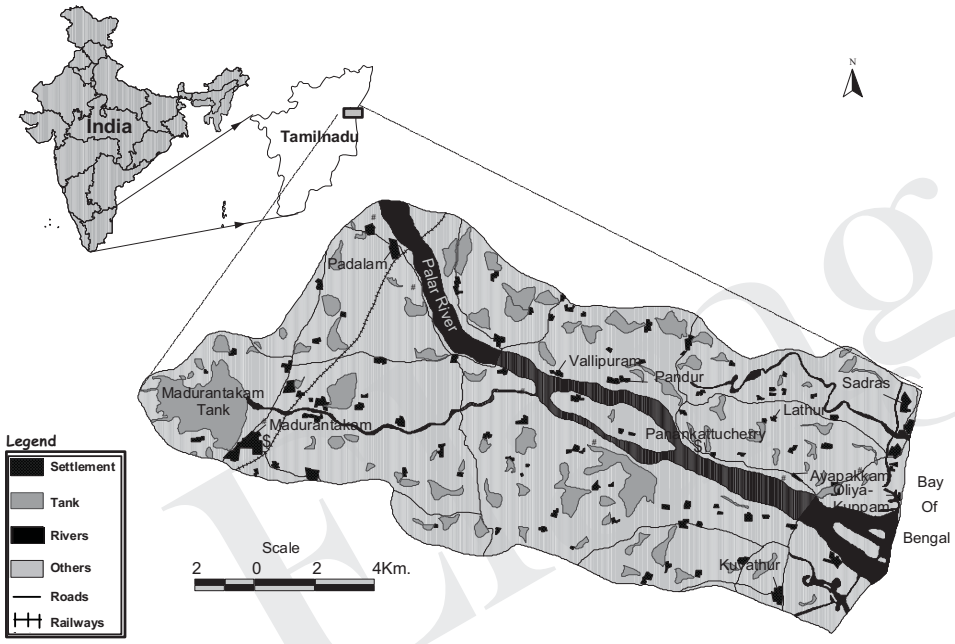

Fig. 1: Part of the Lower Palar River Basin, Southern India

$$\frac{\delta}{\delta x}\left[K_{xx}\frac{\delta h}{\delta x}\right]\frac{\delta}{\delta y}\left[K_{yy}\frac{\delta h}{\delta y}\right]+\frac{\delta}{\delta z}\left[K_{zz}\frac{\delta h}{\delta z}\right]-W=S_s\frac{\delta h}{\delta t}$$

Where,

K_{xx}, K_{yy}, K_{zz} = components of the hydraulic conductivity tensor
h = potentiometric head
W = source or sink term,
S_s = specific storage
t = time

The Finite-difference computer code MODFLOW (McDonald and Harbaugh, 1998) numerically approximates this equation, and we used to simulate the groundwater flow in the study area. The pre and post processor developed by the United States Department of Defense Groundwater Modelling System (GMS) was used to give input data and process the model output.

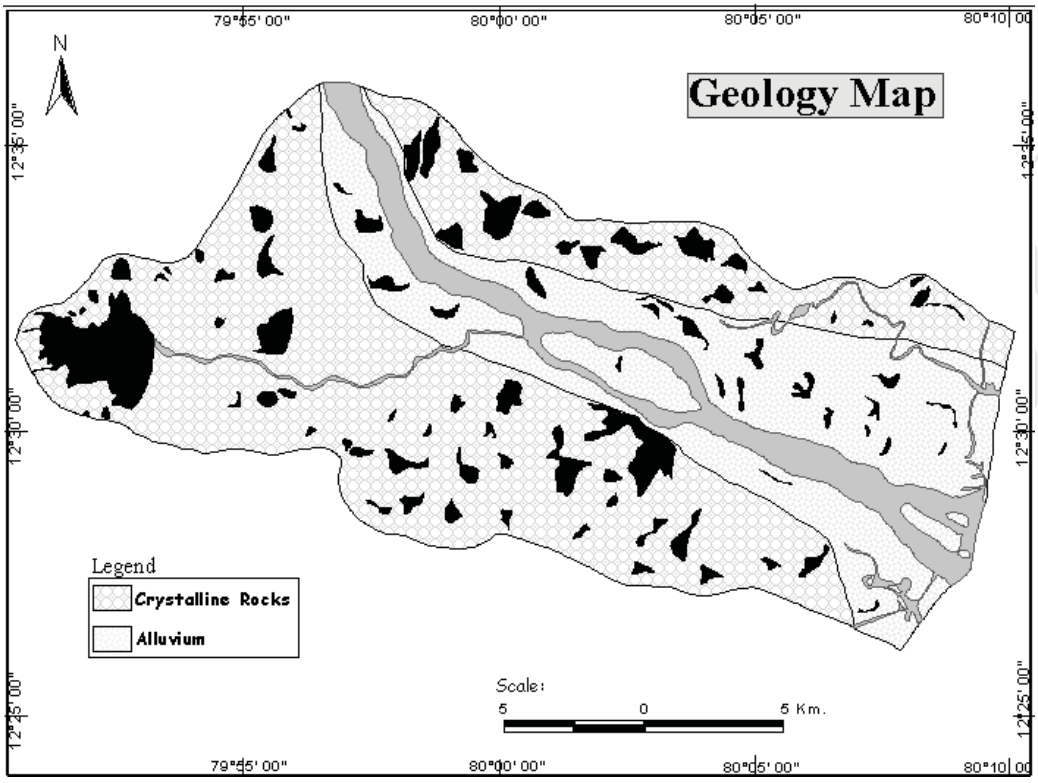

Fig. 2: Geological map of the study area

Discretisation of the Lower Palar River Basin

The model grid covering 392 km^2 of the study area was discretised into 4800 cells with 70 rows and 40 columns, and vertically by 2 layers (Fig.3). The length of model cells is 500 m along the east-west direction and 500 m along the north- south direction of the study area. The vertical cross-section of this system along A-A' and B-B' is shown Figures 3a and 3b respectively.

Boundary Conditions

The boundary conditions are specified for the supper surface of the modelled area. The

northern, southern and western boundaries of the study area have alluvial thickness less than one meter. Hence, they are simulated are no-flow boundaries (Fig.2). The northwestern part of the study area, which is the catchment's area, is simulated as variable head boundary. The eastern parts of the study area is bounded by Bay of Bengal Sea, boundary along this part is simulated as constant head boundary. Palar River, a seasonal River, flows only during the months of November and December, divides the study are into two halves, is simulated as a River boundary. Numerous storage tanks are present in the study area. A flux boundary due to recharge from rainfall and irrigational return is considered at the top of the surface.

Hydrogeological Stresses

The groundwater stresses includes the groundwater abstractions and recharge that an aquifer systems experiences. The abstractions of the study area include water needs of the study area is for irrigation, industrial and domestic purposes. Agricultural is the main activity of the study area. Landuse pattern of the study area depicts that about 210 sq.km of the land is used for irrigational activities, of which 147 sq.km of irrigational land is mainly dependent on groundwater. Industrial pumping includes present actual supply of 2 MGD (Million Gallons a Day) for the Madras Atomic Pumping Station (MAPS) from 8 wells spread along the banks of the Palar River in the village Panankattucherry (Fig.4) Ayapakkam, village pumps about 0.75 MGD (Million Gallons per Day) of water for an industrial plant. Vallipuram, a village supplies about 0.5 MGD of water for drinking water for Chennai city outskirts. Apart from these pumping, domestic pumping for household needs was calculated based on the population. The recharge to the aquifer system is from rainfall, irrigation and

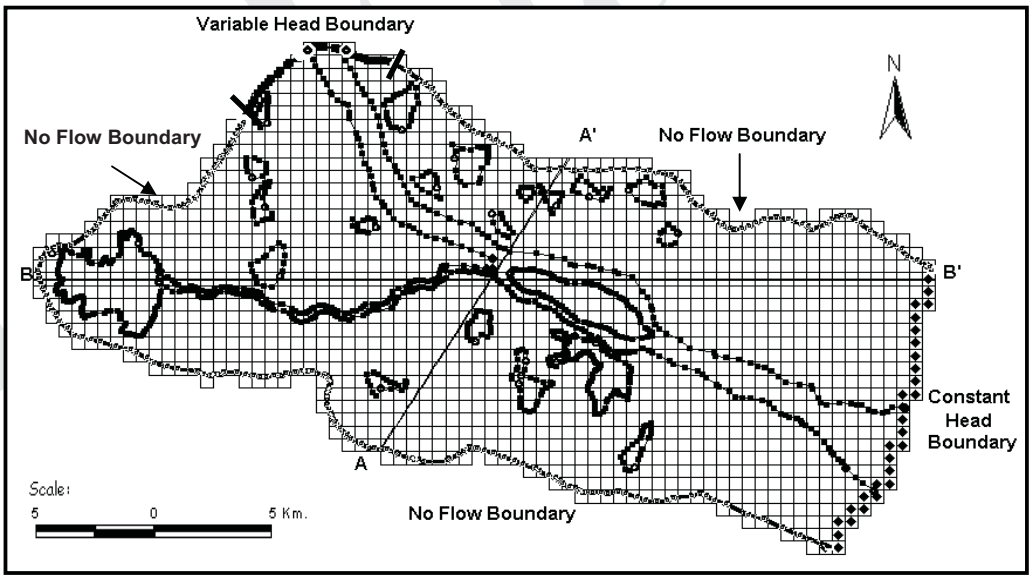

Fig. 3: Discretization of the study area

inflow from the river and storage tanks. Rainfall is the principal source of groundwater recharge. A comparison between the monthly rainfall value and consequent variation of groundwater level for a span of 60 years revealed that the groundwater is replenished whenever the monthly rainfall exceeds 60 mm. Numerous storage tanks are present in the study area, there contribution towards groundwater recharge was also considered.

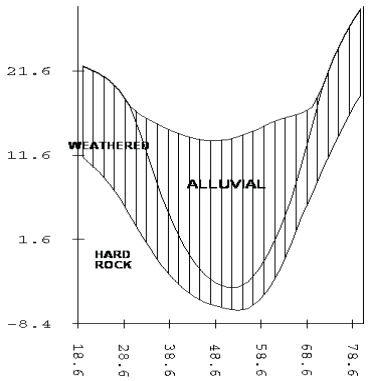

Fig. 3a: Cross-section along A-A'

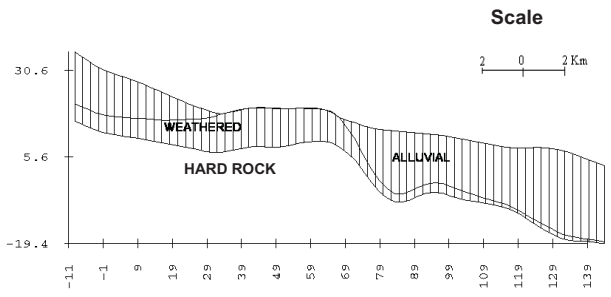

Fig. 3b: Cross-section along B-B'

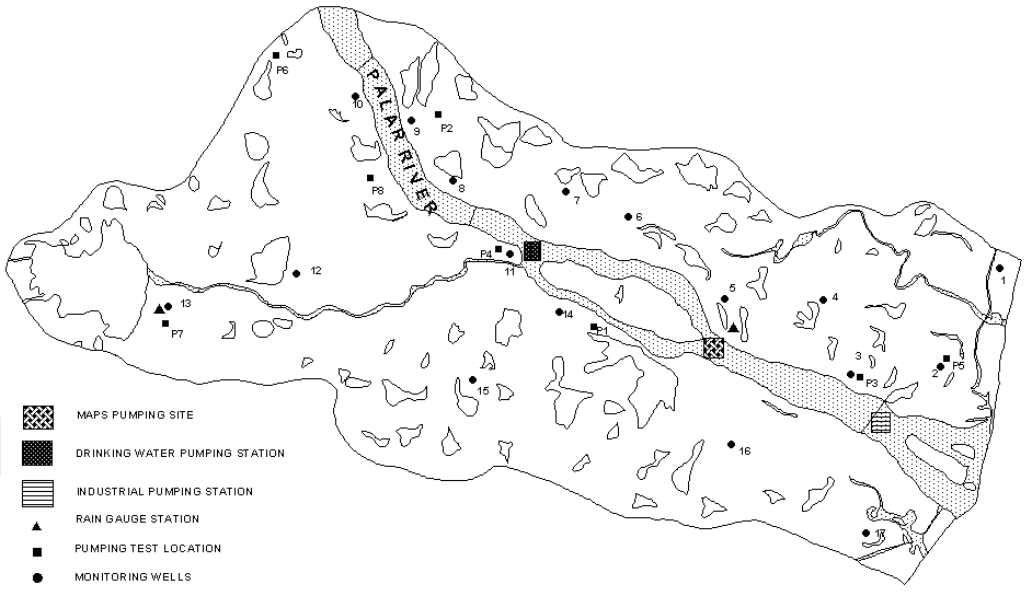

Fig. 4: Monitoring well location map of the study area

CALIBRATION

The calibration strategy was to initially vary the best-known parameters as little as possible, and vary the poorly known or unknown values the most to achieve the best overall agreement between simulated and observed. Steady state model calibration was carried out to minimise the difference between the computed and field water level conditions. Steady state calibration was carried out with the water level data of January 1991 in 17 wells distributed over the study area. Of all the input parameters, the hydraulic conductivity value is the only poorly known, as only eight pumping tests have been carried out in this area. The lithological variations in the area and borehole lithology of existing large diameter wells were studied. Based on this, it was decided to vary hydraulic conductivity values upto 10% of the pumping test results for both upper and lower sublayers in order to get a good match of the computed and observed heads (Fig. 5). This figure indicates that there is a very good match between the calculated and observed groundwater heads in most of the wells of the study area. Root mean square error and the mean error were minimised through numerous trial runs. Transient state simulation was carried out for a period of 12 years from January 1991 to December 2002 with monthly stress periods and 24 hour time steps. Calibration of transient model was achieved by several trials until a good match between computed and observed heads over space and time was obtained. The hydraulic conductivity values incorporated in the transient model were modified slightly from those calibrated by the steady state model. The correlation between computed and observed groundwater heads for all the wells in steady state and transient condition is shown in Fig. 5 and 6. Based on the close agreement between measured and computed heads from January 1991 to December 2002 at 17 observation wells distributed throughout the aquifer, the transient models were considered to be calibrated satisfactorily.

RESULTS OF SIMULATION

The simulated flow model of the lower Palar River basin depicts the following. There was a fairly good agreement between the computed and observed head values in almost 17 wells. A study of the simulated potentiometric surface of the aquifer indicates that the highest heads are found on the western side of the study area, which is a general reflection of the topography. The simulated and observed groundwater head for the stress period September 2002 is shown in Fig. 7. The computed and observed water head of the wells Vilagam of the study area is shown in Fig. 8. The computed head values mimic observed head values in most of the well locations. Further to test the validity of the calibrated model, sensitivity analyses were carried out on the major model parameters. These analyses showed the sensitivity of the model with respect to changes in model parameters.

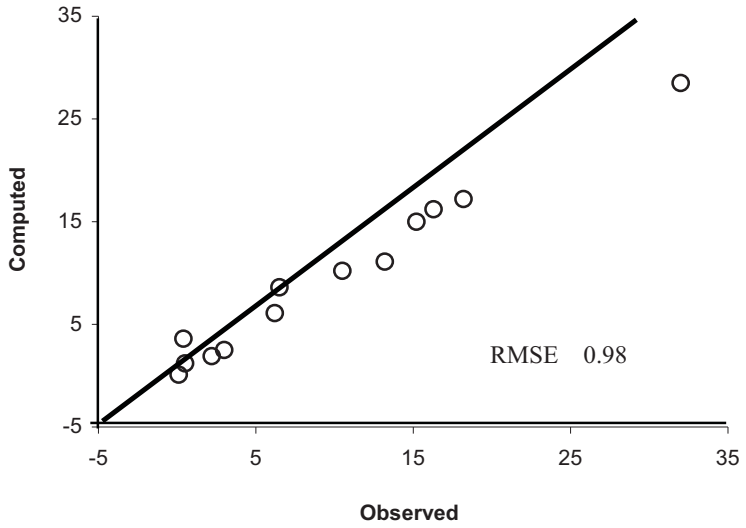

Fig. 5: Comparison of simulated and observed groundwater head after steady state calibration

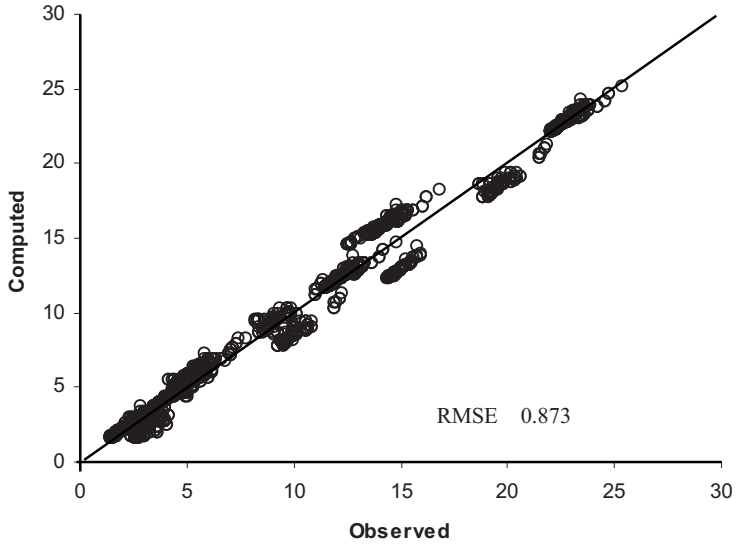

Fig. 6: Comparison of simulated and observed groundwater head after transient state calibration

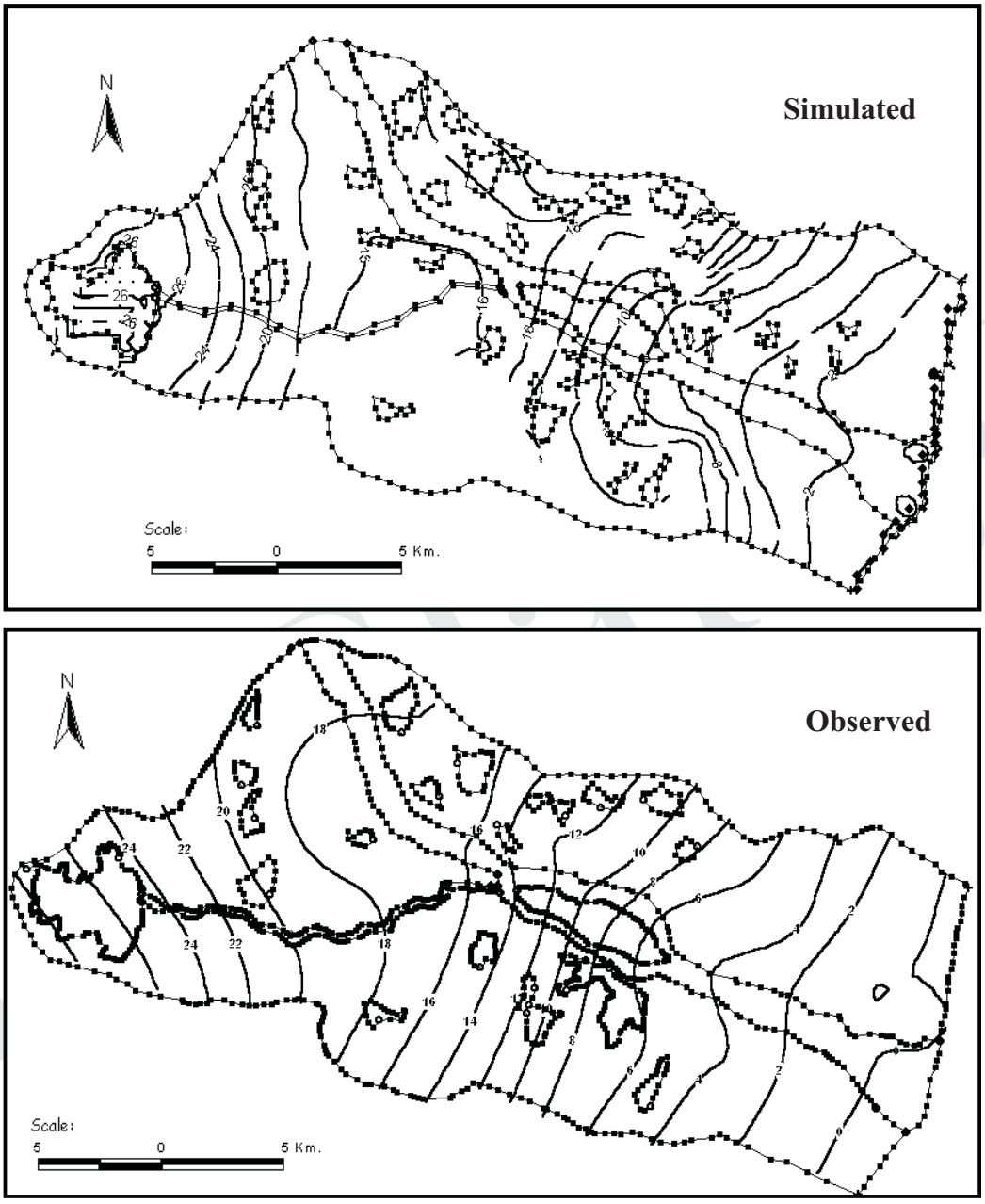

Fig. 7: Regional variation of simulated and observed groundwater head (m above msl) in September 2002

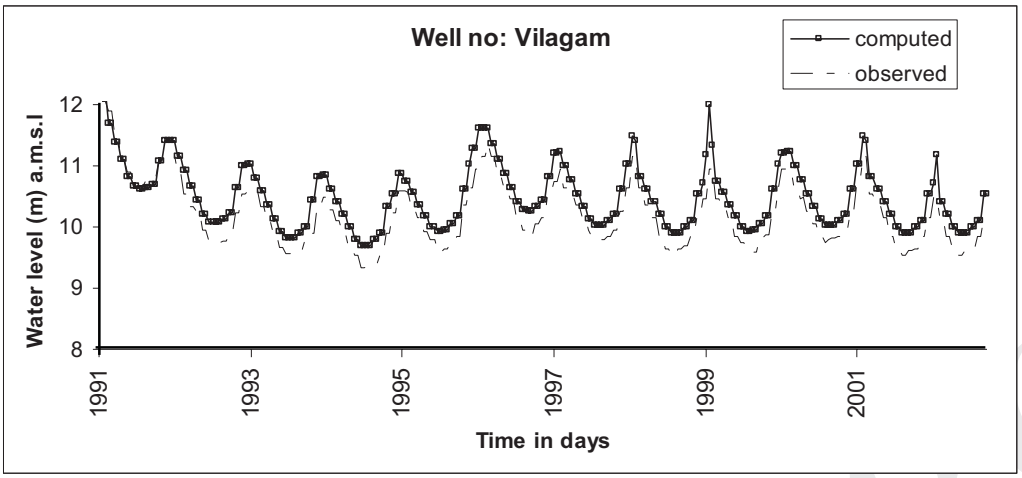

Fig. 8: Simulated and Observed head at wells Vilagam

As groundwater is the major source of water for the industries and agricultural fields located in this region, there has been an increase in pumping over the years. Hence, it is essential to know the behaviour of the system under increased hydrological stress. The groundwater pumping rate for the entire study area was increased by an additional 3 MGD. For these runs, the monthly average rainfall calculated from the 60 years rainfall data was used.

Effect of Increasing in Pumping By 3 MGD

It is anticipated that pumping will be increased by 3 MGD for the expansion of MAPS. Hence, the model was run with an increase of 3 MGD pumping at its existing pumping station. For these runs, the monthly average rainfall calculated from the 70 years rainfall data was used. The predicted regional groundwater head with increase in pumping is shown in Fig. 9. In the well No. 6 located in Pandur village (located on the western side of the pumping station) the groundwater head is lowered by 0.5 to 0.8 m due to increase in pumping (Fig.9a). In the well No. 2 located in Voyalur village (located on the eastern side of the pumping station) the groundwater head is lowered by 0.8 to 1.2 m due to increase in pumping (Fig.9b) extending to a radius of 10 km. The comparison between the wells located on the western and eastern parts of the MAPS site indicates that the groundwater level decreases more on the eastern side. Even under normal rate of pumping the groundwater head is lowered below the sea level during the dry seasons as discussed earlier, where as due to the increase in pumping at the MAPS pumping station, the groundwater water head would decline much lower than the sea level. The flow vectors also indicate that about 1 – 1.5 km inland from the coast would get affected by saline intrusion, resulting in contamination of the groundwater resources. However Public Works Department's proposed new subsurface barrier near the coast on Palar River is likely to prevent sea water intrusion.

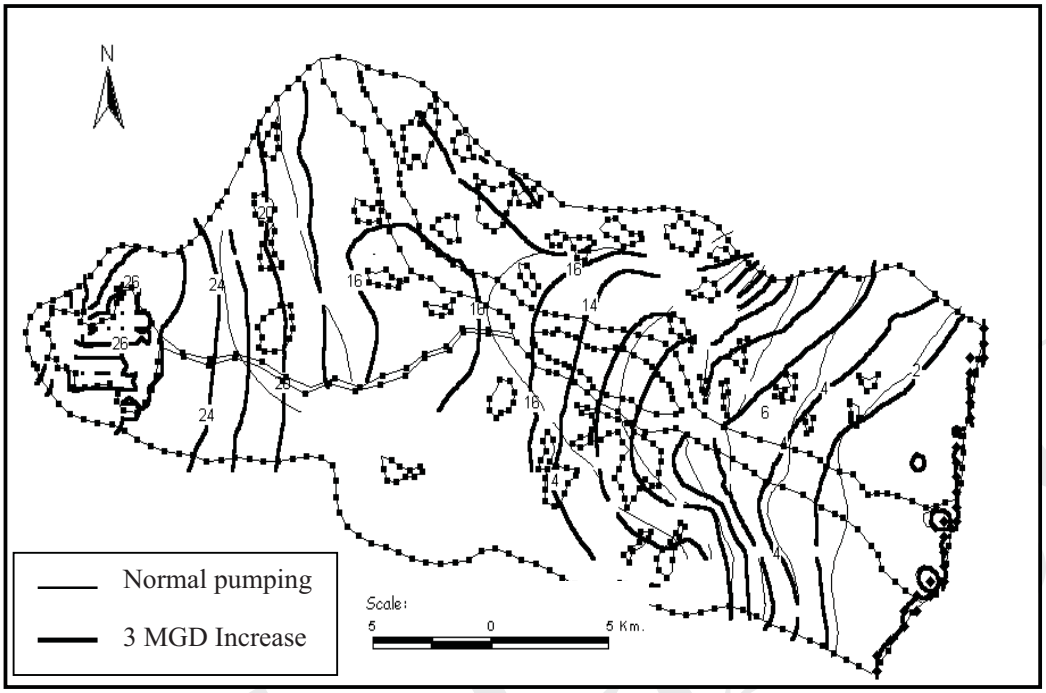

Fig. 9: Predicted groundwater head for September 2010 with increase in pumping by 3 MGD at MAPS pumping site

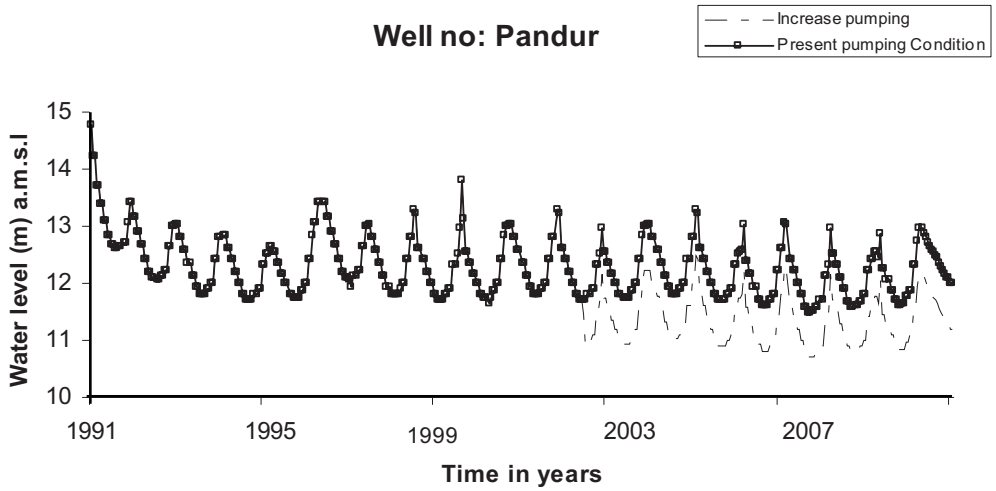

Fig. 9a: Groundwater head with increase in pumping by 3 MGD at well no. 6 Pandur (western side of MAPS site) without subsurface barrier

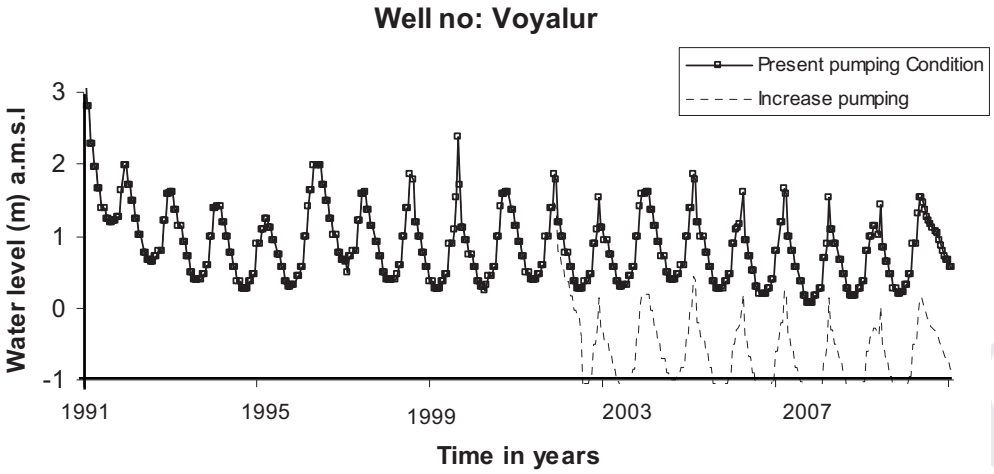

Fig. 9b: Groundwater head with increase in pumping by 3 MGD at well no. 2 Voyalur (eastern side of MAPS site) without subsurface barrier

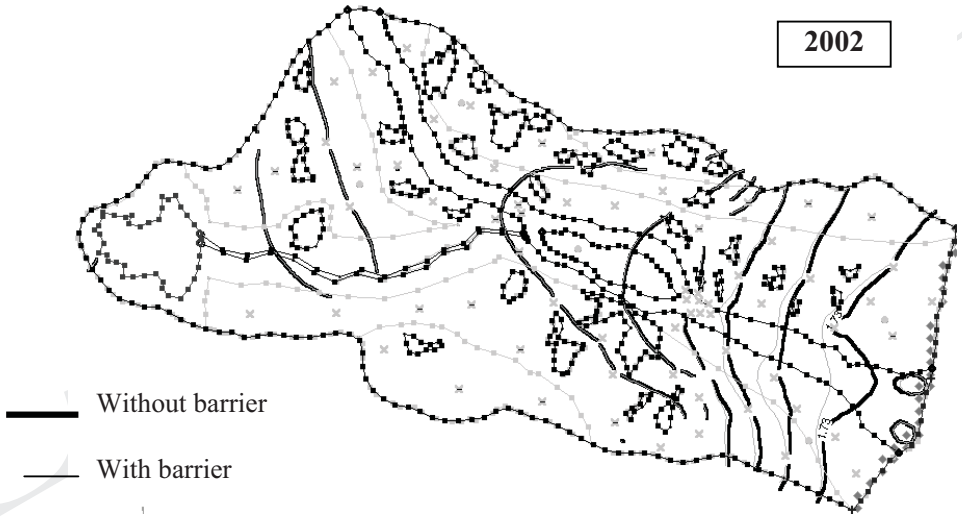

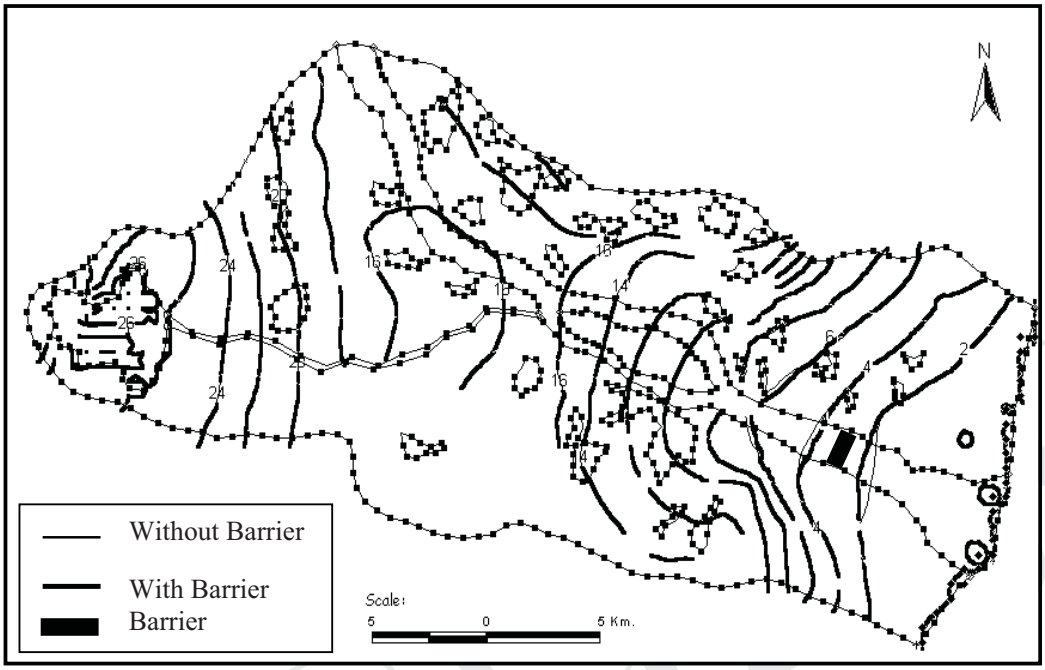

Fig. 10: Predicted regional groundwater head with impact of sub surface barrier on September 2002 & 2003

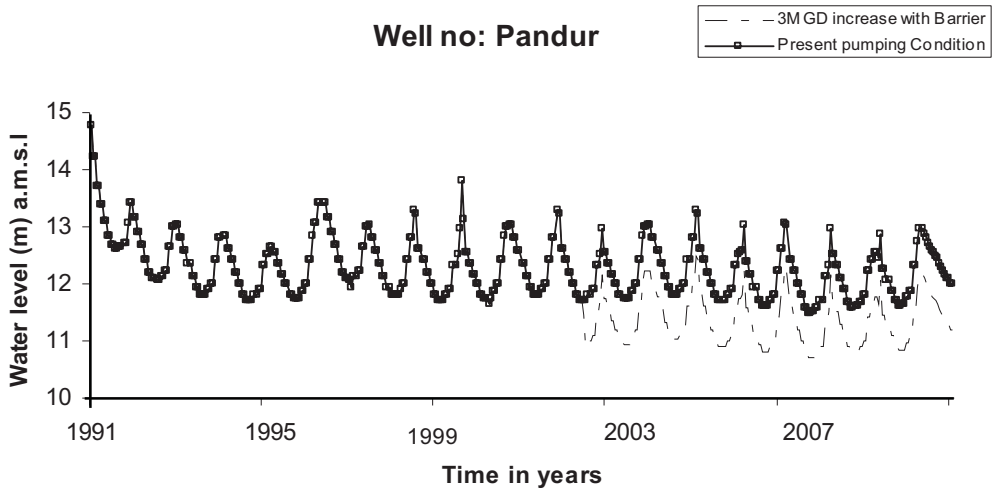

Fig. 10a: Effect on the groundwater head with the construction of subsurface barrier by increasing 3 MGD MAPS site along the upstream side

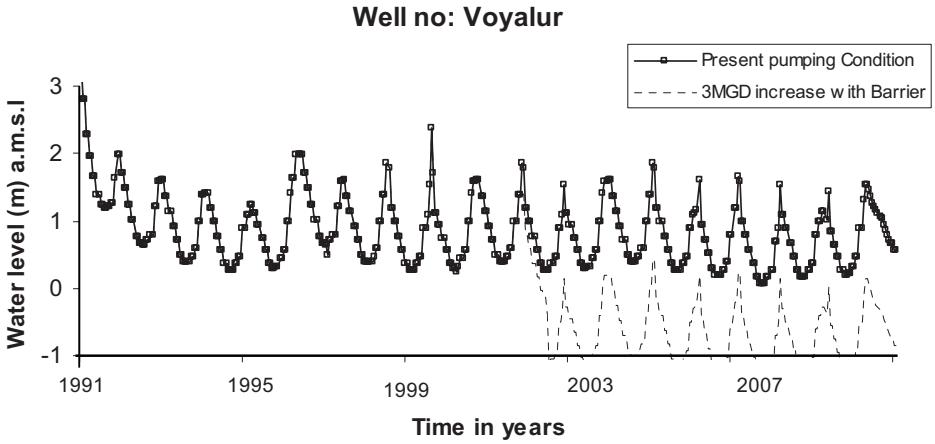

Fig. 10b: Effect on the groundwater head with the construction of subsurface barrier by increasing 3 MGD MAPS site along the downstream side

Effect of Increase in Pumping by 3 MGD at Ayapakkam (Maps Pumping Site)

The expansion of the atomic power station at Kalpakkam will require pumping of 3 MGD in addition to the present level of pumping. As the model prediction of this additional pumping indicated decline in the groundwater table by 0.8 – 1.2 m (explained in previous section), a proposal was made to construct a subsurface barrier across the Palar River to augment the groundwater resources. Hence, the three-dimensional mathematical model of this area developed was used to predict the impact of the subsurface barrier located near Ayapakkam village on the groundwater head. The proposed dimension of the subsurface barrier to stretch across the Palar River is about 1362 m in length and extends to a depth ranging from 3.66 – 6.90 m. The presence of this subsurface barrier was simulated in the model by assigning zero hydraulic conductivity values to the cells where subsurface barrier is located near the village of Ayapakkam. The model predicted an increase in the groundwater head adjoining the barrier (Fig. 10). The impact of the barrier is clearly seen by the decrease in the groundwater head by 0.4 to 0.6 m (Fig. 10a) extending upto a radius of about 1.5 - 2 km along the upstream side of the barrier while on the downstream side the groundwater head would lower by 0.9 to 1.1m (Fig. 10b).

Effect of Increase in Pumping by 3 MGD at Palar Alluvial Region

Simulation of increase in groundwater pumping by 3 MGD distributed over the Palar alluvial region along the upstream without barrier indicates a decline in groundwater by about 0.4 to 0.7m (Fig. 11a) decline. Simulation with subsurface barrier along the upstream indicates a groundwater head by about 0.3 to 0.5 m (Fig. 11b) decline. Palar alluvial region along the downstream without barrier indicates a decline in groundwater by about 0.5 to 0.7m (Fig. 12a). Simulation with subsurface barrier indicates a groundwater head by about 0.6 to 0.9 m (Fig. 12b) decline.

Well: Upstream of MAPS
Inference: about 0.4 to 0.7m decline

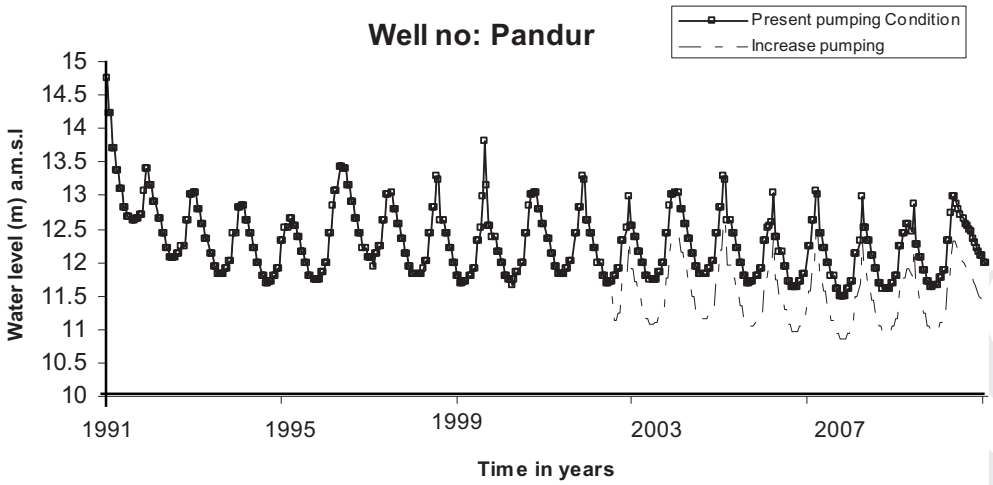

Fig. 11a: 3 MGD increase in pumping- Even distributed over the Alluvial patch of the Palar river (15km radius of MAPS) without Barrier

Inference: about 0.3 to 0.5 m decline

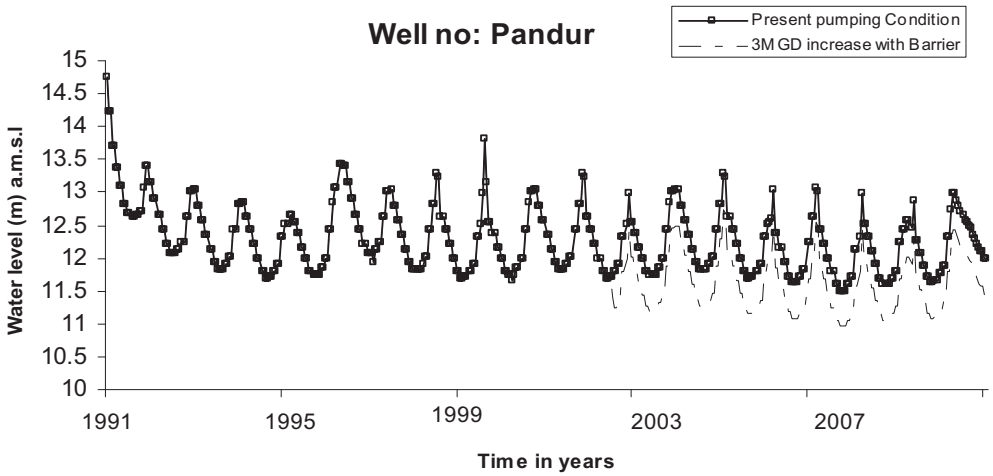

Fig. 11b: 3 MGD increase in pumping- Even distributed over the Alluvial patch of the Palar river (15km radius of MAPS) with Barrier

Well : Down stream of MAPS

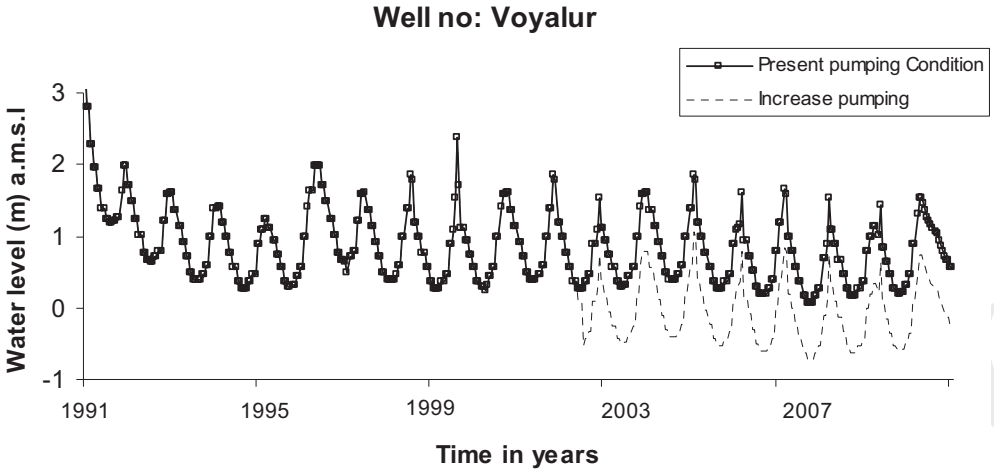

Inference: about 0.5 to 0.7m decline

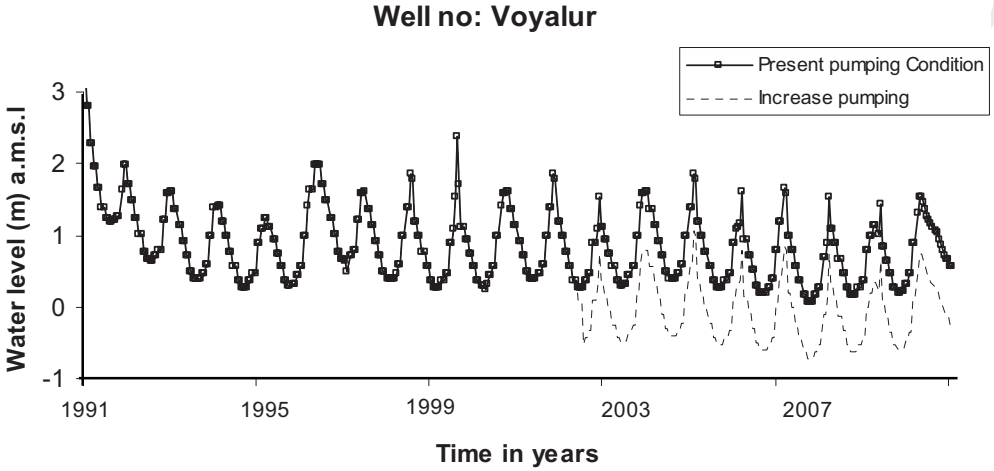

Fig. 12a: 3 MGD increase in pumping distributed over the alluvial patch of the Palar River (15km radius of MAPS) without Barrier

Effect of increase in pumping in the Palar area and its impact with the subsurface barrier is described in the earlier part and is also tabulated in Table.1

Inference: about 0.6 to 0.9 m decline

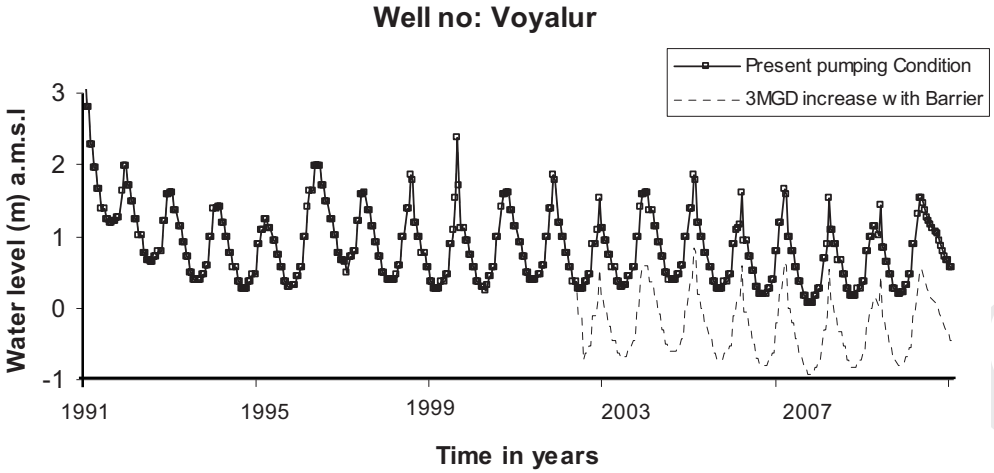

Fig. 12b: 3 MGD increase in pumping distributed over the alluvial patch of the Palar River (15km radius of MAPS) with Barrier

Table 1: Increase in pumping in Palar area

S. No	Scenario	Western side Pandur	Eastern side Voyalur
1.	Addition of 3MGD at Panankattucherry (MAPS) Without barrier	the groundwater head is lowered by 0.5 to 0.8 m	the groundwater head is lowered by 0.8 to 1.2 m
2.	Addition of 3MGD at Panankattucherry (MAPS) With barrier	the groundwater head would lowered by 0.4 to 0.6 m.	the groundwater head would lower by 0.9 to 1.1m
3.	3 MGD distributed over the Palar alluvial region without barrier	the groundwater head decline by 0.4 to 0.7m	the groundwater head decline by 0.5 to 0.7m
4.	3 MGD distributed over the Palar alluvial region with barrier	the groundwater head decline by 0.3 to 0.5 m	the groundwater head decline by 0.6 to 0.9 m
5.	Addition of 3 MGD over the entire Palar region	0.1 to 0.2 m	0.1 to 0.2 m

Saline Water- Fresh Water Interface

The simulated results indicate that this aquifer system is stable under the present pumping rate excepting for a few locations along the coast. The flow vectors also indicate inward

movement of the flow vectors about 2 – 2.5 km inland (Fig.13). Even under normal rate of pumping, the groundwater head is lowered below the sea level during the dry seasons. So, if the pumping is increased by 3 MGD at MAPS pumping station, the villages Chinnakuppam, Periyakuppam, and Oilyakuppam located along the eastern part would be affected by the intrusion of saline water. Seawater has already intruded upto 50-100 m inland in these villages. During the wet season the saline water-fresh water interface gradually moves towards the seaward side. At the present rate of pumping there is no threat to this aquifer.

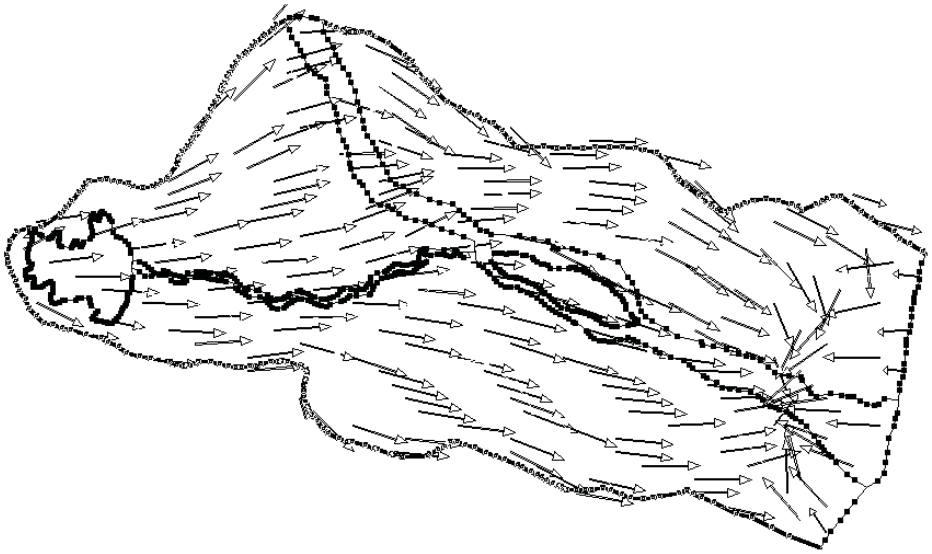

Fig. 13: Groundwater flow vectors showing saline water-fresh water interface during May 2001

CONCLUSION

Simulation of groundwater head was carried in the part of lower Palar River basin, using a finite-difference flow model, for studying the effect construction of sub-surface barrier across the Palar River on the groundwater flow regime in the aquifer system. The model was simulated initially for a period of 12 years (1991-2002). The model was calibrated for steady and transient state conditions. There was a reasonable match between the computed and observed groundwater heads. The model predicted the effect of the subsurface barrier on the groundwater system. It was predicted that there would be an increase in groundwater level by about 0.1 to 0.3 m extending upto a radius of about 1.5 - 2 km along the upstream side of the barrier while on the downstream side the groundwater head would lower by 0.1 to 0.2 m. The aquifer is stable with the present rate of pumping. The model was also used to predict the effect on the groundwater system with an increase in 3 MGD with the present level of pumping from the already existing wells of Panankattucherry (MAPS pumping sites), results in lowering of groundwater head by

0.8–1.2 m on the eastern part extending to a radius of 10 km and 0.5-0.8 m on the western part of this pumping station. The impact of the barrier is clearly seen by the decrease in the groundwater head by 0.4 to 0.6 m along the upstream side of the barrier while on the downstream side the groundwater head would lower by 0.9 to 1.1 m.

Simulation of increase in groundwater pumping by 3 MGD distributed over the Palar alluvial region along the upstream without barrier indicates a decline in groundwater by about 0.4 to 0.7m decline. Simulation with subsurface barrier along the upstream indicates a groundwater head by about 0.3 to 0.5 m decline. Simulation along the downstream without barrier indicates a decline in groundwater by about 0.5 to 0.7m. Simulation with subsurface barrier indicates a groundwater head by about 0.6 to 0.9 m decline.

The favorable areas of this aquifer for construction of new wells is along the alluvial regions i.e. along the flood banks of the Palar River coast were the alluvial thickness is maximum. Groundwater flow regime shows that few locations along the coastal regions have saline water intrusion problem upto 50-100 m inland. The flow vectors also indicate inward movement of the flow vectors about 1 – 1.5 km inland. Even under normal rate of pumping, the groundwater head is lowered below the sea level during the dry seasons.

REFERENCES

[1] Corbet and Bethke., (1992). Disequilibrium fluid pressures and groundwater flow in western Canada sedimentary basin. J Geophys Res. 97(B5): 7203-7217.

[2] Gnanasundar, D. and Elango, L., (2000). Groundwater flow modelling of a coastal aquifer near Chennai city, India. Journal of Indian water resources society vol.20 no.4 pp162-171.

[3] PWD-(Public Works Department)., (2000). Groundwater Perspectives A profile of Kancheepuram district, Tamil Nadu. Public Works Department, pp220.

[4] Rushton.K.R. and Redshaw.S.C., (1979). Seepage and groundwater flow. John Wiley and sons Ltd. NY 330 pp.

[5] Storm, E.W. and Mallory, M.J., (1995). Hydrogeology and simulation of groundwater flow in the Eutaw-Mcshan aquifer and in the Tuscaloosa aquifer system in northeastern Mississippi: U.S Geological Survey Water- Resources Investigations Report 94-4223, pp83.

[6] Senthilkumar, M. and Elango, L., (2001). Numerical simulation of groundwater flow regime in a Part of the Lower Palar River Basin, Southern India. Modelling in Hydrogeology, Eds. Elango & Jayakumar, Allied Publs. pp270.

[7] Senthilkumar, M. and Elango, L., (2004). 'Three- dimensional mathematical model to simulate groundwater flow in the lower Palar River basin, southern India' Hydrogeology Journal, Vol.12, No.4, pp. 197-208.

Numerical Simulation of Groundwater Flow and Solute Transport, L. Elango (ed). pp.151-164

Groundwater Contaminate Transport Modelling

S. Mohan and **S.K. Pramada**

INTRODUCTION

A model is anything that is an approximation of a real system. Groundwater flow models are used to calculate the rate and direction of movement of groundwater through aquifers and confining units in the subsurface. Contaminant transport models simulate the movement and chemical alteration of contaminants as they move with groundwater through the subsurface. The equations that describe the groundwater flow and fate and transport processes may be solved using different types of models. Some models may be exact solutions to equations that describe very simple flow or transport conditions (analytical model) and others may be approximations of equations that describe very complex conditions (numerical models. Analytical models are an exact solution of a specific, greatly simplified, groundwater flow or transport equation. Prior to the development and widespread use of computers, there was a need to simplify the three-dimensional equations because it was not possible to easily solve these equations. Specifically, these simplifications resulted in reducing the groundwater flow to one dimension and the solute transport equation to one or two dimensions. This resulted in changes to the model equations that include one-dimensional uniform groundwater flow, simple uniform aquifer geometry, homogeneous and isotropic aquifers, uniform hydraulic and chemical reaction properties, and simple flow or chemical reaction boundaries. Analytical models are typically steady state and one-dimensional, although selected groundwater flow models are two dimensional (e.g. analytical element models), and some contaminant transport models assume one-dimensional groundwater flow conditions and one-, two- or three-dimensional transport conditions. Well hydraulics models, such as the Theis or Neumann methods, are examples of analytical one-dimensional groundwater flow models. Numerical models are capable of solving the more complex equations that describe groundwater flow and solute transport. These equations generally describe multi-dimensional groundwater flow, solute transport and chemical reactions, although there are one-dimensional numerical models. Numerical models use approximations (e.g. finite differences, or finite elements) to solve the differential equations describing groundwater flow or solute transport. The approximations require that the model domain and time be discredited. In this discretization process, a network of grid cells or elements represents the model domain, and time steps represent the time of the simulation. The accuracy of numerical models depends upon the accuracy of the model input data, the size of the space and time discretization (the greater the size of the discretization steps, the greater the possible error), and the numerical method used to solve the model equations

In recent years groundwater flow and contaminant transport model has become a major part of many projects dealing with groundwater exploitation, protection and remediation. A

groundwater flow model is necessary for the development of a contaminant transport model. The groundwater velocity needed in the transport model is obtained from the flow model.

GROUND WATER CONTAMINATION

Any substances introduced into groundwater by human activities are considered contamination. Natural contamination can also occur if undesirable elements are introduced into groundwater by natural processes. Contaminant levels that exceed acceptable limits result in pollution

There are three general types of contaminants

- Sinking - heavier than water
- Floating - lighter than water
- Compatible or soluble - can mix and dissolve in water

Floating contaminants (also called **LNAPLs** - Light NonAqueous Phase Liquids) tend to be organic compounds and hydrocarbons that are **immiscible** (cannot be dissolved) in water. These contaminants tend to spread out on the groundwater surface in a thin film away from the source of the contamination eg. fuels: gasoline, diesel fuel

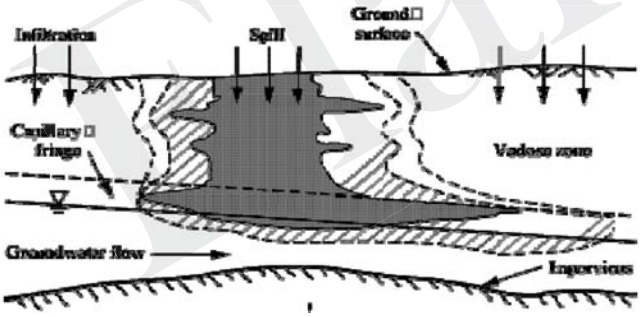

Fig. 1: Migration of NAPL

Sinking contaminants (also called **DNAPLs** - Dense NonAqueous Phase Liquids) tend to accumulate in depressions in the lower surface of the aquifer to which they have been introduced. Eg. chlorinated hydrocarbons such as 1-1-1 trichloroethane, carbon tetrachloride, chlorophenols, chlorobenzenes, tetrachloroethylene, and polychlorinated biphenyls (PCBs).

Compatible contaminants dissolve and mix in the groundwater and are carried along by groundwater flow.

We can categorize ground-water contaminants by their source.

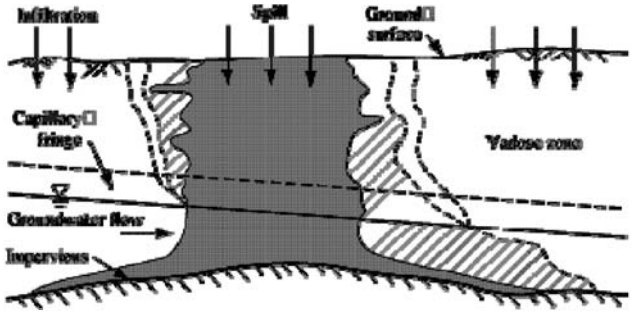

Fig. 2: Migration of DNAPL

1. Sources designed to discharge substances
   - Septic tanks/cesspools
   - Injection wells
   - Land application
2. Sources designed to store/treat/dispose of waste
   - Landfills
   - Surface impoundments
   - Mine wastes
   - Animal burials
   - Storage tanks
   - Radioactive waste disposal
3. Retain substances during transport
   - Pipelines
   - Transfer stations - solid waste
4. Discharge as a result of other activities
   - Irrigation
   - Agriculture/Lawns
   - Road salt
   - Urban runoff
   - Water softeners
5. Sources as conduits to aquifers
   - Poorly constructed wells (observation or monitoring)
   - Excavation - dewatering
6. Naturally occurring that is aided by humans
   - Saltwater intrusion or up(down)coning
   - Coal mines

FATE AND TRANSPORT OF CONTAMINANT

Transport of contaminants in the groundwater system is affected by different processes. They include advection, dispersion, diffusion, adsorption and decay.

Contaminant Transport Mechanisms

There are three basic processes of transport of contaminant:

- Molecular Diffusion
- Advection
- Mechanical Dispersion

Molecular Diffusion: this is the movement of dissolved ions from regions of high concentration to regions of low concentration.

The mass that diffuses is proportional to a concentration gradient that can be described with **Fick's First Law** (in one dimension).

$$F = -D_d\left(\frac{dC}{dx}\right)$$

Where

F = mass flux of solute per unit area,
D_d = diffusion coefficient (L^2/T),
C = solute concentration (M/L^3), and
dC/dx = concentration gradient ($M/L^3/L$).
(-) indicates movement from higher to lower C

For systems where concentration may be changing with time Ficks second law may be applied

$$\frac{\partial C}{\partial t} = D_d \frac{\partial^2 C}{\partial x^2}$$

In porous media, diffusion cannot proceed as fast as it can in water because the ions must follow longer pathways as they travel around mineral grains. In addition, the diffusion can take place only through pore openings. To take these into account an effective diffusion coefficient must be used.

$$D^* = \omega D_d$$

Where, ω is a function of tortuosity and value ranges from 0.01 to 0.5

Advection: this is the movement of contaminants that occurs because they are being carried along with the moving groundwater. The rate of advection is equal to the rate at which the groundwater is flowing. This is the same as the seepage velocity

Darcy Velocity

$v = ki = q/A$

Seepage Velocity relates to actual velocity of particle in soil matrix

$V_a = v/n$

Advective flux $F_a = V_aC$

Mechanical Dispersion: mixing that occurs as the water containing a contaminant(s) flows around the solids in the aquifer media. In reality, groundwater particles are moving faster and slower than the average linear velocity. Three causes of this

1. Fluid will move faster in center of pores than edges
2. Some particles will take longer random paths
3. Some pores are bigger than others allowing for faster flow

Since all water is not traveling at the same speed, mixing occurs along the flow path this **mechanical dispersion** results in a dilution of the solute at the advancing edge of flow.

- **Longitudinal dispersion** is the dispersion in the direction of the flow path
- **Transverse dispersion** this is dispersion out to the sides of the general flow path

In flowing groundwater it is impossible to separate the processes of mechanical dispersion and diffusion. The two are lumped together and treated as a single compound effect called **hydrodynamic dispersion**.

$$D_L = \alpha_L v_x + D^*$$

$$D_T = \alpha_T v_x + D^*$$

where

D_L = longitudinal hydrodynamic dispersion coefficient,
D_T = transverse hydrodynamic dispersion coefficient,
α_L = longitudinal dispersivity, and
α_T = transverse dispersivity.

The effect of hydrodynamic dispersion is to cause a plume of contamination to elongate in the direction of advection as well as to develop a gradient of decreasing concentration from the center to the margins of the plume.

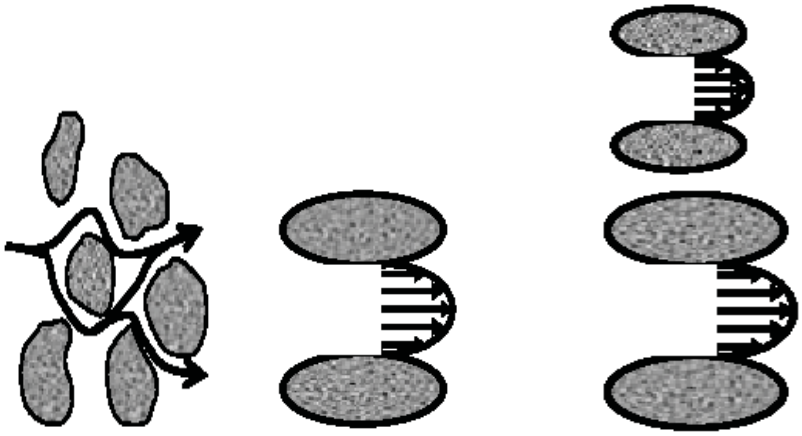

Path length **Friction in Pore** **Difference n pore size**

Fig. 3: Mechanical dispersion

Fate of Contaminants

Chemical reactions may transform one compound into another, change the state of the compound, or cause a compound to combine with other organic or inorganic chemicals. For use in the advection-dispersion equation, these reactions represent changes in the distribution of mass within the specified volume through which the movement of the chemicals is modelled. Chemical reactions in the subsurface often are characterized kinetically as equilibrium, zero, or first order, depending on how the rate is affected by the concentrations of the reactants.

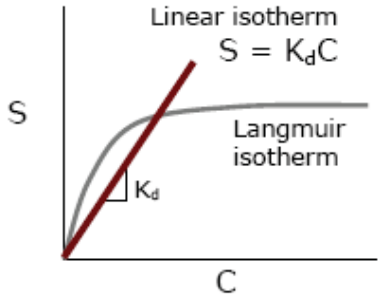

Fig. 4: Different Isotherms

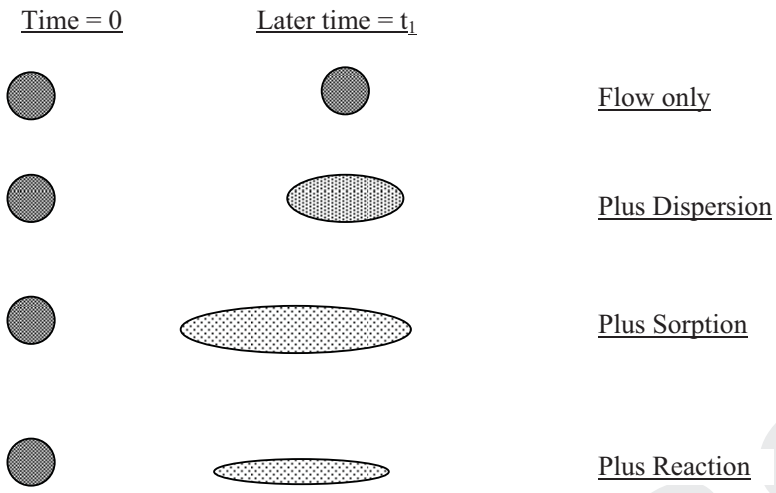

Fig. 5: Schematic diagram of processes effects on contaminant transport for a slug release of contaminant

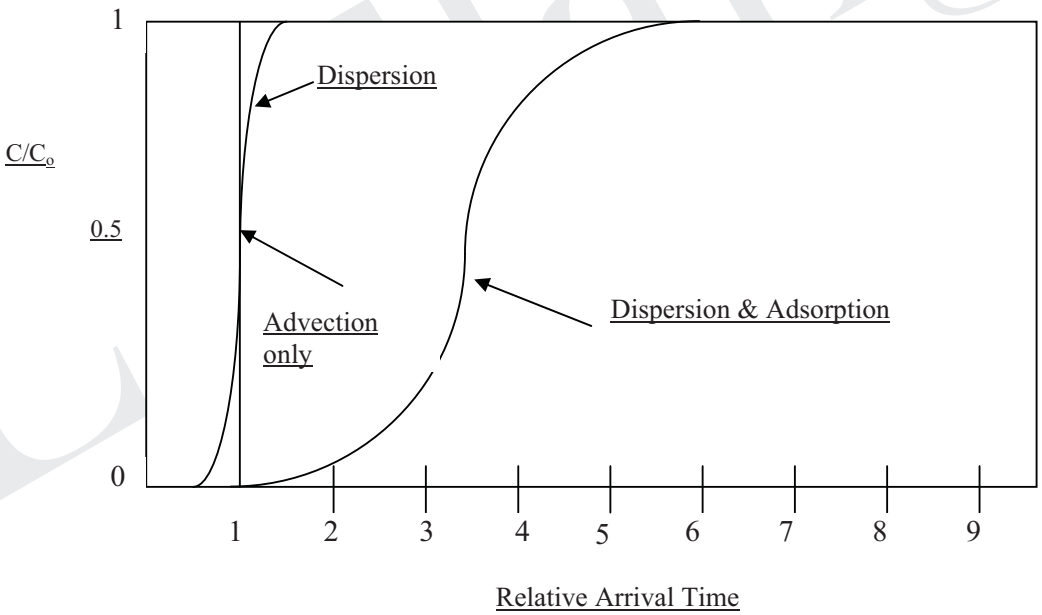

Fig. 6: Breakthrough curves for a constant contaminant source concentration C = Co

Sorption is probably the most important chemical process affecting the transport of organic contaminants in the subsurface environment. Sorption is a type of surface reaction in which the solute stuck to solid surfaces thereby delaying its arrival. Under conditions of linear equilibrium partitioning, the sorption process is represented in the advection dispersion equation as a "retardation factor," R If the retardation factor, R, is equal to 1.0, the solute is nonreactive and moves with the groundwater. Contaminants with lower retardation factors are transported greater distances over a given time than contaminants with larger retardation factors If R = 2 for a given contaminant, it is retarded by a factor of two—in other words, it is moving at half the speed.

Isotherm – a relationship that is not a function of time showing the concentration in solution (C) versus that absorbed (S) on the solid surface.

GOVERNING EQUATIONS OF FLOW AND TRANSPORT

Water Flow in Porous Media

The equation relating Darcy flow of water and conservation of mass of water in 3-D is:

$$\frac{\partial}{\partial x}\left(k_x \frac{\partial h}{\partial x}\right)+\frac{\partial}{\partial y}\left(k_y \frac{\partial h}{\partial y}\right)+\frac{\partial}{\partial z}\left(k_z \frac{\partial h}{\partial z}\right)+W=S\frac{\partial h}{\partial t}$$

Where

x, y, z = principal Cartesian coordinates
h = head
k_i = permeability in the i direction
W = source/sink term
S = specific storage

Transport of Dissolved Contaminant Mass

Let the flux of one particular dissolved constituent into and out of an element of porous media be **F.**

From continuity of mass of the contaminant, we may write:

$$\frac{\partial F}{\partial x}+\frac{\partial F}{\partial y}+\frac{\partial F}{\partial z}+r=\frac{\partial m}{\partial t}=\frac{\partial(nC)}{\partial t}$$

where

r = source/sink term for mass of contaminant due to reactions in aquifer (+ve is a source)
m = mass/unit volume of contaminant
= (porosity • Concentration) = (n • C)

Now the total flux in 1-D, F, has two components:

advective flow $F_a = v_{sx}\, n\, C$ and
dispersive flow $F = -n\, D_x\, \partial C/\partial x$ Thus the total flux in the x direction is:

$F_x = -n\, D_x\, \partial C/\partial x + v_{sx}\, n\, C$

Substituting into the conservation of contaminant mass equation in 1-D we obtain:

$$-\left[\frac{\partial}{\partial x}\left(-n D_x \frac{\partial C}{\partial x} + v_{sx}\, n C\right)\right] + r = \frac{\partial (n C)}{\partial t}$$

which may be simplified to:

$$D_x \frac{\partial^2 C}{\partial x^2} - v_{sx} \frac{\partial C}{\partial x} + \frac{r}{n} = \frac{\partial C}{\partial t}$$ **Advection Dispersion Equation**

Reactions in the Aquifer

Regarding reactions in the aquifer (r term)

r = 0 no chemical reactions

if r is 1^{st} order reaction (radioactive decay, biodegradation

$r = -\frac{\partial (n C)}{\partial t} = -\lambda n C$ (note –ve because loss of mass)

where λ = the decay constant

Considering Sorption

for a linear sorption isotherm $S = K_d C$

Assuming that the r term takes the form

$$r = -\rho \frac{dS}{dt} = -\rho K_d \frac{dC}{dt}$$

Thus the contaminant mass flux Governing Equation becomes:

$$D_x \frac{\partial^2 C}{\partial x^2} - v_{sx} \frac{\partial C}{\partial x} - \left(\frac{\rho K_d}{n}\right)\frac{\partial C}{\partial t} = \frac{\partial C}{\partial t}$$

Rewriting:

$$D_x \frac{\partial^2 C}{\partial x^2} - v_{sx} \frac{\partial C}{\partial x} = \left(1 + \frac{\rho K_d}{n}\right) \frac{\partial C}{\partial t} = R \frac{\partial C}{\partial t}$$

And we define R as the retardation coefficient:

$$R = 1 + \frac{\rho K_d}{n}$$

ANALYTICAL SOLUTIONS OF MASS TRANSPORT EQUATIONS IN ONE DIMENSION WITH CONTINUOUS INJECTION

The mass transport equation in one-dimensional space without reaction term is written as

$$\frac{\partial C}{\partial t} = D_x \frac{\partial^2 C}{\partial x^2} - v_x \frac{\partial C}{\partial x}$$

where v_x is the linear ground-water velocity in the x direction and D_x is the dispersion coefficient.

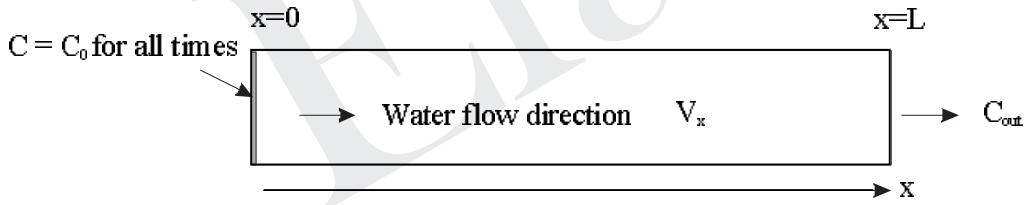

Fig. 7: Problem of one-dimensional mass transport with a continuous source

The boundary conditions for system are

$C(0,t) = C_0$, **for t >= 0**

$C(\infty,t) = 0$, **for t >=0**

with the initial condition (at t = 0): $C(x,0) = 0$ for $0 < x < \infty$

It is assumed that flow is in the x-direction at a constant velocity v_x and a longitudinal dispersion coefficient (D_x), defined as $\alpha_L v_x + \tau D_m$ (τ is the tortuosity of a medium and D_m is the molecular diffusion coefficient). The solution of Eq with boundary conditions

$$C(x,t) = \frac{C_0}{2}\left[erfc\left(\frac{x - v_x t}{2\sqrt{D_x t}}\right) + e^{\frac{xv_x}{D_x}} erfc\left(\frac{x + v_x t}{2\sqrt{D_x t}}\right)\right]$$

erfc () is the complementary error function. The complementary error function erfc() is related to the error function erf() by $erfc(-\beta) = 1 + erf(\beta)$, $erfc(\beta) = 1 - erf(\beta)$, and $erf(-\beta) = -erf(\beta)$. Values of erf () and erfc () are presented in Table 1.

PRACTICE PROBLEM

A landfill is leaking leachate with a chloride concentration of 725 mg/l, which enters the aquifer. Compute the concentration profile in one year. The given properties are

Hydraulic conductivity = 3 * 10^{-5} m/s; dh/dl = 0.002; Effective porosity = 0.23

D* = 1*10^{-9} m^2/sec; Dispersivity = 1.5m

Solution

Average linear velocity = (k *dh/dl)/n = 2.61*10^{-7} m/sec

Longitudinal dispersion coefficient

DL = Dispersivity * average linear velocity+ Molecular diffusion coefficient
=1.5 ***2.61***10^{-7}+1*10^{-9} = =3.91 *10^{-7} m^2/sec; t=1 year=3.15 *10^7 sec; Co=725 mg/l

$$C(x,t) = \frac{C_0}{2}\left[erfc\left(\frac{x - v_x t}{2\sqrt{D_x t}}\right) + e^{\frac{xv_x}{D_x}} erfc\left(\frac{x + v_x t}{2\sqrt{D_x t}}\right)\right] =$$

$$= \frac{725}{2} erf\left[\frac{(x - 8.22)}{7.02}\right] + \exp\left(\frac{2.61x}{3.91}\right) erfc\left[\frac{(x + 8.22)}{7.02}\right]$$

Table 1: Values of erf() and erfc()

x	erf(x)	erfc(x)
-3.0	-1.000000	2.000000
-2.8	-0.999925	1.999925
-2.6	-0.999764	1.999764
-2.4	-0.999311	1.999311

x	erf(x)	erfc(x)
-2.2	-0.998137	1.998137
-2.0	-0.995323	1.995323
-1.8	-0.989091	1.989091
-1.6	-0.976348	1.976348
-1.4	-0.952285	1.952285
-1.2	-0.910314	1.910314
-1.0	-0.842701	1.842701
-0.8	-0.742101	1.742101
-0.6	-0.603856	1.603856
-0.4	-0.428392	1.428392
-0.2	-0.222703	1.222703
0.0	0.000000	1.000000
0.2	0.222703	0.777297
0.4	0.428392	0.571608
0.6	0.603856	0.396144
0.8	0.742101	0.257899
1.0	0.842701	0.157299
1.2	0.910314	0.089686
1.4	0.952285	0.047715
1.6	0.976348	0.023652
1.8	0.989091	0.010909
2.0	0.995323	0.004677
2.2	0.998137	0.001863
2.4	0.999311	0.000689
2.6	0.999764	0.000236
2.8	0.999925	0.000075
3.0	1.000000	0.000000

Table 2: Solution of the Problem

x(m)				erf(b)	erf(c)	Con (mg/l)
0						725
1	-1.02849	1.31339	0.667519	1.852544	0.062426	671.6687
2	-0.88604	1.45584	1.335038	1.78668	0.037505	647.8141
3	-0.74359	1.59829	2.002558	1.703731	0.021497	617.7617
4	-0.60114	1.74074	2.670077	1.602915	0.01216	581.2323
5	-0.45869	1.88319	3.337596	1.484208	0.007377	538.2329
6	-0.31624	2.02564	4.005115	1.348482	0.005257	489.1131
7	-0.17379	2.16809	4.672634	1.197651	0.004243	434.6024
8	-0.03134	2.31054	5.340153	1.034812	0.003217	375.7901
9	0.11111	2.45299	6.007673	0.883858	0.001602	321.0497
10	0.25356	2.59544	6.675192	0.718959	0	260.6226
11	0.39601	2.73789	7.342711	0.572247	0	207.4396
12	0.53846	2.88034	8.01023	0.444622	0	161.1756
13	0.68091	3.02279	8.677749	0.336222	0	121.8805
14	0.82336	3.16524	9.345269	0.246526	0	89.36558
15	0.96581	3.30769	10.01279	0.174461	0	63.24207
16	1.10826	3.45014	10.68031	0.118507	0	42.95864
17	1.25071	3.59259	11.34783	0.076799	0	27.83976
18	1.39316	3.73504	12.01535	0.047238	0	17.12367
19	1.53561	3.87749	12.68286	0.027587	0	10.0004
20	1.67806	4.01994	13.35038	0.015586	0	5.649865
21	1.82051	4.16239	14.0179	0.009048	0	3.279872
22	1.96296	4.30484	14.68542	0.00597	0	2.164186
23	2.10541	4.44729	15.35294	0.004636	0	1.680565
24	2.24786	4.58974	16.02046	0.003721	0	1.348815
25	2.39031	4.73219	16.68798	0.002397	0	0.86883

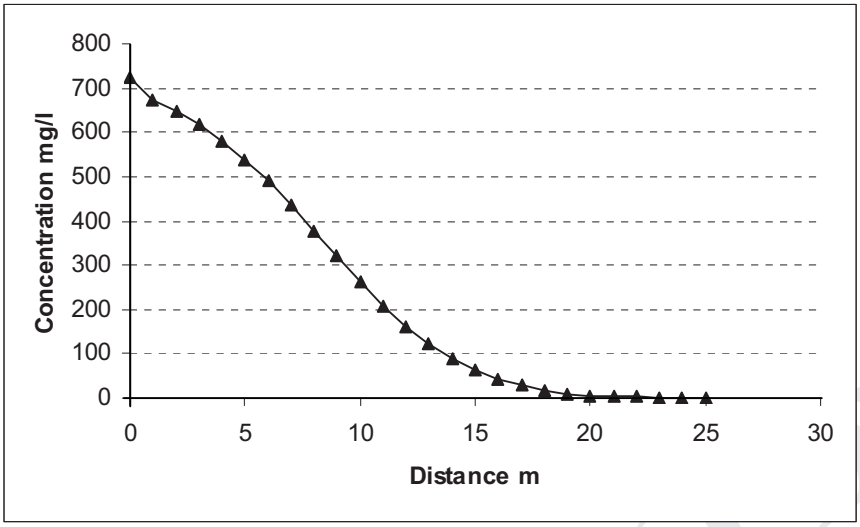

Fig. 8: Concentration profiles in the direction of flow for a continuous source

NUMERICAL SOLUTIONS OF MASS-TRANSPORT EQUATIONS

The numerical approaches are a family of computer-based techniques for solving contaminant transport equations. They approximate forms of the advection-dispersion equation as a system of algebraic equations, or alternatively simulate transport through the spread of a large number of moving reference particles. Whatever the procedure used, it invariably has to be coded for solution on a high-speed computer.

Numerical approaches easily accommodate variability in flow and transport parameters (e.g., hydraulic conductivity, porosity, dispersivity, cation exchange capacity, and etc.). This flexibility in representing parameters facilitates modelling of layering or other more complex patterns of variability in two and three dimensions. One can simulate the complex plumes that occur with real problems. Thus, numerical approaches are readily adapted to site-specific problems and thus are particularly useful in practice.

Various public domain numerical mass transport codes are available. The most commonly used codes include MT3DMS, SUTRA, HST3D. MT3DMS is the modular three-dimensional transport model (MT3D) with significantly expanded capabilities. SUTRA is a two-dimensional solute or energy transport finite-element code for saturated or unsaturated flow. The HST3D is a heat and transport three-dimensional code with integrated finite difference scheme.

Numerical Simulation of Groundwater Flow and Solute Transport, L. Elango (ed). pp.165-171

Assessment of Groundwater Contamination around the Hyderabad TSDF, Andhra Pradesh

V.V.S. Gurunadha Rao, S. Sankaran and **K. Mahesh Kumar**

INTRODUCTION

Andhra Pradesh Pollution Control Board (APPCB) has constructed a Treatment Storage Disposal Facility (TSDF) under Hyderabad Solid Waste Management Project for disposal of hazardous wastes generated by industries in and around Hyderabad city with Australian aid. The facility is created by Ramky Industries over 20 hectares land in the Khazipally industrial area on the already existing industrial solid waste dump site. The TSDF is situated near Dindigal village in the Dindigal Reserve Forest area, Ranga Reddy District, Andhra Pradesh. The study area is located about 25 km NW of Hyderabad city on the Medak road. The watershed covering TSDF spread over 75 sq. km (Fig. 1).

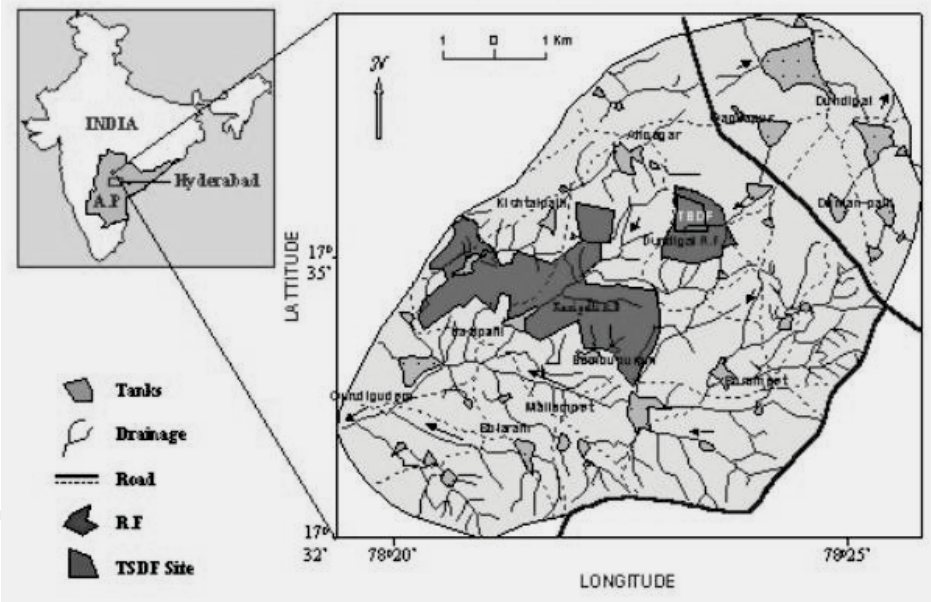

Fig. 1: Location map of TSDF Watershed, Dindigal and surroundings

LANDFILL DESIGN

The TSDF is designed for disposal of hazardous solid waste from CETPs, STPs and other industrial solid wastes. The top weathered part of the ground surface has been

excavated and an in situ clay liner of 1 m thickness has been made on the fractured formation. HDPE liner of 1 mm thickness was laid above the clay liner followed by drainage net of 5 mm and gravel of 30 cm to drain the leachate from the TSDF. The drain pipes of leachate collection well have been laid in this lining. A second set of layers of HDPE liner of 1mm, drainage net and gravel has been laid over the bottom set of liners. Third set of layers consists of HDPE liner of 1 mm, drainage net of 5 mm followed by industrial solid waste of 10.3 m thickness. For tipping of TSDF has been carried out by set of layers of 30 cm of clay, 30 cm of gravel, 60 cm of loamy fine sand followed by HDPE liner (Gurunadha Rao et al, 2004). The final tipping of TSDF has been carried out by layers of drainage net of 5 mm, coarse sand of 60 cm and loamy fine sand of 60 cm on which one can grow small grass vegetation, which is aimed to reduce the infiltration as well as surface runoff due to rainfall (Fig. 2).

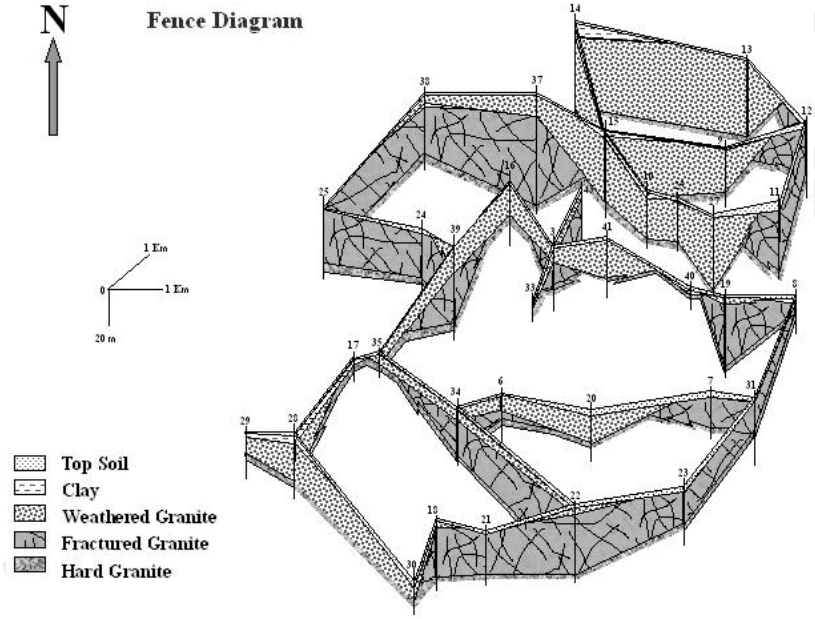

Fig. 2: Fence diagram of litho units in TSDF Watershed

GEOPHYSICAL INVESTIGATIONS

The geomorphological features of the TSDF watershed indicate that the TSDF is situated on the ridge part of the area. The topographic feature divides the natural drainage into two different watersheds having different flow directions, one towards the Dommarapochampalli- Dindigal villages. A major Quartz vein running North – South abetting the eastern boundary of the site plays a significant role on the hydrodynamics of the area. A dolerite dyke running almost East-West direction has been inferred from magnetic surveys, which is very massive near Ganapathi Sachidnanda Dathapeeta Ashram and further

east. The dyke has almost pinched out and disappeared as we move close to and within the TSDF site. The extension of the above dyke was traced through magnetic surveys near the North – East portion of the TSDF site. The dolerite dyke, which is a plutonic intrusion, has been totally disturbed and altered by the major quartz vein (NS), which is a later magmatic activity. This structural feature and tectonic activity has created intense weathering and fracturing of hard rocks in the eastern side of the TSDF site area (Fig. 3).

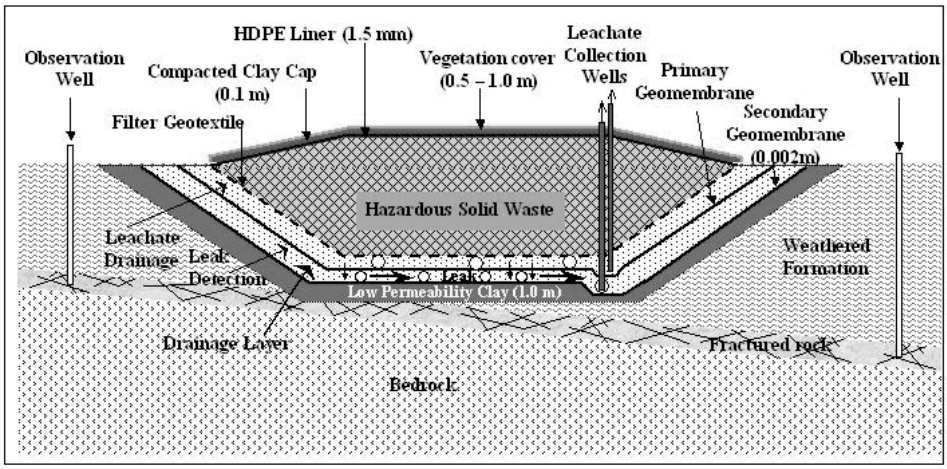

Fig. 3: Vertical Cross Section of TSDF Landfill (APPCB), Dundigal, R.RDistrict, A.P.

GEOHYDROLOGICAL INVESTIGATIONS

The TSDF has been constructed on the ridge part of the watershed in the granitic terrain, which is also a deep water table area in the Dindigal village. There are 14 observation wells around the first cell (2 ha) of TSDF for monitoring of groundwater level as well as water quality. The loading of hazardous waste in the first cell have commenced during November 2002 and tipping of the cell has been completed during December 2003. In addition to the observation wells around TSDF, 43 observation wells have been established in the TSDF watershed. The geophysical investigations carried out have helped to construct the fence diagram and understanding the aquifer geometry. Pre-monsoon and post-monsoon water level and water quality has been monitored and water quality analyzes have been carried for major ions and trace element concentrations. The water level fluctuations during pre-monsoon to post-monsoon vary from 1 – 5 m during the study period. The groundwater quality analyzes indicated presence of toxic trace elements exceeding the WHO limits. The TDS concentration has varied from 1000 – 6000 mg/l within the TSDF with a background TDS concentration around 1000 mg/l in the watershed (Gurunadharao et al., 2004).

As far as the leachate generation from the first cell is concerned the output from the HELP model indicate the designed landfill with embedded liners seems to be a best design for minimizing the leachate contact with groundwater regime. The average hydraulic head generated within the tipped landfill will be about 1.1 m, which occurs during rainy season, and it will reduce to a 0.9 m during rest of the period. The hydraulic head may be acting as a driving force for leachate migration within the landfill. The water samples collected from leachate collection well have shown TDS concentration exceeding 10000 mg/l.

GROUNDWATER FLOW AND MASS TRANSPORT MODEL

The water level collected during June 2001 has been assumed to be under equilibrium condition and same have been used for construction of groundwater flow model (Fig. 4).

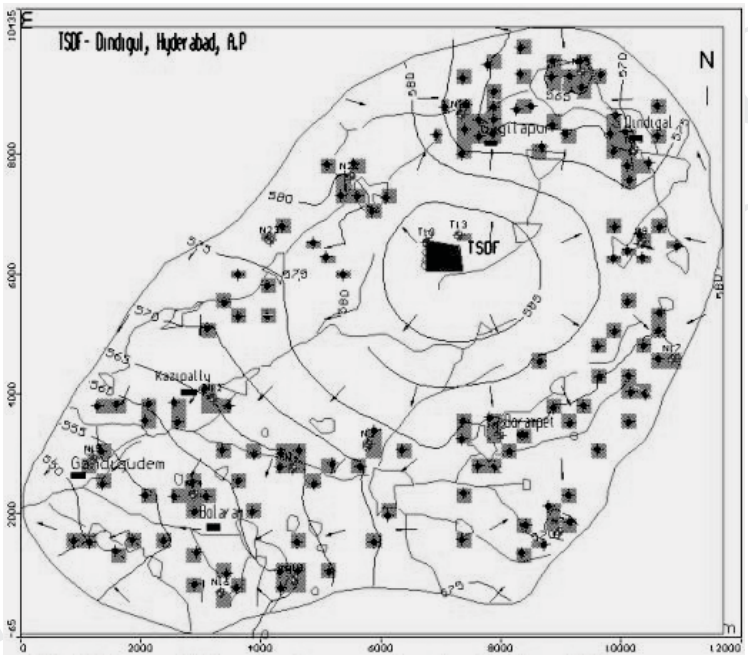

Fig. 4: Computed Water level contours in m(amsl)-June 2001

The computed hydraulic head distribution has been compared with observed data and found matching closely. The computed groundwater velocity in the study area has been about 15 m/year. The leachate concentration of 2000 mg/l has been applied as source loading over 20 ha area and consequent migration pattern for next 100 years has been predicted (Figs. 5a & 5b).

The computed TDS concentration for 20 years shows that the contaminant from the TSDF could migrate only to about 200 m all around from first cell with slight increase in migration towards north. Further the contaminant could hardly migrate to about 600 m around the TSDF during next 100 years (Gurunadha Rao et al, 2004). Thus the status of likely groundwater contamination from the TSDF operations for next 100 years could be limited to a small area within the TSDF. Thus the present TSDF seems on a safe location as regards geological and prevailing hydrogeological conditions. If some heavy pumping occurs in the Gagilapur and Dindigal villages, there could be a possibility of extension of contaminant migration further towards north of TSDF in future.

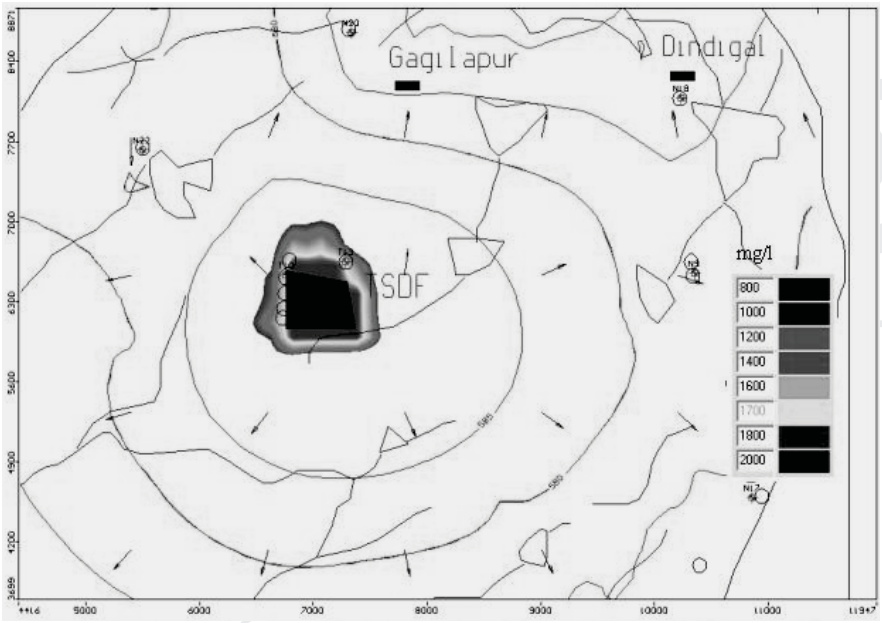

Fig. 5a: Predicted Contaminant Migration TDS (mg/l) from TSDF-100 Years (First Layer)

CONCLUSIONS

It is suggested to monitor the water level and water quality in the northern part more often to ascertain changing groundwater scenario from time to time. It is imperative to control groundwater pumping in the Gagilapur and Dindigal villages as it may influence reversal of hydraulic gradient from TSDF site towards the above two villages. The monitoring of the observation wells around TSDF should be continued for water levels and water quality for detection and compliance monitoring purposes. If there occurs a sudden rise in concentrations or water level, the cause for such increase has to be investigated in detail as TSDF is a hazardous wastes storage facility. The precautions provided in the first cell development and closure may be continued stringently for adjacent cells development

in future. The exact amount of leachate collected from each cell has to be documented from time to time to improve landfill design strategies for reducing leachate generation from the facility.

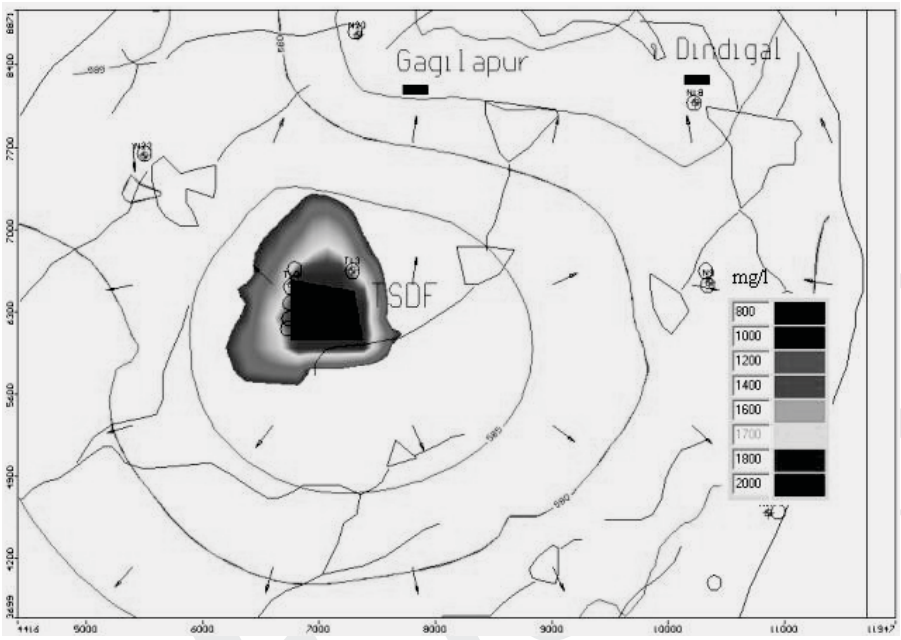

Fig. 5b: Predicted Contaminant Migration TDS (mg/l) from TSDF-100 Years (Second Layer)

REFERENCES

[1] Gurunadha Rao, V.V.S., Sankaran, S., Chandrasekhar, S.V.N. and Mahesh Kumar, K., (2004). Assessment of Groundwater Contamination around Hyderabad TSDF at Dindigal, R.R. District, A.P. Tech Rep. No. NGRI/2004-GW-419, pp. 112.

[2] Gurunadha Rao, V.V.S., (2004). Geoenvironmental studies for Waste Disposal around Hyderabad. In Refresher course on Water Management. Academic Staff College and Centre for Water Resources, JNTU, Hyderabad. Feb 2-22.

[3] CAGP, (1974). Central Groundwater Board Canadian assistance Groundwater project report, Central Groundwater Board (SR).

[4] Anderson M.P. and Woessner, W.W., (1992). Applied groundwater modelling - simulation of flow and advective transport. Academic press. San Diego, CA., U.S.A.

[5] Gurunadha Rao, V.V.S., Dhar, R.L. and Subrahmanyam, K., (2002). Assessment of groundwater contamination in Patancheru and Bolaram Industrial Development Areas. Water, Soil and Air Pollution, Vol.

[6] Nilson Guiger and Thomas Franz, (1996). Visual MODFLOW: Users Guide. Waterloo Hydrogeologic, Waterloo, Ontario, Canada.

[7] McDonald, J.M. and Harbaugh, A.W., (1988). A modular three-dimensional finite difference groundwater flow model. Techniques of Water resources Investigations of the U.S. Geological Survey Book.6, pp.586.

[8] Schneider, W.J., (1970). Hydraulic implications of solid waste disposal. U.S. Geological Survey Circular 601 F.

[9] Relis, P. and Dominski, A., (1987). Beyond the crisis: Integrated waste management. Santa Barbara, CA: Community Environmental Council.

[10] Zheng, C., (1990). MT3D, a Modular three-dimensional transport model for simulation of advection, dispersion and chemical reactions of contaminants in groundwater system prepared for the U.S. Environmental Protection Agency .

Numerical Simulation of Groundwater Flow and Solute Transport, L. Elango (ed). pp.173-192

Mass Transport Modelling: A Case Study in Upper Palar River Basin (South India)

M. Thangarajan

PRE-AMPLE

Pollutant migration in the groundwater was quantified in upper Palar river basin through Mass transport modelling study (Thangarajan, 1999). The study area lies in a hilly terrain of North Arcot district of Tamilnadu (Fig. 1). The untreated effluents from about 650 tanneries have polluted the groundwater system. Seepage of the effluents in unlined canals has been causing pollution of groundwater (Krishnawamy & Haridass, 1984; Teekaraman & Farooque Ahmed, 1982; Margam, unpublished data). The area of high groundwater pollution has been progressively expanding. The situation has become all the more precarious in view of a meager surface water potential in the area where most of the requirements for irrigation, industry and drinking purposes are being met from groundwater resources. It is, therefore, imperative to ensure that the quality of groundwater should be maintained below permissible levels. In order to accomplish this objective, it is imperative to reliably quantify the system and predict its further response to the continued input of pollutants. The former needs reliable data on all the characteristic parameters of the aquifer at a sufficient number of points in space and time while the latter requires mass transport modelling of the polluted groundwater regime.

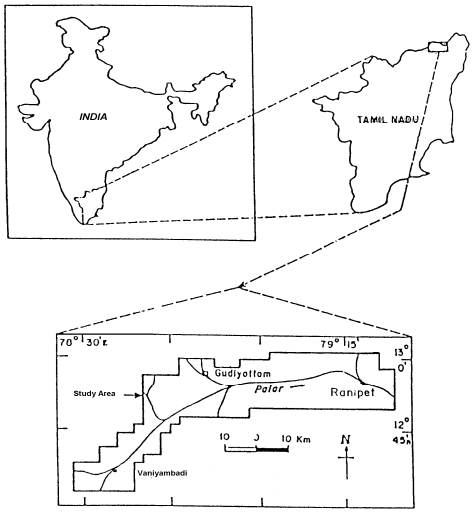

Fig. 1: Location map of the upper Palar river basin

ABOUT THE STUDY AREA

The river Palar and its tributaries the Malatar, Guddar and Poini drain the study area (Fig 2), covering about 1650 km^2. The river originates in the highlands of Nandi-durg in the Kolar district of Karnataka (South India) and flows in a southwesterly direction to Vaniyambadi in Tamilnadu. It then flows northeast towards the confluence with the River Guddar (Pallikonda) and then flows east till it joins the Bay of Bengal. The Palar anaicut (barrage) forms the eastern boundary of the model area. It is an ephemeral river and it flows only for about 10-15 days a year, during flood season. The climate of the area is basically tropical. The normal annual rainfall in the area is about 1050 mm. The area receives rainfall during the southwest and northeast monsoons. The predominant soil types in the area are black soil and red loamy soil. Groundwater occurs mostly in weathered and fractured parts of the crystalline rocks. Along the river course, one can encounter highly permeable sand layers and pebbles which have good groundwater potential and this lead to the establishment of a number of tanneries all along the course of river Palar from Vaniyambadi in the west and Palar anaicut (barrage) in the east.

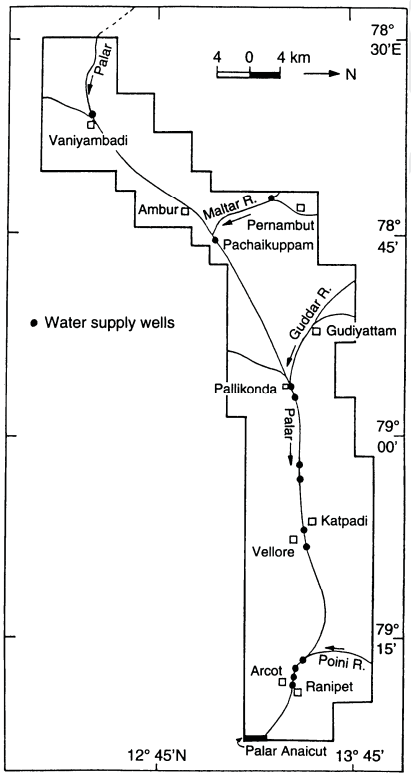

Fig. 2: Model boundary with important towns and water supply wells

GEOLOGICAL SETTINGS

Venkatanarayana & Thangarajan (1994), Gupta & others (1994), Chakrapani (1984) and UNDP (1971) have described the details of geomorphologic, geological and structural features controlling the groundwater regime in the area. Geologically, the study area is covered by crystalline rocks of Archaean age consisting of charnokites, granites, gneisses and quartzites. The alluvium occurring in the area is of a fluviatile origin and restricted to the courses of rivers and major streams; it consists of gravel, fine to coarse sand and clay.

The occurrence and behavior of groundwater are controlled by the physiography, climate and geological conditions including lithology, texture and structure. Charnokites, granites and gneisses represent the bedrock formations. Generally the bedrock aquifers are of a heterogeneous nature due to variations in lithology and structure over a short distance. The sediment rock is represented by alluvium along the stream course. Groundwater occurs under phreatic conditions in the weathered mantle and under semi-confined to confined conditions in joints, cracks, fractures and sheared zones of the bedrock. The groundwater occurs under phreatic condition in the Palar River alluvium bed. The depths to the water table range between 3-30 m in crystalline rocks and 2-8 m in the river alluvial formation. The lineament map of the study area (Fig. 3) reveals that it is tectonically disturbed with having high intensity fractured zones. The minimum groundwater level is 160 m (amsl) at Palar anaicut (eastern model boundary) and the maximum level is 400 m (amsl) at the Palar river western model boundary entry point. The topography is highly undulating near the hilly area due to isolated hills and has a gentle gradient of 0.0024 along the river course.

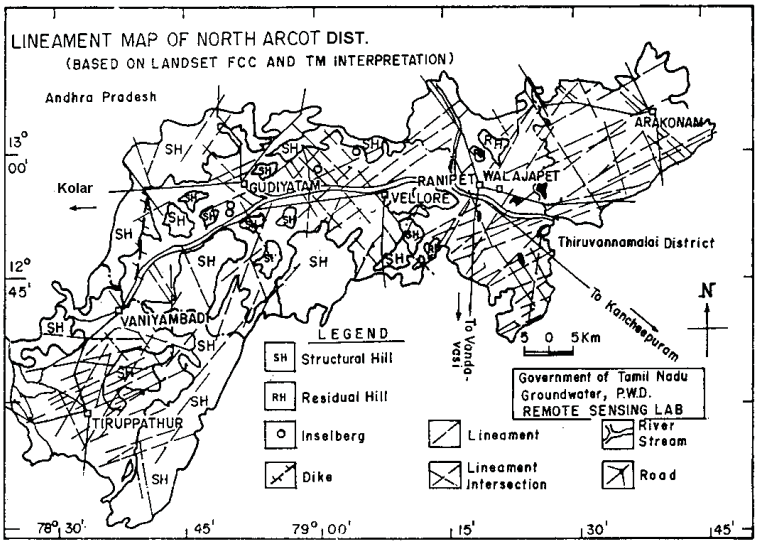

Fig. 3: Lineament map of the study area (source: PWD, Govt. of Tamilnadu)

TANNING INDUSTRIES

The processing of raw skin and hides otherwise called tanning is an ancient craft in India. The tanning industry began in 1914 at Walaja Town (Fig 4) in North Arcot District of Tamilnadu (India) and now it is one of the important tanning centers in India where about 650 tanneries have been in operation in an area of more than 1650 km^2 (Fig 4). These tanneries use calcium carbonate, sodium chloride, sodium sulphide, sodium dichromate and sulphuric acid for processing the raw hides and skins. The effluents are generally untreated and are discharged into the neighboring fields and irrigation tanks. The effluents overflow these tanks and stagnant pools and finally reach the Palar River course. The characteristic parameters of the untreated tannery effluents are shown in Table 1. Nearly 30 million / per

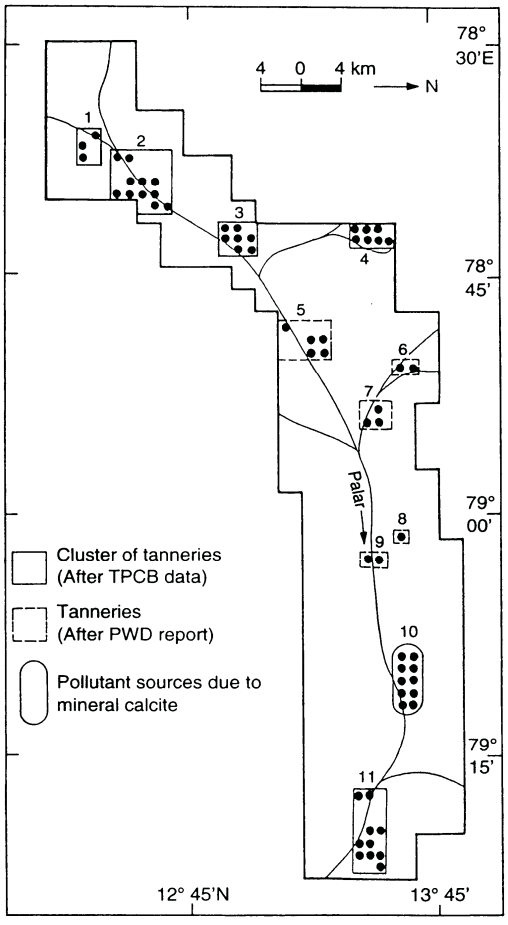

Fig. 4: Location of clusters of tanneries

day (MLD) of untreated effluents were discharged at different points and it is estimated that about 100000 tons of total dissolved solids (TDS) are entering the groundwater system every year. More than 11000 hectares of agricultural land had been affected due to tannery effluents (Krishnawamy & Haridass, 1984; Teekaraman & Farooq Ahmed, 1982; Margam, unpublished data). Some tanneries around Vaniyambadi and Ambur dispose of their untreated effluents directly in the river Palar. Recently at some places common effluent treatment plants have been put up to treat the effluents before discharging in to the soil. These plants treat only organic and biological and not the inorganic pollutants. The seepage rate of polluting effluent through the riverbed is very high due to large hydraulic conductivity. After infiltrating through the unsaturated zone, pollutants reach the water table and migrate through advective transport and hydrodynamic dispersion.

Table 1: Characteristic parameters of tannery effluents (after Teekaraman and Farooque Ahmed, 1982)

Parameter	Type of tanning			Remarks
	Vegetable tanning	Chrome tanning	Finishing units	
PH	5.5-115.	7.5-10	5.6	All values except pH values are expressed in mg/l
Total dissolved solids	1680-26.520	9000-20000	4400	
Suspended solids	160-6300	1250-6000	800	
Chloride	500-7100	1900-26200	600	
Sulphate	80	-	2040	
Chromium (Bivalent)	-	125-200	20	
B.O.D.	400-4200	2000-3000	900	
C.O.D.	1000-10300	5100-7200	276	

GROUNDWATER QUALITY

The groundwater quality of samples taken twice a year from 12 existing dug wells (depth range 5-15 m) for the period from 1970 to 1993 has been monitored by Public Works Department of the Government of Tamilnadu. The analysis of water samples is shown in Table 2. The TDS concentration 'C' observed in the field at 12 dug wells for the period July 1980, 1984 and 1992 are shown in Fig. 5. One notices that TDS concentration is high in the clusters 1, 2, 3 and 4 and it also rises during the year 1984 and is slightly reduced during 1992. Table 2 indicates that the major ions such as sodium, magnesium and chloride, and total hardness are all on the high side in corroboration with the high TDS. The pH values ranges from 7.3 to 8.0 indicating that the groundwater is alkaline in nature. Table 3 gives the variation of water quality (minimum and maximum) at Ambur (cluster 3) for the years 1970, 1982 and 1994. The water quality data for 1994 was making available later and therefore this data could not be incorporated in the present model study.

Table 2: Results of chemical analysis of water samples (S&R sodium absorption ratio; all values except pH are in mg/l)

Zones	Village	pH	TDS	CO	HCo	SO	Cl	Na	SAR
2	Thutipet	7.5	3840	60	488	84.9	1539	913	12.4
3	Thorvozhi	8.0	3840	60	610	99.4	1628	1025	13.6
4	Pernambut	8.0	6400	120	549	84.5	3115	1430	14.3
6	Ammankuppam	7.0	4200	150	1159	24.5	1540	948	16.8
8	Kathivadi	7.3	3000	50	366	96.0	1026	713	10.9
9	Uppupettai	7.3	1500	30	305	86.0	1575	708	9.7
10	Katpadi	7.3	1500	30	183	24.9	743	391	8.5

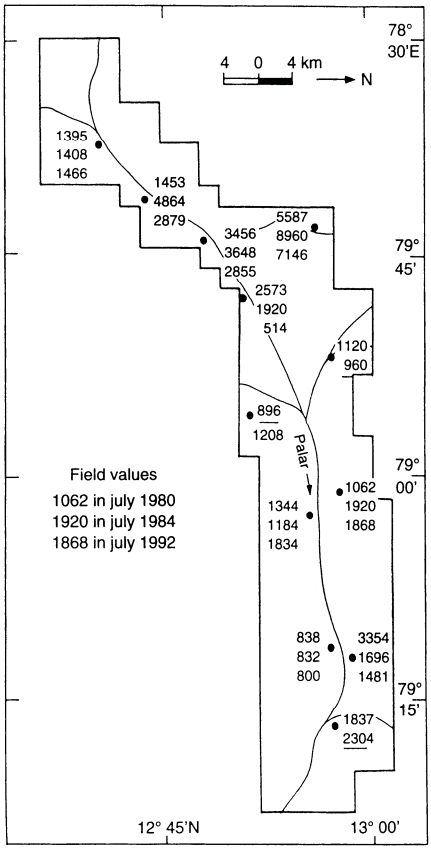

Fig. 5: Comparison of observed TDS concentration in mg/l for July 1980, 1984 and 1992

Table 3: Chemical analysis of water samples at Ambur (cluster no. 3) for the years 1970, 1982 and 1994

Parameters (All values except pH in mg/l)	1970*		1982*		1994*	
PH	7.5	8.3	7.6	8.0	7.8	8.4
TDS	640	3200	3200	4000	6500	10100
HCO_3	292	610	430	610	2300	3200
Cl	198	1864	1347	1630	3261	5034
Na	80	483	738	1025	1564	2323
SO_4	@16	196	60	100	374	864

* Teekaraman and Farooque Ahmed (1982)
@ PWD-GW (1994)

MATHEMATICAL MODELLING OF THE SYSTEM

The available geo-hydrological data helps to conceptualize a single layer phreatic aquifer system with an aquifer thickness of 10 m (Alluvial sand thickness) in the river course and 30 m thickness (weathered part of aquifer system) elsewhere. A two-dimensional groundwater flow model was constructed and an alternating direction implicit method was used to solve the finite different groundwater flow equation (1) and method of characteristics was used to solve the advection part of mass transport equation (2).

GROUNDWATER FLOW EQUATION

$$\frac{\delta}{\delta x}\left(K_{xx}\frac{\delta h}{\delta x}\right)+\frac{\delta}{\delta y}\left(K_{yy}\frac{\delta h}{\delta y}\right)+\frac{\delta}{\delta z}\left(K_{zz}\frac{\delta h}{\delta z}\right)=S_s\frac{\delta h}{\delta t}\pm W. \tag{1}$$

MASS TRANSPORT EQUATION

$$\frac{\partial C}{\partial t}=\frac{\partial}{\partial x_i}\left(D_{ij}\frac{\partial C}{\partial x_j}\right)-\frac{\partial}{\partial x_i}(CV_i)-\frac{C'W^*}{\varepsilon}+\sum_{k=1}^{S}R_k \tag{2}$$

The study area was divided into 976 nodes (active cells) with a grid interval of 1.3 km (Fig. 6). Initially, a groundwater flow model was constructed based on the available geo-hydrological data. All these nodes are required to be assigned various characteristic parameters including 'T', 'S' and 'W' at all the node points. Here, h is the dependent variable on 'T', 'S' and 'W' and that is the solution of Equation (5). The available database was, however, quite sparse. Notwithstanding, efforts were made to arrive at reasonable

guesstimates of the characteristic parameters for which no data is available. Making use of the field conditions, nearby field data, and interpolation, the initial parameters were arrived at, for which known data is available. Subsequently, the aquifer parameters (T and S) were modified through model calibration.

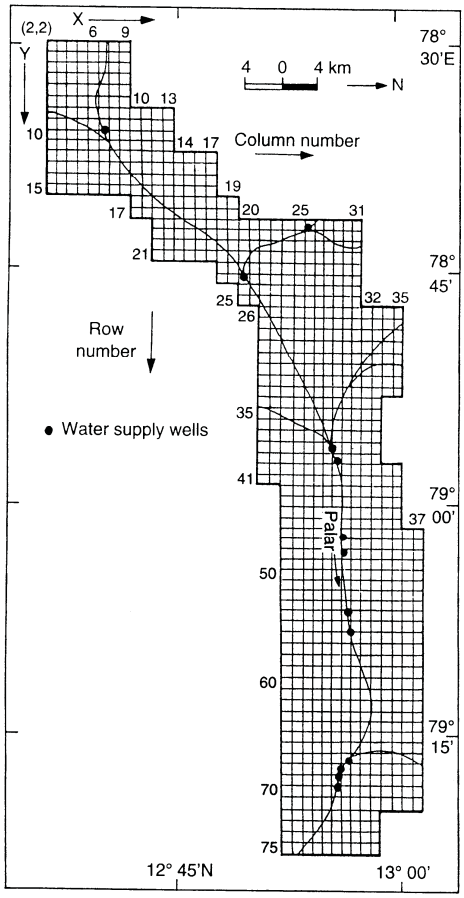

Fig. 6: Grid map of the study area

ASSUMPTIONS USED IN THE MODEL

The groundwater flow regime model was prepared only for the shallow aquifer zone tapped by dug wells (up to 30 m thickness). This implies that the deeper fractured zones do not take part either in the groundwater flow or in the mass transport. The aquifer is also treated as an equivalent porous medium in the regional scale for modelling purpose. The TDS concentration in the surficial effluents was assumed to be 30000 mg/l during the period

July 1980 to July 1984 (Based on the data collected during 1994 and report of Teekaraman & Farooque Ahmed, 1982). However, subsequently many tanneries appear to have started using semi-processed hides as their raw material. This has resulted in a reduction of TDS concentration in their effluents during 1984-1992. Therefore, a uniform TDS concentration of 20000 mg/l was assumed in the surficial effluents for all the tanneries after July 1984. Table 4 gives the quantities of effluents discharged at the surface in kilolitre (kl)/day for the periods before July 1980 and from July 1984 until the present date. While the figures for zones 1, 2, 3, 4 and 11 have been adapted from the data supplied by Tamilnadu Pollution Control Board (TPCB). The values for zones 5, 6, 7, 8, 8 and 10 were guessed based on the field reconnaissance and those are not only due to tannery effluents but also due to local soil conditions and the operation of a few other chemical industries.

Table 4: Untreated effluents discharged at the surface from various cluster of tanneries

Cluster no.	Location	Rate of effluent discharge (kl/day)	
1	Vaniyambadi (South)	300	500
2	Vaniyambadi (North)	6030	10050
3	Ambur	2250	3750
4	Pernambut	1968	3280
5	Vengili	960	1600
6	Gudiyattam	384	640
7	Pallikonda (North)	526	960
8	Veduganthagal	192	320
9	P. Satyamanglam	384	640
10	Arumparithi	4920	8200
11	Ranipet	5760	9600

The quantity of fluid effluents seeping to the groundwater system was assumed to be 30% of the surficial effluents. It was also assumed that on a conservative basis the solvent reaching the water table has a solute concentration, which is 40% of that present at the surface. The remaining 60% of the solutes may get absorbed in the unsaturated zone or carried away by the runoff. Table 5 gives the load (C'W) at corresponding source nodes in the aquifer for different periods. These have been computed in accordance with the above assumption, which, of course, need to be validated.

An effective porosity of 0.2, longitudinal dispersivity of 30 m and transverse dispersivity of 10 m were uniformly assumed for the entire area. The model was calibrated in

two stages, steady state and transient condition (Gupta & others, 1994). It was also assumed that TDS do not influence the density and viscosity values, which may affect the groundwater flow and pollutant migration.

Table 5: Total pollution load (C'W) reaching the aquifer from various tanneries

Cluster no.	Location	Pollutant load (kg/day)		
		July 1980	Aug 1980-July 1984	Aug 1984-July 1992
1	Vaniyambadi (South)	1080	1792	1188
2	Vaniyambadi (North)	21780	36154	23958
3	Ambur	7956	13206	8751
4	Pernambut	6930	11593	7623
5	Vengili	3600	5976	3960
6	Gudiyattam	1440	2390	1584
7	Pallikonda (North)	2160	3585	2376
8	Veduganthagal	720	1195	792
9	P. Satyamanglam	1440	2390	1584
10	Arumparithi	18490	30627	30295
11	Ranipet	21600	35856	23760

HYDROGEOLOGICAL PARAMETERS

Aquifer Parameters (T and S)

The aquifer parameters, transmissivity 'T' and storage coefficient i.e., specific yield 'S_y' were estimated through 5 dug well pumping tests within the study area. The estimated 'T' values outside the river varied from 1 m^2/h to 7 m^2/h and one value at riverbed is 80 m^2/h. Thus out of 976 nodes, the 'T' values were estimated only at 5 points and it was interpolated albeit subjectively. Specific yield 'S_y' values were available at only 5 locations. Here the diversity is still more pronounced. Out of 5 pumping test values of specific yield, 4 values are about 0.01. Therefore, specific yield values were assigned as 0.01.

Input to the System

Recharge due to rainfall was estimated at selected points using water balance technique. The rainfall recharge rate works out to be 10% of the mean annual rainfall. The quantity of rainfall recharge for the year 1980 works out to be 165×10^6 m^3 (million cubic meter (mcm)) for an average rainfall of 1000 mm. The rainfall data collected from 9 rain gauge stations located in the study area were used in calculating recharge. Irrigation return seepage rate was assumed to be 30% of used water and it works out to be 75×10^6 m^3 per year. The inflow and outflow across boundaries were calculated based on interpolated values of 'T' and hydraulic gradient. The inflow from western, southern and northern boundaries is worked out to be 20 million m^3 per year.

Output from the System

The groundwater abstraction for irrigation and industries were estimated as 230×10^6 m^3 per year. Village-wise well inventory was made using well particulars and their usage by PWD-GW from dug and bore wells located in various administrative blocks. Block-wise draft was calculated by using the data on number of wells and number of pumping hours in a day. Tamilnadu Water Supply & Drainage (TWAD) Board had estimated the groundwater abstraction as 20×10^6 m^3 per year from water supply wells (Fig. 2) in the riverbed of Palar. About 8 million m^3 per annum goes as effluent seepage to the stream.

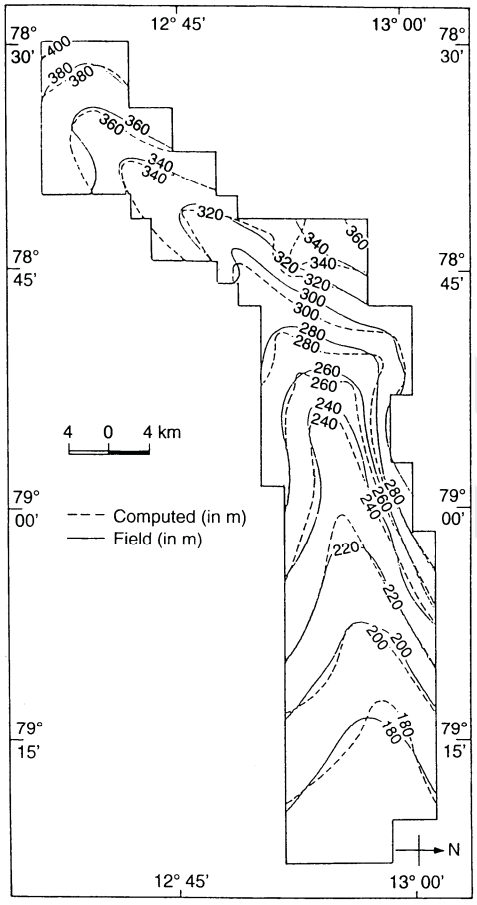

Fig. 7a: Comparison of computed vs. observed water level contours for July 1980

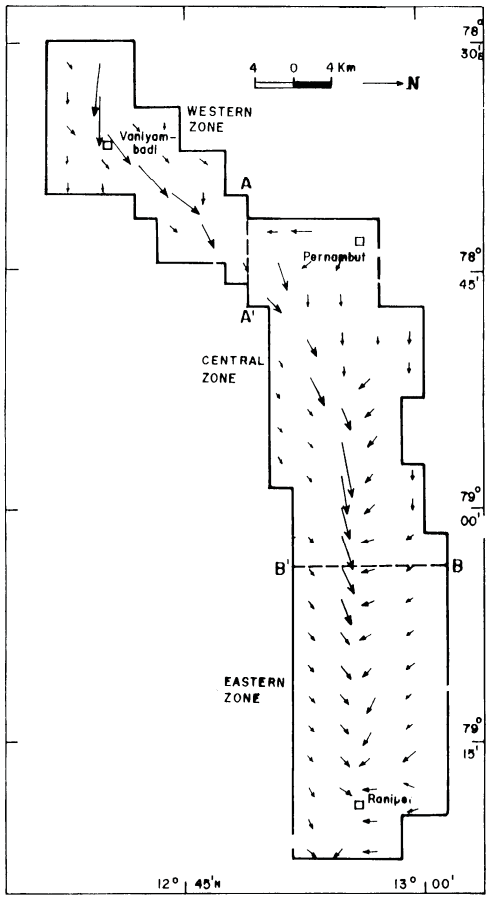

Fig. 7b: Computed groundwater flow velocity vectors

Model Calibration

The actual values and spatial distribution of 'T' values were calibrated assuming steady state condition in the year 1980. Input and output stresses along with 'T' values were progressively modified till better matches of observed and computed values were obtained for steady state condition (Fig. 7). The calibrated node-wise T values along with estimated field values are shown in Fig. 8. The modified input and output quantities and boundary flows arrived at after model calibration are shown in Fig.9 and 10, respectively.

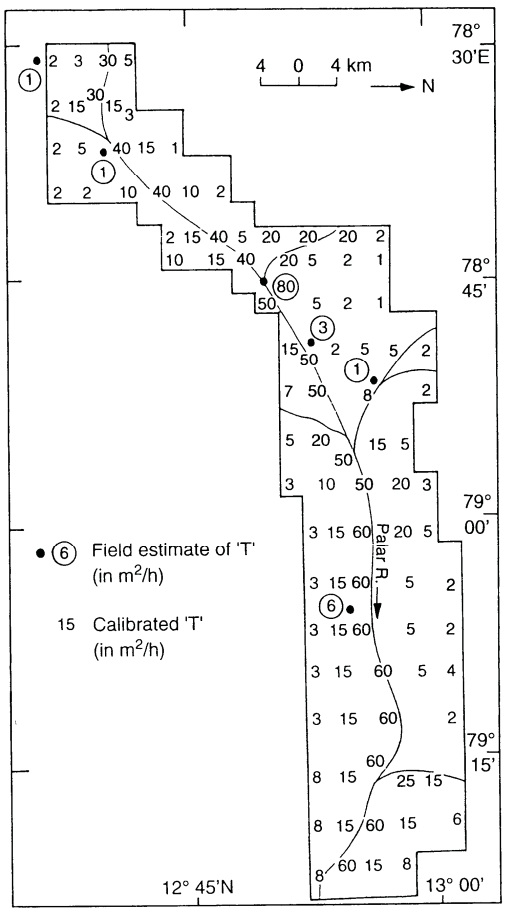

Fig. 8: Node-wise distribution of transmissivity values in m2/hr (Calibrated model)

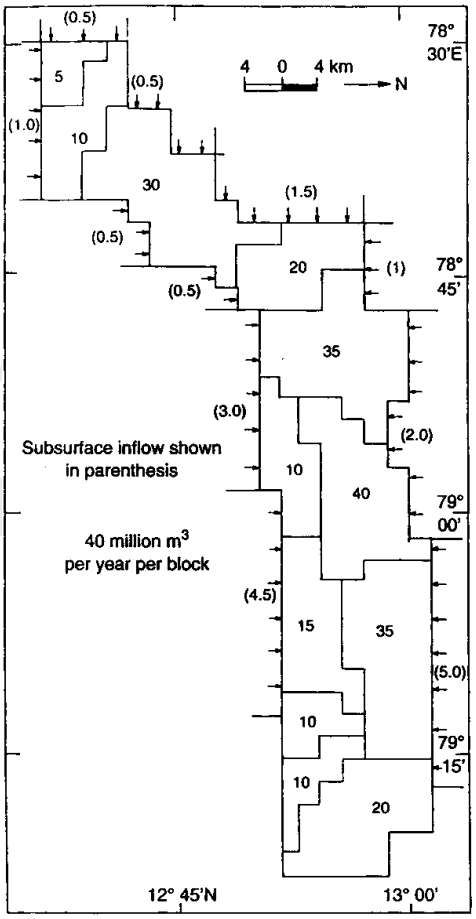

Fig. 9: Block-wise distribution of input quantities (Calibrated model)

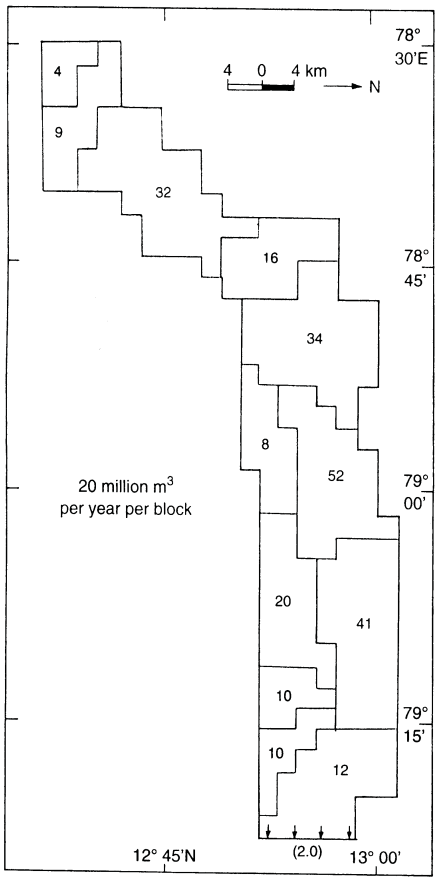

Fig. 10: Block-wise distribution of output quantities (calibrated model)

Mass Transport Modelling

The computer software of USGS (Konikow & Bredehoeft, 1978)) was used to solve the mass transport equation (2). Method of characteristic (MOC) was used to solve the advective transport and finite difference approximation was used to solve the dispersion part of equation (2). As stated earlier, various parameters from Tables 4 and 5 were assigned to the corresponding nodes as point source.

Steady State Condition

TDS concentration 'C' was then calculated at all node points for July 1980, a date up to which the system was assumed to be in a steady-state condition. There was a mismatch between observed and computed values of 'C'. Therefore, efforts were made to obtain a reasonably better match by modifying the magnitude and distribution of the pollutant load.

However, the situation could not be improved much. This may be due to a variety of factors, the most important of which are lacunae and inaccuracies in the database. The computed and observed values of TDS concentration are shown in Fig. 11.

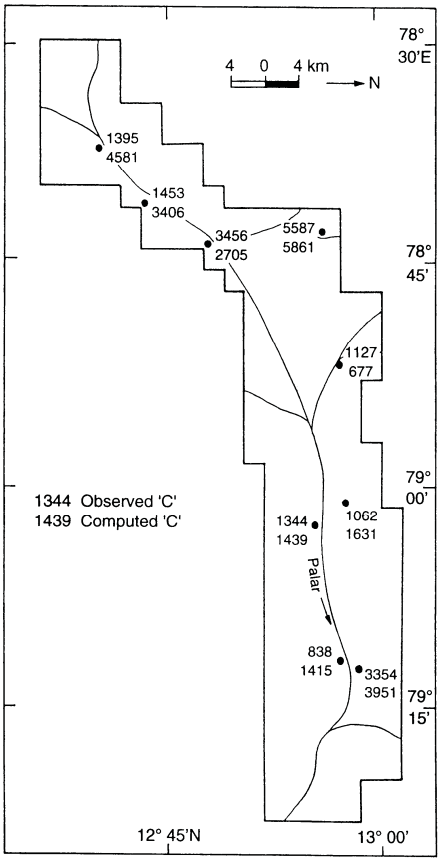

Fig. 11: Comparison of computed vs observed TDS concentration in mg/l for July 1980

Transient State Condition

Even though the steady-state model could not reproduce the observed at all the points, a time variant simulation was carried out. This was done in two stages; for the period August 1980 to July 1984 and then for August 1984 to July 1992. The situation during these periods was distinguished on the basis of the information that the TDS concentration in the surface effluents from tanneries before 1984 was highly (30000 mg/l) than that after 1984 (20000 mg/l). The pollution load reaching the groundwater system at various clusters during this period is shown in column 4 of Table 4. The computed 'C' for 1984 is higher than the observed values. These anomalies, however, could not be rectified during model calibration

due to non-availability field estimates either for model parameters or the stresses (pollutant load). The computed TDS concentrations 'C' for July 1984 are shown in Fig. 12.

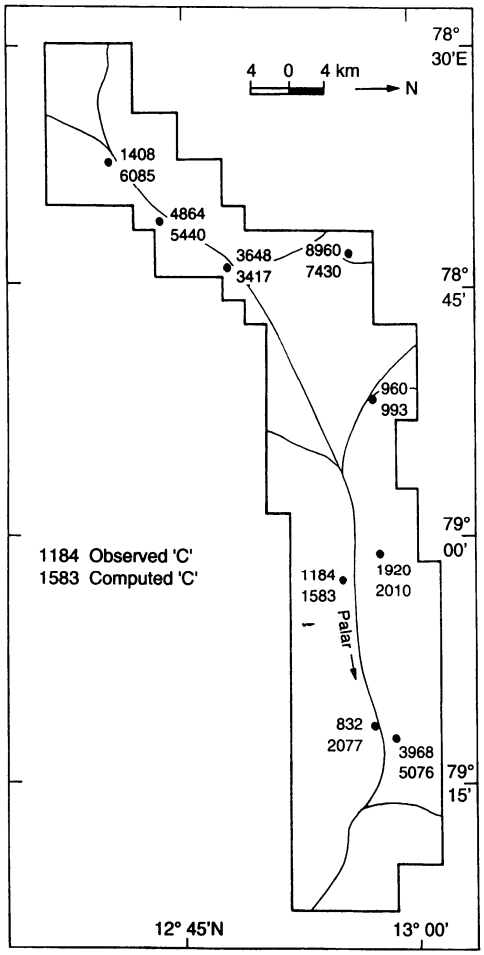

Fig. 12: Comparison of computed vs. observed TDS concentration in mg/l for July 1984

The simulation for the period July 1984 to July 1992 was started with the computed TDS concentration 'C' as shown in Fig. 12. The pollutant load was assumed to be invariant during 1984-1992 and is shown in column 5 of Table 4. The computed and observed values of 'C' for 1992 are shown in Fig. 13. It should be mentioned here that the present model is only to illustrate the feasibility of applying modelling techniques to study this problem and to use it for prediction of system behavior for some further scenarios.

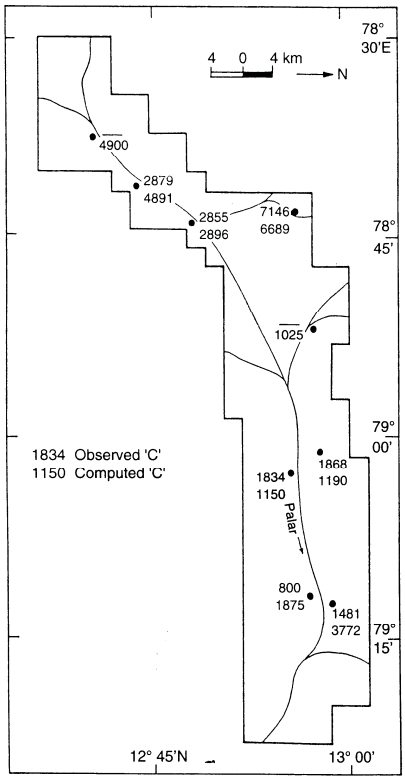

Fig. 13: Comparison of computed vs. observed TDS concentration in mg/l for July 1992

Sensitivity Analysis

The importance of varying transmissivity, dispersivity, and C'W (TDS pollution load at the source) on TDS concentration was studied. The variations caused in TDS concentration "c" at some selected node points as result of some variations in these parameters are shown in Table 6.

Transmissivity – this parameter was changed by 20% (upwards and downwards) of the value shown in Fig. 8 at each node. The change in the transmissivity affects the groundwater velocity causing redistributi0on of solute concentration. In general, the higher the transmissivity, the faster is the movement of the solute. Therefore, the concentration is reduced near the sources and increased away from it when the transmissivity is increased and vice versa (see columns 4 and 5 of Table 6).

Dispersivity – the *longitudinal dispersivity* was increased to 50 m and 100 m (from 30 m). The *transverse dispersivity* was taken as one-third of the longitudinal dispersivity and

was thus also changed in accordance with the longitudinal dispersivity. No significant change in the TDS concentration was noticed due to increase in the dispersivity (see columns 6 and 7 of Table 6). This shows the advection and not dispersion and not dispersion is the predominant mode of solute migration.

TDS pollution load at source points (C'W) – the effect of varying this parameter by 20% (upwards and downwards) at 62 source points (nodes) was examined and it was found that TDS concentration 'C' rises with an increase in the pollution load C'W and vice-versa (see columns 8 and 9 of Table 6).

Table 6: Variation of TDS concentration for a few node points by carrying T, At, and C'

(T_o – transmissivity for calibrated model m^2/h); A_t – 30 m (longitudinal dispersivity); C' – 12000 mg/l (concentration); T_oC – TDS concentration of T_1=(80% of T_o), A_t and C'; T_2C - TDS concentration for T_2=(120% of To), At and C'; AtC – TDS concentration for A1=50 m, ToC'; A2C – TDS concentration for A2=100 m, ToC'; C1'C – TDS concentration when C1'=9600 mg/l, At, Toi, C2'C – TDS concentration when C2' = 14400 mg/l, At, To)

Node	T_o M^2/h	T_oC mg/l	T_1C mg/l	T_2C mg/l	A_1C mg/l	A_2C mg/l	C_1'C Mg/l	C_2'C mg/l
8,12	8	5225	5050	4145	5176	5057	4261	6189
12,16	30	4791	4558	4064	4771	4721	4094	5725
19,20	30	3305	3455	2805	3276	3207	2675	3934
30,19	3	6833	6703	5909	6837	6842	5486	8180
22,27	30	2103	2362	2192	2084	2039	1852	2354
31,31	15	1013	952	830	1000	969	847	1178
32,45	8	2019	2103	1821	1990	1921	1643	2395
29,47	7	1546	1517	1263	1519	1458	1264	1828
32,59	30	1912	1912	1621	1924	1949	1563	2261
34,60	30	4243	4436	3339	4185	4115	3396	5030

Prognosis

A reliable prognosis of the pollutant migration is possible only if a validated model is available. Notwithstanding the shortcomings of the present model, it could be used to prognosticate some general inferences. The following two scenarios were considered for predicting the extent of pollution in the area at the end of a 20-year period.

The TDS load remains at the present level during the entire period of prediction.

The TDS load is reduced to half of the present level. The TDS load is a result of both the effluents discharged from the tanneries and the leaching of the previously adsorbed solutes in the unsaturated zone. Thus, effectively the overall discharges from the tanneries are assumed to reduce to about 25% of the present level.

The predicted TDS concentration level (scenario-1) for the year 2012 is shown in Fig. 14. A graphical view of path-lines due to advection in the western zone is presented in Fig. 15a for the year 1992 and predicted path-lines migration is shown in Fig. 15b for the year 2012. It can be seen that the TDS concentration 'C' progressively increased in the area due to continuous addition to solids to the groundwater. The area in which TDS content in groundwater may be more than 4000 mg/l is likely to be doubled within the next two decades from the present size.

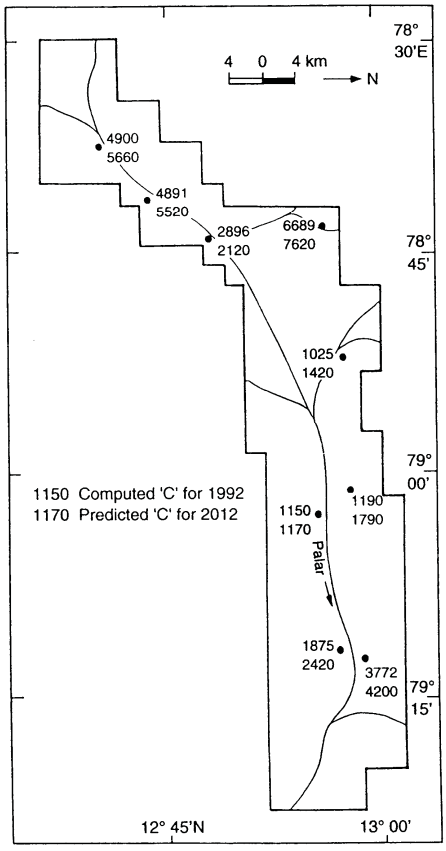

Fig. 14: Predicted TDS concentration in mg/l for July 2012 (scenario-1)

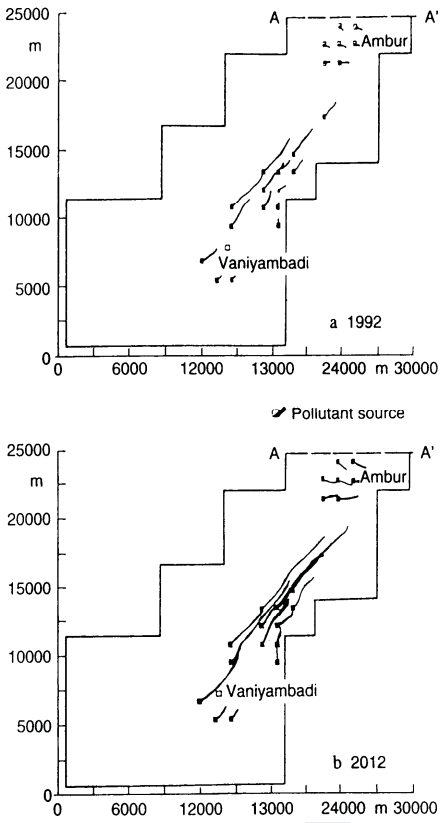

Fig. 15: Predicted path-line migration for July (a) 1992 and (b) 2012 (scenario-1)

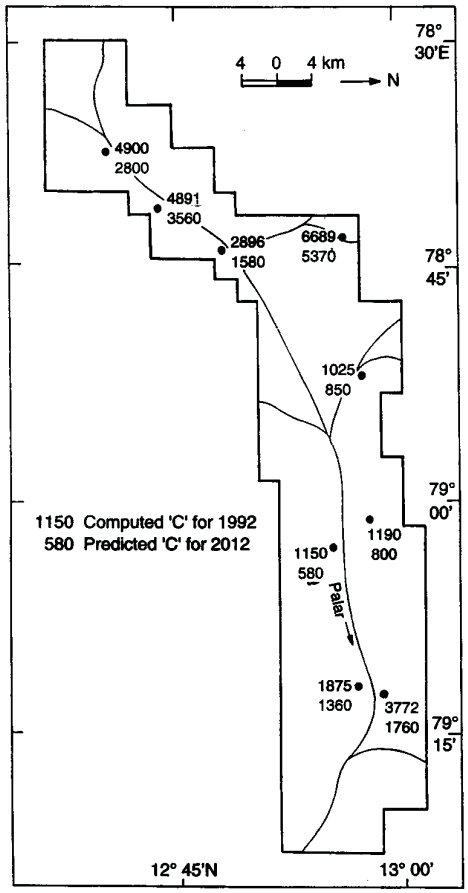

Fig. 16: Predicted TDS concentration in mg/l for July 2012 (scenario-2)

Fig. 16 shows a comparison of computed and observed TDS concentration 'C' for scenario-2. It can be seen that at the end of a 20-year period (2012) TDS concentration 'C' will be reduced but may still be quite high at some locations.

RESULTS AND DISCUSSIONS

Despite lacunae in the database for the modelling of pollutant migration in the aquifer, it is shown indisputably that if tannery effluents continue to be discharged at the present level, both as regards the volume and TDS concentration, groundwater pollution will continue to increase. It is noted from Fig. 16 that even if tannery effluents are reduced to 25% of the present level, even after 20 years, the TDS concentration in groundwater will not be reduced

to 50% of the original level (1992). However, an exact quantification of the affected area and concentration of pollutants in groundwater is possible only if one could make a valid model based on a more representative and accurate database.

REFERENCES

[1] Chakrapani, R., (1984). Hydrogeological conditions in North Arcot District. Central Groundwater Board, Tech. Report, 33p.

[2] Gupta, C. P., Thangarajan, M., Rao, V.V.S.G., Ramachandra, Y.M. and Sharma, M.R.K., (1994). Preliminary study of groundwater pollution in the Upper Palar basin and feasibility of mass transport modelling to predict pollutant migration. NGRI Tech. Rept., no. 94-GW-168, 45p.

[3] Konikow, L.F. and Bredehoeft, J.D., (1978). Computer model of two dimensional solute transport and dispersion in groundwater: Techniques of water-resources investigations of the USGS Chapter C2, Book 7, pp.1-79.

[4] Krishnaswamy, R. and Haridass, G., (1981). Groundwater Pollution by tanneries in Tamilnadu (India). In: Proceedings of on International Symposium on Quality of Groundwater, Noodwijkerhout, The Netherlands (Eds. W. van Duijvenbooden, P. Glasbergen and H. van Lelyveld), pp. 287-290.

[5] Teekaraman, N. and Farooque Ahmed, (1982). Tanneries vs agriculture in North Arcot District. Soil Survey and Landuse Organization, Special Report No. 20, Vellore, pp. 1-45.

[6] Thangarajan, M., (1999). Numerical simulation of groundwater flow regime in a weathered hard rock aquifer. Journal of Geological Society of India, Vol. 53, No. 5, pp. 561-570.

[7] Thangarajan, M., (1999). Quantification of pollutant migration in Upper Palar river basin Environmental Geology, 38(4), pp 285-295.

[8] UNDP., (1971). Groundwater investigations in Tamilnadu (Phase 1); Tech. Rep., New York, 88p.

[9] Venkatanarayana, B. and Thangarajan, M., (1994). Geomorphological studies in Upper Palar basin in Tamilnadu. 31st Annual Convention and Seminar on Geosciences of Energy and Environment, NGRI, Hyderabad, pp. 31-32.

Numerical Simulation of Groundwater Flow and Solute Transport, L. Elango (ed). pp.193-200

Prediction of Groundwater Contaminantion in Patancheru IDA and Environs, Medak District, Andhra Pradesh: A Post Audit

V. V. S. Gurunadha Rao

INTRODUCTION

Water is a part of the natural environment with many complex parallel roles and functions. Water as a landscape element and as a chemically active mobile substance is always on continuous move through the surface and sub-surface. Frequent handling of polluting substances on the ground surface involve interventions with water quality in view of the fact that water is an excellent solvent, chemically active and always on the move according to the laws controlling the hydrodynamics of the water cycle. Once caught by the moving groundwater, pollutants tend to move along with the groundwater, unless chemical reactions along the groundwater pathways influence mobility of the pollutant.

Water carries pollutants through invisible and visible landscapes. On the local scale, water soluble compounds used in agriculture (fertilizers), industrial refuse, solid waste deposits, etc., may be caught by water and produce groundwater pollution, which will remain undetected until the polluted water passes through a local well. Similarly, refuse disposed on land surface may be leached by water, and ultimately transferred to the river. Effect of pollution may show up further downstream where the river water is being used for some vulnerable purpose like irrigation. On regional scale, pollutants emerging from land use activities in upstream areas of a river basin are being transferred into lakes along the river and finally to the downstream area. Environmental management and protection would mean that decisions have to balance dependencies against threats in the region.

Groundwater modelling has become an important tool for planning and decision-making process involved in groundwater management. For managers of water resources, models may provide essential support for regulations and engineering designs affecting groundwater. This is particularly evident with respect to groundwater protection and aquifer restoration. Assessment of the validity of modelling-based-projections is difficult and often controversial. The success or failure of a model depends on the availability of field information (quality and completeness of data) and the type and quality of the mathematical tools (software). The natural starting place for groundwater contamination is with the mass transport processes. These processes determine the extent of plume spread and the geometry of the concentration distribution. Advection is by far the most dominant mass transport process in shaping the plume. Hydrodynamic dispersion is usually a second order process. The magnitude and direction of advective transport is controlled by:

- the configuration of water table or piezometric surface,
- the presence of sources or sinks,
- the permeability distribution within the flow field, and
- the shape of flow domain.

All these parameters are important in controlling the groundwater velocity, which drives advective transport. Adding dispersion to advective transport can cause important changes in the shape of a plume. Other important process is sorption and irrespective of the model describing sorption, the process is of paramount importance in controlling contaminant transport.

Reliability of groundwater model predictions typically depends on the correctness of the conceptual model, availability and quality of model data and the adequacy of the prediction tools. Conceptualization and characterization are sufficiently understood to meet project objective, and then the conceptual model may be translated into a mathematical model. Such a mathematical model typically consists of a set of governing equations and boundary conditions for groundwater flow and transport simulation. Relating such a mathematical model to a particular system requires specific values for system parameters, stresses and boundary conditions as well as rate coefficients. The application of geo-chemical and transport models requires simplifying assumptions with respect to system processes, stresses and geometry, a procedure referred to as model schematization. Efficient model schematization starts early during conceptualization and characterization process and continues into the code selection, model design or construction and model attribution and calibration phases of a modelling project. Determination of site boundaries is based on (a) natural site characteristics (topography, soils geology, hydrology, biota and chemistry) (b) current and past land use and (c) known or suspected extent of site-related contaminants. Investigations of groundwater contamination should include areas of potential source up-gradient and potential migration paths down–gradient from a vulnerable source location. Data from existing sources are gathered by identifying data sources and collecting and organizing relevant data into a manageable database.

Transferring data into a conceptual model is rather intuitive process consisting of (1) qualitative and quantitative data interpretation of individual data elements and grouped data within a particular data type, (2) analysis of spatial and temporal relationships between various data types, and (3) relating data types and interpreted data to elements of specific system (i.e. processes, structure, state and stresses). The source, transport, fate and resulting distribution of each targeted chemical (e.g. inorganic and/or organic chemical constituents, tracers or isotopes) in the transport phenomenon are conceptualized in the second step. In the case of unknown sources, source locations and strengths are hypothesized from the conceptualized transport and fate processes and actual distribution of chemicals. The conceptual models are described and visualized using cross-sections and regional maps. Surface characterization at the near ground-surface is made considering vegetation related

(including plant releases and uptake) and rainfall related chemical exchanges with subsurface system.

Geological and geomorphologic and geo-chemical characterization considers petrologic, mineralogical and geo-chemical factors and composition with respect to their spatial and temporal variations. Geological maps and cross-sections, sub-surface investigation logs, and stratigraphic columns are used in conjunction with surface characterization, geophysical data and geo-chemical data and analysis to develop a part of the geological and geo-chemical framework that represent the distribution of lithological units and mineralogical and geo-chemical compositions as transport system materials. The groundwater system is characterized and quantified by determining the type, amount, temporal variation and spatial distribution of groundwater recharge and discharge using surface, subsurface and hydro-geological analysis. Further more, reaction and flow paths of indicative chemical species are analyzed for information regarding the groundwater flow system. The groundwater system is quantitatively defined in terms of boundary conditions, flow paths and potentiometric surfaces and groundwater regime budget. Transport system characterization analyses the presence, transport and fate of the chemical species in both space and time. At this stage relevant physical and chemical processes of the transport system are mathematically described and quantitatively attributed. Transport processes include advection, dispersion, adsorption, volatilization, ion exchange and biotransformation. The final result of this analysis is a characterized mass transport process model. An adequate computer code is chosen to simulate groundwater flow and mass transport processes.

GROUNDWATER FLOW MODEL

Slice successive over relaxation is a method for solving large systems of linear equations by means of iteration. This method is implemented in the SSOR package of MODFLOW by dividing the finite difference grid into vertical slices and grouping the node equations into discrete sets, each set corresponding to a slice. In every iteration, these sets of equations for each slice are processed. They are first expressed in terms of the change in computed head between successive iterations. The set of equations corresponding to the slice is then solved directly by Gaussian elimination treating the terms for adjacent slice as known quantities. The values of head change computed for the slice are then multiplied by an acceleration factor, generally taken between 1 and 2. The computed heads are taken as the final values of head change in that iteration for the slice. This procedure is repeated for each slice in sequence until all slices in the three-dimensional array have been processed, thus completing a domain iteration. The entire sequence is then repeated, until differences between the computed head values in successive iterations is less than the chosen criterion at all nodes in the grid. The solver checks for the maximum change in the solution at every cell after completion of every iteration. If the maximum change in the solution is below a set convergence tolerance then the solution has converged and the solver stops. Otherwise a new iteration is started (McDonald and Harbaugh, 1988).

MASS TRANSPORT MODEL

Mass transport in three dimensions (MT3D) is a computer model for simulation of advection, dispersion and chemical reactions of contaminants in three-dimensional groundwater flow systems (Zheng, C, 1990). The model is used in conjunction with a block-centered finite difference flow model, MODFLOW, and is based on the assumption that changes in concentration field will not measurably change the flow field and uses a mixed Eulerian-Lagrangian approach to the solution of the advection-dispersion equation, based on a combination of method of Characteristics (MOC) and the modified method of characteristics (MMOC). Longitudinal dispersivity is specified as a characteristic of the soil type (related to the tortuosity of interconnected pores), which tends to spread out contaminant mass along the advective path of the plume. The horizontal transverse (plume width) and vertical transverse (plume thickness) dispersivities are assigned as ratios (fractions) of the longitudinal dispersivity as required by MT3D. The molecular diffusion coefficient is also to be given as input. The hydrodynamic dispersion coefficient is computed as the product of the dispersivities and velocity (mechanical dispersion) plus the molecular diffusion coefficient. The MOC uses a conventional particle tracking technique based on a mixed Eulerian-Lagrangian method for solving the advection. The dispersion, sink/source mixing and chemical reaction terms are solved with the finite difference method (Zheng, C, 1990).

PATANCHERU WATERSHED, MEDAK DISTRICT, A.P.

The Patancheru Industrial Development Area (IDA) forms part of catchment of Nakkavagu, a tributary of Manjira River. The area covers about 120 sq. km under Patancheru Mandal of Medak district, A.P. (Fig.1). The industries are located around Patancheru village on both sides of National Highway from Hyderabad to Mumbai. The industrial estate has been established during 1977 and more than 200 industries are functioning since then dealing in production of pharmaceuticals, paints and pigments, metal treatment and steel rolling, cotton and synthetic yarn and engineering goods. Most of these industries are using various inorganic and organic chemicals as raw material in the manufacturing and processing units. These industrial effluents (mostly untreated) are discharged into various unlined channels and streams up to 1995. The Common Effluent Treatment Plant (CETP) of Patancheru has been established during 1995 and was situated adjacent to Peddavagu. The CETP treats various untreated effluents from a number of industries and treated wastewater is let out into Peddavagu. The wastewater discharged from the CETP contains total dissolved solids (TDS) concentration ranging from 4000 to 5000 mg/1.

The Pamulavagu, Peddavagu and Nakkavagu streams while carrying effluent contributes as a diffuse source of contamination all along its stream course up to confluence with Manjira River near Gowdcherla village. The alluvium around Nakkavagu is a result of paleo-channel course of Manjira River and forms a potential groundwater-bearing zone. Contaminants on reaching groundwater table through stream-aquifer interaction migrate in

the aquifer system mostly through advective dispersion. The rate of movement and consequent spread of pollutants depends upon the hydraulic gradient and groundwater velocity. To determine the groundwater velocity distribution a groundwater flow model was constructed. The computed velocity distribution was used to analyze advective and dispersive transport to determine contaminant migration in the area.

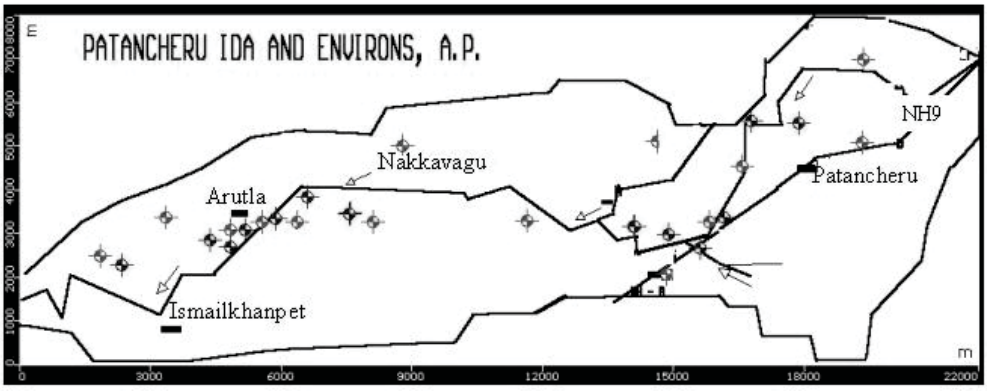

Fig. 1: Observation Well in Nakkavagu Watershed, Medak district, A.P.

Estimation of aquifer parameters is essential for quantifying the groundwater resources and also to determine well characteristics. Pumping tests were carried out on 10 wells including bore wells, filter points and dug wells. High transmissivity values were obtained in alluvial formations, despite limited aquifer thickness. The transmissivity was found to vary from 140 m^2 /day in granites to 1300 m^2/day in alluvium. The permeability values as high as 50-75 m/day are found in the alluvium around Arutla village. Intensive groundwater irrigation has resulted in stream aquifer interaction around this village.

The well inventory and lithologic data collected from tube wells indicated that top weathered aquifer having 10-12 m thickness was underlain by a fractured layer. The most important process contributing to the mass transport in groundwater is advection. Longitudinal dispersion is relatively significant but transverse dispersion could be negligible. The total dissolved solids (TDS) concentration in contaminant was selected for a detailed model study because (a) it's concentration remained relatively constant in effluent ranging between 1000-4000 mg/L along different reaches of Nakkavagu, and (b) it showed a uniform background level of about 300 mg/L in native groundwater. The initial stage in developing the flow and TDS concentration solute transport models was to define the region of interest and establish boundary conditions for flow and solute transport. The surface water while seeping through the bed of Nakkavagu carries effluent to groundwater regime thereby contaminating groundwater up to a distance of 600-800 m on the East of Nakkavagu.

The simulated model domain of Patancheru IDA and environs consist of 51 rows and 88 columns and 2 layers covering an area of 22000 m x 8000 m. The top layer consists of 10-15 m thick alluvium along Nakkavagu or a weathered zone in granite and was underlain by 10-15 m fracture zone. The simulated vertical section has a total thickness of 30 m in the model. The outflow from groundwater flow model was estimated in terms of a constant head node at the confluence of Nakkavagu with Majira River by assuming outflow towards Manjira River. The groundwater recharge @ 110 mm/year has been fed to simulate distributed recharge to aquifer system from the first layer in the recharge package. The location of pumping centers in the watershed have been dense in Arutla area compared to rest of the area, which forcing induced migration effluents from Nakkavagu (Fig. 2).

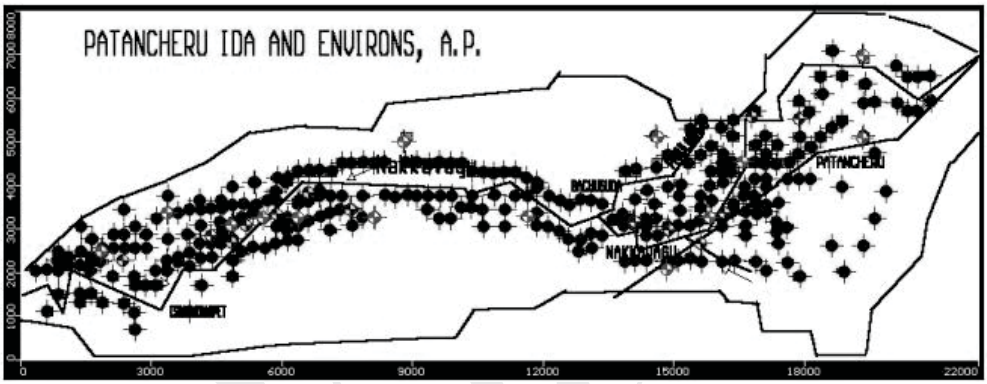

Fig. 2: Location of Pumping Wells in Nakkavagu Watershed

Continuous seepage from Peddavagu, Pamulavagu and Nakkavagu streams was simulated as additional input in the model as there was always some effluent flow in Nakkavagu at Ismailkhanpet Bridge even during summer months. The computed Water level contours have been compared with observed data during 1997 (Fig. 3).

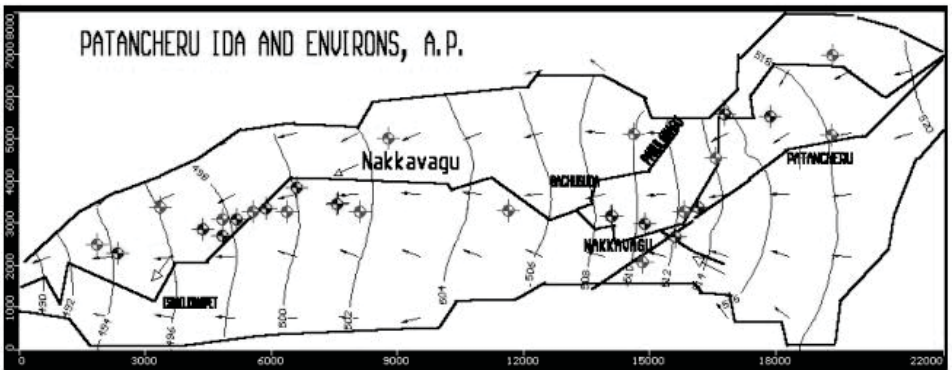

Fig. 3: Computed Water Level in m (amsl) in Nakkavagu Watershed-June 1997

The values of dispersivity in longitudinal and two transverse directions (Y and Z) were assumed to be 50 m, 5m and 0.05 m respectively. The tendency for α_L to be about 10 times larger than α_{TH} and for α_{TV} to be much smaller than either of them is in line with the concentrations determined in the area. The relatively smooth decline of TDS concentration away from the Nakkavagu suggests a relatively constant rate of loading. Thus a constant TDS concentration at different nodes on Nakkavagu was assigned varying from 3500 mg/L at source near Patancheru and 1000 mg/L away from the source at about 18 km downstream of Nakkavagu near Ismailkhanpet. The computed iso-concentration contours indicate that the plume is expanding and follows the hydraulic gradient implying that advection is the dominant mechanism of spreading. Qualitatively shape of the plume indicates that longitudinal dispersion is more significant than transverse dispersion. The contaminant migration was to be found extending up to 500-600 m from Nakkavagu on the eastern part during last 20 years (1997) (Fig. 4).

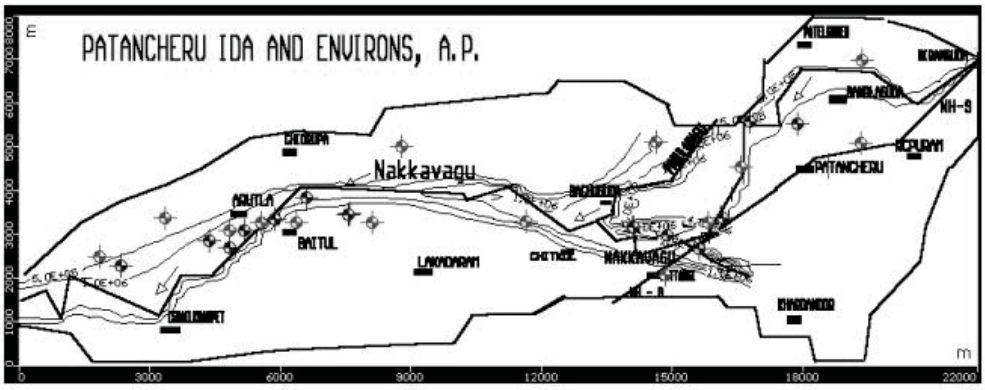

Fig. 4: Computed TDS Contaminated Migration (µg/l)-June 1997 (20 Yrs)-Calibration

Further model predictions were made for next 20 years. The post audit of water quality in the watershed carried out during 2000 – 03 has helped to validate the model predictions. In general the post audit water quality analyses at most of the problem areas were found to be elevated than the predicted TDS. The modelling study has helped in gaining a better insight of the hydrogeologic set up and assessment of contaminant migration due to mass transport processes. Over-exploitation of groundwater in the alluvial parts of Nakkavagu has resulted in decline of water table, resulting in further contamination of groundwater through stream aquifer interaction. Remedial measures like reduction of concentration of effluent in wastewater let out into streams from CETP and individual industries have been suggested to contain elevated concentration of TDS (Gurunadha Rao et al., 1999).

CONCLUSIONS

The groundwater modelling is a prognostic tool for assessment and management of groundwater potential as well as pollution due to discharge of effluents on ground surface. The case studies illustrated the applicability of flow and mass transport models for assessing the contaminant migration. These studies will help in planning development of organized geohydrologic and water quality database for preparation of reliable groundwater flow and mass transport models for understanding and prediction of likely contaminant migration in groundwater from effluent sources and for designing of necessary remedial measures. Periodical post audits are required in view of elevated concentrations noticed in the area due to earlier loadings as well as over exploitation of groundwater for irrigation. The confidence gained from the post audit of groundwater flow and mass transport modelling can be better used in decision-making process.

REFERENCES

[1] Franz, T. and Guiger, N., (1990). FLOWPATH. A Two-dimensional horizontal aquifer simulation model. Waterloo hydrogeologic software, Waterloo, Ontario, Canada.

[2] Guiger, N. and Franz, (1996). Visual MODFLOW. A three dimensional model for groundwater flow and mass transport. Waterloo hydrogeologic software, Waterloo, Ontario, Canada

[3] Gurunadha Rao, V.V.S., Subrahmanyam, K., Yadaiah, P. and Dhar, R.L., (1999). Assessment of groundwater pollution in the Patancheru Industrial Development Area and its environs, Medak district, Andhra Pradesh, India. In Impacts of urban Growth on Surface Water and Groundwater Quality (Proceedings of IUGG 99, Symposium HS5, Birmingham, July 1999) IAHS Press Publ.No.259, pp.99-109.

[4] Konikow, L.F. and Bredehoeft, J.D., (1978). Computer model of two dimensional solute transport and dispersion in groundwater: Techniques of water-resources investigations of the USGS, Chapter C2, Book 7, pp.90.

[5] Pollock, (1990). MODPATH a post processor for MODFLOW software.

[6] McDonald, J.M. and Harbaugh, A.W., (1988). A modular three dimensional finite-difference groundwater flow model. Techniques of Water Resources Investigations of the U.S. Geological Survey Book.6, pp.586.

[7] USGS Open files Report 89-381, "Documentation of Computer Programs to compute and Display pathlines using Results from US Geological Survey Modular Three-dimensional Finite Difference Groundwater Flow Model, by David W.Pollock.

[8] Zheng, C., (1990). MT3D, a Modular three-dimensional transport model for simulation of advection, dispersion and chemical reactions of contaminants in groundwater system prepared for the U.S. Environmental Protection Agency.

Numerical Simulation of Groundwater Flow and Solute Transport, L. Elango (ed). pp.201-218

Simulation of Movement of Solutes in Unsaturated Zone by Finite Element Modelling: A Case Study

N. Rajmohan and **L. Elango**

INTRODUCTION

Accumulation of contaminants from agricultural chemicals in the unsaturated zone over the years is a major concern in many parts of the world. Application of agricultural chemicals and dumping of industrial and domestic wastes at the land surface or within the unsaturated zone may have considerable impact on the quality of groundwater. Among these, agricultural chemicals are generally the most significant anthropogenic source of groundwater contamination. Understanding the fate of dissolved chemicals within the unsaturated zone can greatly aid in the prediction of chemistry of water that reaches the aquifers. Investigation of water movement within the soil zone is essential for understanding the factors controlling recharge and groundwater quality. Study of the movement of water and solute within soil profiles beneath agricultural lands is important for a number of reasons. As a result, the unsaturated zone has been a subject of great research interest during the past decade. Most subsurface pollution problems stem from activities involving the unsaturated or vadose zone between the soil surface and the groundwater table. The unsaturated zone hence provides the best opportunities to limit or prevent groundwater pollution. Once contaminants enter groundwater, pollution is essentially irreversible, or can be remediated only with extreme costs. Numerical modelling is becoming an increasingly important tool for analyzing complex problems involving water flow and contaminant transport in the unsaturated zone. There are a number of such models that are currently available. The use of mathematical models in assessing the possible environmental consequences of land use change, relative to the fate of introduced chemicals, is well established in the hydrogeologic community. Growing interest to know the fate of surface applied chemicals resulted in the development of various models of solute transport. HYDRUS-2D is one of the models developed for water balance simulation in variably saturated soils, and it can simulate flow in response to meterological forcing and plant root water uptake. It is fairly well documented, has been widely used and tested, and it is in public domain (Scanlon.et.al., 2002).

FINITE ELEMENT MODEL-HYDRUS-2D

HYDRUS-2D program (Simunek 1996) is a finite-element model for simulating movement of water, heat, and multiple solutes in variably saturated media.

The program numerically solves the Richards' equation for saturated-unsaturated water flow and the Fickian-based advection-dispersion equations for heat and solute transport. The governing flow equation was modified from Richard's equation:

$$\frac{\partial \theta}{\partial t} = \frac{\partial}{\partial x_i}\left[K\left(K_{ij}^{A} \frac{\partial h}{\partial x_j} + K_{iz}^{A} \right) \right] - S$$

where θ is volumetric water content [$L^3 L^{-3}$], h is pressure head [L], x_i are the spatial coordinates [L], t is time [T], K_{ij}^{A} are components of a dimensionless anisotropy tensor K^{A}, K is unsaturated hydraulic conductivity function [L/T^{-1}] given by

$$K(h,x,z) = Ks(x,z)Kr(h,x,z)$$

S is the sink term to account for water uptake by plant roots. It is defined as

$$S(h) = a(h)(LsTp)/(LxLz)$$

where, a(*h*) is the plant water stress function, Tp is the potential transpiration rate, Ls is the width of the surface, Lx is the width of the root zone, and Lz is the depth of the root zone.

A Galerkin type linear finite element method was used to solve the governing equations in this model. An implicit (backwards) finite difference scheme is used to achieve integration in time for both saturated and unsaturated conditions. The resulting equations are solved in an iterative fashion, by linearization and subsequent Gaussian elimination for banded matrices, a conjugate gradient method for symmetric matrices, or the ORTHOMIN method for asymmetric matrices. Additional measures are taken to improve solution efficiency in transient problems, including automatic time step adjustment and checking if the Courant and Peclet numbers do not exceed preset levels. The ability of HYDRUS-2D to converge to a stable solution depends upon the discretization and temporal iteration schemes. A closely spaced mesh is particularly needed for coarse-textured soil with high n-values and small alpha values. This principle is also true for layer interfaces where hydraulic properties change sharply and further applies to the time iteration criteria for minimum time steps. The unsaturated soil hydraulic properties are defined by a set of closed-form equations resembling the 1980 van Genuchten equations.

The HYDRUS-2D model needs the following input data: number of layers in the soil profile, initial water table depth, residual and saturated water contents of each soil layer, parameters of a and n (the coefficient and the exponent in the soil water retention function, respectively), saturated hydraulic conductivity of each soil layer, root water uptake parameters and root distribution in the soil profile. The Table lists some of these inputdata. The residual water content, and the parameters a and n in the soil water retention curves were obtained using the RETC program (Van Genuchten et al., 1991) with the soil water retention data from Skaggs et al. (1981).

CASE STUDY

An intensive field study was conducted in the Palar and Cheyyar river basins, Tamil Nadu, India to understand the variation of major ions and nutrients in the unsaturated zone and groundwater during paddy cultivation. In the study region, there is no systematic study carried out to understand the movement of chemicals in the unsaturated zone by field and modelling techniques. Rajmohan *et al*. (2000) studied the major ion chemistry of groundwater in part of Palar and Cheyyar basins and concluded that silicate-weathering is the probable source of sodium, calcium and magnesium in groundwater in this region. Rajmohan and Elango (2005) have carried out a study on the mobility of major ions and nutrients in the unsaturated zone during paddy cultivation. The study area (Fig. 1) is situated in Kancheepuram District of Tamil Nadu State, India. It forms a part of the Palar and Cheyyar river basins, and is located 70 km west of Chennai city. The study area has dry climatic condition with the maximum temperature of 37 °C during the months of April–May, and minimum air temperature of 21 °C during the months of November–December. It receives an average annual rainfall of 1113 mm of which, 60% is contributed by the north east monsoon (NE) from October to December; the rest is during the south west monsoon (SW), that is from June to September. Alluvium is the most important formation, occurring on both the sides of the river. The alluvium is essentially composed of sand with intercalated clay. In these formations, wells have been dug up to a depth of 23 m. Most of these are bore and dug cum borewells. The water level in these wells fluctuates between 1 and 20 m below the ground level.

The experiment was conducted at an agricultural land located in the village of Ilayanurvellur (Open well, No. 18) (Fig. 1). This site covers an area of 4049 m^2 and is located in alluvial formation. The irrigation need for this agricultural land is met by pumping groundwater from this open well (Well No. 18). Water table in this well fluctuates between 1.8 and 7.7 m below the ground level. Rainfall is the principal source of groundwater recharge in this area.

This agricultural field is intensively cultivated, usually with three crops in a year. Mostly, paddy (rice crop) is cultivated. Sometimes, sugarcane is cultivated, which is a 12-month crop. The main cropping season is from September to January. The second crop season is from February to May and the third from May to August. These crops are mainly dependent on groundwater and rainfall, as surface water supply is not available at this site. In the present study, soil core sampling was carried out during the third crop season that is from May to August and groundwater was used for irrigation. During this study period, paddy is cultivated. The most commonly used fertilizers for paddy are urea, complex fertilizers and muriate potash.

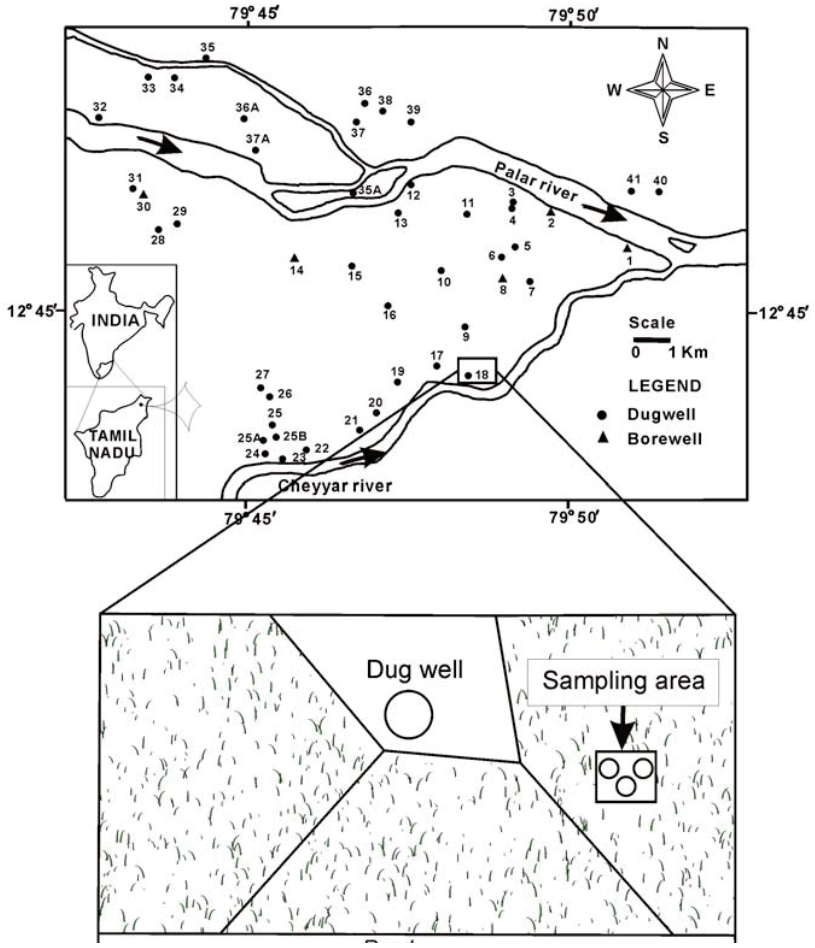

Fig. 1: Location of the study area

METHODOLOGY

Soil core samples were collected at different times. First core sample was collected 3 day before transplantation and fertilizer application. In order to derive a representative value, three core samples were collected during each sampling event, and an arithmetic mean was used. Soil core samples were collected by coring up to 1 m depth and sub samples were collected at every 10 cm interval. Care was taken by collecting the sub samples from the center of the core and neglecting the outer portions. The soil samples were placed in a plastic container at 4°C in the field itself. The collected samples were divided into two parts in the laboratory and one part of the samples was used to determine the concentration of $N\text{-}NO_3$

and soil moisture. The other part of the samples was air-dried and used for the analysis of pH, electrical conductivity (EC), major ions, nutrients, organic carbon and grain size analysis. Twenty grams of each sample was used for grain size analysis by the pipette method (Krumbein and Pettijohn, 1938). Soil moisture was measured from weight loss of oven dried sample at 105 °C. EC and pH were measured using digital meters from 1:5 soil solution prepared from air-dried soil sample

Major anions such as Cl, HCO_3 and SO_4 were measured from 1:5 soil solutions. Chloride and HCO_3 were measured by volumetric method and sulphate was measured by barium chloride method using spectrophotometer (APHA, 1995). Nitrate in the freshly collected soil samples was determined by the method described by Jackson (1958). Air-dried soil samples were used for the analysis of available nitrogen (alkaline permanganate method), available phosphorus (Olsen's method) and available potassium (ammonium acetate leaching method) (Muthuvel *et al*., 1990). The organic carbon content was determined by Walkley–Black (1934) method. All the analysis was carried out with triplicate and arithmetic mean was used.

During this study, groundwater samples were collected once in a month from the experimental site for 18 months. Additionally, groundwater samples were also collected during the soil core sampling period. Water samples were collected in clean polythene bottles. All sampling bottles were soaked with 1:1 HNO_3 and washed using double distilled water. At the time of sampling, sampling bottles were thoroughly rinsed two to three times using the groundwater to be sampled. EC, pH and temperature of groundwater samples were measured in the field immediately after sample collection using a portable digital meters. Water level was recorded using a water level recorder. Samples collected were transported to the laboratory on the same day and they were filtered using 0.45 mm Millipore filter paper and acidified with nitric acid (Ultra pure, Merck) for cation analyses. For nutrient and anion analyses, these samples were stored below 4 °C. The samples were analysed for major ions (Na^+, Ca^{++}, Mg^{++}, K^+ , Cl^-, SO_4^{2-}, HCO_3^-) and nutrients (Si-H_4SiO_4, N-NO_3 and P-PO_4) as per the procedures given in APHA (1995). The analytical precision for the measurements of ions was determined by calculating the ionic balance error, which is generally within 5%.

FINITE ELEMENT MODELLING

Model Input Parameters

Finite Element Discretization

The finite element mesh is constructed for the 5 m column by dividing the flow region into triangular elements whose shapes are defined by the co-ordinate nodes that form the element corners (Neuman *et al*., 1974). Small finite element mesh size were given at and near the soil surface, that is, up to 10 cm, as highly variable meteorological factors can cause fast changes in the pressure head. Similarly, closer mesh intervals were given for the lower 10 cm of the column. In general, the size of the mesh along the *x* direction was 0.04 m and

along *y* direction it varied from 0.01 to 0.02 m. Thus, the column of 5 m length was divided into 250 nodes with 248 meshes.

Soil Layers and Properties

The number of soil materials and layers were decided based on the field data. The soil core collected from the top 1 m of the unsaturated zone and its grain size analysis indicate that there are seven different zones. As soil coring was not carried out beyond 1 m, the same soil type was considered from 1 to 5 m of the column. Thus, seven layers were considered in the 5 m column, based on the variation in soil characteristics. Analyses of the soil core for the contents of sand, silt and clay, were used to input the soil hydraulic properties for modelling. Grain size analysis of a soil core sample shows that it is generally sandy with silt and clay. The sand percentage is between 65 and 85 (Table 1). These data were used in the model for determination of the unsaturated soil hydraulic properties. The soil hydraulic properties were estimated by the Genuchtan (1980) equation in HYDRUS model itself using neural network predictions technique developed by US Salinity laboratory (Simunek *et al*., 1999). The calculated soil hydraulic properties based on the percentage of sand, silt and clay are given in Table 1.

Table 1: Soil hydraulic properties before and after model calibration

Layers	Depth (cm)	Before calibration						After calibration					
		θr	θs	α	n	Ks	l	θr	θs	α	n	Ks	l
A	0–10	0.035	0.385	2.8	1.81	1.20	0.5	0.030	0.391	2.4	2.10	1.20	0.5
B	10–20	0.036	0.391	2.1	1.73	1.10	0.5	0.030	0.397	1.9	1.60	0.90	0.5
C	20–30	0.032	0.385	1.6	1.62	1.03	0.5	0.029	0.399	1.3	1.46	0.78	0.5
D	30–60	0.031	0.389	2.7	1.73	1.31	0.5	0.027	0.393	2.5	1.59	0.92	0.5
E	60–80	0.030	0.395	2.3	1.82	1.02	0.5	0.025	0.396	2.0	1.47	0.76	0.5
F	80–90	0.038	0.385	2.6	1.73	1.11	0.5	0.031	0.395	2.3	1.50	0.85	0.5
G	90–500	0.030	0.391	2.4	1.62	0.91	0.5	0.029	0.399	2.1	1.43	0.73	0.5

θr = residual water content (cm^3/cm^3), θs = saturated water content (cm^3/cm^3), α = inverse of air entry value (or bubbling pressure) (cm^{-1}), n = pore size distribution index, Ks = Saturated hydraulic conductivity (m/d), l = pore connective parameter.

Solute Properties and Boundary Condition

The dispersivity and diffusion co-efficient are important parameters in solute transport process. The dispersivity for chloride and nitrate used in the model are given in Table. 2. The diffusion co-efficient for chloride in water is assumed to be 0.20 m^2/d and for N-NO_3 to be 0.016 m^2/d. These values were derived from the soil characteristics of this area and from the

literature (Hutson and wagenet, 1992; De Vos *et al*., 2002; Paramasivam *et al*., 2002; Saadi and Maslouhi, 2003). In the case of nitrate, plant uptake and denitrification were considered with a degradation factor of 0.01 (Clark, 1994; Paramasivam *et al*., 2002). Atmospheric boundary condition was assumed at the top of the column and variable head boundary condition was considered at the lower boundary. The atmospheric boundary condition varies depending upon the amount of rainfall, irrigation and evaporation. The actual variation in rainfall and water depth in the irrigation land was measured regularly in the field and used in the model. The evaporation is assumed as 40% of irrigation water. In the case chloride and nitrogen, third-type (solute flux-type) boundary condition was applied (Van Genuchten and Alves, 1982). In addition to these, a limiting value of surface pressure head is also provided. The minimum allowed pressure head at the soil surface is usually set between 100 and 150m. In this study, it is assumed as 100m. However, the variation in this value could not affect the result and it is confirmed by test runs.

Initial Condition and Model Calibration

The initial conditions were derived primarily from the field study. The initial conditions necessary for this model include pressure head and concentration. The initial concentration values used for model simulation are given in Table 2. These values were derived form the analysis of the soil cores collected 3 d before transplantation. The model was initially run with field input parameters (Tables 1 and 2) to model the movement of chloride in the column. The concentration computed by the model was compared with the field data. Then, the model was run by varying certain input parameters such as evaporation, bulk density, diffusion co-efficient and dispersivity. All these parameters were varied within the reasonable limit of 10% and the sensitivity of the model results to these parameters was

Table 2: Soil texture and initial conditions of chloride and nitrate and their longitudinal dispersivities for model simulation

Layers	Soil texture (%)			Longitudinal dispersivity (m)	Initial condition	
	Clay	Silt	Sand	Cl & N-NO3	Cl (mg/kg)	N-NO3 (mg/kg)
A	2.08	10.6	87.3	0.009	75	1.47
B	2.40	18.0	79.6	0.008	62	0.97
C	2.48	18.1	79.4	0.007	55	0.85
D	2.77	12.4	84.8	0.010	70	1.2
E	2.90	13.9	84.1	0.008	61	0.99
F	2.72	17.3	80.0	0.007	62	1.1
G	2.96	23.7	73.4	0.006	60	1.0

studied. Calibration was carried out by varying these input parameters within the reasonable limit, and compared the simulated concentrations of chloride with observed field data. The values actually used in the model after calibration, are given in Table 2. After the simulation of chloride concentration, the model was run to simulate the concentration of nitrate. It is assumed that 6% of the applied fertilizer nitrogen becomes $N\text{-}NO_3$. Petrovic (1990) reported that 4–10% of applied nitrogen fertilizer becomes $N\text{-}NO_3$. Initially, all these model runs were made for one irrigation cycle. The model was run with a time step of 1 d with a time increment of a minute.

Model Results

After calibration and testing, the model was used to simulate the concentrations of chloride and nitrate in the soil zone. The model results were initially obtained for the study period of 100 d after transplantation and then, simulation was carried out for a period of 1 year (three crops).

Chloride

The simulation was carried out initially for one crop season (third crop season) and the computed results were compared with the observed field data to a depth of 1 m (Fig. 2). It shows that there is an agreement between model results and the observed field data. During the irrigation practice, the concentration of chloride varies in the top 1 m. Fig.7 shows that the chloride ion from the irrigated field reaches the groundwater zone (500 m) after about 45 d. Fig.8 shows that movement of mass through the unsaturated zone is controlled by the recharging water from the irrigated land. Hence, most of the fluctuation in chloride mass takes place (i.e. from 0.0173 g/m^3 to 0.274 g/m^3 in the upper zone) during irrigation period, that is, up to 55 d. After that (i.e. after harvest) the mass of chloride reaches the level measured before the commencement of irrigation. The fluctuation in the mass of chloride with respect to time in the lower layers is less significant as inferred from the linear nature of the curve (Fig. 3).

Nitrogen

Similar to that of chloride, initially the model was simulated for one crop period (third crop season) and compared with field data for nitrogen (Fig. 4). The computed nitrogen trend in the unsaturated zone is reasonably matched with field data. The nitrogen concentration in the unsaturated zone varies significantly during irrigation period due to intense agricultural activities. The mass of nitrogen varies from 0.0011 g/m^3 to 0.0109 g/m^3 in the 30–60 cm layer (Fig. 5).

Further, after the completion of irrigational activity (i.e. after 55 d) the mass of nitrogen remains almost constant. This is inferred from the linear nature of the curve for mass in Fig. 5.

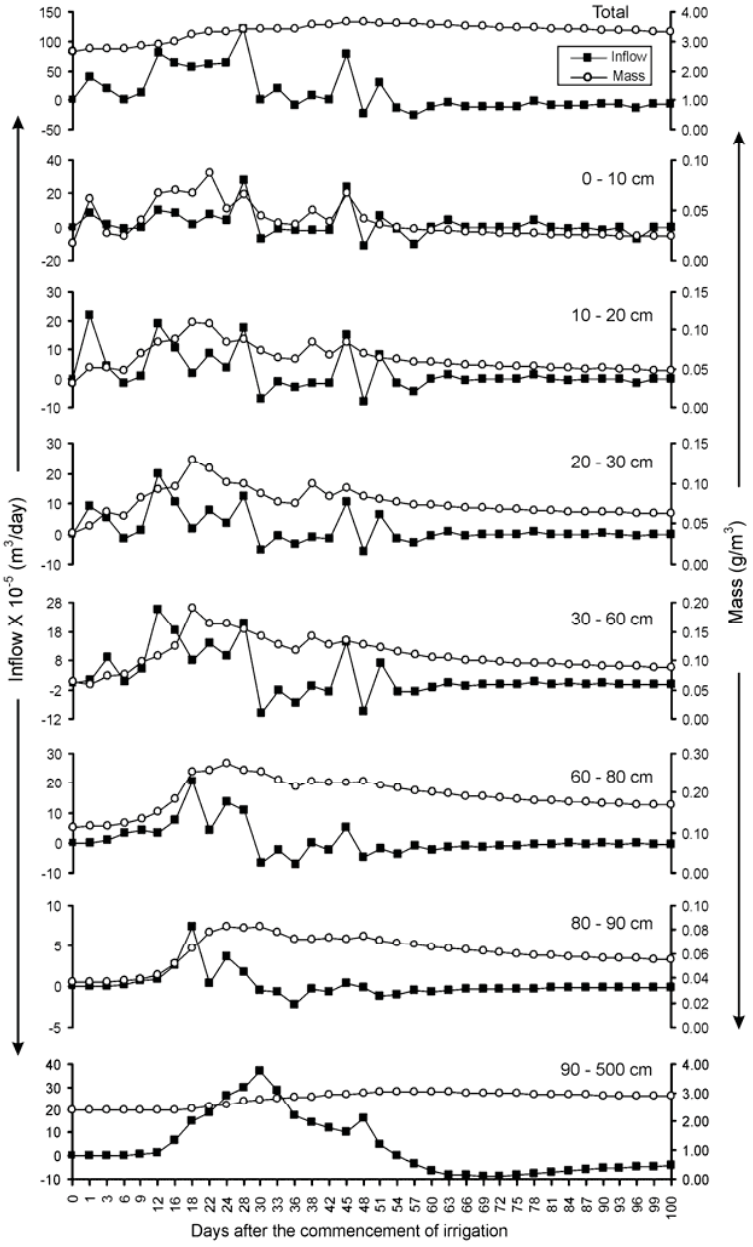

Fig, 2: Simulated and observed concentration of chloride

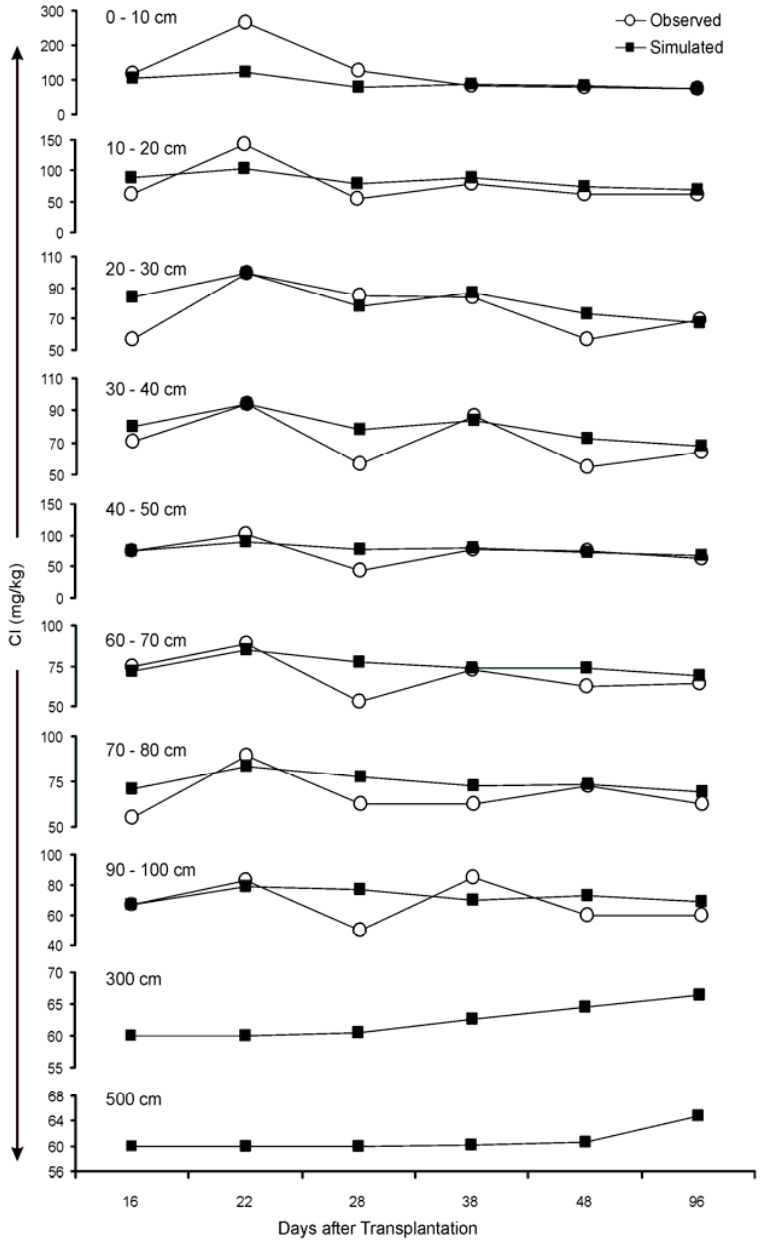

Fig.3: Simulated water inflow and mass of chloride

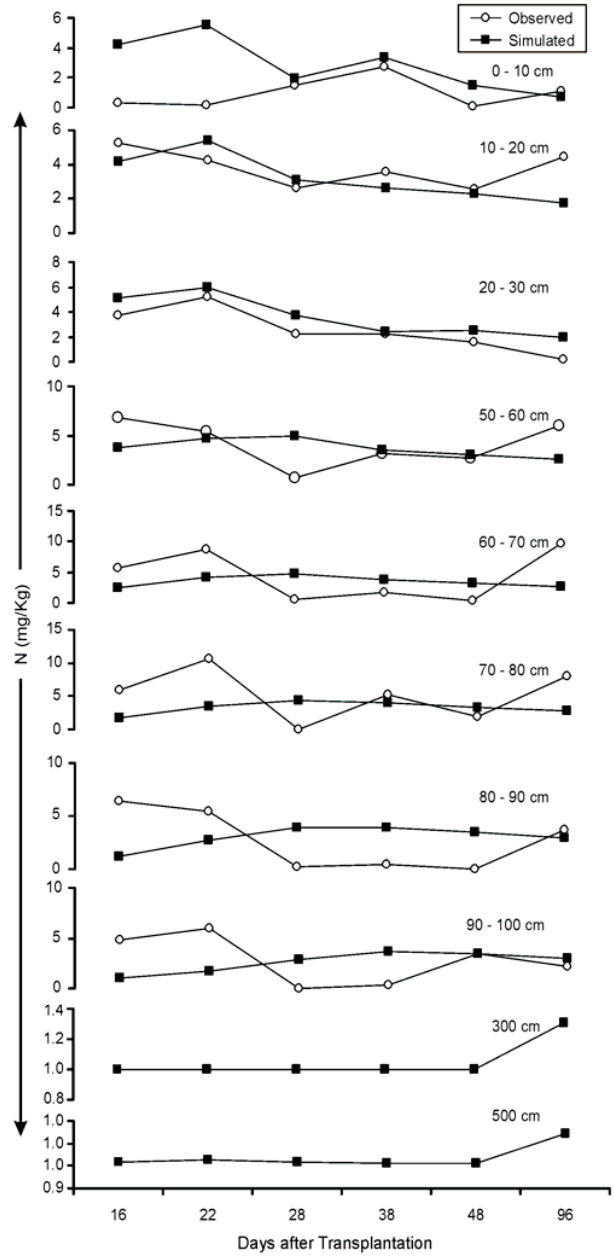

Fig.4: Simulated and observed concentration of nitrogen

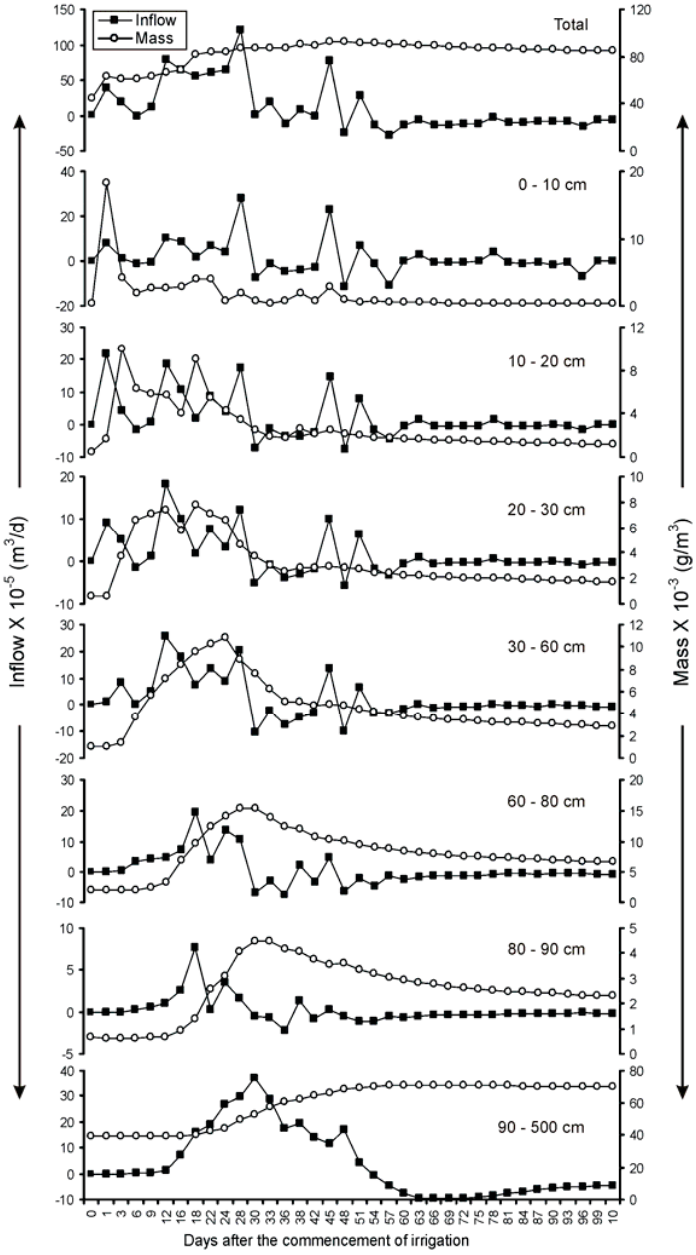

Fig. 5: Simulated water inflow and mass of nitrogen

Model Prediction

The model was then used to predict the concentration of chloride and nitrogen in the unsaturated zone under different irrigation practices. The model was run for a 1-year and a 5-year period with the usual and increased application of fertilizer. These model runs were made by assuming the same input parameters. The daily average rainfall and evaporation data calculated for the past 6 years were used. The model run was made for the period starting from May 1999.

Model Results for Three Crops (1 year)

The results of the model run for three crop periods (third crop (May – August), first crop (September – January), second crop (February – May)) show that the concentration varies significantly during the third and second cropping period (Fig. 6). The first crop period, however, shows lower levels of variation in concentration due to monsoon. During this period, unsaturated zone may be flushed by infiltrating water and increases the ionic concentration in groundwater. Fig.2 apparently shows this variation and rising groundwater level by monsoon increases the major ions and nutrients concentration in groundwater. However, concentration increases in nitrogen is observed initially after that diluted by late monsoon. Model results show that in groundwater zone, chloride varies from 60 to 68 mg/l during this 1-year simulation. In the case of nitrate, it is fluctuated between 3.4 and 3.5 mg/l in the groundwater zone. The overall fluctuation during the three crops period is mainly due to variation in rainfall, fertilizer application and evaporation. The model predictions indicate that even though there is a variation in the concentration of these ions, no upward or downward trend is observed. In general, the concentration of chloride and nitrate in 40–50 cm fluctuate between 55 and 95 mg/kg, 1.2 and 5.4 mg/kg, respectively (Fig. 6). Similarly, in groundwater, chloride varies from 60 to 65 mg/l and nitrate varies from 3.4 to 3.5 mg/l.

Model Results for 5-year Period

Assuming that the fertilizer application and other input parameters are similar, the model was run for 5 years from May 1999, considering three paddy-cropping seasons. The results indicate that the concentrations of chloride and nitrogen fluctuate significantly (Fig. 7). Fig.7 shows that the concentrations of ions fluctuate in a cyclic trend during the simulation period. This trend is mainly because of rainfall during monsoon and evaporation in summer period. In the 40–50 cm layer, the concentrations of chloride and nitrate vary from 45 to 95 mg/kg and 1.7 and 5.3 mg/kg, respectively. In groundwater zone, the concentration of chloride fluctuates between 60 and 68 mg/l and nitrate from 3.4 to 3.5 mg/l. Despite this cyclic trend, there is no significant over all upward or downward trends in the concentrations of ions in the unsaturated zone. It is further observed that these ions in the groundwater zone do not increase during the simulation period.

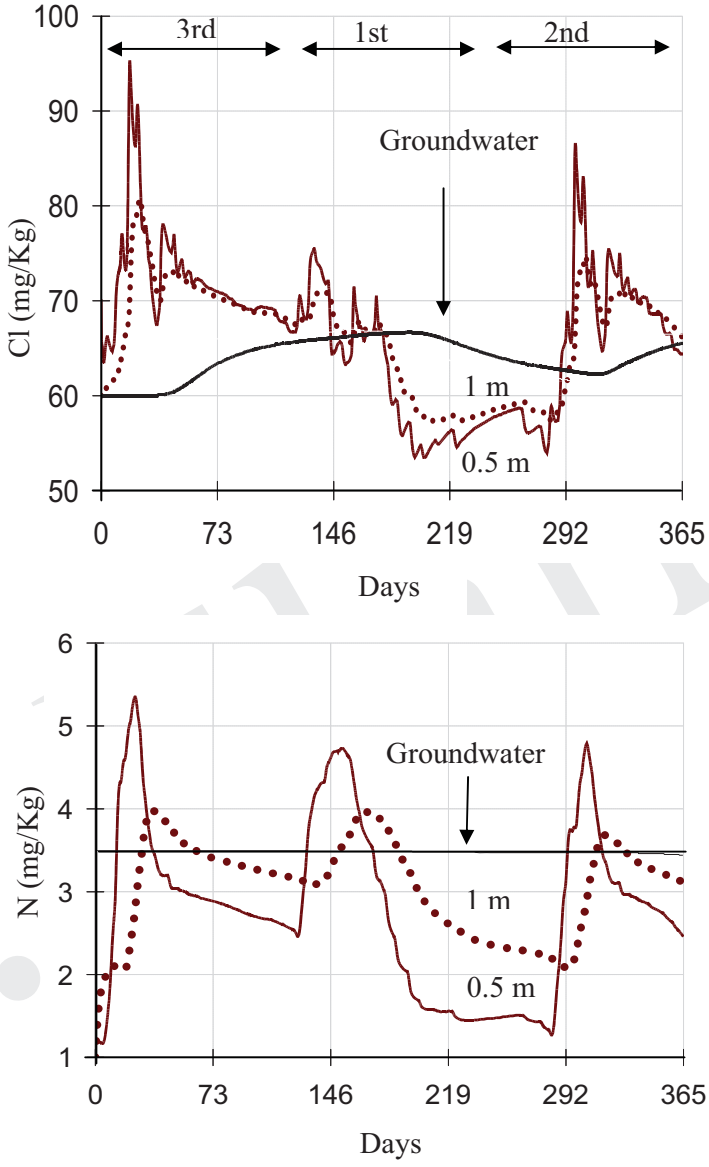

Fig. 6: Simulated chloride and nitrogen at different depths for one year period

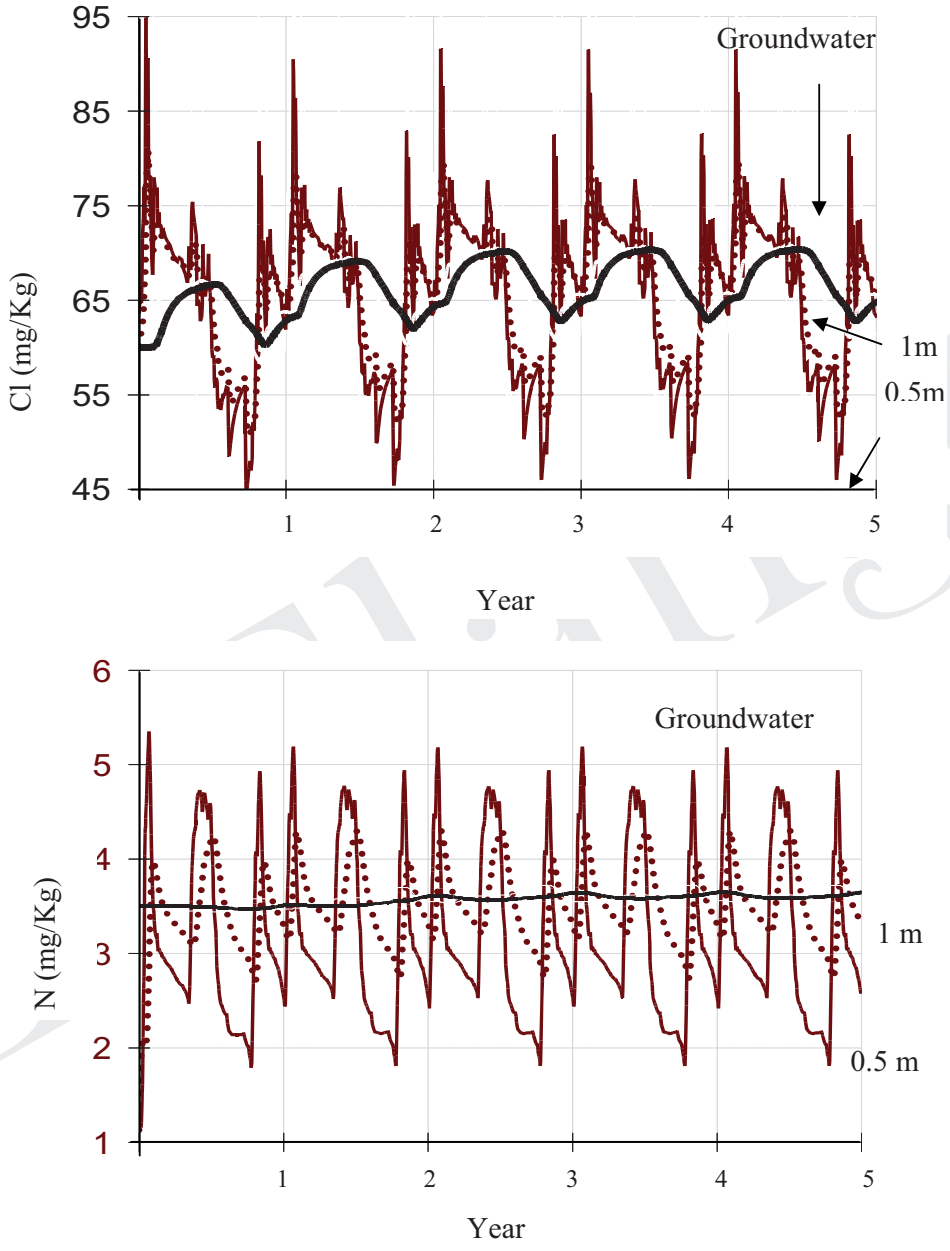

Fig. 7: Simulation of chloride and nitrogen for five year period

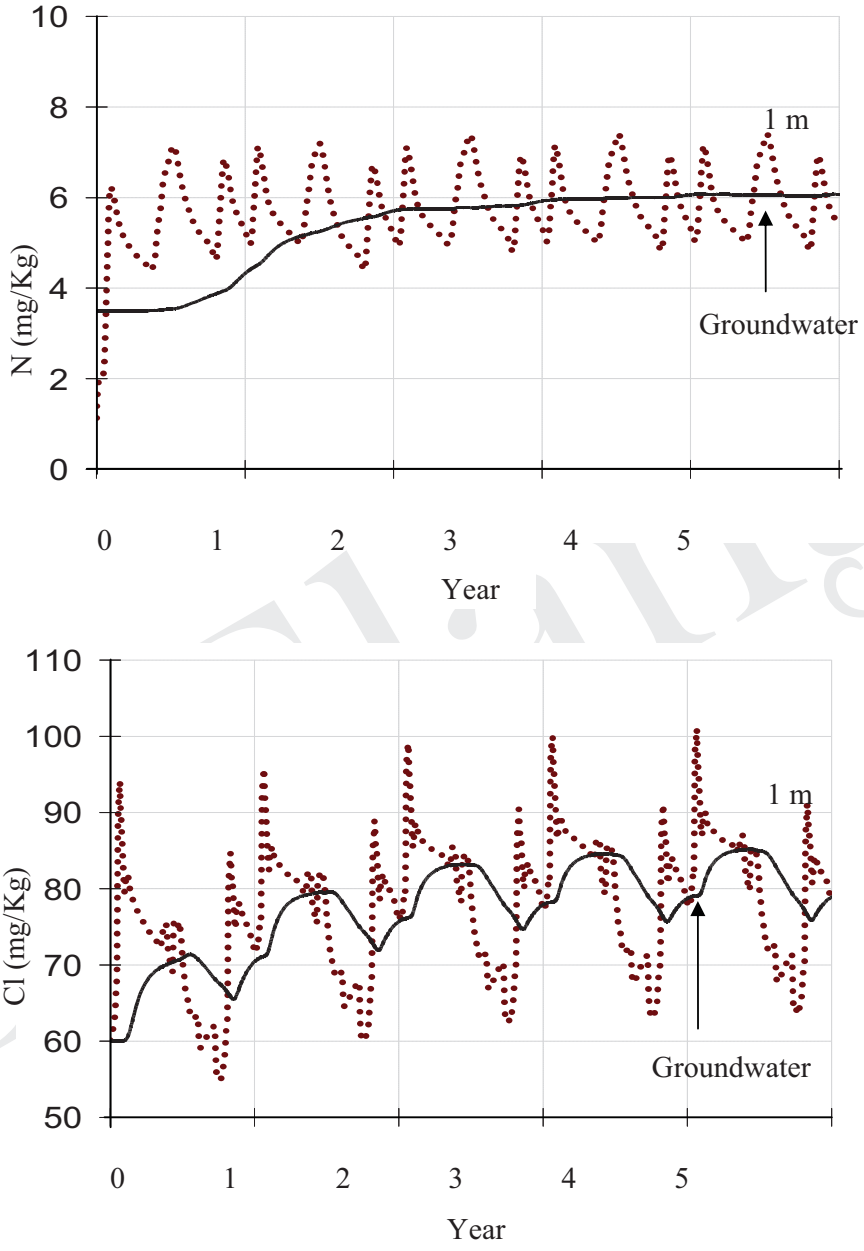

Fig. 8: Simulated chloride and nitrogen concentrations during excess fertilizer applications (2-fold) for 5-year period

Model Results with Excess Fertilizer Application for 5-year Period

The model was also used to predict the effect of excess fertilizer application on unsaturated zone and groundwater. During this simulation, application of fertilizer was doubled and other model parameters were kept as in earlier predictions. The results of the 5-year run with increased fertilizer application indicate an increase in the concentration of chloride and nitrate in the unsaturated zone and groundwater (Fig. 8). A two-fold increase in fertilizer usage results in an increase of 20 mg/kg of chloride and 3 mg/kg of nitrogen in top 1 m of the unsaturated zone. Similarly, the concentrations of chloride and nitrogen in the groundwater increase by 17 mg/l and 2.3 mg/l, respectively. However, this increase in the concentrations seems to stabilize at the end of the fifth year. The model predicts that there is no threat to the groundwater quality due to the present use of fertilizers.

CONCLUSIONS

The out come of the study expresses that the concentrations of chloride, sulphate and bicarbonate in the unsaturated zone increased during irrigation due to the application of fertilizer and evaporated irrigation water. Solute transport modelling indicates that the simulated results reasonably match with the observed trend. Simulated concentrations of chloride and nitrate for a 5-year period indicate that the concentration of these ions fluctuates in a cyclic manner (from 60 to 68 mg Cl/l and 3.4–3.5 mg N/l in groundwater) with no upward and downward trends. Influence of excessive fertilizer application on groundwater was also modelled and it predicts an increase of about 17 mg/l of chloride and 2.3 mg/l of nitrogen in the groundwater of this area when the application of fertilizers increased into 2 fold. Thus, the study concluded that there is no threat to the groundwater quality due to the present level fertilizer usage.

REFERENCES

[1] APHA, (1995). Standard methods for the examination of water and wastewater, 19th ed. American Public Health Association, Washington DC, USA.

[2] Clark, J., (1994). Evaluation of nitrogen movement beneath a leather leaf fernery. Master's thesis. Univ. of Florida, Gainesville.

[3] De Vos JA., Raats PAC. and Feddes, RA., (2002). Chloride transport in a recently reclaimed Dutch polder. Journal of Hydrology 257:59-77.

[4] Genuchten, VMT., (1980). A closed form equation for predicting the hydraulic conductivity of unsaturated soils. Soil Science Society of American Journal 892–898.

[5] Genuchten, VMT. (1985). Convective–dispersive transport of solutes involved in sequential first order decay reactions. Computers and Geosciences 11:129–147.

[6] Hutson, JL. and Wagenet, RJ., (1992). LEACHM: Leaching Estimation and Chemistry Model: A process-based model of water and solute movement, transformation, plant uptake and chemical reactions in the unsaturated zone. Water Resour. Inst., Cornell Univ., Ithaca, NY.

[7] Jackson, ML., (1958). Soil Chemical Analysis 227–255.

[8] Krumbein, WC. and Pettijohn, PJ., (1938). Manual of sedimentary petrography, New York, Appleton Centuary Co., Inc. 540.

[9] Muthuvel, P., Udayasoorian, C., Duraiswamy, P., Palanivel, A. and Rakkiyappan, P., (1990). Introduction to Soil Analysis, Palaniandavar Printers, Coimbatore, India.

[10] Neuman, SP., Feddes, RA. and Bresler, E., (1974). Finite element simulation of flow in saturated–unsaturated soils considering water uptake by plants, Third Annual Report, Project No. A10-SWC-77, Hydraulic Engineering Lab, Technion, Haifa, Israel.

[11] Paramasivam, S., Alva, AK., Fares, A. and Sajwan, KS., (2002). Fate of Nitrate and Bromide in an Unsaturated Zone of a Sandy Soil under Citrus Production. Journal of Environmental Quality 31:671-681.

[12] Petrovic, AM., (1990). The fate of nitrogenous fertilizers applied to turfgrass. Journal of Environmental Quality 19:1–14.

[13] Rajmohan, N., Elango, L., Ramachandran, S. and Natarajan, M., (2000). Major ion correlation in groundwater of Kancheepuram region, South India. Indian Journal of Environmental Protection 20:188–193.

[14] Rajmoan, N. and Elango, L., (2005) Mobility of major ions and nutrients in the unsaturated zone during paddy cultivation: a field study and solute transport modelling approach, Journal of Hydrological Processes (in press).

[15] Saadi, Z. and Maslouhi, A., (2003). Modelling nitrogen dynamics in unsaturated soils for evaluating nitrate contamination of the Mnasra groundwater. Advances in Environmental Research 7:803-823.

[16] Scanlon, B., Christman, M., Reedy, R., Porro, I., Simunek, J. and Flerchringer, G., (2002) Intercode Comparisons for Simulating Water Balance of Surficial Sediments in Semiarid Regions. Water Resource Research, Vol. 38, No.12. P59-1 – 59-16

[17] Simunek, J., Sejna, M. and Genuchtan, VT., (1999). Hydrus-2D/Meshgen-2D: simulating water flow and solute transport in two-dimensional variably saturated media. US Salinity Laboratory, Agriculture Research Service, Riverside, California.

[18] Van Genuchten, MT. and Alvès, WJ., (1982). Analytical solutions of the one-dimensional convective–dispersive solute transport equation, US Department of Agriculture Technical Bulletin No 1661. 151 pp

[19] Van Genuchten, M.Th., F.J. Leij and S.R. Yates., (1991). The RETC code for quantifying the hydraulic functions of unsaturated soils, version 1.0. EPA Report 600/2-91/065. U.S. Salinity Laboratory, Agricultural Research Service, USDA, Riverside, California. 85 p.

[20] Walkley, A. and Black, IA., (1934). An examination of the Degtjareff method for determining soil organic matter and proposed modification of the chromic acid titration method. Soil Science 37:29–38.

Numerical Simulation of Groundwater Flow and Solute Transport, L. Elango (ed). pp.219-226

Assessment of Groundwater Pollution from Red Mud Ponds in Hindalco- Belgaum Works Watershed, Karnataka

V.V.S. Gurunadha Rao

INTRODUCTION

An upcoming problem in the recent times is that of the groundwater pollution. Indiscriminate disposal of industrial waste, extensive use of chemicals in agriculture such as fertilizers and pesticides and a host of other human interventions have been causing pollution of water resources. The pollution after effecting soils and surface water extends to the groundwater system through downward gravitational movement as well as lateral dispersion and advective migration. Fractures, fissures, joints etc., provide additional preferred pathways for a fast migration of pollutants. With the increase in industrialization and the increasing use of groundwater, it is imperative to study the movement of contaminants in an aquifer to predict their migration. This can help planners in working out necessary remedial and preventive measures. Such studies also help evolve useful guidelines for future planning of waste disposal operations and for controlling the existing pollution plumes.

GROUNDWATER FLOW AND MASS TRANSPORT MODELLING

The partial differential equation describing three-dimensional transport of contaminants in groundwater (Bear, 1979, Javandel, et. al, 1984, Anderson and Woessner, 1992) can be written as

$$\frac{\partial}{\partial}\frac{C}{t} = \frac{\partial}{\partial x_i}\left[D_{ij}\frac{\partial C}{\partial x_j}\right] - \frac{\partial}{\partial x_i}(v_i C) + \frac{q_s}{\theta}C_s + \sum_{K=1}^{N} R_k. \qquad (1)$$

where

C concentration of contaminants dissolved in groundwater
t time
x_i distance along the respective Cartesian co-ordinate axis
D_{ij} hydrodynamic dispersion coefficient
v_i seepage or linear pore water velocity
q_s volumetric flux of water per unit volume of aquifer representing sources (positive) and sinks (negative)
C_5 concentration of sources or sinks
θ porosity of the porous medium
R_k chemical reaction term

Assuming that only equilibrium controlled linear or non-linear sorption and first order irreversible rate reactions are involved in the chemical reactions, the chemical reaction term can be expressed as (Grove and Stollenwerk, 1984)

$$\sum_{k=1}^{N} R_k = -\frac{\rho_b}{\theta}\frac{\partial \overline{C}}{\partial t} - \lambda\left[C + \frac{\rho}{\theta}\overline{C}\right]. \tag{2}$$

where

ρ_b the bulk density of the porous medium

$\overline{C}$ the concentration of contaminants sorbed on the porous medium

λ the rate constant of the first-order rate reactions

rewriting

$$\frac{\rho_b}{\theta}\frac{\partial \overline{C}}{\partial t} = \frac{\rho_b}{\theta}\frac{\partial C}{\partial t}\frac{\partial \overline{C}}{\partial C} \tag{3}$$

We can rewrite equation(1) by substituting eqs. (2) and (3) as

$$\frac{\partial C}{\partial t} = \frac{\partial}{\partial x_i}\left[D_{ij}\frac{\partial C}{\partial x_j}\right] - \frac{\partial}{\partial x_i}(v_i C) + \frac{q_s}{\theta}c_s - \frac{\rho_b}{\theta}\frac{\partial \overline{C}}{\partial C}\frac{\partial C}{\partial t} - \lambda\left(C + \frac{\rho_b}{\theta}\overline{C}\right) \tag{4}$$

Rearranging terms we get

$$R\frac{\partial C}{\partial t} = \frac{\partial}{\partial x_i}\left[D_{ij}\frac{\partial C}{\partial x_j}\right] - \frac{\partial}{\partial x_j}(v_i C) + \frac{q_s}{\theta}c_s - \lambda\left(C + \frac{\rho_b}{\theta}\overline{C}\right) \tag{5}$$

where R is called the retardation factor, defined as

$$R = 1 + \frac{\rho_b}{\theta}\frac{\partial \overline{C}}{\partial C}. \tag{6}$$

Equation (5) is the governing equation underlying the solute transport model.

The transport equation is linked to the flow equation

$$v_i = -\frac{K_{ii}}{\theta}\frac{\partial h}{\partial x_i}. \tag{7}$$

where

K_{ii} a principal component of the hydraulic conductivity tensor

h hydraulic head

The hydraulic head is obtained from solution of three dimensional groundwater flow equation through MODFLOW software (McDonald and Harbaugh, 1988)

$$\frac{\partial}{\partial x_i}\left[K_{ii}\frac{\partial h}{\partial x_j}\right] + q_s = S_s\frac{\partial h}{\partial t} \tag{8}$$

where S_5 is the specific storage of the porous material.

The numerical approaches for solving the mass transport equations are based on computer-based particle tracking methods. They are approximate forms of the advection - dispersion equation (5) as a system of algebraic equations or alternatively simulating transport through spread of a large number of moving reference particles. These numerical approaches deal with variability of flow and transport parameters (hydraulic conductivity, porosity, dispersivity etc.).

Velocity values are computed by applying Darcy's equation using calculated hydraulic heads and porosity values (Konikow and Bredehoeft, 1978). For steady state flow, the water level configuration of July 1997 was considered and the groundwater flow equation was solved once and thereby a single velocity field was determined for the mass transport simulation for all times. Dispersion is accounted for in the particle motion by adding to the deterministic motion a random component, which is a function of the dispersivities. The mean concentration for each grid block is calculated as the sum of the mass carried by all the particles located in a given block divided by the total volume of water in the block.

INDAL ALUMINA PLANT WATERSHED, BELGAUM

One of the main tailings of Aluminium industry is red mud, which is a kind of hydrous silt muddy, highly alkaline solid waste produced by physical and chemical treatments of bauxite in alumina (Al_2O_3) production. As red mud is harmful to the ecological environment, the safety of its storage has become an environmental problem of concern for Alumina industry in the country. HINDALCO-Belgaum works (formerly INDAL) was established during 1970 and in the production process of alumina, the red mud slurry is generated. The effluent is stored in two ponds constructed in an area of 70 hectares up to 1984. The process has been changed during 1985 to a dry process known as red mud stacking. The present day effluent in ponds contains dissolved Sodium Carbonate (Na_2CO_3) and small amounts of NaOH drained from the red mud stacking area. Rainfall falling on the red mud stacking area is being collected in two ponds. Seepage from bed of the ponds and leachate from stacking area may carry Na_2CO_3 and NaOH to the groundwater regime. The effluent TDS concentration on reaching groundwater table migrates with groundwater velocity.

The watershed is spread over 75 sq. km in basaltic terrain on the northern periphery of Belgaum town (Fig. 1).The watershed is drained by Markandeya River in the north. Detailed geophysical and hydrogeological investigations have been carried out in and around the

watershed. Electrical resistivity soundings were carried out to know aquifer geometry. The soundings have not detected presence of any fractures around the ponds. Periodical water level and water quality was monitored at 30 observation wells during 1998–1999. Detailed chemical analysis was carried out for estimation of concentration of TDS, Sodium Carbonate and Caustic soda in the effluent ponds as well as in the groundwater samples (Dhar et al, 1999).

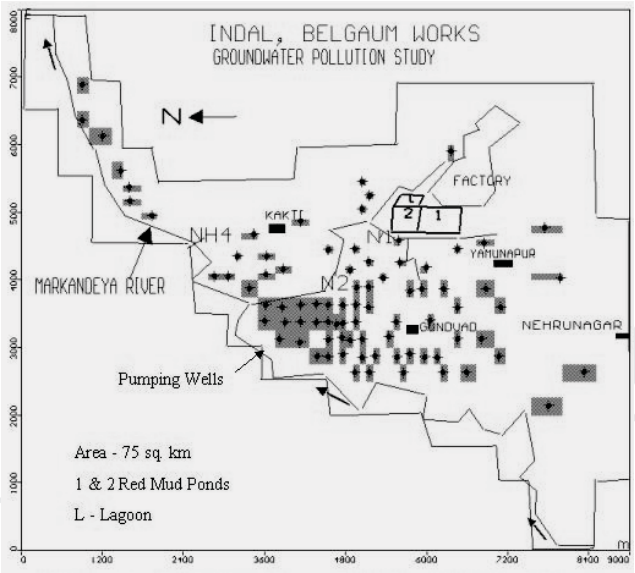

Fig. 1: Location of HINDAL CO-Belgaum Works Watershed, Belgaum, Karnataka

GROUNDWATER FLOW AND MASS TRANSPORT MODELS

A number of irrigation wells are pumping groundwater between Gaundvad village and Markandeya River. Dug well cross-sections and lithologs of drilled bore wells indicated that top weathered zone has a thickness of 15-20 m and it is underlain by a fractured layer of 20-30 m thickness. Aquifer parameters were estimated by carrying out 3 pumping tests and estimated permeability values are found ranging from 0.1 m/day in the upland to 2 m/day near the river. The boundary conditions assigned are river boundary on Markandeya River and small inflow from east (Fig. 2).

Natural recharge of 65 mm/yr was given as input to the flow model. The seepage from red mud ponds is simulated as additional recharge (130 mm/yr) from the ponds. The groundwater flow model simulation was carried out by using visual MODFLOW software. Steady state flow model was calibrated for the water level configuration of July 1998 and the groundwater velocity vectors indicate the predominant flow direction (Fig. 3). The water level data of 14 observation wells is used for flow model calibration.

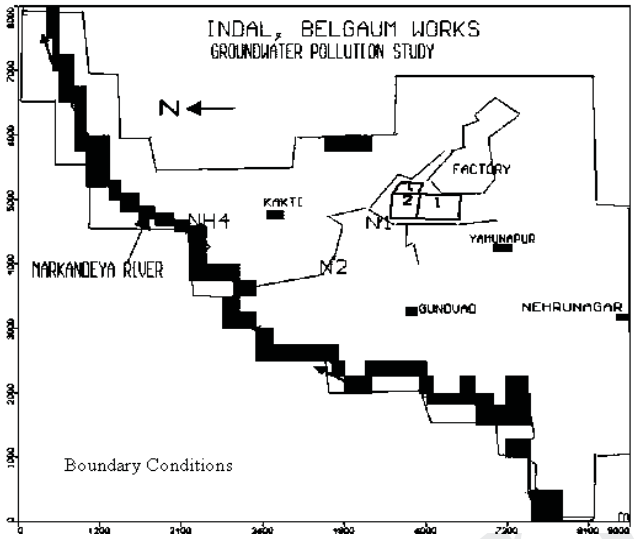

Fig. 2: Boundary Conditions Simulated in the Groundwater Flow Model

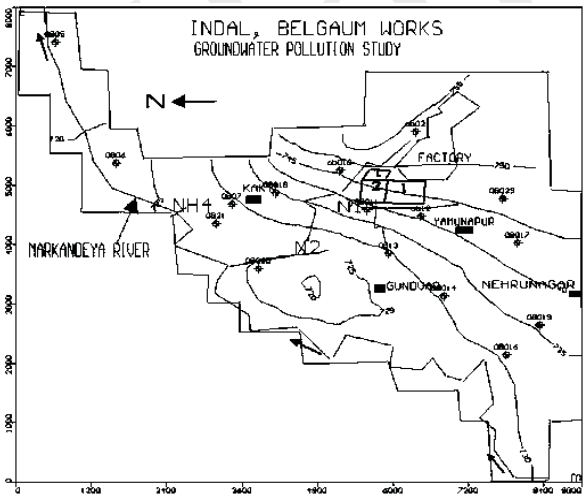

Fig. 3: Computed groundwater level contours in m (amsl) June 1998

The mass transport model is coupled to the flow model by the velocity terms. The TDS concentration in the effluent was selected for mass transport modelling. The transport of contaminants is simulated by adding reference particles and moving them in a prescribed manner in groundwater. Advection is accounted by moving each particle by a distance in the direction of flow that is determined by the product of magnitude of groundwater velocity and size of the time

step. Dispersion is accounted for in particle motion by adding to the deterministic motion a random component, which is a function of the dispersivities. The mean concentration for each grid block is calculated as the sum of mass carried by all particles located in a given block divided by total volume of water in the block. The values of dispersivity in the longitudinal and two transverse directions (Y and Z) are assumed to be 50 m, 5m and 0.05 m respectively. Constant TDS concentration of 2000 mg/l was assigned at the water table just below the red mud ponds. Mass transport for simulation of advection, dispersion and chemical reactions of contaminants in three-dimensional groundwater flow system has been carried with the help of MT3D computer software. The computed and observed iso-concentration of TDS for 1998 is found to be in good agreement. The advective transport makes TDS concentration (Contaminant) to move about 350-400 m from ponds during last 28 years with an average groundwater velocity of 20 m/year during calibration phase.

The mass transport model was used to compute concentrations for same amount loading of effluent in the ponds for next 20 years in the first layer and second layer (Fig. 4 & 5 respectively). Significantly the predicted TDS concentration for 2018 indicates that the TDS concentration plume does not extend beyond Gaundvad village. Periodical monitoring of groundwater quality data measured by HINDALCO-Blegaum works has helped to make a post audit of the predicted contaminant concentrations. It was found that the water quality data of 2003 indicate that the contaminant concentrations at the measured wells are found to be even less than the predicted contaminant concentrations. Thus the mass transport modelling has provided a worst-case design. It could be possible that the porous matrix may be retarding more than the simulated conditions.

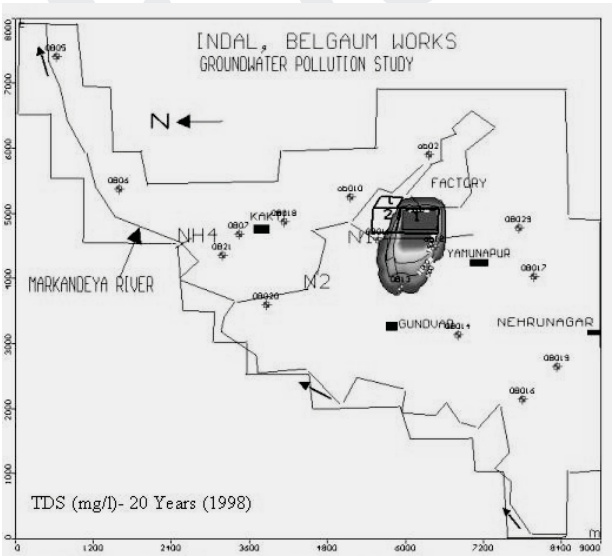

Fig. 4: Computed TDS concentration (mg/l)-June 1998

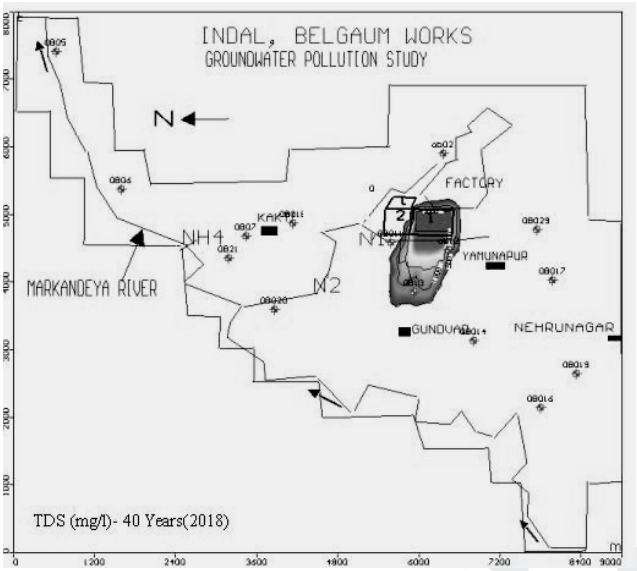

Fig. 5: Predicted TDS concentration (mg/l)-June 2018

CONCLUSIONS

Groundwater flow and mass transport modelling is a power tool for assessment of groundwater contamination due to effluent discharges from industrial areas. The groundwater modelling has reached a stage that predictions can be visualized, which may help the Industrial policy makers for taking remedial actions in advance. As model calibration and parameter estimation are keyed to a set of historical data, the confidence in and reliability of the calibration process is proportional to the quality and comprehensiveness of the historical record. The accuracy of a model's predictions is the best measure of its reliability. If model is to be used for prediction relating to a problem or system that is of continuing interest to the society, then field monitoring should continue and the model should be periodically post-audited to incorporate new information. A recent post audit of groundwater quality data from the observation wells in the watershed are has helped validate modelling results, thereby helped the HINDALCO management ascertain that the measures taken up by them to control the contaminant migration in groundwater from the red mud stacking area are working well.

REFERENCES

[1] Anderson M.P. and Woessner, W.W., (1992). Applied groundwater modelling – simulation of flow and advective transport. Academic press. San Diego, CA., U.S.A.

[2] Bear, J., (1979). Hydraulics of groundwater. McGraw Hill, NewYork, pp.210.

[3] Burnett, R.D. and Frind, E.O., (1987). An alternating direction Galerkin techniques for simulation of groundwater contaminant transport in three dimensions, 2-Dimensionality effects. Water Resour. Res. 23 (4), p.695-705.

[4] Dhar, R.L, Gurunadha Rao, V.V.S., Subrahmanyam, K. and Yadaiah, P. Assessment of groundwater contamination in Patancheru and Bolaram Industrial Development Areas, Medak District, Andhra Pradesh, India. Tech Rep. No. NGRI-GW-Environ-236, pp.105.

[5] Dhar, R.L., Singh, V.S., Gurunadha Rao, V.V.S., Ananda Rao, V., Sarma, M.R.K., Prakash, B.A. and Krishnan, V., (1999). Assessment of the impact of red mud stacking on groundwater regime around INDAL Alumina plant, Belgaum, Karnataka. Tech. Rep. No. NGRI- 99 – GW-256, pp.79.

[6] Javandel, I., Doughty, C. and Tsang, C.F., (1984). Groundwater transport: Handbook of Mathematical models. American Geophysical Union, Water Resources Monograph 10, pp.228.

[7] Grove, D.B. and Stollenwork, K.G., (1984). Computer model of one-dimensional equilibrium controlled sorption processes. U.S. Geol. Survey Water Resources Investigations Report 84-4059, pp.58.

[8] Konikow, L.F. and Bredehoeft, J.D., (1978). Computer model of two dimensional solute transport and dispersion in groundwater. U.S. Geol. Surv. Water Resour. Invest. Book 7, Chapter C2, pp.90.

[9] Guiger, N. and Franz, T., (1996). Visual MODFLOW: Users Guide. Waterloo Hydrogeologic, Waterloo, Ontario, Canada.

[10] McDonald, J.M. and Harbaugh, A.W., (1988). A modular three-dimensional finite-difference groundwater flow model. Techniques of Water resources Investigations of the U.S. Geological Survery Book.6, pp.586.

[11] Zheng, C., (1990). MT3D, a Modular three-dimensional transport model for simulation of advection, dispersion and chemical reactions of contaminants in groundwater system prepared for the U.S. Environmental Protection Agency.

Numerical Simulation of Groundwater Flow and Solute Transport, L. Elango (ed). pp.227-235

Mass Balance Modelling and Its Concepts: A Case Study

L. Elango and **R. Kannan**

INTRODUCTION

Groundwater chemistry is largely a function of the mineral composition of the aquifer through which it flows. As groundwater moves along its path from recharge to discharge areas, a variety of hydrogeochemical processes alter its chemical composition. These hydrogeochemical processes vary spatially and temporally, depending on the geology and chemical characteristics of the aquifer. Generally, hydrogeochemical processes are broadly classified into three types as water rock interaction, evaporation and dilution. Further, they are classified into several types such as precipitation and dilution, weathering and dissolution, ion exchange processes, oxidation and reduction, over saturation and precipitation of minerals, evaporation and evapotranspiration, which control the chemical composition of groundwater. The occurrence of chemical processes can be rebuilt and if the processes continue in future we can predict the groundwater contamination before using mass balance modelling. To carryout this study the following steps has to be followed.

1. Identifying the current physio-chemical nature (Composition, EC, pH & Eh) of the groundwater system.
2. Understanding the fundamental hydrogeochemical processes that can take place in an aquifer of a particular geological formation
3. Developing a conceptual model of the system
4. Identifying the chemical characteristics of the system in terms of the net geochemical mass balance reactions between initial and final waters and also predict the future trends of groundwater quality.

MODELLING DATA REQUIREMENTS

Data is the primary variable used to do modelling of any kind. Accuracy of the modelling depends on the precession of the data used. Data required for mass balance modelling can be divided in to two categories as physio-chemical data and experimentally derived data. Physio-chemical data (Table 1) to be collected depend on the purpose of the study. Experimentally derived data on equilibrium and rate constants are thermodynamic data (equilibrium constants and enthalpy values for the common chemical reactions).

Certain properties of the solids such as adsorption and neutralization capacities cannot be predicted from the solution analysis so solid phase data (Table 2) is also necessary for hydrogeochemical modelling.

Table 1: Physio-chemical data collection for geochemical modelling

Data	Use
Major ions	Calculation of solution complexes, saturation indices
pH	Ion speciation/complexation and mineral solubility
Eh	Ion speciation/complexation and mineral solubility of Redox-sensitive elements
Temperature	Stability of groundwater pH, Dissolution control
Dissolved Gasses	O2: quality measure of Redox potential CO2: stability of groundwater pH
Minor/Trace elements Clay and oxyhydroxide	Mineral equilibria
Trace metals	Mineral equilibria, competitive adsorption
Organic compounds	Complexation, oxygen consumption, sorption reactions
Stable isotopes	Water signature, mineral reactions
Unstable isotopes	Age dating

Table 2: Solid phase data

Data	Potential impact on system
Carbonate minerals	Mineral solubility control on solution concentration
Clay minerals	Exchange capacity, Mineral solubility control
Ferric and manganese oxyhydroxide	Mineral solubility control, adsorption substrates for minor /trace elements
Pyrite	Mineral solubility control, source of acidity under oxidizing condition
Silicate minerals	Sources of many dissolved constituent
Organic carbon	Adsorbent medium, reducing agent, source of dissolved carbon

Data related to equilibrium and reaction rate is also essential to carry out hydrogeochemical modelling. Knowledge on common water/rock/gas interactions that are taken place in the subsurface are useful to understand the possibility of chemical reactions in a particular aquifer system. Similarly mass balance modelling will lead to quantify the the chemical processes that are taking place in an aquifer. Some of the common water/rock/gas interactions or chemical processes are given below.

Process	**Example Chemical reaction**
Gas equilibrium	$2CO_2(g) + H2O \Leftrightarrow CO_2\ (aq) + H_2CO_3$
Ion speciation	$H_2CO_3 \Leftrightarrow HCO_3^- + H^+$
Ion complexation	$Ca_2^+ + HCO_3^- \Leftrightarrow CaHCO_3^+$
Mineral dissolution/precipitation	$CaCO_3 \Leftrightarrow Ca_2^+ + CO_2^-$
Oxidation/reduction	$CH_2O + O_2 \Leftrightarrow CO_2 + H_2O$
Adsorption/desorption	$FeOH_2^+ + Ag^+ \Leftrightarrow FeOHAg^+ + H^+$
Solid solution	$CaCO_3 + xMg_2^+ \Leftrightarrow Ca1\text{-}x\ MgxCO_3 + xCa_2^+$

BASIC APPROACHES FOR HYDROGEOCHEMICAL MODELLING

There are two basic modelling approaches can be adopted to do mass balance modelling. They are,

1. Forward method of hydrogeochemical modelling
2. Inverse method hydrogeochemical modelling

Forward Method of Hydrogeochemical Modelling

The forward method applies to the situations where the data may only be available from one point along the flow path. In this case the investigator wishes to know how the aquifer system will respond to the addition of a reactant or some other change in the environmental condition. This model uses equilibrium constants for all the potential reactions allowed by the model; therefore reactants will dissolve if they are under-saturated and products may be formed if adding the reactant causes a mineral to become saturated in the solution. The result of the model calculations once again consists of a suite of reactive phases; however, their reactivity is constrained by mass balance and thermodynamic equilibrium (Fig. 1).

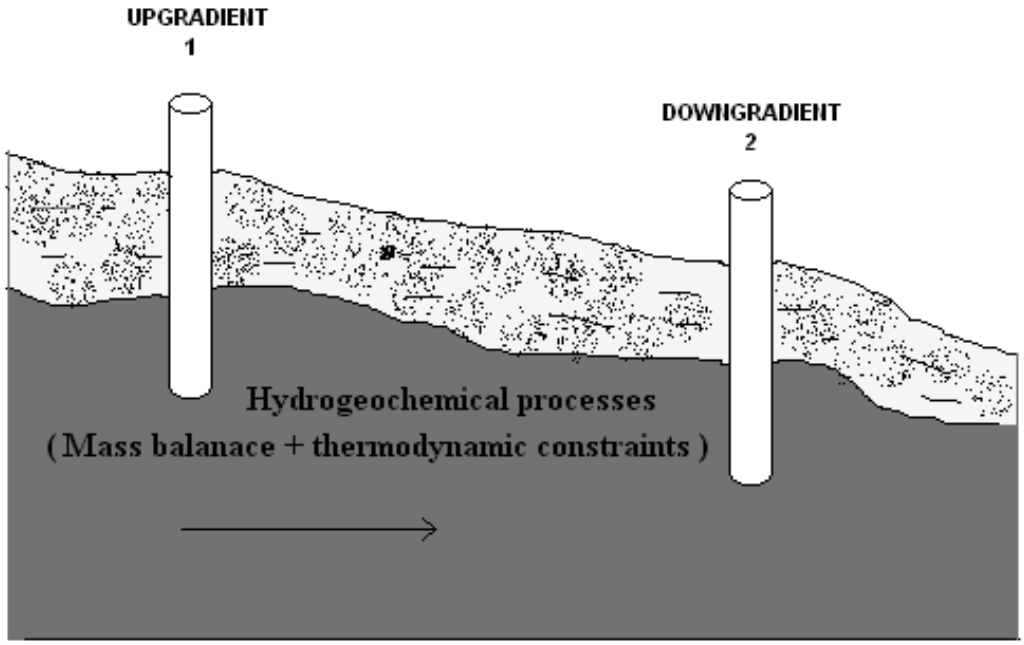

Fig. 1: Forward modelling concepts

Initial water composition at 1 + Reactants = Predicted water composition at 2 + Products.

Several software are there for forward modelling. PHREEQE (PH Redox Equilibrium Equations) was developed by the U.S. Geological Survey (Parkhurst, 1980) and has been enhanced in the PHREEQC version (Parkhurst, 1995) by the ability to model surface complexation with diffuse double layer model and reactive transport.

Inverse Mass Balance Modelling

The inverse method applies to situations where sufficient data are available to define the flow path and changes in groundwater composition along the flow path (Fig. 2). It is assumed that reactive solids and gases along the flow path have produced the changes in composition, but the suit of reactive phases has not been identified nor is the amount of reactive phases that are dissolving or precipitating known (Deutsch, 1997). Models are developed consisting of suites of reactive phases that are known to occur in the aquifer. The mass balance calculations are made to account and the reactive phases that are suggested will produce a reaction of the following form (eq. 1):

Initial water composition +Reactants = Final water composition + Products – (1)

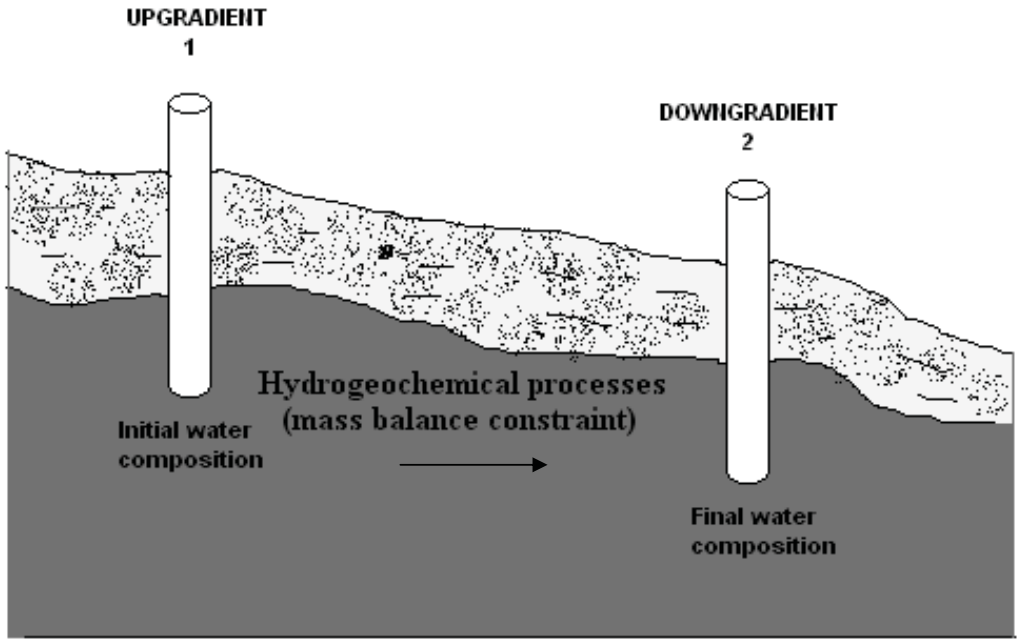

Fig. 2: Inverse mass balance modelling concept

Some of the most popular models based on this concept are WATEQF (Plummer et al., 1976), BALANCE (Parkhurst et al., 1982), MINTEQ (Felmy et al., 1983) and NETPATH

(Plummer et al., 1991). NETPATH is an interactive Fortran 77 computer program used to interpret net geochemical mass balance reactions between initial and final water along a hydrologic flow path (Fig. 2). Plummer et al., (1991) insisted that in constructing net geochemical mass balance reactions, it is necessary to select truly evolutionary initial and final waters, such as waters sampled along the flow path in a confined regional groundwater system, or laboratory waters sampled sequentially from a reactor. Various authors have studied hydrogeochemical processes, aquifer attenuation capacity and unsaturated zone chemical processes using these software codes. Elango et al., (2003) identified the major hydrogeochemical processes in the saturated zone of the Lower Palar River basin, Tamil Nadu, India. In this area Kannan (2005) has carried out a study on the hydrogeochemical processes in the unsaturated zone using NETPATH.

APPLICATIONS AND USES

The mass balance modelling can be useful to identify the hydrogeochemical process responsible for groundwater chemical composition along a flow path. By identifying the chemical process one can predict the surface water leakage in to groundwater. The chemical processes may increase or decrease the dissolved ions in the water. Thus by identifying and quantifying the chemical process we can define the aquifer attenuation capacity, which will help to know the aquifer vulnerability to pollution. Forward modelling can be used to predict the future trends of groundwater quality if certain chemical processes take place in an aquifer. Similar concept can be used to predict the unsaturated zone filtering capacity.

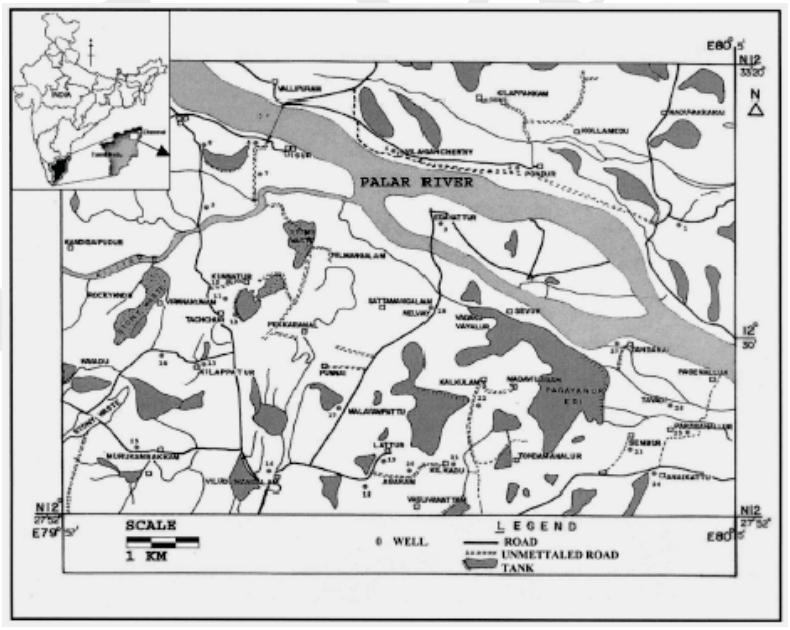

Fig. 3: Study area and well location map

INVERSE MASS BALANCE MODELLING: A CASE STUDY

The net geochemical mass balance reactions between initial and final water were identified and quantified for selected flow paths in a part of Lower Palar River Basin, Tamil Nadu, India. The study area is situated 75 km south of Chennai City, Tamil Nadu, India (Fig. 3). It is a semiarid region with temperatures ranging between 23 and 42^{o}C. The annual rainfall is about 1100 mm from the southwest monsoon (June to September), northeast monsoon (October to December) and rains during the transitional period. Palar that flows through this area is a non-perennial river active only during the months of October, November and December. It, however, has not flowed since 1999, due to scanty rainfall in the catchment area. This region is intensively irrigated and agriculture is the main source of livelihood. Paddy, sugarcane and groundnut are the main crops.

Geology and Hydrogeology

Topographically, the northern and southern parts of the study area slope towards the river, but regionally towards east. The basement is composed of Precambrian Charnockite, outcrops of which are seen in the western and southwestern parts of the area. The alluvial flood plain is constituted by sandy clay overlying the basement rock. The thickness of alluvium varies from 10 to 30 m along the Palar River banks. Boulders and clay patches are also present at some locations. The alluvium and weathered crystalline charnockite form an aquifer system, where groundwater occurs in an unconfined condition. The major sources of groundwater recharge are precipitation and the Palar River itself. The groundwater head fluctuates from 2 to 7 m below ground level in the study area. Hydraulic conductivity of the alluvium varies from 20 to 30 m/day and specific yield from 0.037 to 0.18. Weathered zone thickness varies from 0 to 7 m, and its hydraulic conductivity from 0.5 to 2.5 m/day.

Model Considerations

After a systematic study in the study area 5 pairs were selected along the flow path, which are Well Nos.14 & 12, 11 & 9, 12 & 10, 15 & 16, and 8 & 7. Another three wells - Well Nos. 14, 12 and 16 were selected for single well inverse mass balance modelling by considering successive monthly samples as initial and final waters.

Calcium, magnesium, sodium, potassium, chloride, carbon and sulphur concentrations were considered for mass balance modelling. Geochemical processes considered for modelling are 1. Calcite equilibrium, 2. NaCl equilibrium, 3. Gypsum equilibrium, 4. Illite equilibrium, 5. Ca/Na exchange and 6. Mg/Na exchange. These processes were selected based on the hydrogeology and the mineralogy of the formations of the study area. NaCl equilibrium is also included to explain the increase of chloride along the flow path. Kaolinite equilibrium and silicate weathering processes were not considered in the model due to lack of aluminium and silica data. These processes were chosen during the mass balance modelling of all initial and final waters (Table 2 & 3).

Model Results

A number of possible models have been suggested, each with certain chemical processes that would have given rise to the chemistry of final water. Certain chemical processes are suggested in almost all these models because calcium, sodium and bicarbonate ions are present in considerable amounts in the study area. Calcite and ion exchange processes, therefore, repeatedly occur in the models. In order to obtain a single model, NETPATH modelling was repeated by considering these processes.

Mass balance model shows that halite dissolution, Mg/Na ion exchange process, Ca/Na ion exchange process and calcite dissolution are the dominant processes that control the chemistry of the groundwater along the flow paths considered for modelling. Illite precipitation and gypsum dissolution is also involved to a certain extent. These are responsible for the magnesium and low potassium ion concentrations. In ion exchange processes, the aquifer matrix adsorbs Ca ion and Na is released to groundwater (Table 4 & 5). Release of Mg to groundwater and Na adsorption by aquifer matrix is observed in most of the models, except in the flow path between Well Nos. 12 and 10, wherein the irrigation return flow could have increased the concentration of Na (Table 4 & 5). The exchange reactions between Ca or Mg and Na are given below (equations 2 & 3) as explained by Martinez and Bocanegra (2002).

$$2Na^{+}\text{-}X+Ca^{2+} \Rightarrow 2Na^{+}+Ca\text{-}X^{2} \quad (2)$$

$$2Na^{+}+Mg\text{-}X^{2} \Rightarrow 2Na\text{-}X+Mg^{2+} \quad (3)$$

X- stands for matrix

The calculated cation exchange capacity (CEC (meq/100g) = 0.7 (%clay) + 3.5 (%OC)) value of selected well samples of the study area ranges from 20–27 meq/100g (Table 3), which suggests that mixed type of clay is present in the study area. Various authors have reported CEC values for mixed clay minerals. Chapelle (1983) recorded 20-30 meq/100g for the Aqua aquifer in Maryland, USA. Martinez and Bocanegra (2002) observed CEC values to vary from 20-40 meq/100g for mixed clay sediments of The Mar del Plata aquifer. This type of mixed clay content is probably responsible for the ion exchange process

Table 3: Calculated cation exchange capacity of selected wells in the study area

Well No.	Depth (m)	Sediment description	Clay %	Organic carbon %	CEC meq/100g
6	1	Sand clay loam	28.4	0.12	20.30
7	1	Clay loam	35.9	0.30	26.18
11	1	Loam	23.4	3.00	26.88

Table 4: Results of mass balance modelling of chemical processes in the groundwater from selected wells along flow path

Initial water	Final water	Calcite 1	NaCl 2	Gypsum 3	Illite 4	Exchange (Ca/Na) 5	Exchange (Mg/Na) 6
14	12	0.13265	0.45393	0.00510	-0.18036	-0.19720	-0.51603
11	09	-0.04935	1.51279	0.01097	-0.04935	-0.01425	-1.03520
12	10	-0.10613	-3.75642	-0.17427	0.43335	-0.13248	0.08644
15	16	0.06916	0.36016	0.00361	-0.14658	-0.11261	-0.25713
8	7	1.25437	7.91227	0.02675	0.24675	-0.44571	-1.34442

1, 2, 3, & 4 - (+ve) indicates dissolution and (- ve) indicates precipitation

5 & 6 - Exchange (Ca/Na)– (+ve) indicates Ca adsorption and Na release (-ve) Na adsorbed and Ca release.

- Exchange (Mg/Na)- (+ve) Mg adsorption and Na release, (-ve) Na adsorbed and Mg release.

Table 5: Results of single well mass balance chemical processes in groundwater from selected wells

Initial Water	Final Water	Calcite 1	NaCl 2	Gypsum 3	Illite 4	Exchange Ca/Na 5	Exchange Mg/Na 6
14	14	0.10201	1.15392	0.01802	-0.01736	-0.21010	-0.85254
12	12	-0.12346	-1.74162	-0.00761	0.00009	-0.18985	0.88653
16	16	0.00055	-0.42780	0.00230	0.00529	-0.28010	-0.51337

1, 2, 3, & 4 - (+ve) indicates dissolution and (- ve) indicates precipitation

5 & 6 - Exchange (Ca/Na)– (+ve) indicates Ca adsorption and Na release (-ve) Na adsorbed and Ca release.

- Exchange (Mg/Na)- (+ve) Mg adsorption and Na release, (-ve) Na adsorbed and Mg release.

In certain parts of the study area, calcite precipitation, halite precipitation, reverse ion exchange and illite dissolution are found to reduce the calcium, bicarbonate and Na ion concentration and increase the potassium ion concentrations of groundwater. Carbonate weathering is one of the main processes as suggest by modelling. Calcite dissolution contributes relatively more Ca to the water so that it is mostly of the Ca-HCO_3 type. Due to the lack of silica data silicate weathering processes could not be studied.

REFERENCES

[1] Elango, L., Kannan, R. and Senthil Kumar, M., (2003). Major ion chemistry and identification of hydrogeochemical processes of groundwater in a part of Kancheepuram district, Tamil Nadu, India. Environmental Geosciences, Vol. 10, No. 4, pp. 157-166.

[2] Chapelle, F. H., (1983). Groundwater geochemistry and calcite cementation of the Aquia aquifer in Southern Maryland. Water Resources Research, 19 (2), 545-558.

[3] Felmy, A.R, Girvin, D.C. and Jenne, E.A., (1983). MINTEQ: A computer programme for calculating Geochemical Equilibria. U.S.Environmental Protection Agency.

[4] Kannan, R., (2005). Identification of aquifer vulnerability to pollution with special emphasis to unsaturated zone. Unpublished Ph.D. Thesis, Anna University, Chennai, India, pp. 142.

[5] Martinez, D. E. and Bocanegra, E., M., (2002). Hydrogeochemistry and cation exchange processes in the coastal aquifer of Mar Del Plata, Argentina. Hydrogeology Journal, 10, 393-408.

[6] Plummer, L. N., Prestemon, E. C. and Parkhurst, D. L., (1991). An interactive code (NETPATH) for modelling NET geochemical reactions along a flow PATH. U.S. Geological Survey: Water-Resources Investigations Report, 91-4078, pp. 227.

[7] Parkhurst, D.L., Thorstenson, D.C. and Plummer, L.N., (1980). Phreeqe – A computer program for geochemical calculations. U.S. Geological Survey.

[8] Parkhurst, D.L., Plummer, L.N. and Thorstenson, D.C., (1982). BALANCE- a computer program for calculation chemical mass balance. U.S. Geological Survey.

[9] Parkhurst, D.L., (1995). User's Guide to phreeqc, a computer model for speciation, reaction path, advective transport and inverse geochemical calculations U.S. Geological Survey.

[10] Deutsch, W.J., (1997). Groundwater Geochemistry: Fundamentals and Applications to contamination. Lewis Publishers, New York, USA, pp 150.

Numerical Simulation of Groundwater Flow and Solute Transport, L. Elango (ed). pp.237-244

Stochastic Modelling of Groundwater Flow in a Weathered Gneissic Formation

A. Chaudhuri, M. Sekhar, M. Descloitres and **A. Legchenko**

INTRODUCTION

Stochastic analyses of flow in porous formations exhibiting heterogeneity due to variation in hydraulic conductivity have been the subject of considerable research over the past several years (Rubin, 1995). The behaviour is quite complex in the case of hard rocks and geophysical investigations are useful for characterizing such typical formations (Hyndman, 2000). Integrating geophysical measurements in hydrogeological modelling provides a better understanding of fluid flow processes in such complex groundwater environments (Guadagninia et al., 2004). The groundwater flow in the granitic gneissic crystalline rocks, which are one of the abundant formations in the peninsular India is governed by a complex and irregular weathered zone along with the underlying deeper fractured formation. The present paper discusses the simulations of groundwater flow in the weathered zone using integration of stochastic modelling with information from the geophysical investigations.

GEOPHYSICAL INVESTIGATIONS

The 2D resistivity imaging (or electrical resistivity tomography) is useful to survey electrical properties of the subsurface in complex environments (Loke, 2000). In this study a multi-electrode imaging system Syscal R2 manufactured by Iris Instruments was used to produce an electrical cross section along a profile across the stream at the outlet of Moole Hole experimental watershed (Legchenko et al., 2005).

Magnetic Resonance Sounding (MRS) method (Legchenko et al., 2004) measures a magnetic resonance signal generated from subsurface water molecules. Measurements are made varying pulse magnitudes that reveal the depth and thickness of water-saturated layers. MRS results give an estimate of water content and hydraulic conductivity at depth and can be correlated with bore well hydraulic tests. In the field investigations, Numisplus equipment manufactured by Iris Instruments was used to perform soundings along the same profile where the 2D electrical imaging was carried out. A 50 m x 50 m, loop was used along the profile, shifted by 25 or 50 m laterally.

GEOPHYSICAL RESULTS

The Fig. 1 presents the results of the geophysical survey carried out at the outlet zone of the experimental watershed. The results show the 2D distribution of the resistivity down to

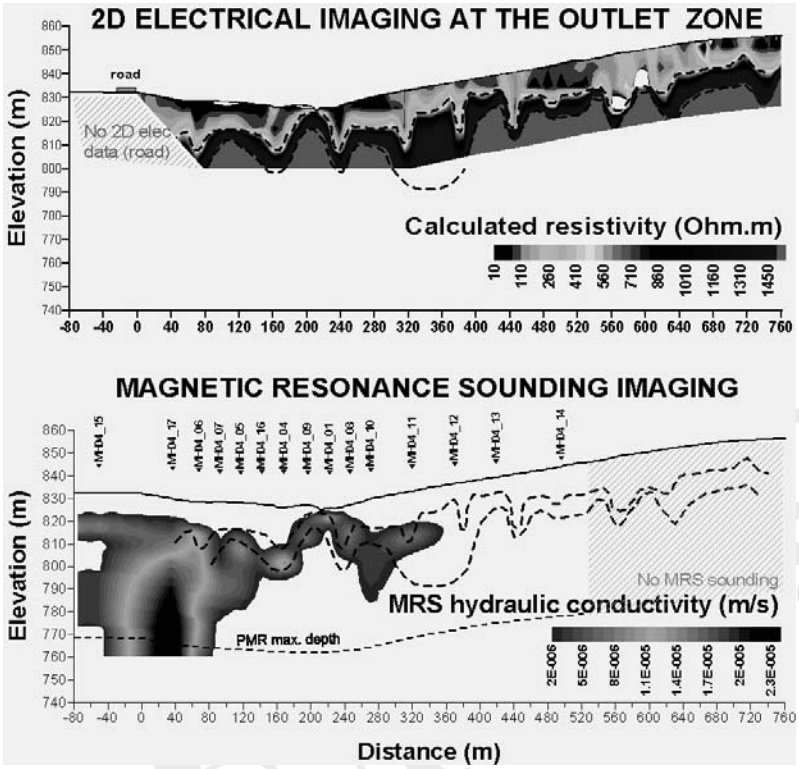

Fig. 1: Comparison between 2 D electrical imaging (above) and Magnetic Resonance Sounding results (below) at the outlet of Moole Hole watershed. The isocontours 400 and 1500 Ohm.m are drawn using dashed lines to facilitate the comparison.

25 m depth. The 2D electrical imaging outlines the distribution of electrically conductive or resistive zones that corresponds to alterite (clayey to sandy) and to the fresh rock respectively. The shape of the resistive bedrock exhibits a highly heterogeneous pattern mainly due to the dip angle (75° to the South West) of the foliated gneissic formations. The alteration processes take place non-uniformly at depth. The MRS results show a highly heterogeneous distribution of the hydraulic conductivity along the profile. In Fig. 1 at the left, a deep structure containing 1 to 2 % of water and a hydraulic conductivity of $2x10^{-5}$ ms^{-1} is measured. An additional survey at 250 m perpendicular to this structure shows that this reservoir vanishes, and hence does not correspond to a major feature of the watershed, and is consequently not taken into account in the modelling. In the central part of the profile, the MRS results are showing a pattern that follows the resistivity isocontours. This strongly suggests that the weathered zone, between the clayey zone (upper part) and the fresh rock (lower part) behaves as an upper aquifer. The bore wells show a fractured aquifer below this weathered aquifer, not evidenced in MRS because the amount of water in this

deep zone is probably less than 0.5%. When the water table is high (during monsoon season) the lateral groundwater flow observed in the weathered zone plays a significant role on the water balance of the watershed. From the 2D electrical imaging, it is possible to make a hypothesis about the shape of the weathered zone. From additional 2D electrical profiles (not shown here) elsewhere on the watershed the weathered part is found to follow the same pattern.

STOCHASTIC GENERATION OF THE WEATHERED ZONE

The objective is to generate a profile of weathered zone, which resembles the electrical profile. Fig. 2 shows the random variables to characterize the weathered zone. The steps for generating a typical profile are given in Chaudhuri et al. (2005).

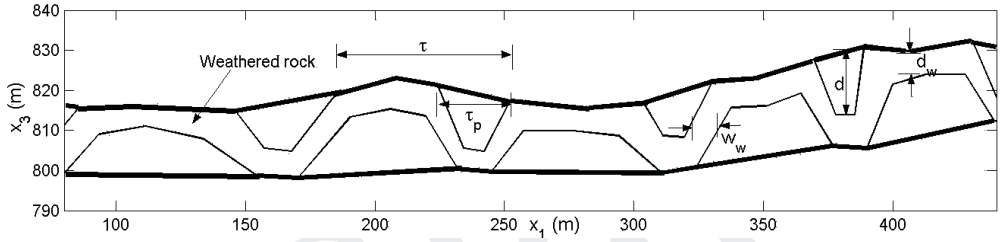

Fig. 2: The cross section of weathered rock modelled from the data of 2D electrical imaging

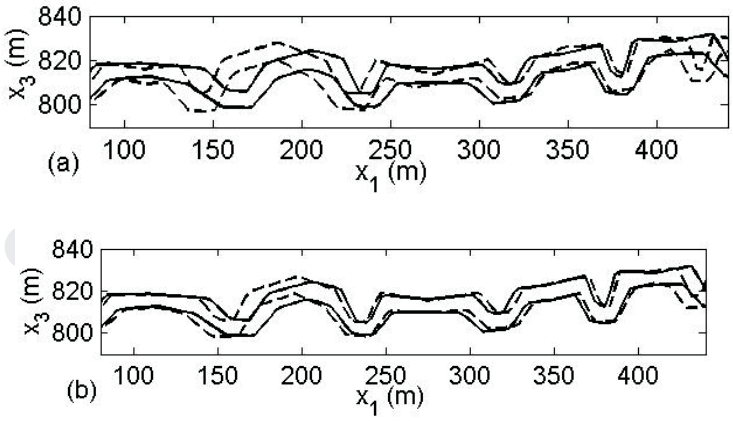

Fig. 3: A realization of the weathered zone generated (broken line) at 15 m way from the available profile (solid line) for two different correlation lengths (a) $\lambda_g = 50$ m and (b) $\lambda_g = 200$ m.

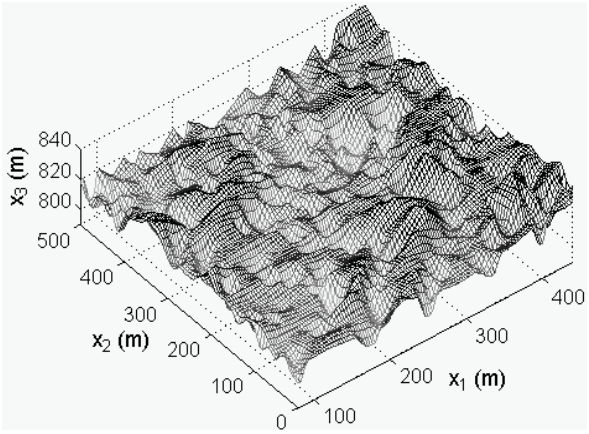

(a)

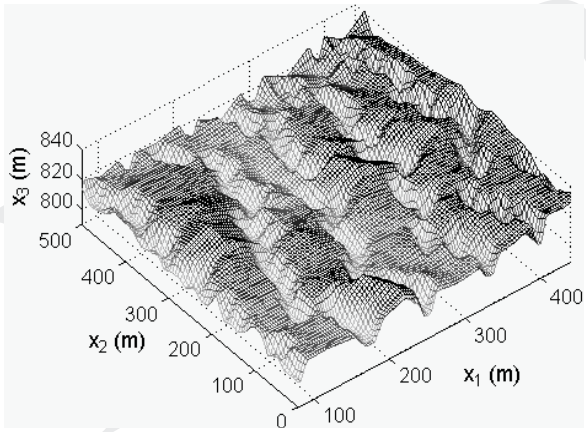

(b)

Fig. 4: The realizations of top surface weathered zone for (a) $\lambda_g = 50$ m and (b) $\lambda_g = 200$ m

As may be seen in the Fig. 3b, a realization of the generated profile of the weathered zone at 15 m way matches closely with that obtained using geophysics for $\lambda_g = 200$ m. Here λ_g is the correlation length, which defines the continuity of higher permeable weathered zone along the flow direction. Fig.4 shows the higher permeable channels in the weathered zone along x_2 axis for a larger λ_g. The correlation function of the random conductivity field is given as,

$$\rho(x_1, x_2, x_3) = \exp\left(-\left(\frac{x_1}{\lambda_1}\right)^2 - \left(\frac{x_2}{\lambda_2}\right)^2 - \left(\frac{x_3}{\lambda_3}\right)^2 \right) \tag{3}$$

where λ_1, λ_2 and λ_3 are three correlation lengths defining the random hydraulic conductivity along the Cartesian coordinates. The covariance matrix of the element hydraulic conductivity is obtained by using the above correlation function and the distance between the centroid of any two elements. This matrix is used to generate the realization of the element hydraulic conductivity for Monte Carlo simulation.

FLUX CALCULATION

The equation for flow in a porous media and the Darcy velocity are given as,

$$\frac{\partial}{\partial x_i}\left(K_{ij}(\mathbf{x}) \frac{\partial H(\mathbf{x})}{\partial x_j} \right) = 0 \text{ , and } v_i(\mathbf{x}) = -K_{ij}(\mathbf{x}) \frac{\partial H(\mathbf{x})}{\partial x_j} \tag{4}$$

where $\mathbf{K}(\mathbf{x})$ is the hydraulic conductivity tensor and $H(\mathbf{x})$ is the hydraulic head. Using finite element method the governing equation for flow can be expressed as

$$[K]\{H\} = \{H_0\} \tag{5}$$

Here $[K]$ is conductivity matrix, $\{H\}$ is the vector of heads at nodes and the vector $\{H_0\}$ consists of all flux and head boundary conditions. The flow velocity in an element is obtained by averaging of that at all Gauss points inside the element. In the present study hydraulic conductivity tensor is considered as isotropic. Here flow occurs along x_2 axis with a gradient taken as 1 in 125, while lateral fluxes are zero along $x_1 = 80\,\text{m}$ and $x_1 = 400\,\text{m}$. The flux entering through the section $x_2 = 0$ is given as $q = \sum_{p=1}^{N_B} v_{p_2} A_p$. Here N_B is the number of elements along section $x_2 = 0$, v_{p_2} and A_p are respectively the flow velocity along x_2 axis and area at the boundary of p^{th} element.

RESULTS AND DISCUSSION

The flow occurring in the weathered zone between the two thick lines in Fig. 2 is modelled in this study. The flow domain is modelled as (i) an unstructured random field, and

(ii) a structured random field using 2D electrical imaging. The zone with hydraulic conductivity, $K < 1\times10^{-8}$ ms^{-1} assessed by MRS is considered as impermeable. For the case of unstructured random field, the geometric mean of hydraulic conductivity and standard deviation of log conductivity are $K_G = 5.382\times10^{-7}$ ms^{-1} and $\sigma_f = 1.754$. In the case of structured random field the weathered zone is assumed to have two zones, one with $K_1 < 1\times10^{-6}$ ms^{-1} and the other with 1×10^{-7} ms^{-1} $< K_2 < 1\times10^{-6}$ ms^{-1}. Their statistical properties are given as $K_{G1} = 3.385\times10^{-6}$ ms^{-1}, $\sigma_{f_1} = 0.601$ and $K_{G2} = 1.602\times10^{-7}$ ms^{-1}, $\sigma_{f_2} = 1.081$. The mean ($\overline{q}$) and standard deviation (σ_q) of the total flux as obtained by Monte Carlo simulation for a few cases are given in Table 1.

Table 1: Comparisons of mean and standard deviation of flux for different cases

Case	Statistical parameters					Mean (m^3s^{-1})	Standard deviation (m^3s^{-1})
	λ_1	λ_2	λ_3	λ_g	n		
I	20 m	20 m	10 m	50 m	3	9.01×10^{-5}	1.03×10^{-5}
II	40 m	40 m	20 m	50 m	3	8.86×10^{-5}	1.27×10^{-5}
III	20 m	20 m	10 m	200 m	3	10.60×10^{-5}	0.81×10^{-5}
IV	40 m	40 m	20 m	200 m	3	10.38×10^{-5}	1.09×10^{-5}
V	20 m	20 m	10 m	50 m	4	9.55×10^{-5}	0.86×10^{-5}
VI	40 m	40 m	20 m	50 m	4	9.38×10^{-5}	1.14×10^{-5}
VII	20 m	20 m	10 m	200 m	4	10.91×10^{-5}	0.76×10^{-5}
VIII	40 m	40 m	20 m	200 m	4	10.69×10^{-5}	1.09×10^{-5}
IX	20 m	20 m	10 m	Unstructured		5.01×10^{-5}	0.72×10^{-5}
X	40 m	40 m	20 m	Unstructured		4.07×10^{-5}	1.18×10^{-5}

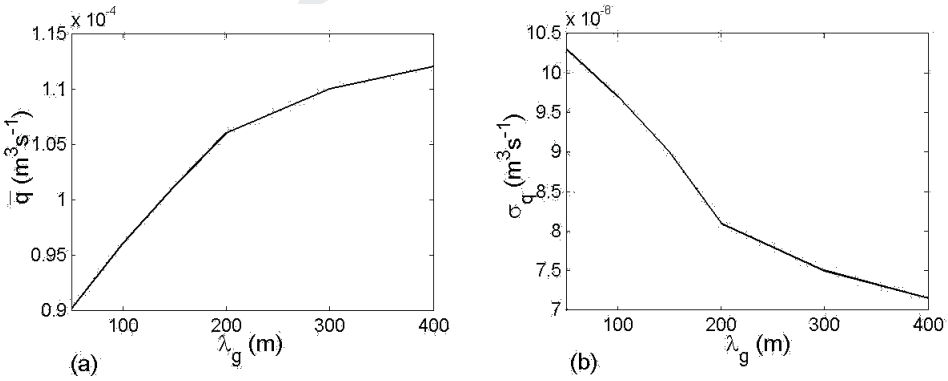

Fig. 5: (a) Mean and (b) standard deviation of flux for different correlation length

The mean flux for the unstructured case is estimated approximately 50% of the case with structured random field. The effect of different statistical parameters characterizing the 3D structured heterogeneous conductivity field on the flux has been studied. Fig. 5 shows that for a larger correlation length (λ_g), the mean flux is higher while the standard deviation is lower. Since the higher value of 'n' in equation (1) corresponds to a lower variance of the distance between two consecutive intrusions (τ), the standard deviation is less for a higher value of 'n' while the mean is larger. Table 1 shows that for the case with higher λ_1 , λ_2 and λ_3 results in a lower mean and a higher standard deviation of flux whereas higher λ_g gives a higher mean and lower standard deviation.

CONCLUSIONS

Geophysical investigation by 2D electrical imaging and MRS reveal the complexity of the distribution of the permeable weathered zone, which may be characterized as bimodal. The stochastic modelling of the flow domain as an unstructured random hydraulic conductivity field results in a significantly lower mean flux with higher uncertainty in comparison to that obtained by modelling it as a structured random field. The continuity of higher permeable weathered zone resulting from high correlation of the structures in the direction of flow produces a higher mean and a lower standard deviation of flux. In contrast the higher spatial correlation of hydraulic conductivity field results in a lower mean and a higher standard deviation of flux. These results suggest the necessity to perform more geophysical 2D profiles to understand the continuity of the structures along the flow path. Future modelling is planned to consider the anisotropic behavior of the hydraulic conductivity tensor and attempts to combine both shallow weathered and deeper fractured zones.

REFERENCES

[1] Chauduri, A., Sekhar, M., Descloitres, M. and Legchenko, A., Stochastic modelling combined with geophysical investigations for groundwater fluxes at watershed scale in the weathered gneissic formations of South India. Proceedings of ModelCARE-2005, The Hague, Netherlands, June 2005.

[2] Guadagninia, L., Guadagninia, A. and Tartakovskyb, D. M., Probabilistic reconstruction of geologic facies, Journal of Hydrology, 294, 57--67, 2004.

[3] Hyndman, D.W., Geophysical and Tracer Characterization Method, The Handbook of Groundwater Engineering, Edited by Dellur, J. W., 2000.

[4] Legchenko A., Baltassat J-M., Bobachev A., Martin C., Robain H. and Vouillamoz J-M., Magnetic resonance sounding applied to aquifer characterization. Journal of Groundwater, 42, (3), 363-373, 2004.

[5] Legchenko, A., Descloitres, M., Bost, A., Ruiz, L., Reddy, M., Sekhar, M.Mohan Kumar, M. S. and Braun, J.J., Â- Characterization of anisotropic crystalline basement aquifers using Magnetic Resonance Soundings (Southern India). IRD-IISc report, 140 p, 2005.

[6] Loke, M.H., Electrical imaging surveys for environmental and engineering studies. Technical note from Geotomo software, www.geoelectrical.com, 2000.

[7] Rubin, Y., Flow and Transport in Bimodal Heterogeneous Formations, Water Resources Research, 31, 2461-2468, 1995.

Author Index

Editor's Profile

L. Elango is a Professor, presently heading the Department of Geology, Anna University, Chennai, India. His research interests are hydrogeochemistry and groundwater modelling. He is a hydrogeologist with a Masters Degree in Science (Applied Geology) from University of Madras, Masters Degree in Engineering (Hydrology & Water Resources Engineering) and a Ph.D in Hydrogeology from Centre for Water Resources, Anna University. He carried out his postdoctoral work at the University of Birmingham under Indian National Science Academy and The Royal Society fellowship programme. He has published about 45 research papers in various journals and edited two books. So far six students have completed their Ph.D. thesis under his guidance. He has organised training programmes/workshops and conferences in the field of Hydrogeology. He has organised an International workshop on Modelling in Hydrogeology under UNESCO's International Hydrology Programme in the year 2001. He has carried out a number of sponsored research projects on hydrogeology. Some of the international projects were carried out by him in collaboration with the British Geological Survey, Australian Research Council and Moscow State University. He has also carried out many consultancy projects for organisations and companies of international repute. He has traveled wide around Asia, Australia, Europe, North America and South America on various assignments. He is a member of International Association of Hydrological Science, International Association of Hydrogeologists, Association of Geoscientists for International Development, Institution of Engineers and Association of Indian Water Resources Society. He is an Associate Editor of two international journals namely, the American Association of Petroleum Geologist's Journal of Environmental Geosciences and International Association of Hydrogeologist's Hydrogeology Journal.

ISBN - 81 - 7764 - 923 - X

ALLIED PUBLISHERS PRIVATE LIMITED